THE UNIVERSITY of TULSA

Department of Petroleum Engineering

Fluid Flow Projects

Seventy Fourth Semi-Annual Advisory Board Meeting Brochure and Presentation Slide Copy

May 12, 2010

Tulsa University Fluid Flow Projects
Seventy Fourth Semi-Annual Advisory Board Meeting Agenda
Wednesday, May 12, 2010

Tuesday,
May 11, 2010

Tulsa University High-Viscosity Oil Projects
Advisory Board Meeting
University of Tulsa – H. A. Chapman Stadium, OneOK Club
3112 East 8th Street
Tulsa, Oklahoma
8:00 – Noon

Tulsa University High-Viscosity Oil Projects and Tulsa University Fluid Flow Projects
Workshop Luncheon
University of Tulsa – Mayo Village – Student Activity Center
11th & Delaware
Tulsa, Oklahoma
12:00 – 1:00 p.m.

Tulsa University Fluid Flow Projects Workshop
University of Tulsa – H. A. Chapman Stadium – OneOk Club
3112 East 8th Street
Tulsa, Oklahoma
1:00 – 3:00 p.m.

Tulsa University High-Viscosity Oil Projects, Tulsa University Fluid Flow Projects and
Tulsa University Paraffin Deposition Projects
Tour of Test Facilities
University of Tulsa North Campus
2450 East Marshall
Tulsa, Oklahoma
3:30 – 5:30 p.m.

Tulsa University High-Viscosity Oil Projects and Tulsa University Fluid Flow Projects
Reception
H. A. Chapman Stadium – OneOk Club
3112 East 8th Street
Tulsa, Oklahoma
6:00 – 9:00 p.m.

Wednesday, May 12, 2010

Tulsa University Fluid Flow Projects
Advisory Board Meeting
University of Tulsa – H. A. Chapman Stadium – OneOK Club
3112 East 8th Street
Tulsa, Oklahoma
8:00 a.m. – 5:00 p.m.

Tulsa University Fluid Flow Projects and Tulsa University Paraffin Deposition Projects
Reception
University of Tulsa – H. A. Chapman Stadium – OneOk Club
3112 East 8th Street
Tulsa, Oklahoma
5:30 – 9:00 p.m.

Thursday, May 13, 2010

Tulsa University Paraffin Deposition Projects
Advisory Board Meeting
University of Tulsa – Collins Hall – Heritage Room
2905 East 8th Street
Tulsa, Oklahoma
8:00 a.m. – 1:00 p.m.

Tulsa University Fluid Flow Projects
Seventy Fourth Semi-Annual Advisory Board Meeting Agenda
Wednesday, May 12, 2010

8:00 a.m.	**Breakfast – Allen Chapman Activity Center - Gallery**	
8:30	**Introductory Remarks**	Cem Sarica
8:45	**TUFFP Progress Reports**	
	Slug Flow Evolution in Three-Phase Gas-Oil-Water Flow in Hilly Terrain Pipelines	Gizem Ersoy
	Low Liquid Loading Three-Phase Flow	Kiran Gawas
10:30	**Coffee Break**	
10:45	**TUFFP Progress Reports**	
	Effects of High Oil Viscosity on Slug Liquid Holdup in Horizontal Pipes	Ceyda Kora
	Effect of Pipe Diameter on Drift Velocity for High Viscosity Liquids	Ben Jeyachandra
12:00 p.m.	**Lunch – Mayo Village – Student Activity Center**	
1:15 p.m.	**TUFFP Progress Reports**	
	Investigation of Slug Length for High Viscosity Oil-Gas Flow	Eissa Alsafran
	Immediate Continuation of High Oil Viscosity Two-Phase Flow Research	Ben Jeyachandra
	High Pressure – Large Diameter Multiphase Flow Loop	Cem Sarica
2:45	**Coffee Break**	
3:00	**TUFFP Project Reports**	
	Transient Gas/Liquid Two-Phase Flow Modeling	Michelle Li
	Liquid Unloading from Gas Wells	Ge (Max) Yuan
4:00	**New TUFFP Web Site**	Lori Watts
4:15	**Potential New Research Direction**	Cem Sarica
4:30	**TUFFP Business Report**	Cem Sarica
4:45	**Open Discussion**	Cem Sarica
5:00	**Adjourn**	
6:00	**TUFFP/TUPDP Reception – H. A. Chapman Stadium – OneOk Club**	

Table of Contents

Executive Summary **1**

Introductory Presentation **5**

TUFFP Progress Reports

Executive Summary 13
Slow Flow Evolution of Gas-Oil-Water Flow in Hilly-Terrain Pipelines – Gizem Ersoy Gokcal
Presentation 21
Report 41

Executive Summary 73
Low Liquid Loading Gas-Oil-Water in Pipe Flow – Kiran Gawas
Presentation 77
Report 103

Executive Summary 123
Effects of High Oil Viscosity on Slug Liquid Holdup in Horizontal Pipes – Ceyda Kora
Presentation 137
Report 149

Effect of Pipe Diameter on Drift Velocity for High Viscosity Liquids – Benin Chelinsky Jeychandra and Dr. Abdel Al-Sarkhi
Presentation 165
Report 179

Investigation of High Viscosity Oil Two-Phase Slug Length in Horizontal Pipes – Eissa Al-Safran
Presentation 193
Report 207

Continuation of High Oil Viscosity Two-Phase Flow Research – Benin Chelinsky Jeyachandra
Presentation 223
Report 239

Executive Summary 251
High Pressure – Large Diameter Multiphase Flow Loop – Scott Graham and Cem Sarica
Presentation 255

Executive Summary 271
Transient Two-Phase Flow Modeling – Michelle Li
Presentation 273
Report 301

Executive Summary 333
Liquid Unloading from Gas Wells – Ge (Max) Yuan
Presentation 335
Report 355

TUFFP Business Report

Presentation 369
Introduction 377
Personnel 379
Membership 381
Equipment and Facilities 383
Financial Status 385
Miscellaneous Information 391

Appendices

Appendix A – Fluid Flow Projects Deliverables 393
Appendix B – Fluid Flow Projects Advisory Board Representatives 399
Appendix C – History of Fluid Flow Projects Membership 405
Appendix D – Contact Information 411

Executive Summary

Progress on each research project is given later in this Advisory Board Brochure. A brief summary of the activities is given below.

- *"Investigation of Gas-Oil-Water Flow"*. Three-phase gas-oil-water flow is a common occurrence in the petroleum industry. The ultimate objective of TUFFP for gas-oil-water studies is to develop a unified model based on theoretical and experimental analyses. A three-phase model has already been developed. There are several projects underway addressing the three-phase flow.

- *"High Viscosity Oil Two-phase Flow Behavior"*. Oils with viscosities as high as 10,000 cp are produced from many fields around the world. Current multiphase flow models are largely based on experimental data with low viscosity fluids. The gap between lab and field data may be three orders of magnitude or more. Therefore, current mechanistic models need to be improved with higher liquid viscosity experimental results. Modifications or new developments are necessary.

  An earlier TUFFP study conducted by Gokcal showed that the performances of existing models are not sufficiently accurate for high viscosity oils with a viscosity range of 200 – 1000 cp. It was found that increasing oil viscosity had a significant effect on flow behavior. Mostly, intermittent flow (slug and elongated bubble) was observed in his study. Based on his results, this study focused on the slug flow.

  Gokcal (2008) developed a translational velocity closure relationship for all inclination angles. Moreover, he developed a slug frequency correlation. Our current efforts in this project continue at multiple fronts:

  1. *Translational Velocity Study:* Diameter effect on the drift velocity is being investigated theoretically and experimentally. The tests with 6 in. ID pipe have been completed during this period. 6 in. data and previously acquired 3 in. and 2 in. data are used to assess the effect of diameter on the drift velocity. Moreover, CFD modeling of drift velocity is performed using Fluent. The results agree with the experimental results.

  2. *Slug Length Study:* Dr. Eissa Al-Safran of Kuwait University continued investigating the slug length for high viscosity oils which was started as his sabbatical research assignment. In an earlier study by Gokcal (2008) slug lengths were found to decrease with increasing liquid viscosity and follow a log-normal distribution.

  3. *Slug Liquid Holdup Study:* One of the important closure relationships of the slug flow is the slug liquid holdup. Current experimental study focuses on the investigation of the slug liquid holdup. During this period, a new capacitance probe is developed to measure the holdup. The probe has been successfully tested against the quick closing valve data. The new probe allows faster data acquisition and expands the testing range. .

- *"Droplet Homo-phase Interaction Study"*. There are many cases in multiphase flow where droplets are entrained from or coalesced into a continuous homophase. For example, in annular mist flow, the liquid droplets are in dynamic equilibrium with the film on the walls, experiencing both entrainment and coalescence. Very few mechanistic models exist for entrainment rate and coalescence rate. Understanding the basic physics of these phenomena is essential to model situations of practical interest to the industry. Droplet homo-phase covers a broad range of possibilities.

  A past sensitivity study of multiphase flow predictive models showed that, in stratified and annular flow, the variation of droplet entrainment fraction can significantly affect the predicted pressure gradient. Although better entrainment fraction correlations were proposed, a need was identified to experimentally investigate entrainment fraction for inclined pipes. At the last Advisory Board meeting, the results of the experimental results for various inclination angles were presented. The results showed the dependency of entrainment fraction to the inclination angle of the pipe. Several dimensionless groups correlating the entrainment fraction for all inclination angles has been identified and verified with the experimental data from the open literature. The current focus will be on the modeling side and the effective use of Magrini's data. A new reliable model for all inclination angles or a modification of an existing model will be the target of the future work. The project is assigned to Dr. Abdel Al-Sarkhi, a Research Associate Professor of Petroleum Engineering.

- *"Simplified Transient Flow Studies"*. TUFFP's simplified transient flow studies project proposal ranked high in our previous questionnaires. The objective is to develop a simplified transient model as

a screening tool. Significant progress is made in this project since the last Advisory Board meeting. Two simplified transient models using two-fluid and drift flux approaches were developed. Model predictions are compared with the TUFFP transient flow data. Two-fluid model is found to perform well for all flow patterns using a steady-state flow pattern prediction model with possible non-convergence problems between the flow patterns. Flow pattern independent drift flux model seems to perform quite well in slug flow, and reasonably well for stratified flow. A detailed report is given in this brochure.

- *"Low Liquid Loading Gas-Oil-Water Flow in Horizontal and Near Horizontal Pipes"*. Low liquid loading exists widely in wet gas pipelines. These pipelines often contain water and hydrocarbon condensates. Small amounts of liquids can lead to a significant increase in pressure loss along a pipeline. Moreover, existence of water can significantly contribute to the problem of corrosion and hydrate formation problems. Therefore, understanding of flow characteristics of low liquid loading gas-oil-water flow is of great importance in transportation of wet gas.

  In a previous study, large amount of data were collected on various flow parameters such as flow patterns, phase distribution, onset of droplet entrainment, entrainment fraction, and film velocity using a model oil with a viscosity range of 25 to 10 cp. The existing oil has been replaced by Isopar L, which has similar fluid properties as wet gas condensate. Several tests have been conducted for both two-phase oil-gas and three-phase gas-oil-water flows. The initial analyses of the results indicate that the onset of the entrainment occurs at lower superficial velocities and increased entrainment fraction at the same superficial velocities when compared with higher viscosity oil test results.

- *"Multiphase Flow in Hilly Terrain Pipelines"*. Three-phase flow in hilly terrain pipelines is a common occurrence. The existence of a water phase in the system poses many potential flow assurance and processing problems. Most of the problems are directly related to the flow characteristics. Although the characteristics of two-phase gas-liquid flow have been investigated extensively, there are very few studies addressing multiphase gas-oil-water flow in hilly terrain pipelines. The general objectives of this project are to thoroughly investigate and compare existing models, and develop closure relationships and predictive models for three-phase flow of gas-oil-water in hilly-terrain pipelines.

  Since the Fall AB meeting, the data analysis has been completed. While the data analysis showed some effect of in-situ water on slug characteristics, by large, no significant systematic effect of water cut could be observed probably owing to the oil and the hilly terrain geometry studied. Comparisons of the data with the predictions of two-phase models such as OLGA and TUFFP Unified model have been made. The comparisons show that design parameters such as pressure gradient and holdups can be predicted well with two-phase models using a lumped liquid phase.

- *"Up-scaling Studies"*. One of the most important issues that we face in multiphase flow technology development is scaling up of small diameter and low pressure results to large diameter and high pressure conditions. Studies with a large diameter facility would significantly improve our understanding of flow characteristics in actual field conditions. Therefore, our main objective in this study is to investigate the effect of pipe diameter and pressures on flow behavior using a larger diameter flow loop.

  This project is one of the main activities of TUFFP, and a significant portion of the TUFFP budget is allocated to the construction of a 6" high pressure flow loop. The concrete foundation and steel supporting structures have been completed. All major equipments have been purchased. They are either on-site or scheduled for delivery. The test section will be completed by the end of May. Piping in the circulation area and the instrumentation/control system will be completed by the end of October. Commissioning of the gas compressor will take place in November with shakedown tests of the entire facility beginning in January. The flow loop is expected to be fully operational in March of 2011. A HAZOP analysis will be arranged with the support from Chevron. This will identify the need for additional safety and measurement devices and finalize the operation procedures.

- *"Liquid Unloading from Gas Wells."* Liquid loading of liquid in the wellbore has been recognized as one of the most severe problems in gas production. At early times of the production, natural gas carries liquid in the form of mist since the reservoir pressure is sufficiently high. As the gas well matures, the reservoir pressure decreases reducing gas velocity. The gas velocity may go below a critical value resulting in liquid accumulation in the well. The liquid accumulation increases the bottom-hole

pressure and reduces gas production rate significantly.

Although significant effort has been made to predict the liquid loading of gas wells, experimental data are very limited. The objective of this project is to better understand of the mechanisms causing the loading and develop new technologies to prevent or remediate liquid-loading problems in gas wells. This project is an experimental and modeling study. Flow characteristics will be observed and measured along the pipe. The effects of well deviation to the liquid loading will be investigated. The Turner model and its modified versions along with other models (including the TUFFP unified model) will be evaluated with experimental results. The existent models will be improved or a new model developed based on the experimental measurements and observations.

- "*Unified Mechanistic Model*". TUFFP maintains, and continuously improves upon the TUFFP unified model. Collaborative efforts with Schlumberger Information Systems continue to improve the speed and the performance of the software.

Current TUFFP membership stands at 14 (13 industrial companies and MMS). Efforts continue to further increase the TUFFP membership level. A detailed financial report is provided in this report. The sum of the 2010 income and the reserve account is projected to be $569,959.00. The expenses for the industrial member account are estimated to be $663,917.24 leaving a negative balance of $93,958.62. Despite of the cost cutting measures implemented this year, 2010 budget has a shortfall as presented primarily due to the high pressure facility construction. Therefore, it is proposed to increase the membership fee from $48,000 to $55,000 effective 2011.

Several related projects are underway. The related projects involve sharing of facilities and personnel with TUFFP. The Paraffin Deposition consortium, TUPDP, is into its fourth phase with 11 members. Tulsa University High Viscosity Oil Projects (TUHOP) Joint Industry Projects is into its third year. TUHOP currently has four members.

Fluid Flow Projects

74th Fluid Flow Projects Advisory Board Meeting

Welcome

Safety Moment

- Emergency Exits
- Assembly Point
- Tornado Shelter
- Campus Emergency
  - Call 9-911
  - Campus Security, ext. 5555 or 918-631-5555
- Rest Rooms

Introductory Remarks

- 74th Semi-Annual Advisory Board Meeting
- Handout
  - Combined Brochure and Slide Copy
- Sign-Up List
  - Please Leave Business Card at Registration Table

Team

- Research Associates
  - Cem Sarica (Director)
  - Holden Zhang (Associate Director)
  - Abdel Al-Sarkhi (Visiting Research Professor)
  - Polat Abduvayt
  - Mingxiu (Michelle) Li
  - Eissa Al-Safran (Collaborator)

Team …

- Project Coordinator
  - Linda Jones
- Project Engineer
  - Scott Graham
- Research Technicians
  - Craig Waldron
  - Brandon Kelsey
- Web Master
  - Lori Watts

Team …

- TUFFP Research Assistants
  - Gizem Ersoy (Ph.D.) – Turkey
  - Kiran Gawas (Ph.D.) – India
  - Ceyda Kora (MS) – Turkey
  - Ge Yuan (MS) – PRC
  - Benin (Ben) Chelinsky Jeyachandra (MS) – India

Guests

- Dr. Xiaoping Li, CUP

Membership and Financial Status

- 14 Members in 2010
  - Rosneft & PEMEX Terminated for 2010
    - Collectively They Owe $136,000 from Past Due Membership Fees
    - Efforts are Underway to Collect the Fees
- Budget Shortfall of $94,000
- 2011 Membership Fee will be Increased to $55,000

2009 Industrial Account Summary

(Prepared April 28, 2010)

Anticipated Reserve Fund Balance on January 1, 2009					**452,358.43**
Income for 2009					
	2009 Membership Fees (14 @ $48,000 - excludes MMS)				**$672,000**
	Two Uncollected 2009 Membership Fees				**(96,000)**
Total Budget					**1,028,358.43**
Projected Budget/Expenditures for 2009					
		Budget	**Revised Budget 2/11/09**	**Expenses 1/8/10**	
90101	Principal Investigator - Sarica	29,251.82	29,074.14	19,562.62	
90103	Co-Principal Investigator - Zhang			-	
90600	Professional Salary - Jones	11,596.24	11,728.00	9,773.32	
90601	Professional Salary - Li	13,157.00	12,875.00	5,031.59	
90602	Professional Salary - Graham	19,923.00	20,149.00	16,790.92	
90603	Professional Salary - Polat	62,000.00	65,000.00	55,434.90	
90701	Technician - Miller	9,943.45	10,016.00	8,036.20	
90702	Technician - Waldron	16,826.00	16,517.00	16,522.92	
90703	Technician - Kelsey	19,097.00	18,746.00	18,746.00	
91000	Graduate Students - Monthly	58,100.00	54,650.00	62,825.00	
91100	Students - Hourly	15,000.00	15,000.00	12,312.97	
91800	Fringe Benefits (33%)	59,992.19	58,805.74	50,132.65	
93100	General Supplies	3,000.00	3,000.00	170,977.31	
93101	Research Supplies	100,000.00	100,000.00	63,248.52	
93102	Copier/Printer Supplies	500.00	500.00	81.99	
93103	Component Parts			1,585.90	
93104	Computer Software	4,000.00	4,000.00	1,023.75	
93106	Office Supplies	2,000.00	2,000.00	1,466.14	
93200	Postage/Shipping	500.00	500.00	3,313.00	
93300	Printing/Duplicating	2,000.00	2,000.00	3,788.79	
93400	Telecommunications	3,000.00	3,000.00	1,649.99	
93500	Membership/Subscriptions	1,000.00	1,000.00	515.00	
93601	Travel - Domestic	10,000.00	10,000.00	9,431.74	
93602	Travel - Foreign	10,000.00	10,000.00	2,203.96	
93700	Entertainment (Advisory Board Meetings)	10,000.00	10,000.00	16,400.50	
94803	Consultants	16,000.00	18,500.00	24,280.33	
94813	Outside Services	20,000.00	20,000.00	25,975.57	
95103	Equipment Rental			2,752.24	
95200	F&A (55.6%)	141,721.35	141,867.93	125,120.26	
98901	Employee Recruiting	3,000.00	3,000.00	3,923.05	
99001	Equipment	600,000.00	400,000.00	319,161.04	
99002	Computers	8,000.00	8,000.00	1,604.61	
99300	Bank Charges	40.00	40.00	30.00	
81801	Tuition/Fees	30,665.00	30,067.00	29,089.00	
81806	Graduate Fellowship			2,608.03	
	Total Expenditures	**1,280,313.05**	**1,080,035.81**	**1,085,399.81**	
Anticipated Reserve Fund Balance as of 12/31/09					**(57,041.38)**

2010 Industrial Account Projections

(Prepared April 26, 2010)

Anticipated Reserve Fund Balance on January 1, 2010					**($57,041)**
Income for 2010					
	2010 Anticipated Membership Fees (13 @ $48,000 - exludes MMS)				**624,000**
	1 Membership Overpayment				**3,000**
Total Budget					**$ 569,959**
Projected Budget/Expenditures for 2008/2009					
		Projected Budget	**Revised Budget April 2010**	**2010 Expenditures (April 2010)**	
90101 - 90103	Faculty Salaries	29,074.14	918.10	981.10	
90600 - 90609	Professional Salaries	47,628.54	53,310.06	53,310.06	
90700 - 90703	Staff Salaries	35,262.50	35,291.52	35,291.52	
91000	Student Salaries - Monthly	41,550.00	43,725.00	43,725.00	
91100	Student Salaries - Hourly	15,000.00	10,000.00	10,000.00	
91800	Fringe Benefits	38,068.16	30,986.49	30,986.49	
81801	Tuition & Student Fees	17,898.00	26,637.00	26,637.00	
92102	Student Fringe		1,762.00	1,762.00	
93100	General Supplies	3,000.00	3,000.00	156.25	
93101	Research Supplies	50,000.00	60,000.00	34,068.38	
93102	Copier/Printer Supplies	500.00	500.00	-	
93104	Computer Software	4,000.00	3,000.00	538.18	
93106	Office Supplies	2,000.00	2,000.00	654.40	
93200	Postage and Shipping	500.00	500.00	269.83	
93300	Printing and Duplicating	2,000.00	2,000.00	83.31	
93400	Telecommunications	3,000.00	1,700.00	456.99	
93500	Membership	1,000.00	1,000.00	90.00	
93601	Travel - Domestic	10,000.00	10,000.00	1,405.32	
93602	Travel - Foreign	10,000.00	10,000.00	-	
93700	Entertainment	10,000.00	10,000.00	276.87	
94813	Outside Services	20,000.00	20,000.00	9,650.00	
95103	Equipment Rental			500.73	
95200	F&A (55.6%)	93,694.44	79,679.07	79,679.07	
98901	Employee Recruiting	3,000.00			
99001	Equipment	200,000.00	257,868.00	-	
99002	Computers	8,000.00	-	-	
99300	Bank Charges	40.00	40.00		
Total Anticipated Expenditures		**645,215.78**	**663,917.24**	**330,522.50**	
Anticipated Reserve as of 12/31/10					**(93,958.62)**

Salaries are calculated through December 31, 2010

Total TUFFP Income reduced by $136,000 due to uncollected Membership Fees

Agenda

- 8:30 Introductory Remarks
- 8:45 Progress Reports
  - Slug Flow Evolution in Three-phase Gas-Oil-Water Flow in Hilly Terrain Pipelines
  - Low Liquid Loading Three-phase Flow
- 10:30 Coffee Break
- 10:45 Progress Reports
  - Effects of High Oil Viscosity on Slug Liquid Holdup in Horizontal Pipes
  - Effect of Pipe Diameter on Drift Velocity for High Viscosity Liquids

Agenda …

- 12:00 Lunch – Mayo Village – Student Activity Center
- 1:15 Progress Reports
  - Investigation of Slug Length for High Viscosity Oil-Gas Flow
  - Immediate Continuation of High Oil Viscosity Two-phase Flow Research
    - Inclined Pipes
    - Higher Viscosity Oils (1,000 cp – 10,000 cp)
  - High Pressure – Large Diameter Multiphase Flow Loop
- 2:45 Coffee Break

Agenda …

- 3:00 Progress Reports
  - Transient Gas/Liquid Two-phase Flow Modeling
  - Liquid Unloading from Gas Wells
- 4:00 New TUFFP Web Site
- 4:15 Potential New Research Direction
- 4:30 TUFFP Business Report
- 4:45 Open Discussion
- 5:00 Adjourn
- 6:00 TUFFP/TUPDP Reception – OneOK Club

Other Activities

- May 11, 2010
  - TUHOP Meeting
  - TUFFP Workshop
    - Excellent Presentations
    - Beneficial for Everybody
  - Facility Tour
- May 13, 2010
  - TUPDP Meeting

Fluid Flow Projects

Executive Summary of Research Activities

Cem Sarica

Advisory Board Meeting, May 12, 2010

Unified Model

- Objective
  - Develop and Maintain an Accurate and Reliable Steady State Multiphase Simulator
- Past Studies
  - Zhang *et al.* Developed "Unified Model" in 2002 for Two-phase Flow
    - Became TUFFP's Flagship Steady State Simulator
    - Applicable for All Inclination Angles
  - "Unified Model was Extended to Three-phase in 2006

Unified Model …

- Current Activities
  - Code and Software Improvement Efforts

Unified Model …

- Future Activities
  - Continue Improvements in Both Modeling and Software Development

Droplet Homo-phase Studies

- Significance
  - Better Predictive Tools Lead to Better Design and Practices
- General Objective
  - Development of Closure Relationships
- Past Study
  - Earlier TUFFP Study Showed
    - Entrainment Fraction (FE) is Most Sensitive Closure Parameter in Annular Flow
    - Developed New FE Correlation
      - Utilizing In-situ Flow Parameters
      - Limited Data, Especially for Inclined Flow Conditions

Droplet Homo-phase Studies …

- Current Study
  - Liquid Entrainment in Annular Two-Phase Flow in Inclined Pipes
  - Objectives
    - Acquire Data for Various Inclination Angles for 3-in. ID Pipe Using Severe Slugging Facility
      - Existing Data are for 1 and 1 ½ in.
    - Develop a New Closure Relationship

Droplet Homo-phase Studies …

- Status
  - Experimental Study is Completed
    - Entrainment Fraction is Found to Vary with Inclination Angle
    - Performance Analysis of the Existing Correlations is Completed
  - New Dimensionless Groups are Proposed to Correlate Entrainment Fraction
  - Closure Relationship Development will Continue

Three-phase Flow Studies

- Significance
  - Good Understanding of Gas-Oil Flow
  - Poor Understanding of Gas-Oil-Water Flow
- Objective
  - Development of Improved Prediction Models
- Past Studies
  - Oil-Water
    - Trallero (1994), Horizontal
    - Flores (1996), Vertical and Deviated
    - Alkaya (1999), Inclined

Three-phase Flow Studies …

- Past Studies …
  - Three-phase
    - Keskin (2007), Experimental Horizontal Three-phase Study
    - Zhang and Sarica (2005), Three-phase Mechanistic Model Development
    - Need to More Research on Oil-Water Flow
  - Recent Oil-Water Studies with Emphasis on Droplets
    - Vielma (2006), Horizontal Flow
    - Atmaca (2007), Inclined Flow
    - Sharma (2009), Modeling Based on Minimum Energy Concept

Three-phase Flow Studies …

- Current Activity
  - Various Other Projects Contribute to This Project
    - Low-Liquid Loading Three-phase Flow
    - Slug Flow Evolution in Hilly Terrain Pipelines
    - Unified Model and Software Development

Three-phase Hilly Terrain Flow

- Significance
  - Valleys and Hills may Act as Local Separation Devices for Fluids
  - Location, Amount and Residence Time of Water in a Pipe can have Significant Impact on Flow Assurance Issues such as Hydrate Formation and Corrosion

Three-phase Hilly Terrain Flow …

- Past Studies
  - Hilly Terrain Flow of Two Phases has been Studied Extensively
    - Al-Safran, 1999 and 2003
    - Others Outside of TUFFP
  - No Available Research is Found on Three-phase Flow

Three-phase Hilly Terrain Flow …

- Current Project
  - Objectives
    - Observe Flow Behavior and Identify Flow Characteristics
    - Develop Predictive Tools (Closure Relationships or Models) If Needed

Three-phase Hilly Terrain Flow …

- Status
  - Testing is Complete
  - Data Analysis and Model Evaluation are recently Completed
  - No Significant Impact of Water on Design Parameters Could Be Observed

Fluid Flow Projects

Slug Flow Evolution of Gas-Oil-Water Flow in Hilly-Terrain Pipelines

Gizem Ersoy Gokcal

Outline

- Introduction
- Objectives
- Experimental Study
- Preliminary Modeling
- Project Schedule

Introduction

Hilly-Terrain Pipelines Cause

- **Operational Problems**
  - **Flooding of Downstream Facilities**
  - **Severe Pipe Corrosion**
  - **Structural Instability of Pipelines**
- **Flow Assurance Problems**
  - **Hydrates**
  - **Emulsions**
  - **Paraffin Deposition**
  - **Corrosion**

Introduction …

Hydrodynamics

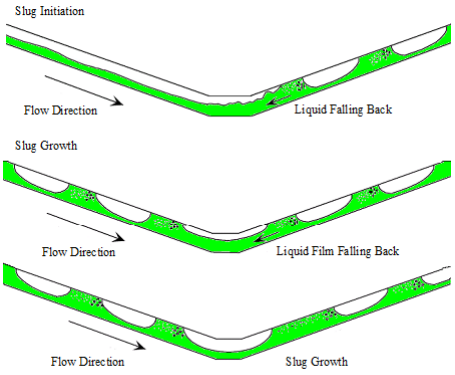

Flow Assurance

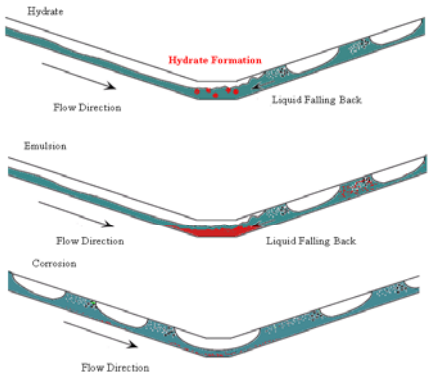

Objectives

- Investigate Gas-Oil-Water Flow in Hilly-Terrain Pipelines
- Develop Closure Models for Flow in Hilly-Terrain Pipelines on
  - Three-Phase Slug Initiation and Dissipation
  - Mixing Status of Phases

Experimental Study

- Experimental Facility
- Instrumentation
- Data Acquisition System
- Test Fluids
- Testing Ranges
- Experimental Results

Experimental Facility

- Extended to 69-m (226-ft) Long
- 50.8-mm (2-in.) ID Pipes
- Single Hilly-Terrain Unit
  - 9.7-m (32-ft) Long Downhill
  - 1.5-m (5-ft) Long Horizontal
  - 9.7-m (32-ft) Long Uphill Sections (L/D=413)
- ±1°, ±2°, ±5° of Inclination Angles

Experimental Facility

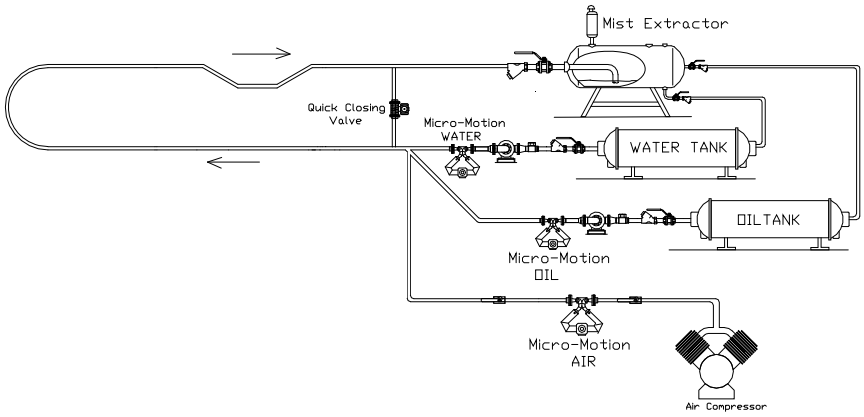

Experimental Facility …

Test Section

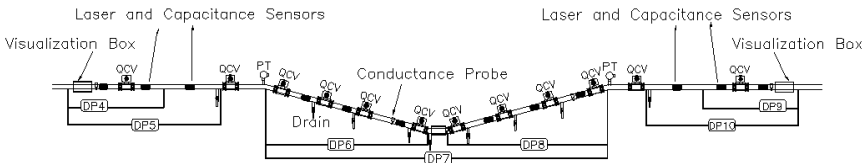

Fluid Flow Projects

Advisory Board Meeting, May 12, 2010

Experimental Facility …

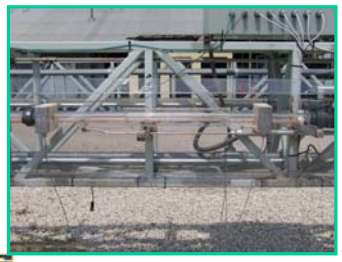

Fluid Flow Projects

Advisory Board Meeting, May 12, 2010

Instrumentation

- Pressure & Differential Pressure Transducers
- Quick-Closing Valves
- Laser Sensors
- Capacitance Sensors
- Cameras

Instrumentation …

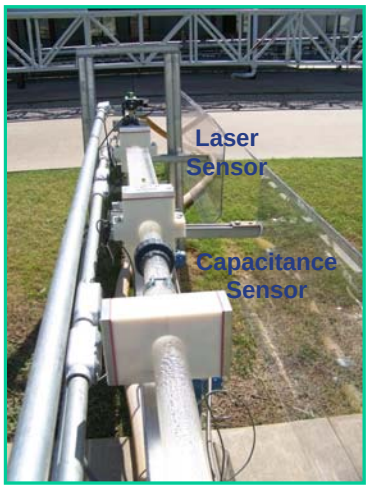

Data Acquisition System

- Lab VIEW™ 7.1 Software
- High-Speed Data Acquisition

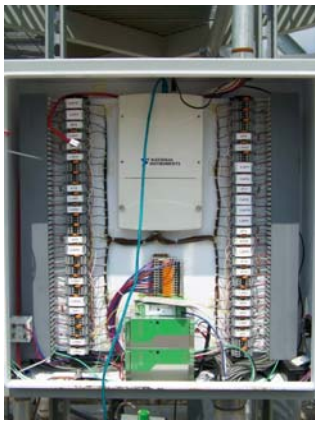

Test Fluids

- Air - Mineral Oil - Water
- Tulco Tech-80 Mineral Oil
  - API: 33.2°
  - Density: 858.75 kg/m^3 @ 15.6 °C (60°F)
  - Viscosity: 13.5 cP @ 40 °C (104 °F)
  - Surface Tension: 29.14 dynes/cm @ 25.1 °C (77.2 °F)

Testing Ranges

- Superficial Oil Velocity
  - 0.04 – 1 m/s
- Superficial Water Velocity
  - 0.025 – 1 m/s
- Superficial Gas Velocity
  - 0.1 – 5 m/s
- Water Fraction
  - 20%, 40%, 60%, 80%
  - 0% and 100% for Preliminary Tests
- Hilly-Terrain Unit
  - 5° for Valley Configuration

Testing Ranges …

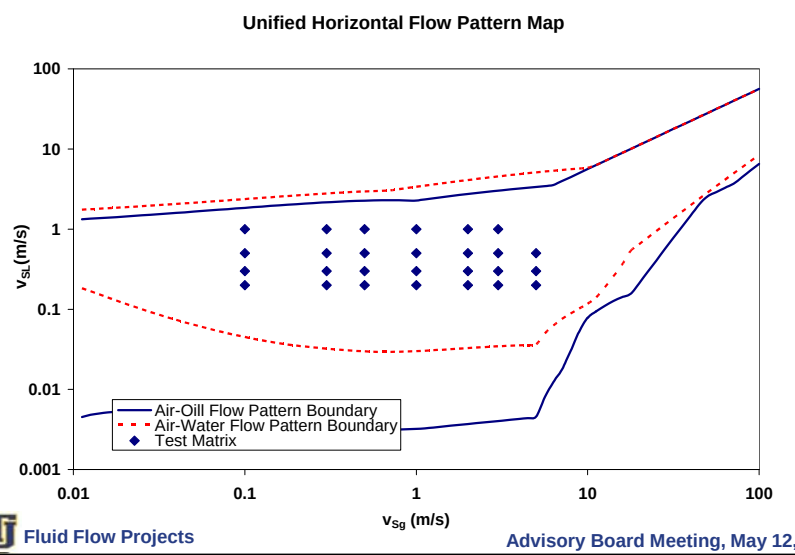

Testing Ranges …

Unified Flow Pattern Map for -5° Inlclination Pipe

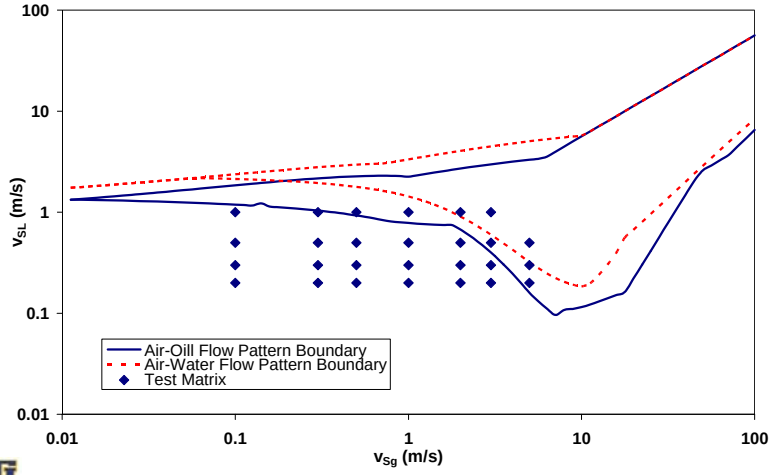

Fluid Flow Projects

Advisory Board Meeting, May 12, 2010

Testing Ranges …

Unified Flow Pattern Map for +5° Inclination Pipe

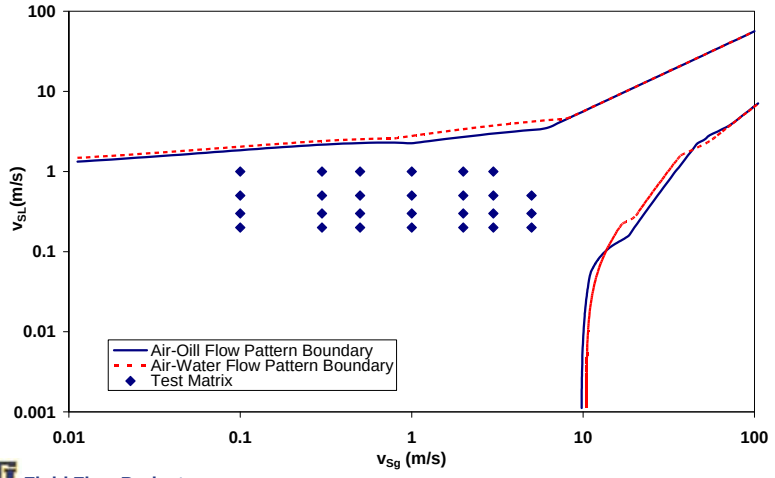

Fluid Flow Projects

Advisory Board Meeting, May 12, 2010

Experimental Results

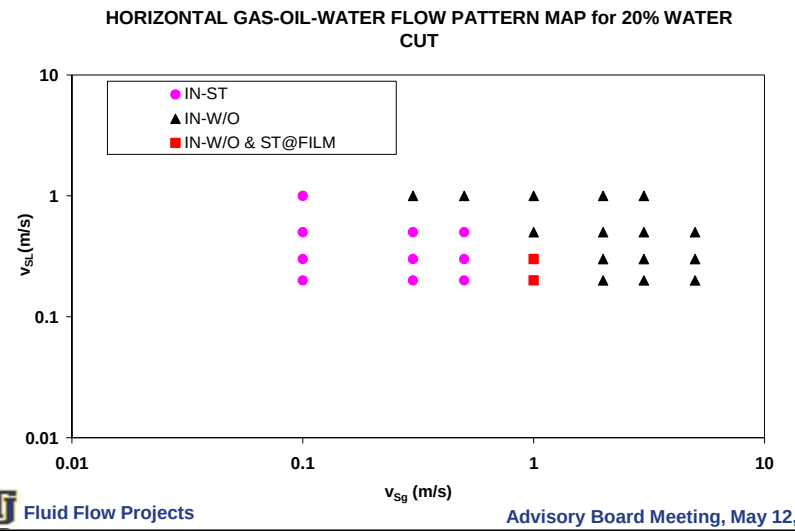

Fluid Flow Projects

Advisory Board Meeting, May 12, 2010

Experimental Results …

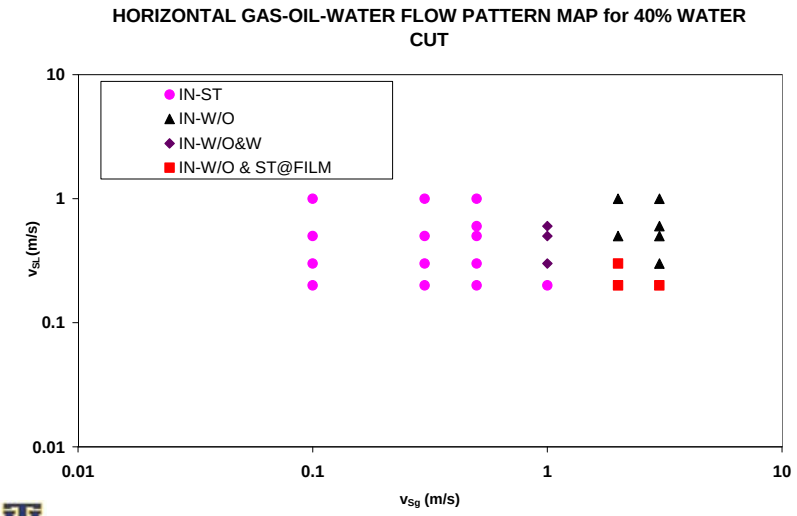

Fluid Flow Projects

Advisory Board Meeting, May 12, 2010

Experimental Results …

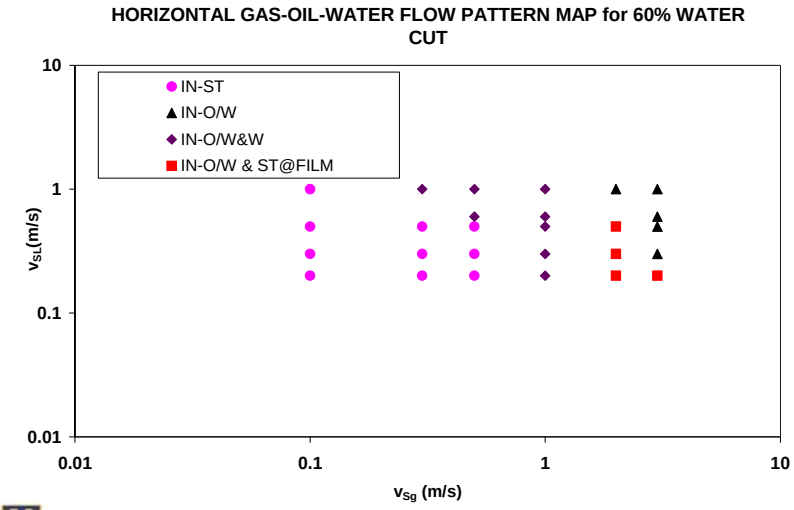

Fluid Flow Projects

Advisory Board Meeting, May 12, 2010

Experimental Results …

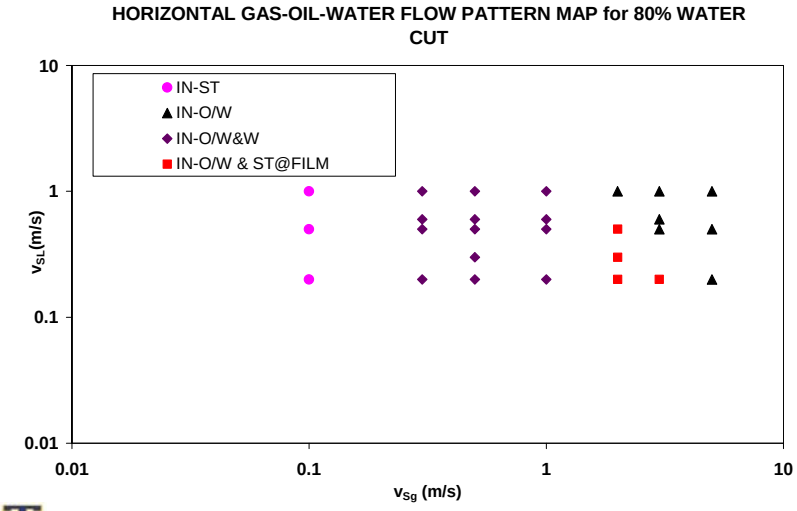

Fluid Flow Projects

Advisory Board Meeting, May 12, 2010

Experimental Results …

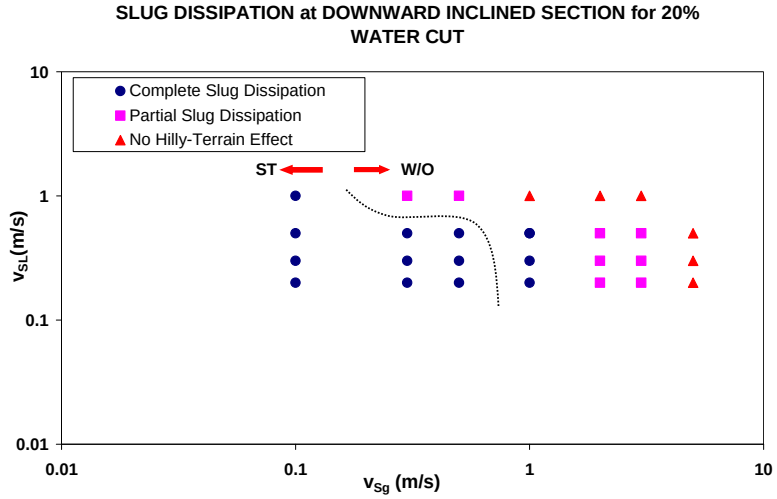

Fluid Flow Projects

Advisory Board Meeting, May 12, 2010

Experimental Results …

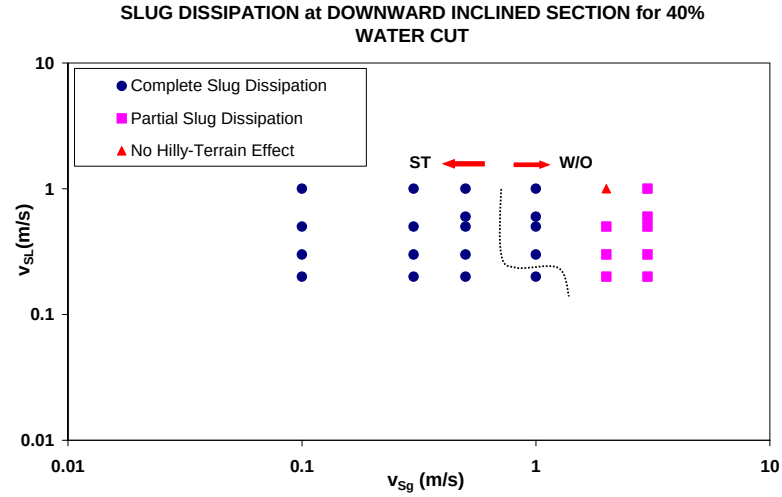

Fluid Flow Projects

Advisory Board Meeting, May 12, 2010

Experimental Results …

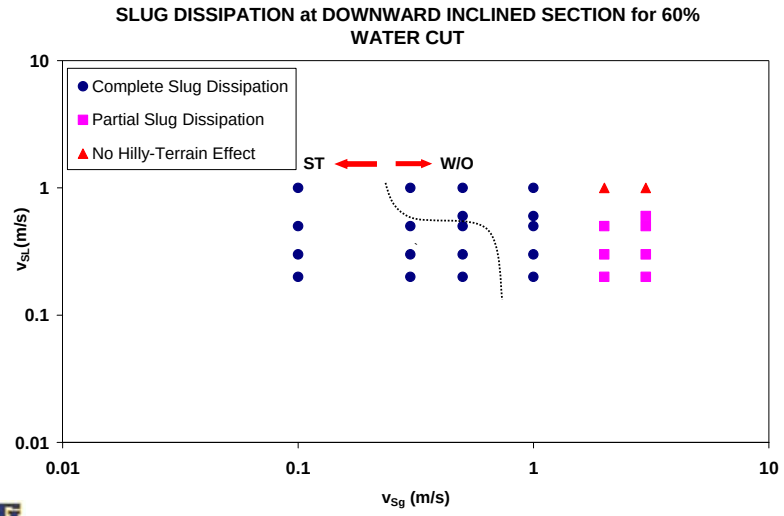

Fluid Flow Projects

Advisory Board Meeting, May 12, 2010

Experimental Results …

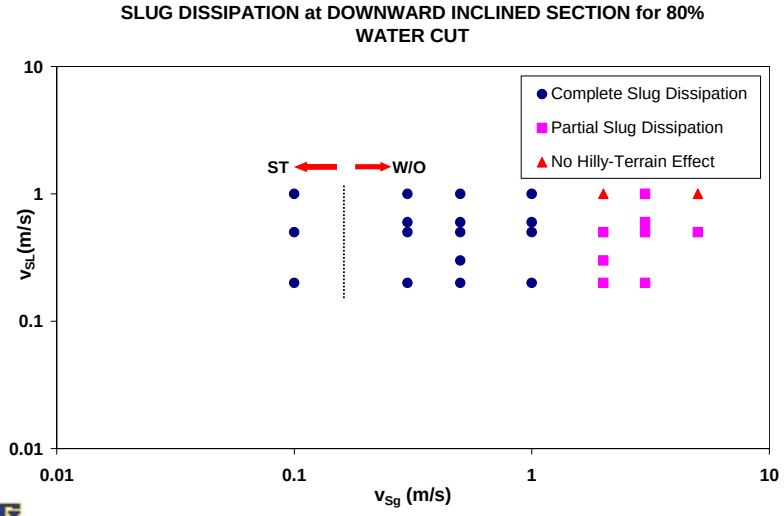

Fluid Flow Projects

Advisory Board Meeting, May 12, 2010

Experimental Results v_{Sg}= 1m/s v_{SL}= 0.5 m/s …

20% Water Cut

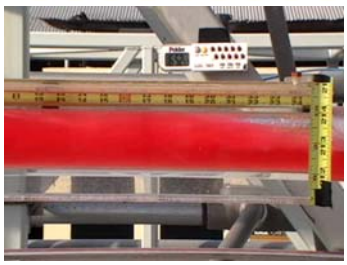

60% Water Cut

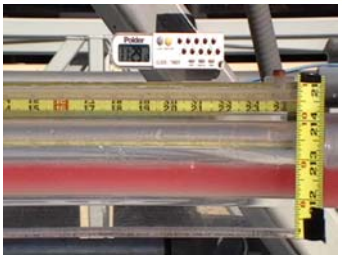

40% Water Cut

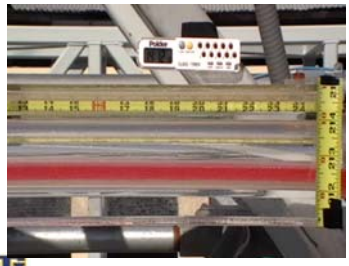

80% Water Cut

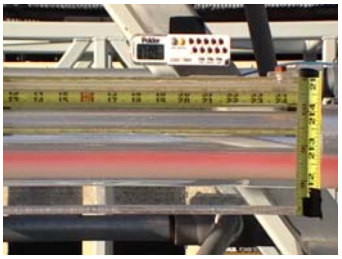

Experimental Results (v_{Sg}= 1m/s v_{SL}= 0.5m/s)…

20% Water Cut

60% Water Cut

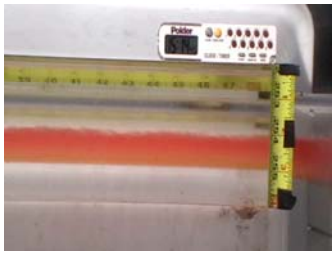

40% Water Cut

80% Water Cut

Experimental Results (v_{Sg}= 1m/s v_{SL}= 0.5m/s)…

20% Water Cut

60% Water Cut

40% Water Cut

80% Water Cut

Experimental Results …

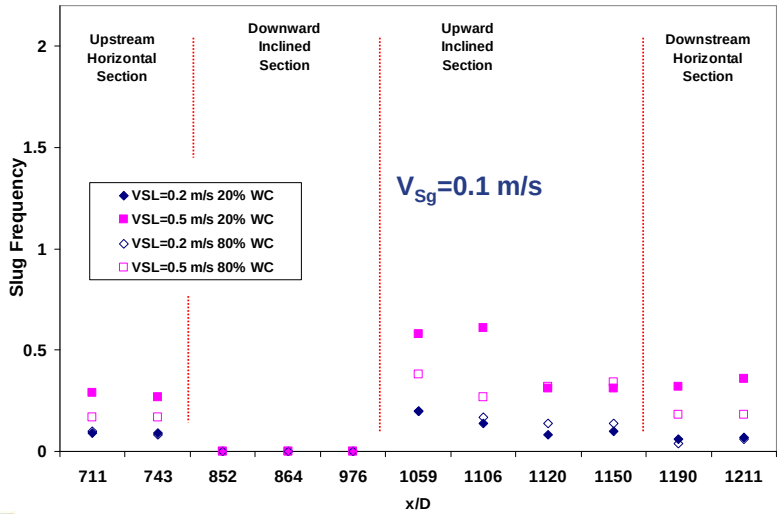

Experimental Results …

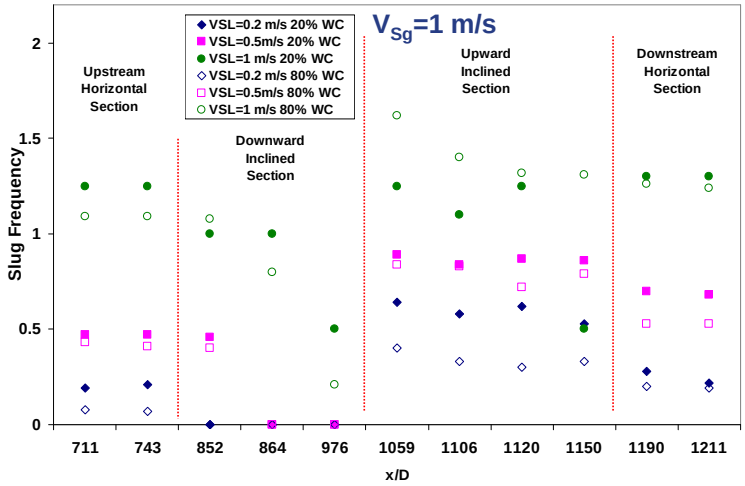

Experimental Results …

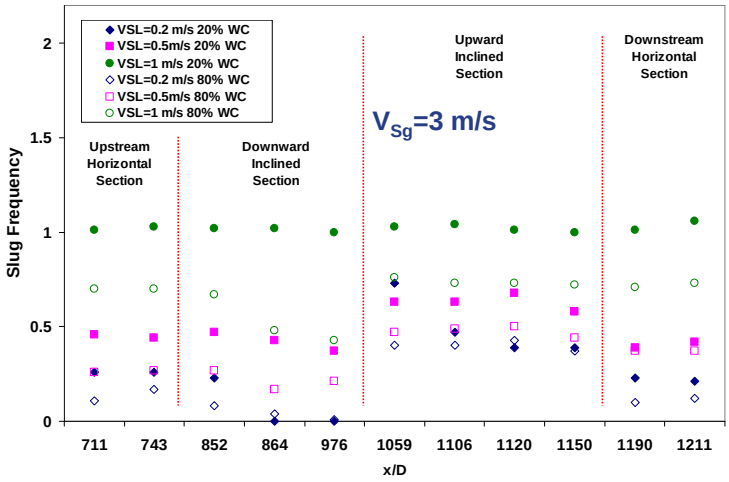

Experimental Results …

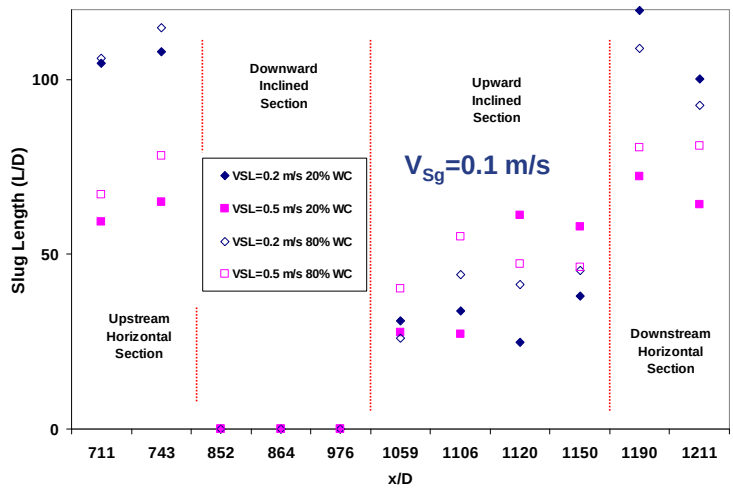

Fluid Flow Projects

Advisory Board Meeting, May 12, 2010

Experimental Results …

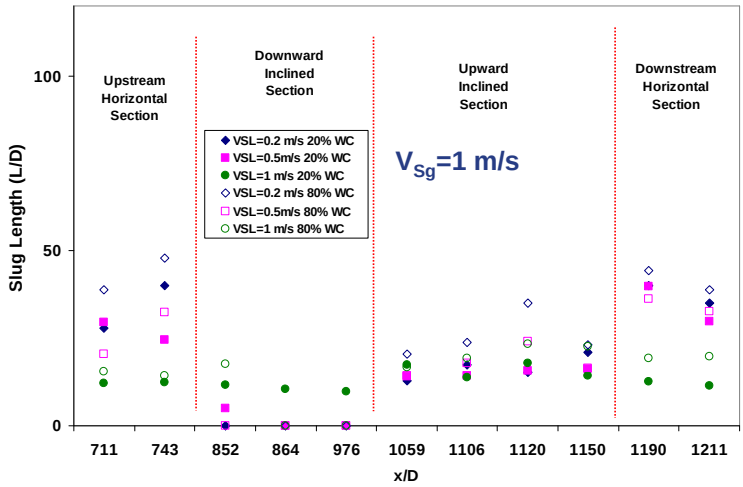

Fluid Flow Projects

Advisory Board Meeting, May 12, 2010

Experimental Results …

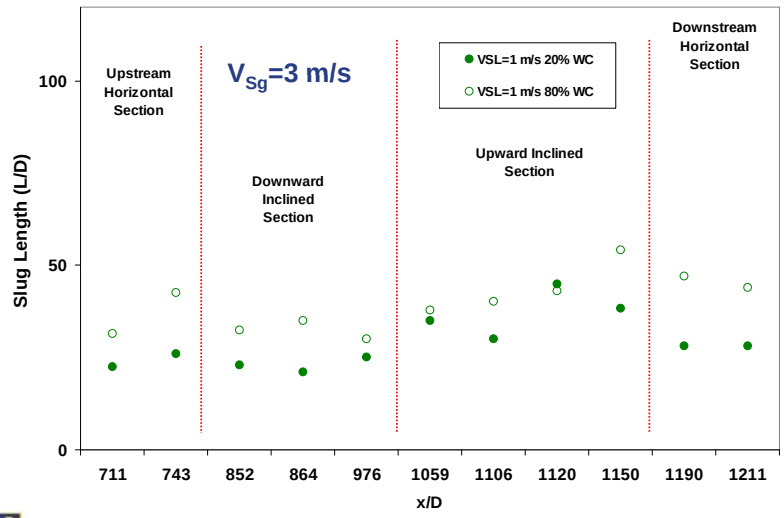

Experimental Results …

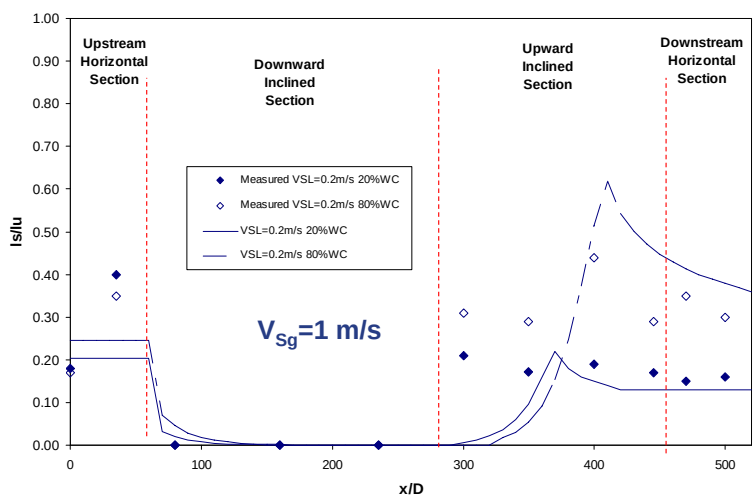

Experimental Results …

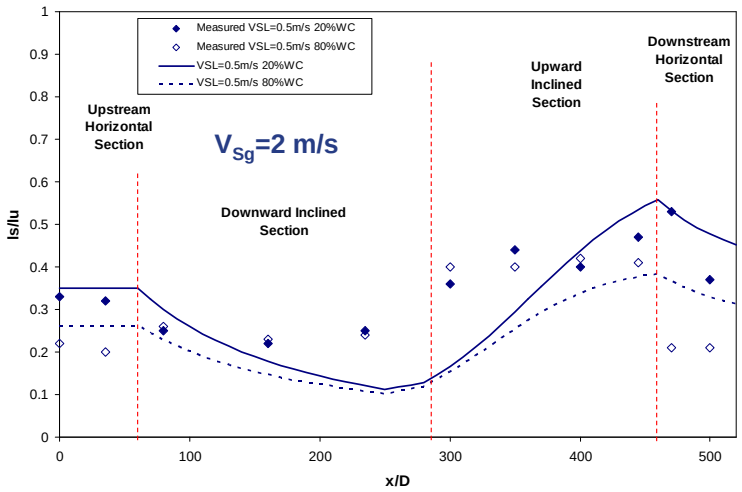

Fluid Flow Projects

Advisory Board Meeting, May 12, 2010

Experimental Results …

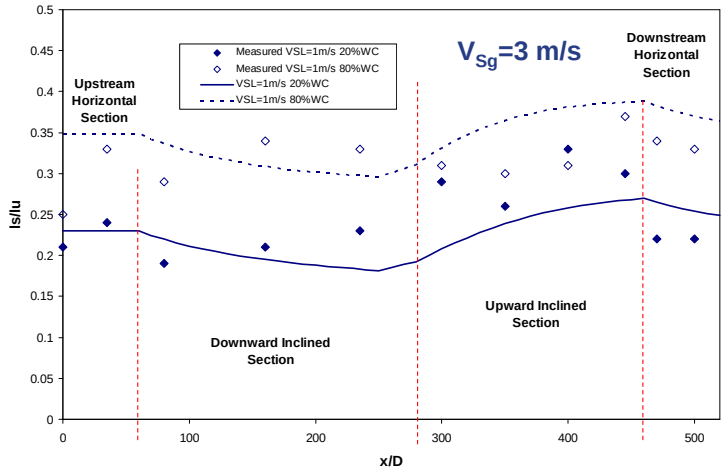

Fluid Flow Projects

Advisory Board Meeting, May 12, 2010

Project Schedule

- Final Report — May 2010

Questions & Comments

Slug Flow Evolution of Gas-Oil-Water Flow in Hilly-Terrain Pipelines

Gizem Ersoy Gokcal

PROJECTED COMPLETION DATES:

Literature Review	Completed
Facility Modifications	Completed
Preliminary Testing	Completed
Testing	Completed
Data Analysis	Completed
Model Development	Completed
Model Validation	Completed
Final Report	May 2010

Objective

The general objectives of this project are:

- to conduct experiments on three-phase gas-oil-water flow in hilly-terrain pipelines,
- to develop closure models for three-phase slug initiation, dissipation and mixing status of phases,
- to validate developed closure models with experimental results.

Introduction

In the petroleum industry, slug flow is the most complex and dominant flow pattern in horizontal and near-horizontal pipes. Numerous studies have been carried out on slug flow in pipelines. Although slug flow in horizontal and inclined pipes has been studied extensively, slug flow in hilly-terrain pipelines which are common in both onshore and offshore production and transportation systems, is still not completely understood.

A hilly-terrain pipeline is a pipeline consisting of horizontal, upward inclined, and downward inclined sections. The standard engineering design method for hilly-terrain pipelines has been to divide the pipeline into various sections of constant slopes, and apply steady state flow models to simulate flow behavior in each section. However, the lack of understanding of how flow characteristics change when these sections are interconnected in hilly-terrain pipelines, prevents enhancing pipeline and downstream facility designs. Some of the most common problems hilly-terrain pipeline causes are operational problems, flooding of downstream facilities, severe pipe corrosion and structural instability of the pipeline, as well as production loss and poor reservoir management due to unpredictable wellhead pressures.

With the challenging field conditions, three-phase gas-oil-water flow becomes more common in oil production. The understanding of three-phase flow is crucial for flow assurance problems such as hydrates, emulsions and paraffin deposition. Corrosion and erosion also depend on the characteristics of three-phase flow in pipes. However, very limited amount of work on three-phase flow has been conducted due to the difficulties of oil-water and gas-liquid flow characterizations.

In the open literature, no studies addressing three-phase slug flow in hilly-terrain pipelines could be found. Since slug flow is such a frequently encountered flow pattern in three-phase flow, a study of slug characteristics for three-phase flow in hilly-terrain pipelines is very crucial for production and pipeline transportation. However, the complexity of slug flow increases from two-phase to three-phase flow. The increased complexity in slug flow necessitates transient solutions, supported by closure models. These closure models should focus especially on the phase distribution throughout the flow, and oil-water interactions, as well as the slug flow characteristics. In this study, these models will be examined and studied.

Experimental Study

Experimental Facility and Flow Loop

The experimental work is being conducted using the TUFFP facility for gas-oil-water flow located at the University of Tulsa North Campus Research Complex. The gas-oil-water facility was previously used by Atmaca (2007) for characterization of oil-water flow in inclined pipes. The facility consists of a closed circuit loop with storage tanks, progressive cavity pumps, heat exchangers, metering sections, filters, test section and separator.

For oil and water phases, there are two storage tanks equipped with valves to control the flow rates. Two progressive cavity pumps are used to maintain the liquid flow rates. There are manual bypass valves after the pumps to obtain low flow rates, and pressure relief valves for excessive pressure control. Copper-tube type heat exchangers are used to control the temperature of the fluid during the tests. After the heat exchangers, manual bypass valves allow the fluids to be pumped back to the respective tanks.

Two separate metering sections are equipped with Micro Motion™ Corriolis flow meters to measure mass flow rates and densities of the fluids, and with temperature transducers for monitoring the temperatures of the fluids. Oil and water flow through filters after the metering section. At the inlet of the test section gas, oil and water flow through the mixing tee to form the gas-oil-water three-phase co-current flow. After the fluids flow through the test section, the mixture is directed to the separator where pressure is set at 20 psig.

The test section is attached to an inclinable boom that makes inclined flow in the loop possible. However, during the three-phase hilly-terrain study, the boom will not be used and the part of the flow loop that is mounted on the boom stay horizontal.

Significant modifications were needed to flow loop to make enough space for the hilly-terrain section and instrumentation. The original gas-oil-water flow loop consisted of two 21.1-m (69.3-ft) long runs connected with a U-shaped bend to reduce the disturbance of the flow pattern due to a sharp turn. The current test section consists of a 21.1-m (69.3-ft) long upstream branch and a 46.7-m (153.2-ft) long downstream branch connected with a 1.2-m (4-ft) long U-shaped PVC bend as shown in Fig. 1. Both of the branches are made of transparent pipes with 50.8-mm (2-in.) diameter.

The upstream branch of the test section consists of a 13.8-m (45.3-ft) long flow developing section (L/D=272.0), two pressure drop sections 1.17-m (3.83-ft) and 2.79-m (9.3-ft) long, one long pressure drop section combining the two short sections, and one 3.1-m (10.2-ft) long fluid trapping section (L/D=108). The entire upstream branch is placed on the boom.

The downstream branch of the test section consists of a 13.8-m (45.3-ft) long flow developing section (L/D=272.0), a 6-m (19.7-ft) long horizontal section with two short pressure drop sections 4.2-m (14-ft) and 2.13-m (7-ft) long, in addition to a 21-m (68.9-ft) long hilly-terrain section (L/D=413.4) followed by a 6-m (19.7-ft) long horizontal section.

The hilly-terrain section simulates a hilly-terrain unit of 9.5 m (31.3 ft) downhill followed by a 1.9 m (6.2 ft) horizontal and 9.5 m (31.3 ft) uphill sections. The inclination angles are ±1°, ±2° and ±5° for the valley configurations.

The horizontal section immediately downstream of the hilly-terrain section was designed and built similar to the horizontal section immediately upstream of the hilly-terrain section.

The 21.1-m long section of the downstream branch is placed on the inclined boom as in the original gas-oil-water facility. The rest of the downstream branch, which is 25.6 m long, is supported by an aluminum base. Schematic diagram of the test section is given in Fig. 2.

Some hazards have been identified through a facility hazard analysis. Polycarbon protective glass is installed around the test section to provide protection in case of a rupture. In addition, the existing equipment such as pumps, flow meters, separator and storage tanks are checked and made operational.

Instrumentation and Data Acquisition

Capacitance sensors, quick closing valves temperature transducers, laser sensors, and pressure and differential pressure transducers are installed along the facility to measure the operating temperature, pressure, differential pressure, total liquid holdup and spatial distribution of the phases.

For data acquisition, Lab View™ 7.1 is used. New hardware, including a high speed data acquisition system is used for absolute and differential pressure transducers and laser and capacitance sensors. With

the instruments connected to high speed data acquisition system, slug flow characteristics are captured and compared more efficiently. For most of the test matrix, a sampling rate of 100 sample/s is found to be acceptable. For high flow rates, the sampling rate can be increased based on the three-phase slug characteristics. The existing program for the low speed data acquisition is updated for three-phase gas-oil-water flow in hilly-terrain studies. A sampling rate of 1 sample/s is selected to collect data for this data acquisition system. The data logging for each test is ten minutes.

Test Fluids

For the experiments of three-phase flow in a hilly-terrain pipeline, fresh water, air and refined mineral oil were chosen as the testing fluids. The refined oil, Tulco Tech 80, was chosen based on its easy separation. The physical properties of Tulco Tech 80 are given below:

- API gravity: 33.2°
- Density: 858.75 kg/m^3 @ 15.6°C
- Viscosity: 13.5 cp @ 40°C
- Surface tension: 29.14 dynes/cm @ 25.1°C
- Interfacial tension with water: 16.38 dynes/cm @ 25.1°C
- Pour point temperature: -12.2°C
- Flash point temperature: 185°C

The properties of Tulco Tech 80 were measured by Chevron labs. As shown in Figs. 3 and 4, the density and viscosity changes with temperature at three different flow rates were measured, respectively.

Experimental Ranges

In this study, 108 tests were conducted for three-phase air-oil-water flow in hilly-terrain pipelines with an inclination angle of ±5° for valley configuration. Although the facility can be modified to run at ±1°, ±2° and ±5° for the valley configurations, the inclination angle for the hilly-terrain unit is set to ±5˚ due to time constraints. This inclination angle is decided to observe the most significant changes in three-phase slug flow. The testing ranges for the three-phase hilly-terrain experiments on the gas-oil-water flow loop are as follows:

Superficial gas velocity: 0.1-5.0 m/s

Superficial oil velocity: 0.04-1 m/s

Superficial water velocity: 0.02-1 m/s

Water fraction: 20, 40, 60 and 80 %

The lower limits of superficial velocities were decided on by the accuracies of the Micro Motion™ flow meters. The higher limits were set by the pressure gradient and facility limits.

The test matrix was arranged in order to include both the flow regime transition from stratified to slug flow and the phase distributions from low water cut to high water cut. For each water cut value, twenty seven data points were taken.

The unified flow pattern maps showing the test matrix for inclination angles for 0˚,-5˚ and 5˚ are shown respectively in Figs. 5-7. The test matrix was selected such that slug flow would exist in the horizontal 2 in. pipe. It should be noted that these flow pattern maps were drawn for each section of the pipeline with a fixed inclination angle. In a hilly-terrain pipeline, the flow pattern in an upstream section may persist in a downstream section for a considerable distance, while the flow pattern prediction may be different.

The observed three-phase flow patterns based on the test matrix for this study are Intermittent-Stratified (IN-ST), Intermittent-Oil Continuous (IN-OC) and Intermittent-Water Continuous (IN-WC) as described in Keskin *et al.* (2007).

Experimental Results

Experiments on hilly-terrain effects on three-phase slug flow characteristics are conducted. Experimental data contains visual observations, differential pressure, average holdup, slug frequency and length.

Three-Phase Flow Patterns

Three-phase gas-oil-water slug flow experiments have been conducted for 20, 40, 60 and 80% water cuts at various flow rates. Three-phase flow patterns have been observed using the video system at the facility. Three-phase flow pattern maps for the horizontal section before hilly-terrain section are shown in Figs. 5-8. For the operational water cuts, slug dissipation at the downward inclined section is shown in Figs. 9–12. For the slug dissipation analysis, flow pattern maps are divided into three categories.

The first category, Complete Slug Dissipation, is the most common case. It is observed mainly at low and

moderate flow rates. In this category, slug flow completely dissipates along the downhill section of the hilly-terrain unit. Most of this category shows Intermittent-Stratified three-phase flow at the horizontal section before the hilly-terrain section. For the Partial Slug Dissipation region, as the second category, the slug flow still survives at downhill section. However, slug frequency decreases. For high superficial gas and liquid velocities slug flow is not affected significantly by the downward inclination. This region corresponds to No Hilly-Terrain Effect as the third region. For the second and third category, liquid phases mix and result in oil and water continuous cases based on the water cut. For the operational conditions and pipelined geometry, it has been observed that none of the Intermittent-Stratified cases at horizontal section before the hilly-terrain section could maintain slug flow at the downward inclined section.

The liquid accumulation at the elbow comes from the mass influx from the downhill section and backward flow from the uphill section, (Zheng, 1991). In the previous studies by Zheng and Al-Safran (2003) of two-phase hilly-terrain pipelines, the flow behavior at the elbow of the hilly-terrain section is coupled and analyzed with the flow conditions of the upstream downhill and downstream uphill sections of the hilly-terrain unit. Al-Safran identified five different cases of flow for slug dissipation at downhill pipe and slug initiation and growth at uphill section of the hilly-terrain section. The observed flow pattern cases based on these studies are (1) complete dissipation in the downhill section with slug initiation at the dip, (2) no hilly-terrain effect, (3) partial dissipation in the downhill section with initiation and growth at the dip, (4) no dissipation in the downhill section with initiation and growth at the dip and (5) no dissipation in the downhill section with growth only at the dip.

The first category is the most common case. In this category, due to the flow rates, slow moving slugs are observed in the horizontal section upstream of the hilly-terrain section. Slug flow completely dissipates along the downhill section of the hilly-terrain unit. Liquid fallback is observed, and there is liquid accumulation resulting in slug initiation at the elbow. This is mainly observed at low and moderate flow rates. As the gas flow rate increases, the hilly-terrain effect is suppressed because of the increased slug velocity. When the gas flow rate is increased to a certain velocity, highly aerated and foamy slugs are formed. Although these slugs are fast, the slug lengths are short. As they enter the downhill section, the segregation of the gas phase in the slug to the top of the pipe resulting in dissipation. Therefore category one is observed again for low v_{SL} and high v_{Sg} values.

The second category is when there is no slug dissipation at downhill section and slug initiation or growth at the elbow. This behavior is mainly observed in high liquid and low gas flow rates. Due to the high frequency and no slug dissipation, liquid accumulation can not be observed at the elbow. Therefore, there is not enough liquid for slug initiation or growth at the elbow.

For the third category, the slug flow survives at downhill section. However, slug frequency decreases in the downhill section. At the elbow section of the hilly-terrain unit, liquid accumulates and results in either slug initiation or slug growth of the surviving slugs based on the slug frequency at the downhill section of the hilly-terrain unit.

No dissipation in the downhill section with slug initiation and growth at the elbow is the fourth category. This behavior is generally observed at moderate liquid flow rates and both moderate and high gas flow rates. When the slugs are fast enough, no dissipation takes place in the downhill section. At the elbow slug initiation and growth takes place.

The category five is no dissipation at the downhill section and slug growth in the bottom elbow. This case is experimentally observed for moderate liquid flow rates. High slug frequency in the downhill section allows liquid accumulation at the elbow, which is picked up by a persistent slug before a slug is initiated.

The experimental data obtained in this study are compared with Al-Safran's flow pattern map. Out of the five categories defined by Al-Safran, only three are observed. The comparisons of the observed three-phase flow are shown in Figs. 9-12 for different water cuts. The figures illustrate the general trend of the category one which decreases with increasing v_{Sg} to a minimum value, then increases again at high v_{Sg}. This trend was also observed in Al-Safran's study. However, no hilly-terrain effect case could not be observed due to facility limits. The partial dissipation with initiation and growth category is observed for relatively higher superficial liquid velocities. The slight differences are speculated to be caused by the difference in liquid properties used in the testing. No dissipation with initiation and growth flow category could not be observed. In Al-Safran's study, this flow category's region was significantly reduced when the inclination angle was increased from 0.915° to 1.93°. Therefore, the disappearance

of this category with a ± 5° hilly-terrain unit corroborates with Al-Safran. The differences in liquid properties can again be speculated to be the reason for not being able to observe category five – no dissipation with growth only. It can shift this flow category's lower boundary to higher superficial liquid velocities.

When the comparisons with Al-Safran's flow categories and observed three-phase flow patterns are observed, no water cut effect is observed. It can be only speculated that water cut has the effect on the liquid viscosity for the dispersed cases which causes the shifts in flow patterns. However, no effect can be observed due to segregated water or slippage.

Pressure Gradient

The pressure gradients from the horizontal sections before and after hilly-terrain unit, downward and upward inclined sections of the hilly-terrain section are shown for low, moderate and high flow rates in Figs. 17-19. Figure 17 shows the pressure drop along the test facility for v_{SL} = 0.2 m/s and v_{Sg} = 0.1 m/s. Intermittent-stratified flow is observed for all of the water cuts at the upstream horizontal section. At the downward inclined section of the hilly-terrain unit, all of the slugs dissipated immediately. Due to gravity, pressure increases at the lower part of the downhill inclined section and positive pressure gradient is observed. At the upward inclined section, slugs are initiated and liquid fallback is observed. As it can be seen in Fig. 17, no discernible effect of water cut can be observed for low flow rates.

Liquid Holdup

The change in average water, total liquid holdup and in situ water cut for an operational case where superficial liquid and gas velocities are low are shown in Fig. 20. Oil and water phases are segregated and slugs dissipate completely at downhill section of hilly-terrain unit. The water and total liquid holdup decreases significantly at downhill section. At the elbow, they start to increase due to the liquid accumulation that is caused by liquid flowing from the downhill and liquid falling back from uphill sections of hilly-terrain section. Due to the initiated slugs, holdup values increase at the uphill sections. The in-situ water cut increases at the downhill sections and reaches a maximum value at the elbow. At the inclined sections water cut decreases back to 20%. Figure 21 shows the changes in average water holdup for different inlet water cuts. The trends of the water holdup are similar for the same operational conditions.

When the superficial velocities are increased, slug flow still exists at the downward inclined section. Therefore, the change in water holdup and water cut along the test section is less dramatic as shown in Fig. 22. Figure 23 shows the holdup trends with varying water cuts. The decrease in water holdup values at the downward inclined section is less severe due to the surviving slugs.

For moderate flow rates, water is completely dispersed in oil. There was no discernable change in water cut and water holdup values (Fig. 24). When the water cut values are increased for the operational conditions, the trend in water holdup values become more similar to previous cases due to the existence of segregated water layer flowing at the bottom of the pipe (Fig. 25).

Slug Frequency

The three-phase slug flow characteristics are investigated by using laser and capacitance sensors in addition to the cameras. The slug characteristics are measured with a sampling frequency of 100 Hz per sensor for time duration of 600 s to acquire statistical information. Due to the large amount of experimental data obtained by the laser and capacitance sensors, two Excel macro programs are developed and used to analyze the data automatically.

During the three-phase slug flow tests, it has been observed that air entrainment at the slug body increases with superficial gas velocity. The existence of the air bubbles in slug flow effects the performance of the sensors by creating jumps on the output signals. A disregard value is defined to filter these jumps from the output signals in the first Excel macro program. Before running the program for each test, the raw output signals are examined to determine voltage thresholds that are used to differentiate between the slug body and elongated bubble for each sensor output. It is found from the experimental results that the output signal for liquid slug region is higher than elongated bubble region for oil continuous flow. On the other hand, the output signal for elongated bubble region is higher that slug region for the experiments with water continuous flow. For oil continuous cases, the first macro then identifies the liquid slug region as "1" when the output signal is higher than the specified threshold value. When the output signal is lower, they are regarded as elongated bubble region and registered as "0". Based on this analysis, slugs are counted by the program. For the water continuous cases slug region is defined as "0" and elongated bubble region as "1". The rest of the analysis is similar to oil continuous cases. During the

signal process, slugs are assumed and analyzed as rectangles (horizontal lines) and film regions as horizontal lines (rectangles) for the oil (water) continuous case. As a final step, the macro determines slug frequency by dividing the number of slugs detected by the laser or capacitance sensors by the test duration and records the time that each slug passes from each sensor.

The time differences that the slug front and back takes to travel from one sensor to another are also detected and given as an output by the first Excel macro program. The time difference that is taken by a slug front and back to travel from one sensor to another is defined as Δt_f and Δt_b, respectively. Since the distance between each two sensors are known, slug front and back velocities can be calculated as

$$v_f = \Delta x / \Delta t_f \tag{1}$$

and

$$v_b = \Delta x / \Delta t_b \,, \tag{2}$$

respectively. Slug growth and dissipation can be analyzed with the relative magnitudes of the slug front and tail velocities to each other. No change in slug length (or frequency) can be observed if the slug front and tail velocities are similar to each other. Slug growth is observed in the cases where slug front velocity is bigger than the slug tail velocity. Slugs dissipate when the slug tail velocity is bigger than slug front velocity, and there is enough pipe length for the flow to be developed fully.

In the second Excel macro program, cross correlation technique is used to find critical time lag to calculate the slug translational velocity. The cross-correlation is a standard method to measure of the extent to which two signals (or series) correlate with each other as a function of the time displacement between them.

Consider two time series, x(tn) and y(tn), where n = 0 ,1 ,2 ,…, N-1. The cross-correlation coefficient is defined as:

$$R_{xy}(\tau) = \frac{C_{xy}(\tau)}{\sqrt{C_y(0)C_y(0)}} \,, \tag{3}$$

If the signals are identical, the cross correlation will be one, and if they are completely dissimilar, the cross correlation will be zero. In Eqs. 9 and 10, x(τ) and y(τ) are time series data when τ is the temporal lag. When the time series x(τ) and y(τ) are identical, the correlation coefficient is called auto-correlation coefficient,

$$C_{xy}(\tau) = \frac{1}{N-\tau}\sum_{n=1}^{N-\tau} x(t_n)\,y(\tau + t_n)\,. \tag{4}$$

$$C_x(0) = \frac{1}{N}\sum_{n=1}^{N} x(t_n)^2 = \overline{x^2}\,. \tag{5}$$

The critical time lag is defined by the value of τ where the cross correlation coefficient is maximum. Based on this analysis, the second Excel macro program finds the critical time lag and translational velocity for each test and for each sensor couples. The output signals from laser and capacitance sensors are used for cross-correlating between different pairs of laser sensors and capacitance sensors that are at the same segment of the test facility, i.e., between LSR1-LSR2, LSR3-LSR4, LSR5-LSR6, LSR5-LSR7, LSR8-LSR9 and CS3-CS4. Then, the translational velocity is easily calculated from the following equation and by the second program automatically:

$$v_t = \frac{\Delta L_{LS2 \to LS1}}{\tau}\,. \tag{6}$$

The time difference for a slug to travel from one sensor to another is defined as Δt_s and calculated by the first Excel macro program for each test. Slug length is calculated by multiplying translational velocity with Δts and can be expressed as:

$$l_s = \Delta t_s * v_t\,. \tag{7}$$

Figures 26-28 show the results of processed laser sensors' data along the test facility for various superficial gas and liquid velocities for 20 and 80% water cuts. Figure 13 shows the resultant frequency changes for the superficial gas velocity of 0.1m/s. This case shows effect of water cut at low superficial gas velocity. For all of the tests in this figure, intermittent-stratified three-phase flow is seen at the horizontal section before the hilly-terrain section. At the downward inclined section, complete slug dissipation is observed for all cases. With the beginning of upward inclined section, slugs are initiated with the liquid accumulation at the elbow section. However, most of the initiated slugs cannot survive until the end of upward inclined section and liquid fallback is observed. Therefore, at the upward inclined section, first an increase and then a decrease in slug frequency is observed. The decrease in frequency is observed to be at the higher parts of the upward inclined section for the higher liquid velocity. For the low operational conditions, water cut effect

on slug frequencies is not significant. However, the effect of water cut is more visible when superficial liquid velocity is increased.

Figure 27 shows the slug frequency along the test section for v_{Sg} = 1 m/s. For the tests with v_{Sg} = 1 m/s, water-in-oil and oil-in-water dispersions are observed for 20% and 80% water cut, respectively. For the superficial liquid velocities of 0.2 and 0.5 m/s, complete slug dissipation is observed. The slug frequency is observed to decrease at the downward inclined section for v_{SL}=1 m/s for both of the water cuts. At the upward inclined section, segregation of liquids is observed due to frequency. This results in difference in slug frequency between 20% and 80% water cuts. However, no significant difference in slug frequencies can be observed with respect to water for the rest of the flow conditions.

When superficial gas velocity increases, water cut effects start to become less significant. In Fig. 28, with the exception of the high superficial liquid velocity test for 20 % water cut, partial slug dissipation is observed at downward inclined section. For the upward section close to the elbow, slug frequency increases due to slug initiation. Slug frequency stays constant along the upward section due to the operational conditions. When the frequency values before and after the hilly-terrain sections are compared, the change in frequency is less significant than the tests with lower superficial gas velocities. For the test with v_{SL}=1 m/s with 20% water cut, three-phase slug flow maintains a constant frequency along the pipe which is not affected by the hilly-terrain geometry.

Translational Velocity

In two-phase flow mechanistic modeling, translational velocity can be obtained with a closure relationship. It is the sum of the bubble velocity in a stagnant liquid, i.e. the drift velocity, v_d, and the maximum velocity in the slug body. Nicklin *et al.* (1962) proposed an equation for translational velocity as,

$$v_t = C_O v_s + v_d \,. \qquad (8)$$

The flow coefficient, C_o is approximately the ratio of the maximum to the mean velocity of a fully developed velocity profile. The translational velocities were obtained by cross-correlating the output signals of the laser sensors.

Figures 29-33 illustrate the linear relationship between the measured translational velocity and the mixture velocity at different water cuts along the test section. As expected, translational velocity increases with increasing mixture velocity. The slope of the linear relationship is almost 1.2 for all cases except 20% water cut. It is checked that, most of the experiments are in turbulent flow regime in this study. For the cases with 20% water cut, experimental translational velocities are compared with translational velocities calculated with Nicklin's correlation for the pure oil and oil-water mixture. Figure 33 shows that the differing C_o value of translational velocities with 20% water cut are not due to the slug flow between air and pure oil phase.

Slug Length

Figure 34 shows mean slug lengths for v_{Sg} = 0.1 m/s at different superficial liquid velocities for 20% and 80% water cuts. The three-phase flow patterns for v_{SL} = 0.2 and v_{SL} = 0.5 m/s are IN-ST for 20% and 80% water cuts. Long slugs at the upstream horizontal section are observed. The slugs dissipate at downward flow. With liquid accumulation, slugs are initiated at the elbow. Slugs with W/O and O/W&W oil-water mixing status are generated due to slug initiation and liquid fallback at the upward inclined section for 20% and 80% water cut, respectively. At the beginning of the upward section, relatively shorter slug lengths are observed. There was no change in behavior with v_{SL} and water cut change. The effect of water cut can not be observed for the slug lengths since both of the flow patterns are dispersed which results in similar fluid properties. Most of the initiated slugs decay before reaching the top of the upward inclined section. The fallback liquid feeds the preceding slug and increases the slug length. However, slug growth and liquid fallback is a cyclic process which results in fluctuations in mean slug length. Long slugs are observed to survive from upward inclined section. Dispersed phases generated at uphill section segregates quickly. The slug lengths for v_{Sg} = 0.1 m/s do not show much water cut effect.

Figure 35 shows measurements for the mean slug length as a function of superficial gas velocity of v_{Sg} = 1 m/s for superficial liquid velocities ranging from 0.2 to 1 m/s for 20% and 80% water cuts. For the slug lengths at the upstream horizontal section, W/O and O/W dispersions are observed for 20% and 80% water cuts, respectively. However, no significant water cut effect can be observed. At the downward inclined section, for superficial liquid velocity of 1 m/s partial slug dissipation is observed. At the upward inclined section, mean slug lengths do not show any dependence to superficial liquid velocity

nor to water cut. At the downstream horizontal section, longer slugs are again observed.

Figure 36 illustrates mean slug lengths for v_{Sg} = 3m/s and v_{SL} = 1 m/s. At these superficial velocities, no dissipation with slug growth is observed at the hilly-terrain section. W/O and O/W dispersions are observed for 20% and 80% water cuts, respectively. The difference in slug lengths is due to the dispersion characteristics. At the upward inclined section, the difference in slug lengths between 20% and 80% water cuts is observed to diminish. Slug lengths are observed to increase for both of the water cut values. At the horizontal section downstream of the hilly-terrain unit, the slugs are relatively longer than the slug at the upstream horizontal section.

Modeling Study

As it is briefly discussed at the previous section, different cases of flow were identified for slug dissipation, initiation and growth along the hilly-terrain section (Al-Safran, 2003). As a first step to model three-phase effects on slug growth and initiation mechanisms, these flow cases will be improved by including the three-phase flow patterns. Experimental results for pressure gradients and average total liquid and water holdups at the upstream horizontal section of the hilly-terrain unit were compared with predictions by the TUFFP unified model.

Zhang *et al.* (2003-Part 1) developed a two-phase unified hydrodynamic model to predict flow patterns, pressure gradient and liquid holdup and slug characteristics in gas-liquid pipe flows for all inclination angles from -90° to 90° inclination angles. The model was based on the entire liquid film as the control volume. The continuity and momentum equations based on liquid film were used to predict flow pattern transitions from slug flow to other flow patterns. The model was also compared with extensive experimental data that included different pipe diameters, flow patterns, inclination angles, fluid physical properties, and gas-liquid flow rates. The comparisons showed very good agreement for both flow pattern and hydrodynamic behavior predictions.

Similar methodology was also applied to three-phase gas-oil-water flow. A three-phase unified model was developed by Zhang and Sarica (2006). Some of the closure relationships for two-phase flow such as gas-liquid interfacial friction factor, liquid entrainment fraction in the gas core, gas void fractions in oil and water in the slug body, slug translational velocity and length were also used with necessary modifications. Experimental validation showed that three-phase unified model performs successfully.

Statistical parameters are used to evaluate the performance of the pressure gradients and holdup predictions by the unified model. These parameters are calculated from two types of errors, relative and actual errors. The relative and actual errors are expressed in Eqs. 2 and 3, respectively.

$$e_{ri} = \left(\frac{q_{i\,Cal} - q_{i\,Mea}}{q_{Mea}} \right) \times 100 . \qquad (9)$$

$$e_i = q_{i\,Cal} - q_{i\,Mea} . \qquad (10)$$

Based on the relative and actual errors, six statistical parameters are defined in Eqs. 4 - 9.

Average percentage relative error is

$$\varepsilon_1 = \left[\frac{1}{N} \sum_{i=1}^{N} e_{ri} \right] . \qquad (11)$$

Average absolute percentage relative error is

$$\varepsilon_2 = \left[\frac{1}{N} \sum_{i=1}^{N} \left| e_{ri} \right| \right] . \qquad (12)$$

Standard deviation about average relative error is

$$\varepsilon_3 = \sqrt{\frac{\sum_{i=1}^{N} \left(e_{ri} - \varepsilon_1 \right)^2}{N-1}} . \qquad (13)$$

Average actual error is

$$\varepsilon_4 = \frac{1}{N} \sum_{i=1}^{N} e_i \qquad (14)$$

Average absolute actual error is

$$\varepsilon_5 = \frac{1}{N} \sum_{i=1}^{N} \left| e_i \right| \qquad (15)$$

Standard deviation about average actual error is

$$\varepsilon_6 = \sqrt{\frac{\sum_{i=1}^{N} \left(e_i - \varepsilon_4 \right)^2}{N-1}} . \qquad (16)$$

where N is the number of data points.

The average percentage relative error, ε_1 and the average actual error, ε_4 are to measure the agreement

between the predicted and measured parameters. The parameter is overestimated if these average errors are positive, and underestimated if they are negative. Individual errors can be either positive or negative, and can cancel each, masking the true performance. The average absolute percentage relative error, ε_2, and the average absolute actual error, ε_3, eliminate the masking effect and indicate how large the errors are on the average. The standard deviations, ε_3 and ε_6, indicate the degree of scattering with respect to their corresponding average errors, ε_1 and ε_4. The TUFFP unified mechanistic model was evaluated with 105 pressure gradient and liquid holdup data of this study with various water cuts.

Table 1 shows the statistical analysis for evaluation of the unified model for pressure gradient. The TUFFP unified model produced positive values of ε_1 and ε_4, indicating overestimation of the pressure gradient. When the data is compared against the TUFFP unified model, the average percentage relative and actual errors are 28% and 32 Pa/m, respectively.

The model evaluation results for average total liquid holdup are shown in Table 2 for the unified model. The TUFFP unified model again produced positive values of ε_1 (17%) and ε_4 (0.10), indicating overestimation of the liquid holdup. When the average water holdup dataset was compared against the unified model, the average percentage relative and actual errors are 32% and 0.07, respectively.

Comparisons of the data with unified model showed good agreement. Considering the unified model's good performance, unified model results were used to generate oil-water mixture fluid properties to be used in the two-phase slug dissipation model by Zhang *et al.* (2003-Part 1).

The model developed by Zhang *et al.* (2003-Part 1) was used to model two-phase slug dissipation and generation in hilly-terrain pipelines. The model was developed from unsteady continuity and momentum equations for two-phase flow.

Figures 37-39 show the comparison of the slug dissipation model with the experimental three-phase slug flow in hilly-terrain facility.

The resulting models will be validated with experimental data and compared with a multiphase flow simulator, OLGA®.

Near Future Activities

The final report will be submitted by May 2010.

References

Al-Safran. E.: "An Experimental and Theoretical Investigation of Slug Flow Characteristics in the Valley of a Hilly Terrain Pipeline," Ph.D. Dissertation, U. of Tulsa, Tulsa, OK (2003).

Keskin, C., Zhang, H.Q., Sarica, C.: "Identification and Classification of New Three-Phase Gas/Oil/Water Flow Patterns," SPE 110221, presented at SPE ATCE, Anaheim, California (2007).

Taitel, Y. and Barnea, D.: "Slug Tracking in Hilly Terrain Pipelines," Paper Presented in SPE ATCE, Houston, TX (1999).

Zhang, H.-Q., Al-Safran, E., Jayawardena, S., Redus, C., Sarica, C. and Brill, J.: "Modeling of Slug Dissipation and Generation in Gas-Liquid Hilly-Terrain Pipe Flow," ASME J. Energy Res. Tech., vol. 125, pp. 161-168 (2003).

Zhang, H.-Q. and Sarica, C.: "Unified Modeling of Gas/Oil/Water Pipe Flow – Basic Approaches and Preliminary Validation," SPE 95749, presented at SPE ATCE, Dallas, TX (2005).

Zhang, H.-Q., Wang, Q., Sarica, C. and Brill, J.P.: "Unified Model for Gas-Liquid Pipe Flow via Slug Dynamics-Part 1: Model Development," ASME J. Energy Res. Tech., vol. 125 (4), pp.266 (2003).

Zhang, H.-Q., Yuan, H., Redus, C.L., and Brill, J.P.: "Observation of Slug Dissipation in Downward Flow," presented at ETCE/OMAE 2000, New Orleans, February, 14-17, 2000.

Zheng, G.: "Two-Phase Slug Flow in Hilly-Terrain Pipelines," Ph.D. Dissertation, U. of Tulsa, Tulsa, OK (1991).

Table 1: TUFFP Model Evaluation Using the Present Study Pressure Gradient Data

Parameter	Statistical Parameters					
	ε_1	ε_2	ε_3	ε_4	ε_5	ε_6
Pressure Gradient	28	34	31	32	36	35

Table 2: TUFFP Model Evaluation Using the Present Study Total Liquid and Water Holdup Data

Parameter	Statistical Parameters					
	ε_1	ε_2	ε_3	ε_4	ε_5	ε_6
Total Liquid Holdup	17	30	31	0.10	0.15	0.14
Water Holdup	23	32	29	0.06	0.07	0.09

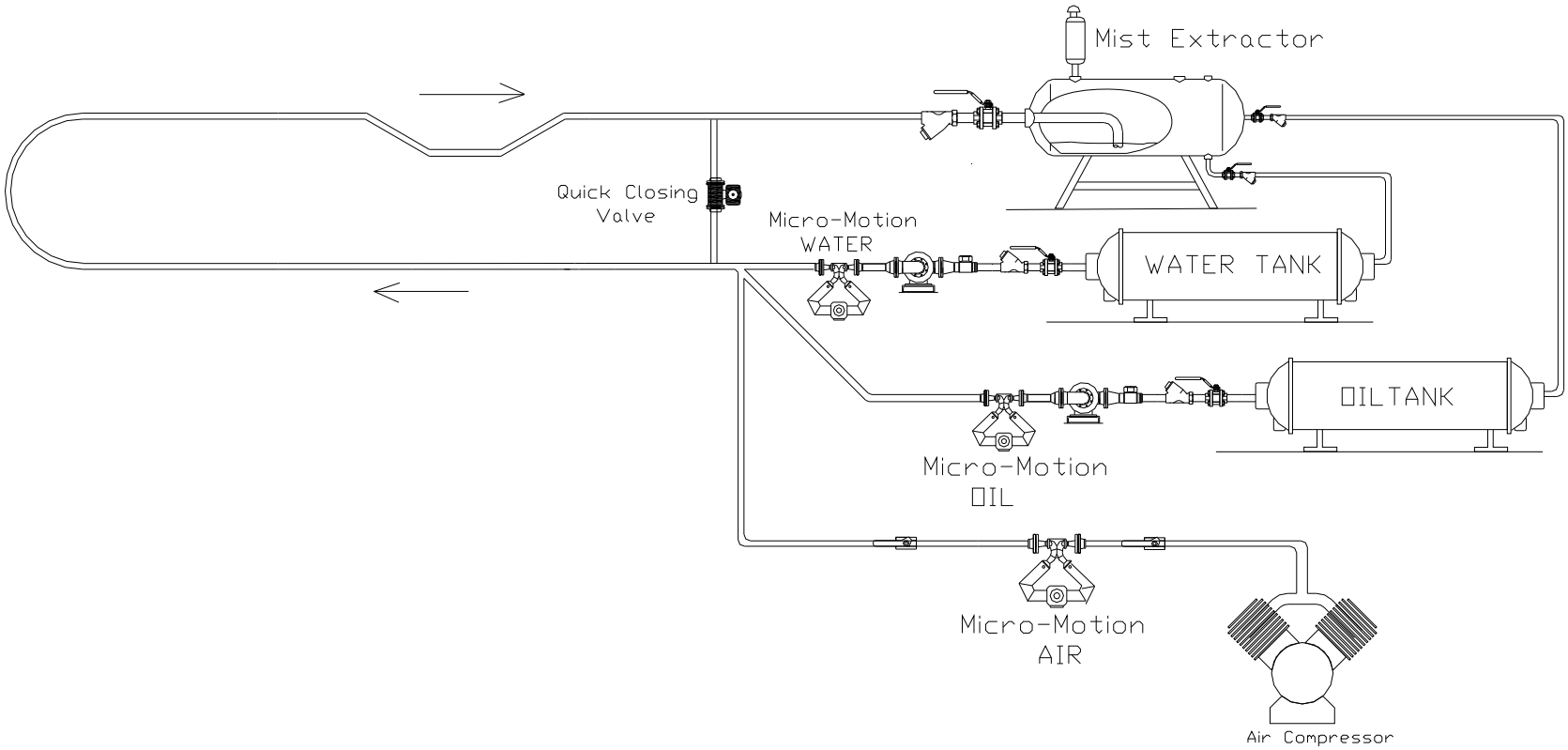

Figure 1: Gas-Oil-Water Facility Schematic

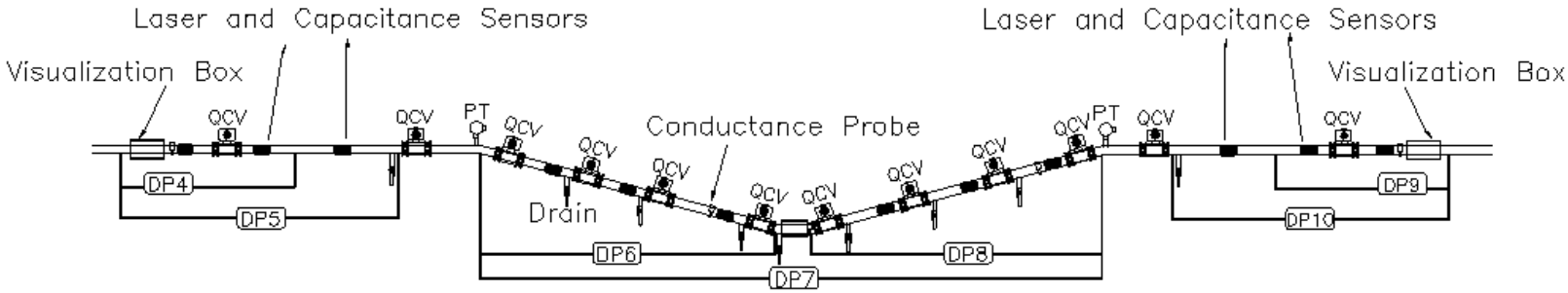

Figure 2: Schematic of Downstream Branch of Test Section

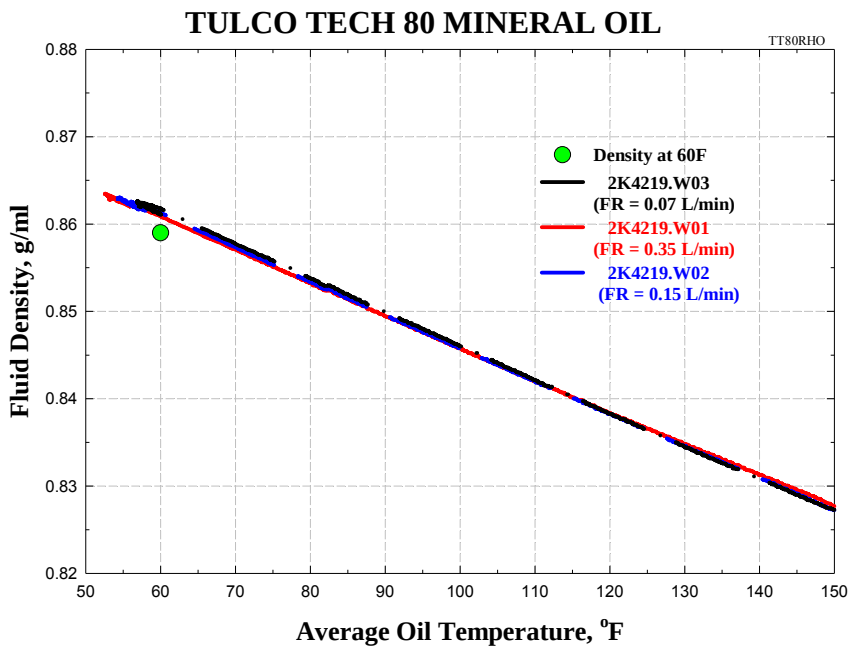

Figure 3: Tulco Tech 80 Oil Density vs. Temperature

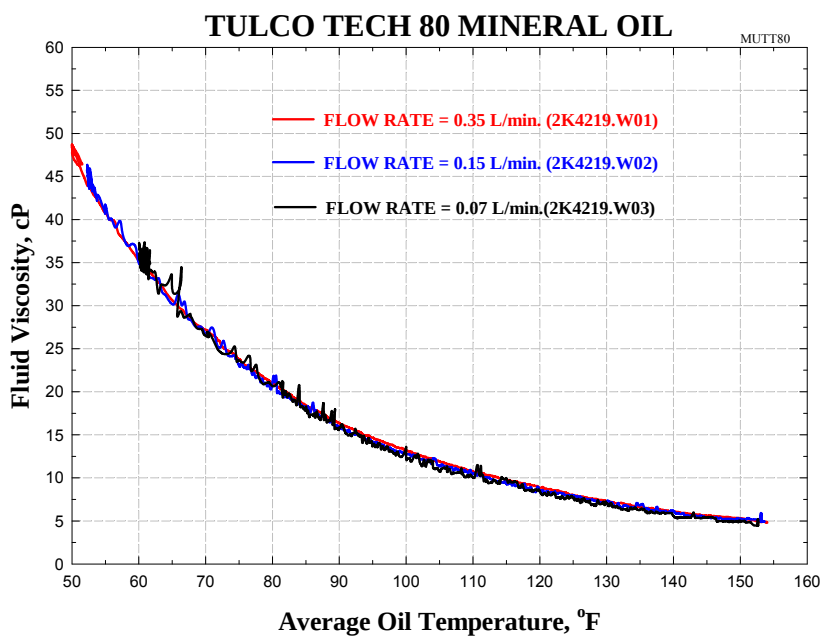

Figure 4: Tulco Tech 80 Oil Viscosity vs. Temperature

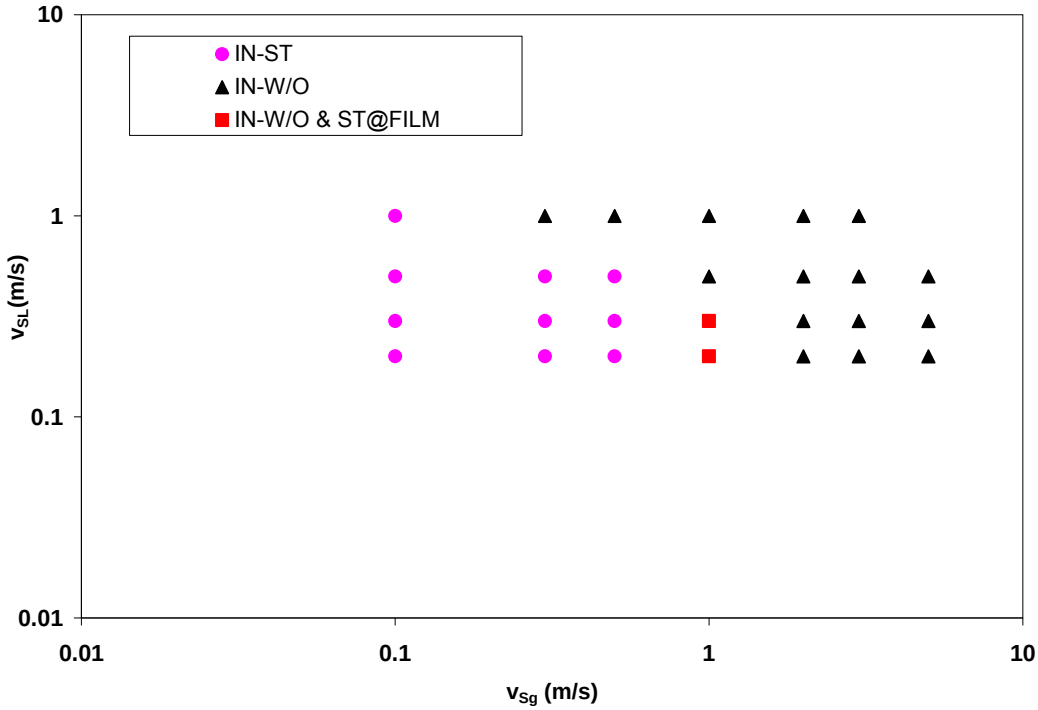

Figure 5: Horizontal Gas-Oil-Water Flow Pattern Map for 20% Water Cut

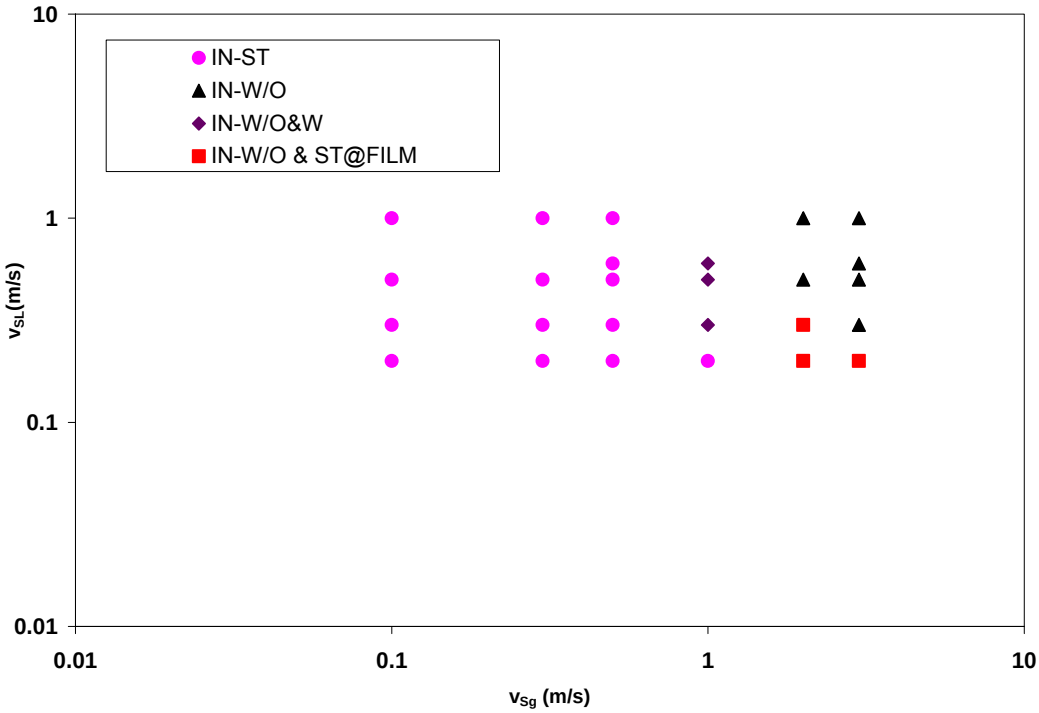

Figure 6: Horizontal Gas-Oil-Water Flow Pattern Map for 40% Water Cut

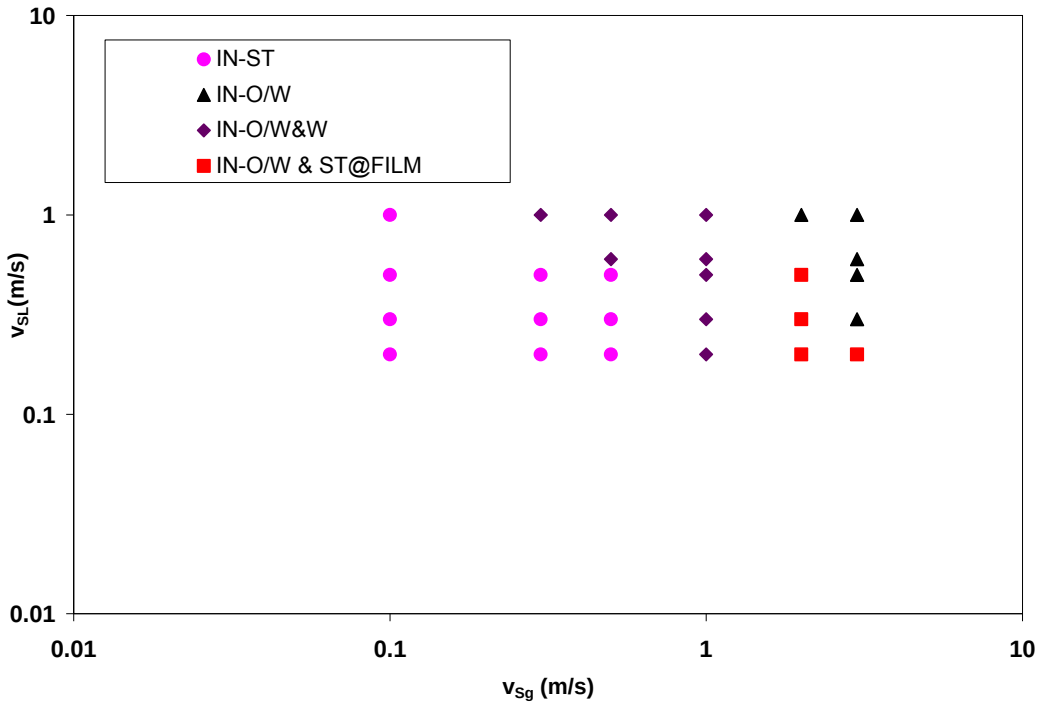

Figure 7: Horizontal Gas-Oil-Water Flow Pattern Map for 60% Water Cut

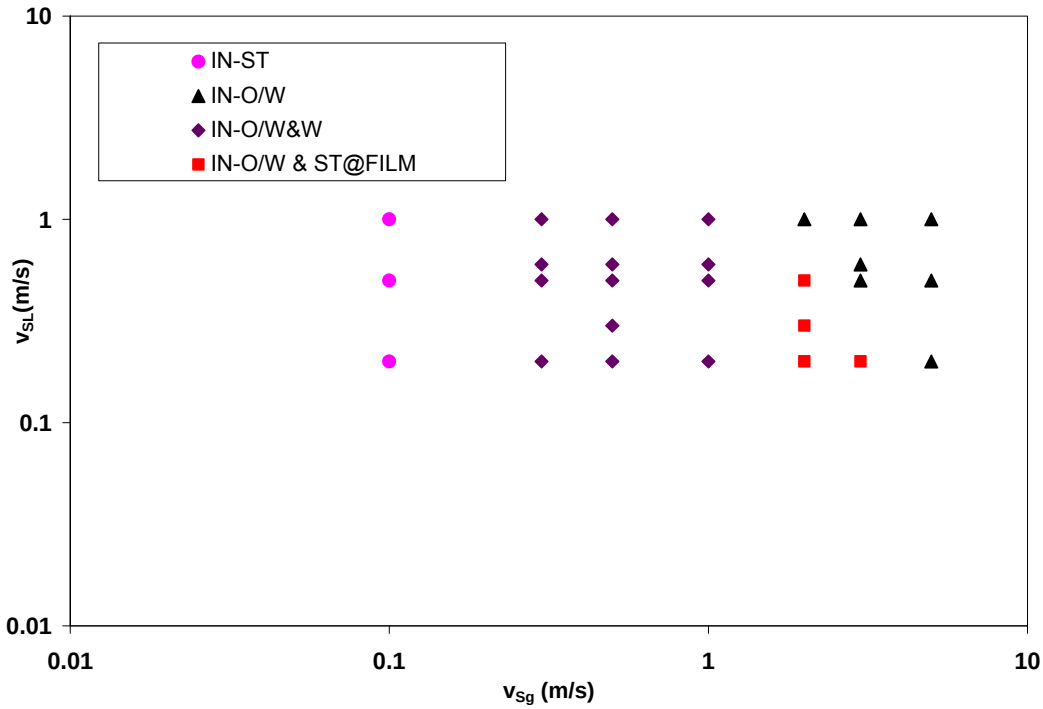

Figure 8: Horizontal Gas-Oil-Water Flow Pattern Map for 80% Water Cut

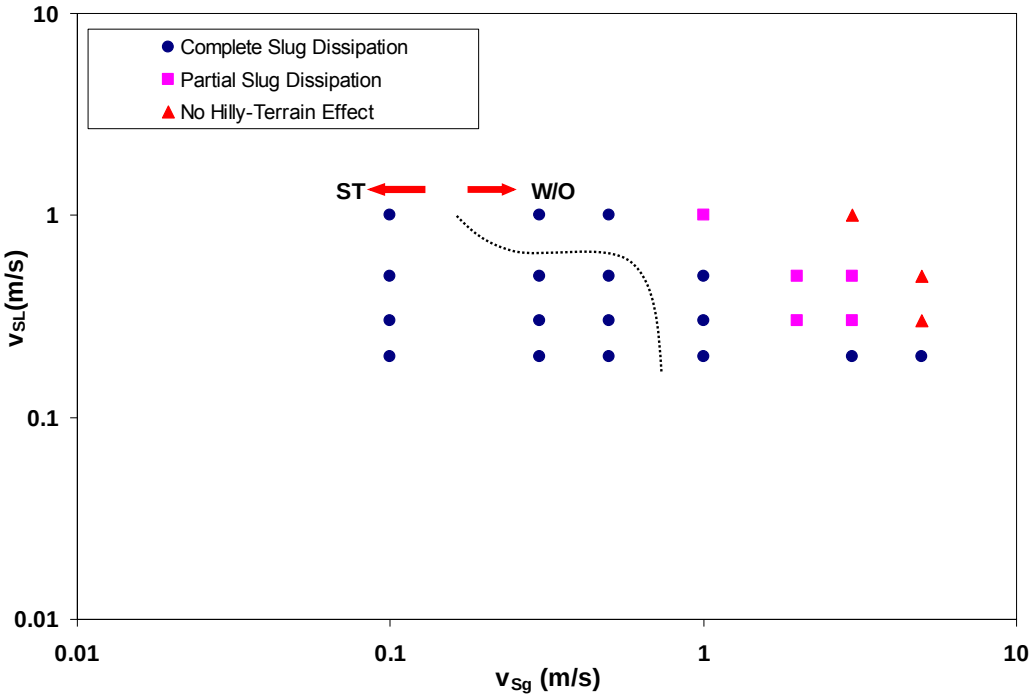

Figure 9: Slug Dissipation at the Downward Inclined Section for 20% Water Cut

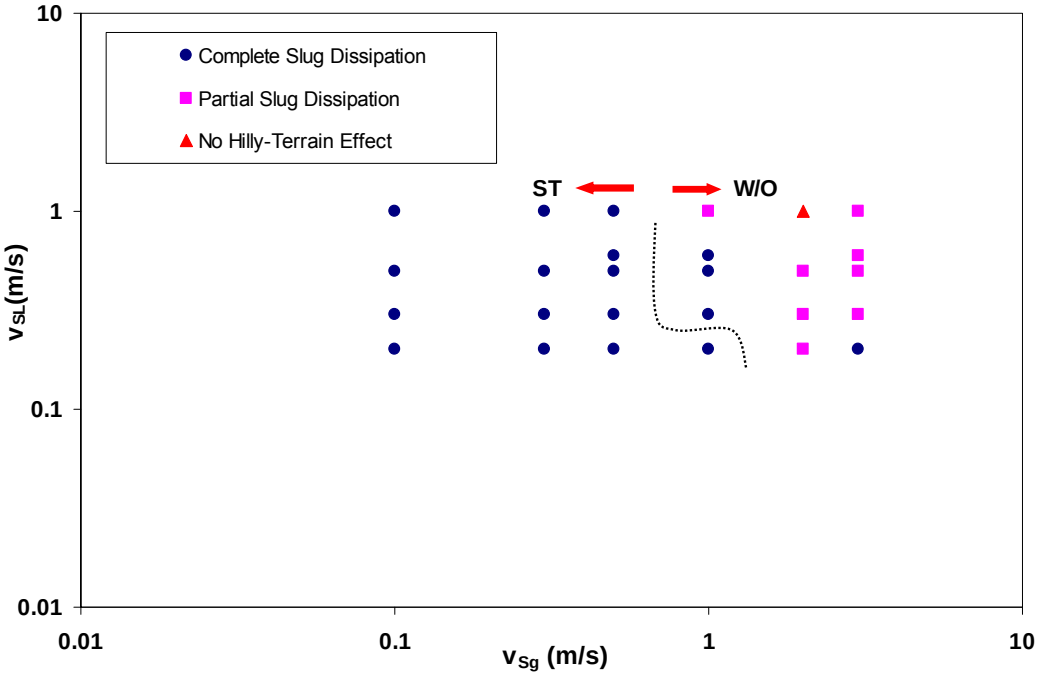

Figure 10: Slug Dissipation at the Downward Inclined Section for 40% Water Cut

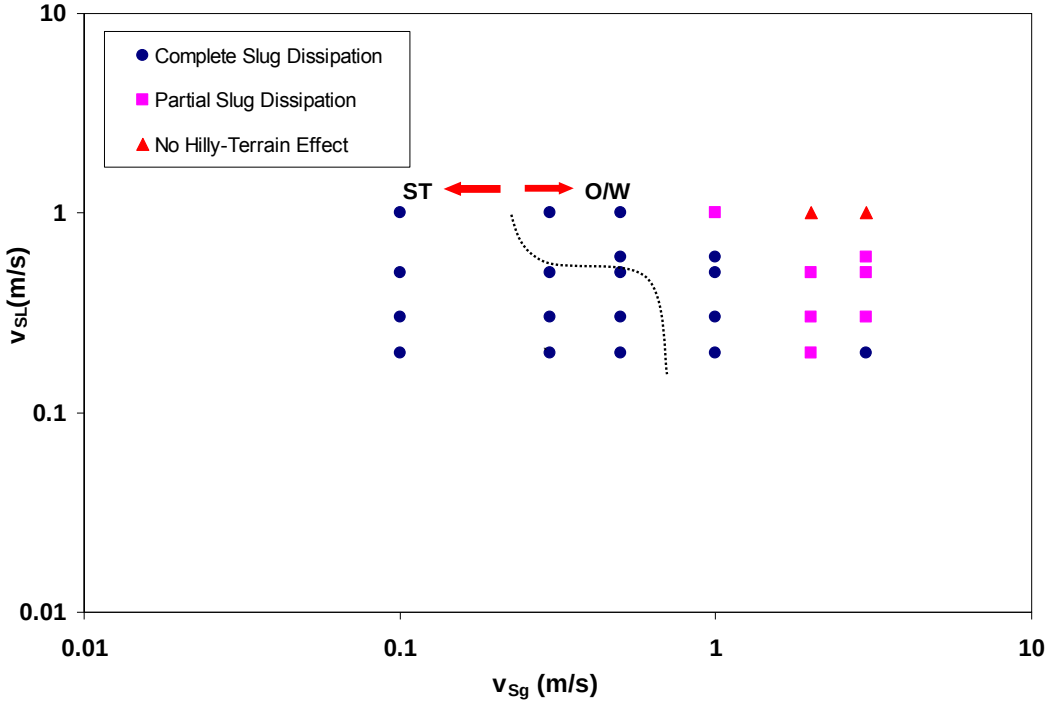

Figure 11: Slug Dissipation at the Downward Inclined Section for 60% Water Cut

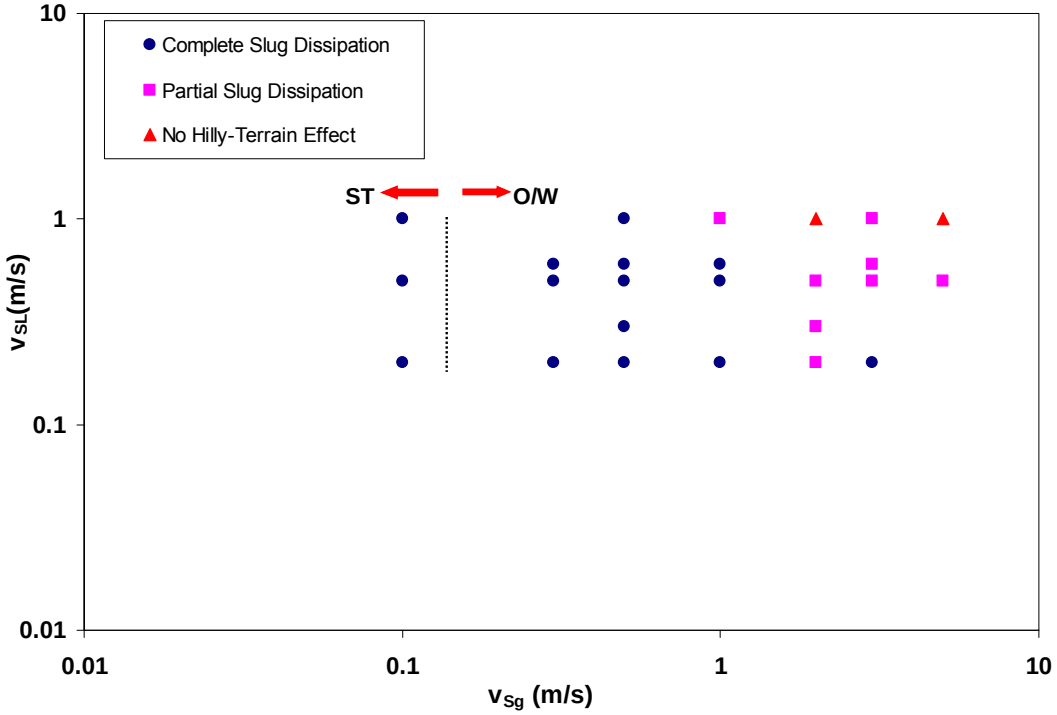

Figure 12: Slug Dissipation at the Downward Inclined Section for 80% Water Cut

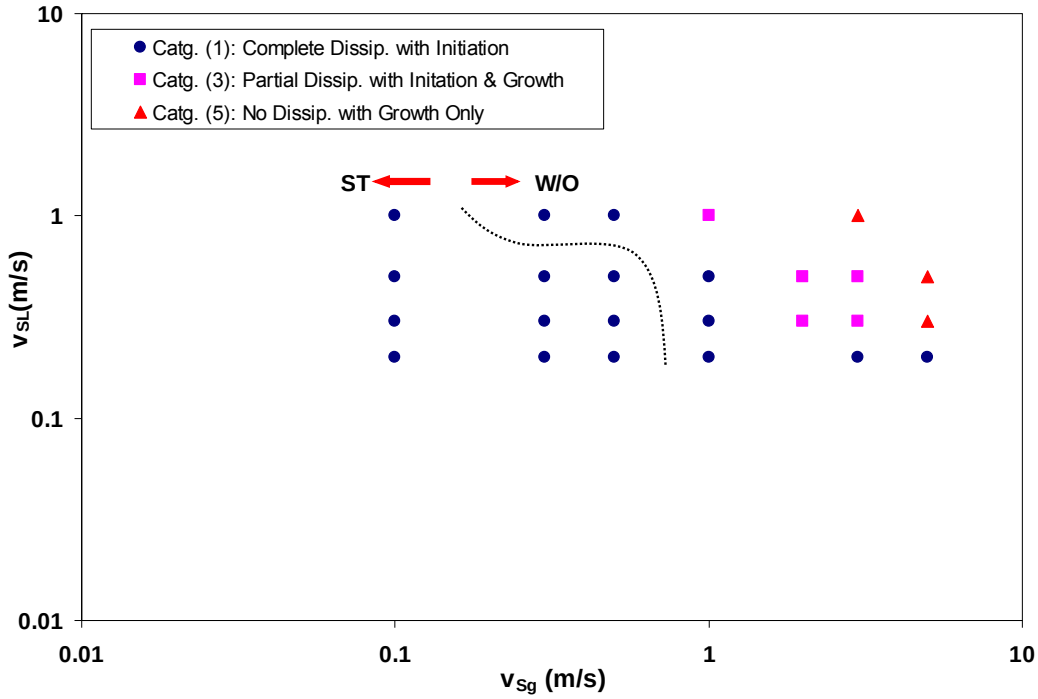

Figure 13: Hilly-Terrain Flow Behavior Map for 20% Water Cut

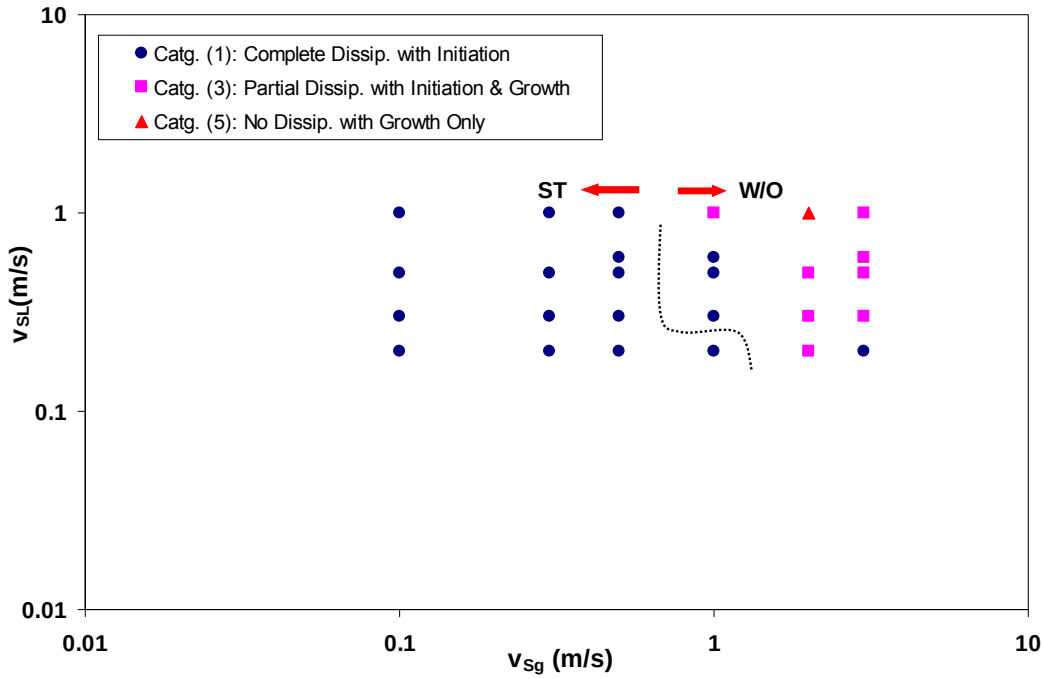

Figure 14: Hilly-Terrain Flow Behavior Map for 40% Water Cut

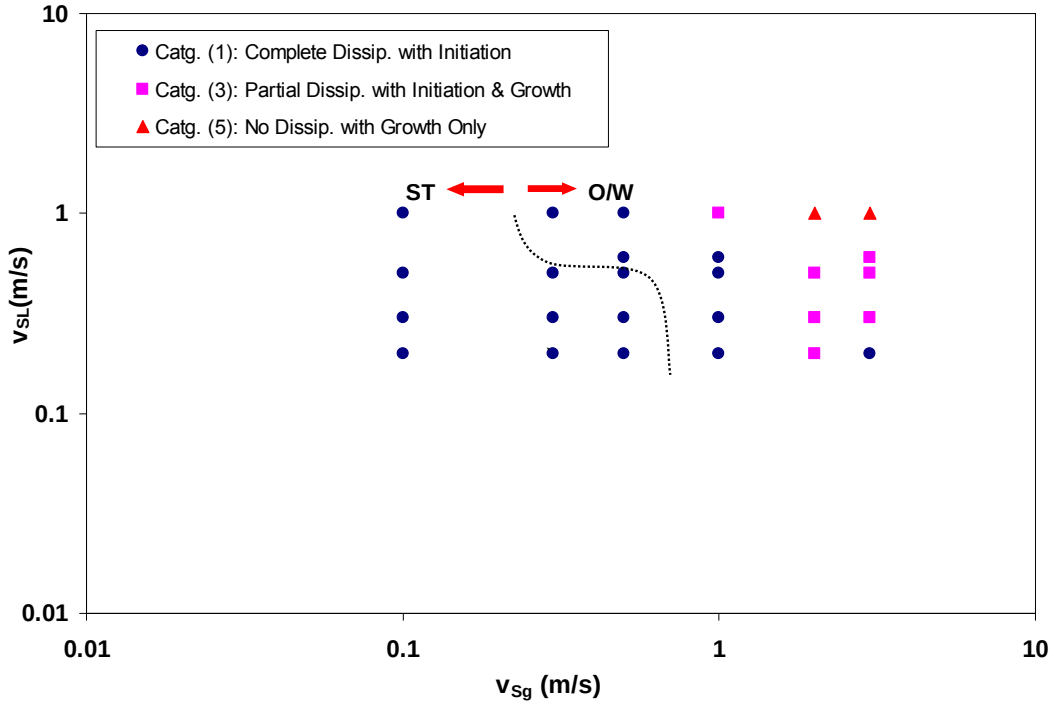

Figure 15: Hilly-Terrain Flow Behavior Map for 60% Water Cut

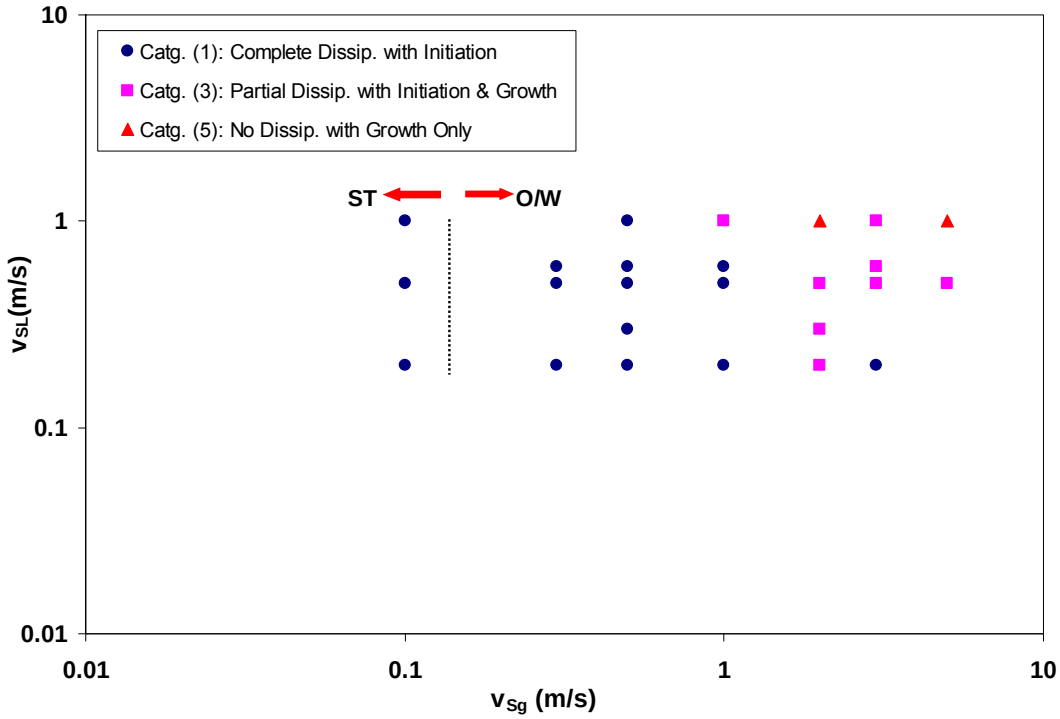

Figure 16: Hilly-Terrain Flow Behavior Map for 80% Water Cut

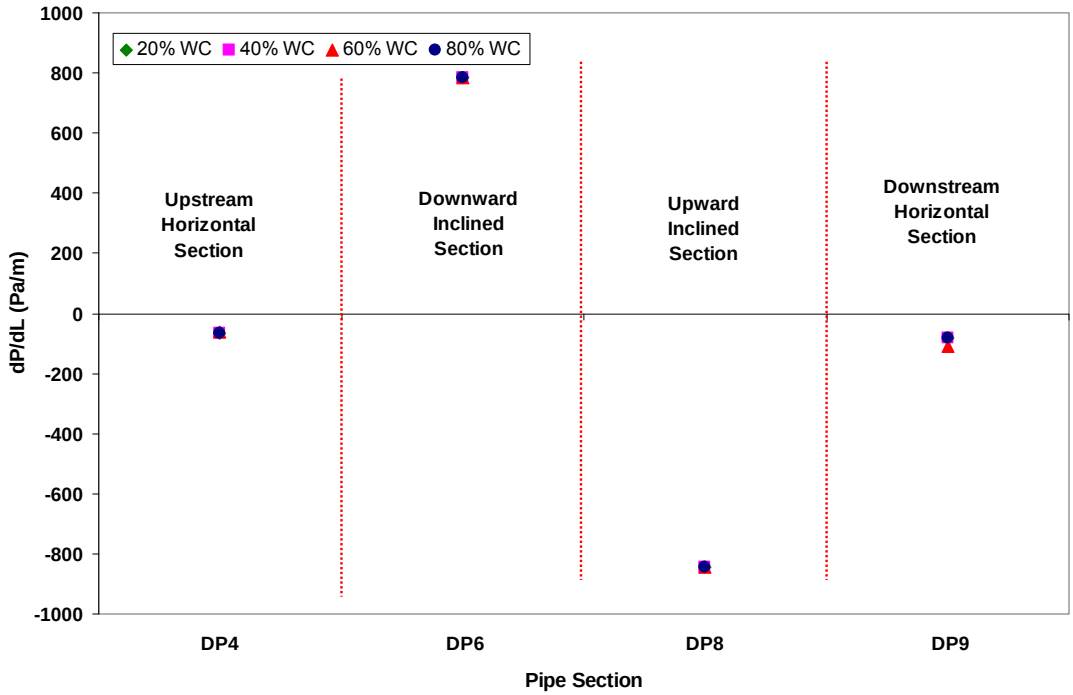

Figure 17: Pressure Gradient along the Test Section for v_{SL} = 0.2 m/s and v_{Sg} = 0.1 m/s

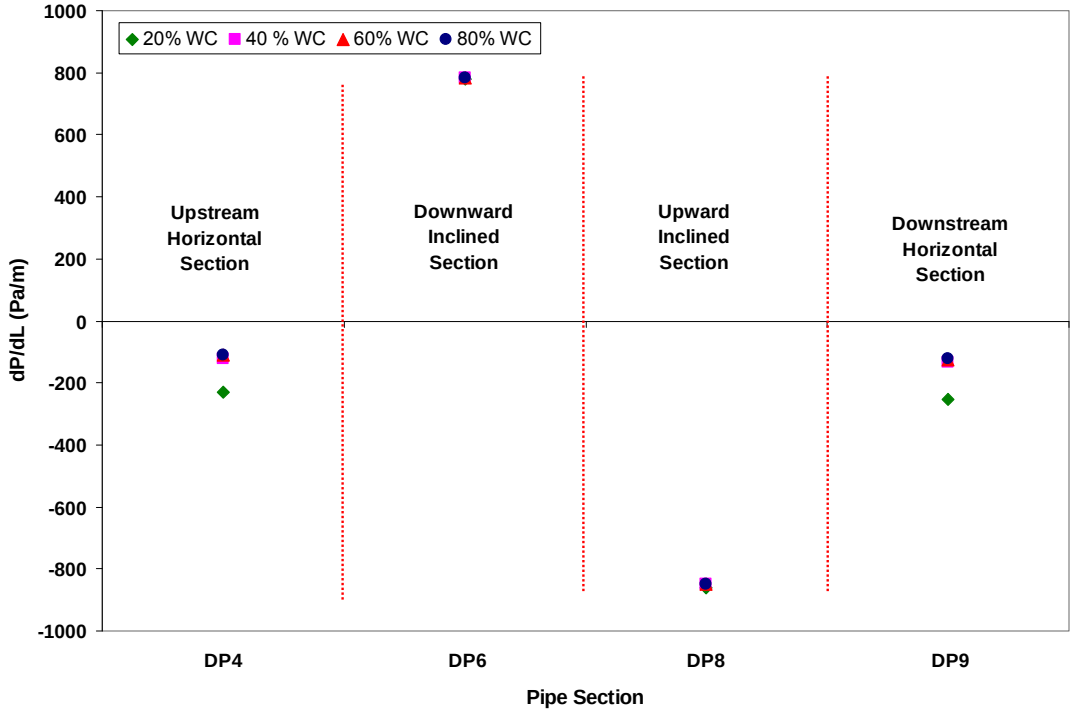

Figure 18: Pressure Gradient along the Test Section for v_{SL} = 1 m/s and v_{Sg} = 0.5 m/s

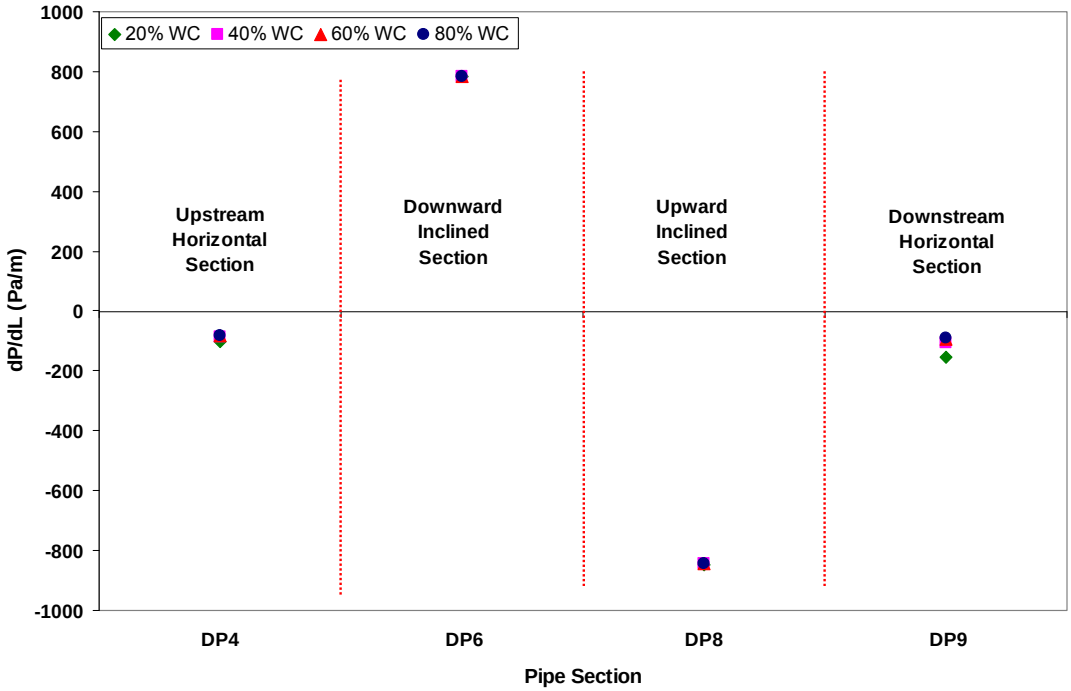

Figure 19: Pressure Gradient along the Test Section for v_{SL} = 0.3 m/s and v_{Sg} = 2 m/s

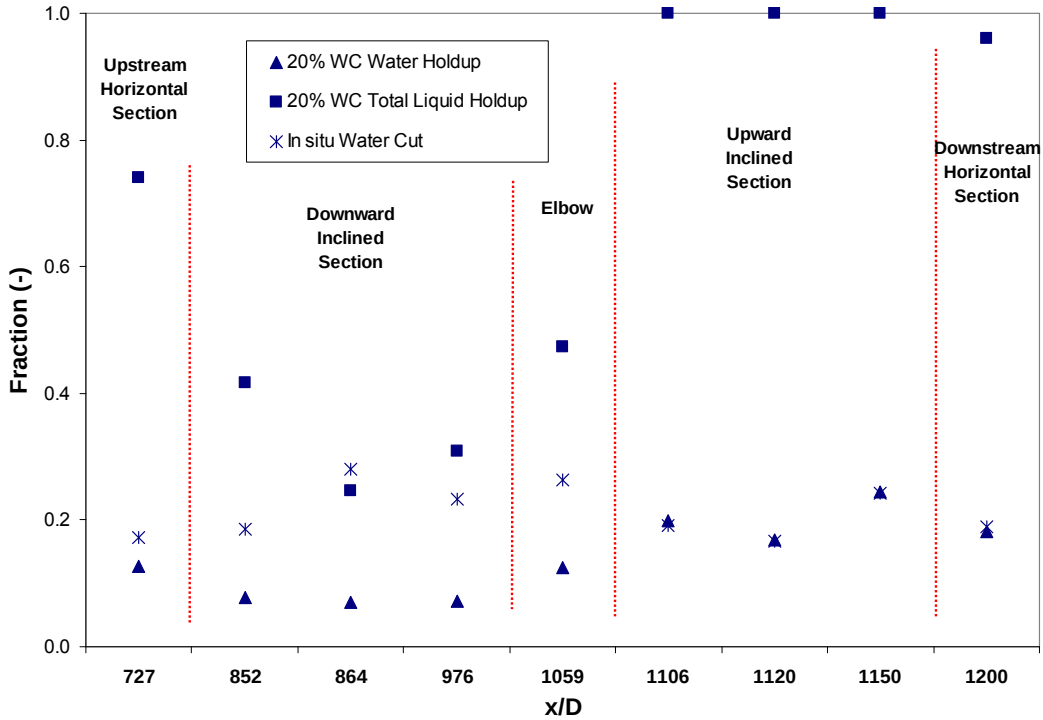

Figure 20: Liquid Fraction Values for v_{SL} = 0.5 m/s and v_{Sg} = 0.1 m/s at 20% Water Cut

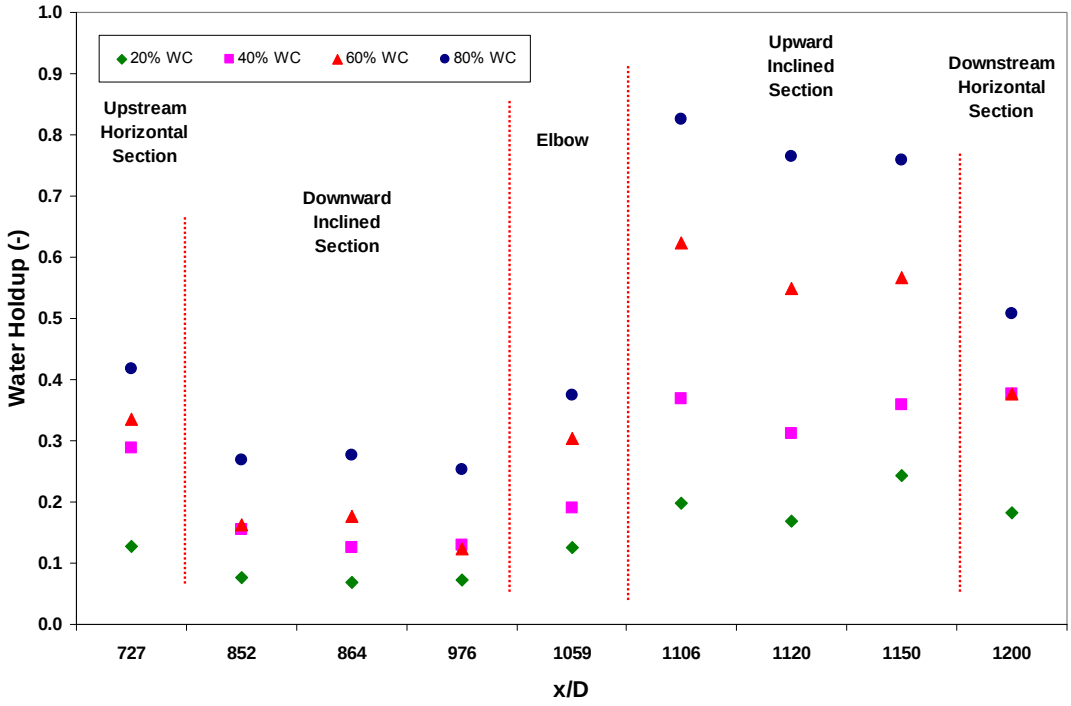

Figure 21: Water Holdup Values for v_{SL} =0.5 m/s and v_{Sg} =0.1 m/s

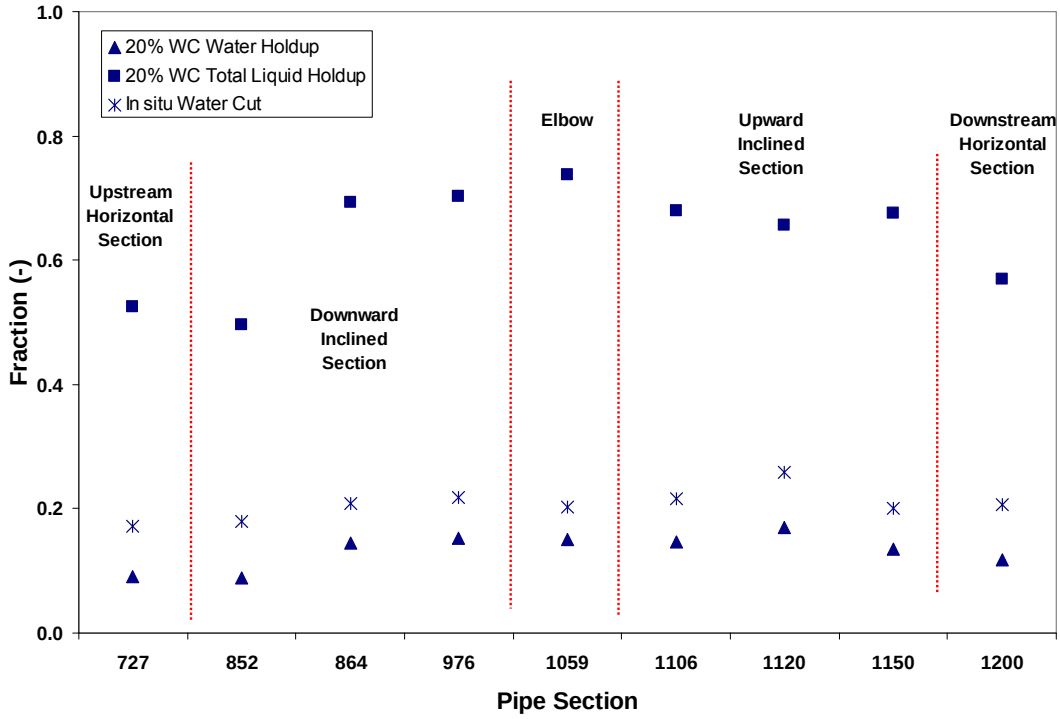

Figure 22: Liquid Fraction Values for v_{SL} = 1 m/s and $v_{S}g$ = 1 m/s at 20% Water Cut

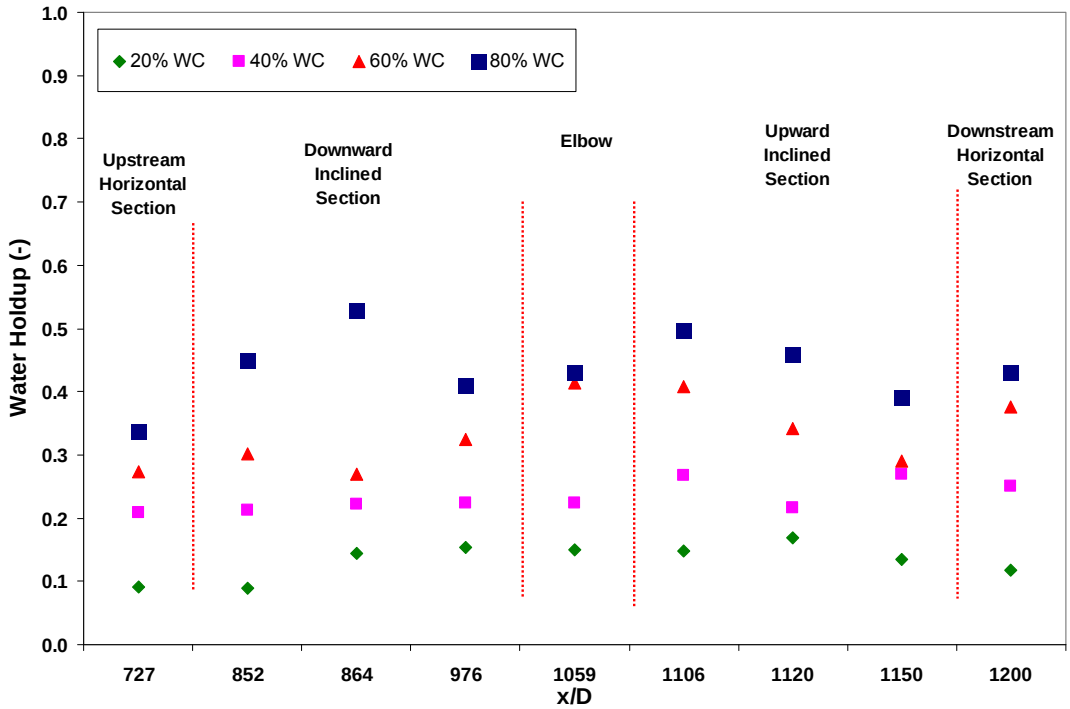

Figure 23: Water Holdup Values for v_{SL} = 1 m/s and v_{Sg} =1 m/s

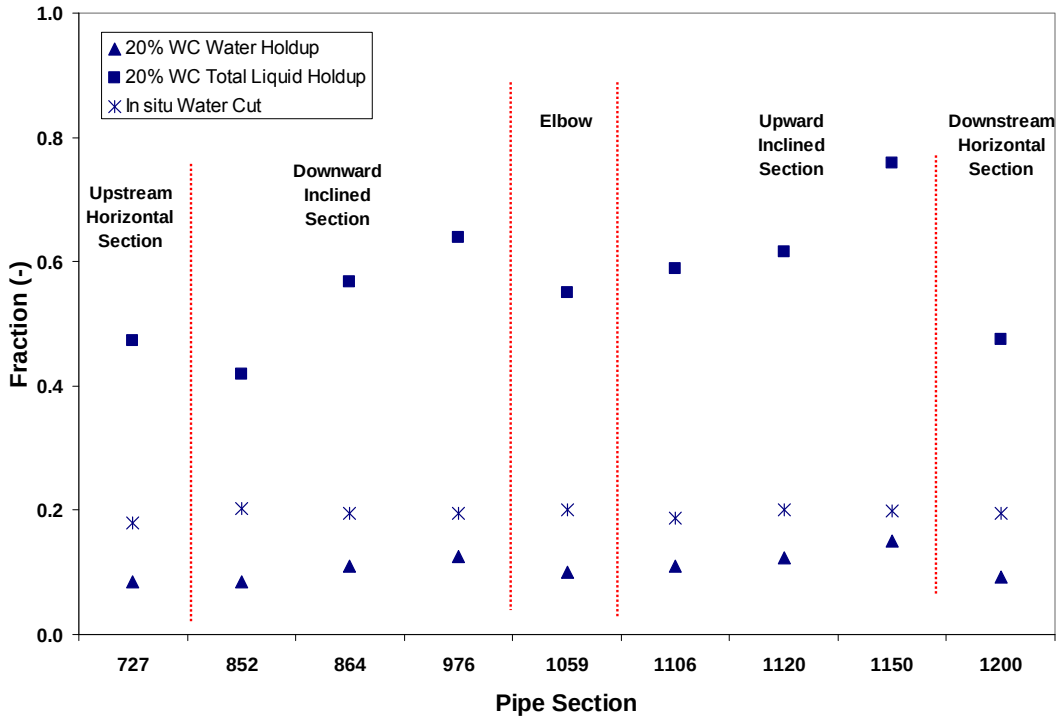

Figure 24: Liquid Fraction Values for v_{SL} = 1 m/s and v_{Sg} = 2 m/s at 20% Water Cut

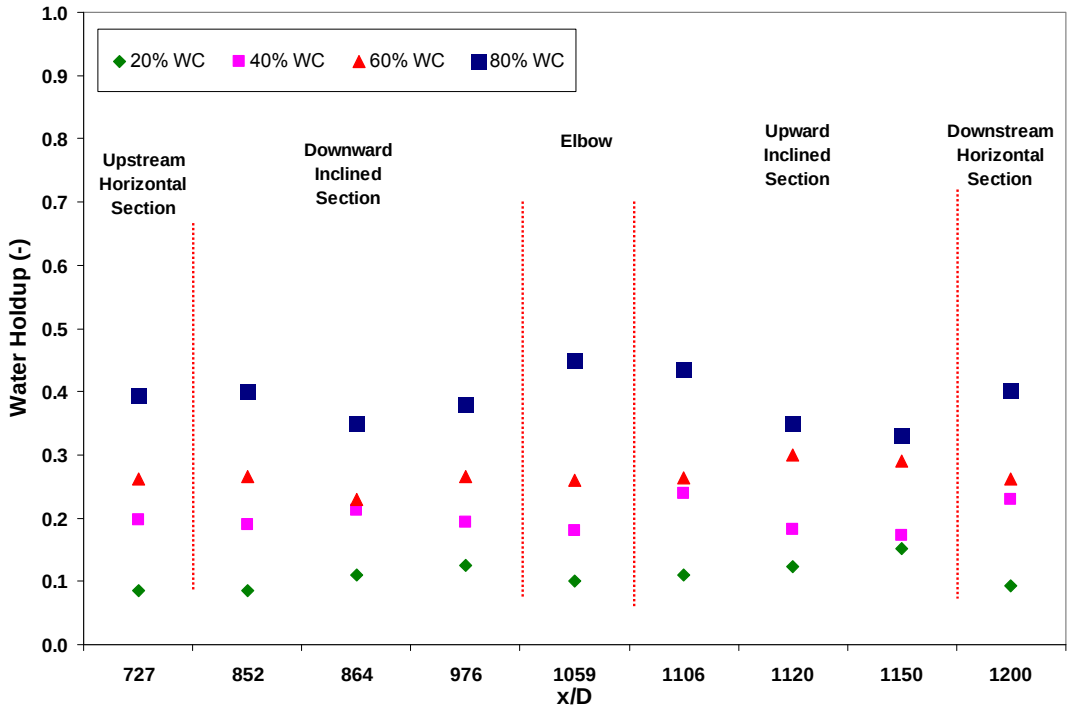

Figure 25: Water Holdup Values for v_{SL} = 1 m/s and v_{Sg} = 2m/s

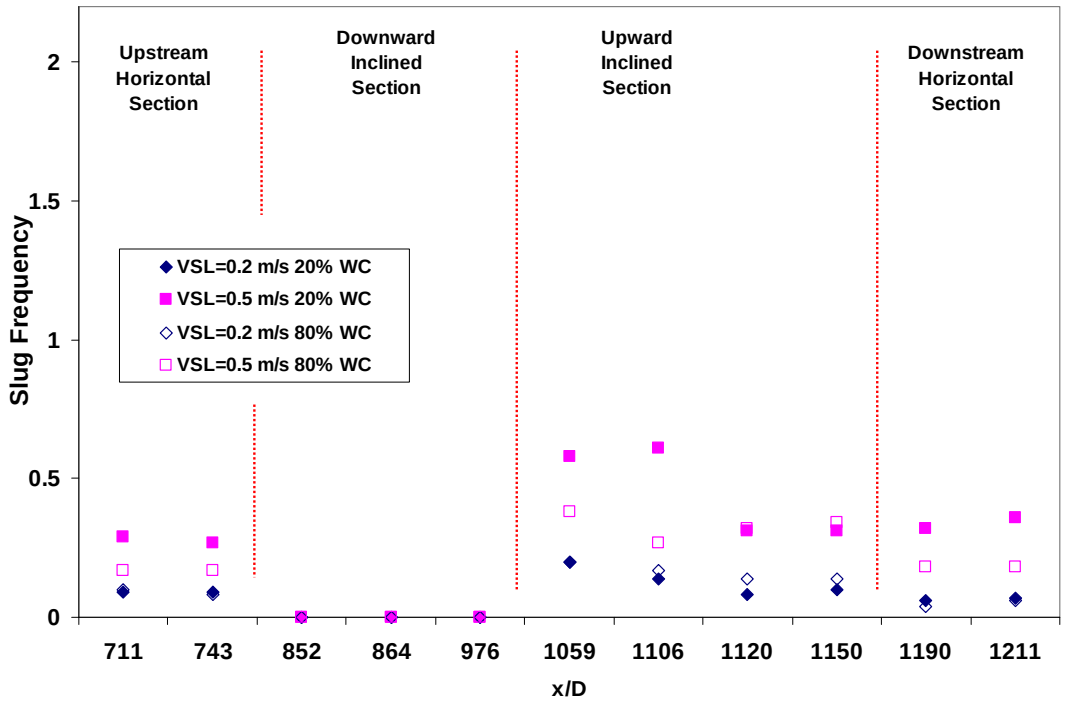

Figure 26: Slug Frequency for v_{Sg} = 0.1 m/s for 20 and 80% Water Cuts

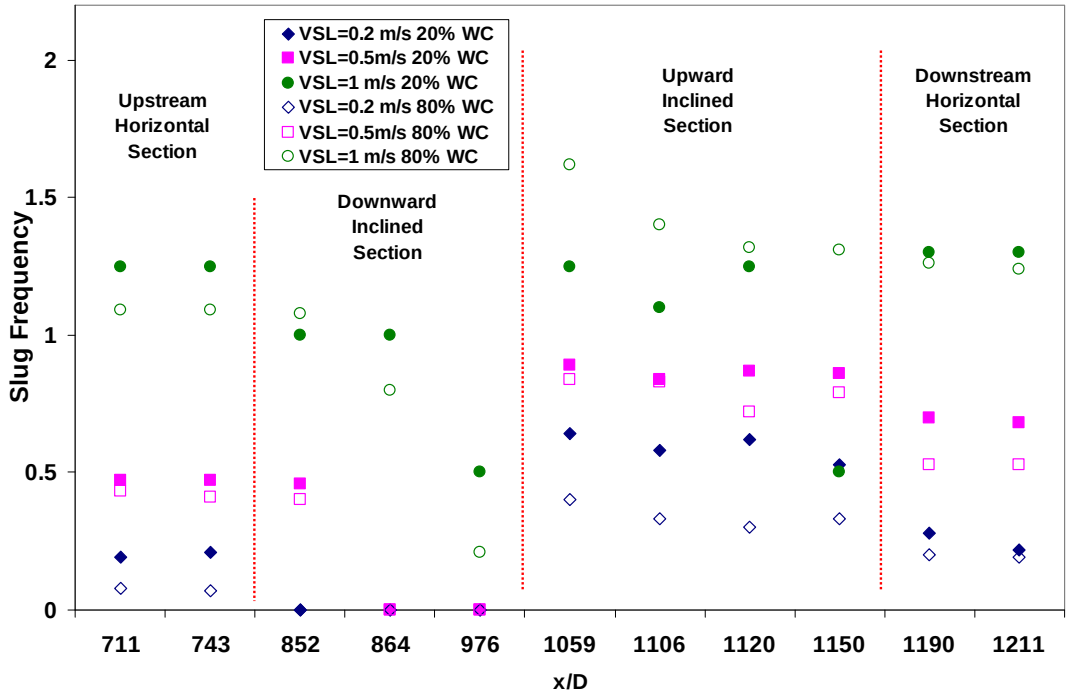

Figure 27: Slug Frequency for v_{Sg} = 1 m/s for 20 and 80% Water Cuts

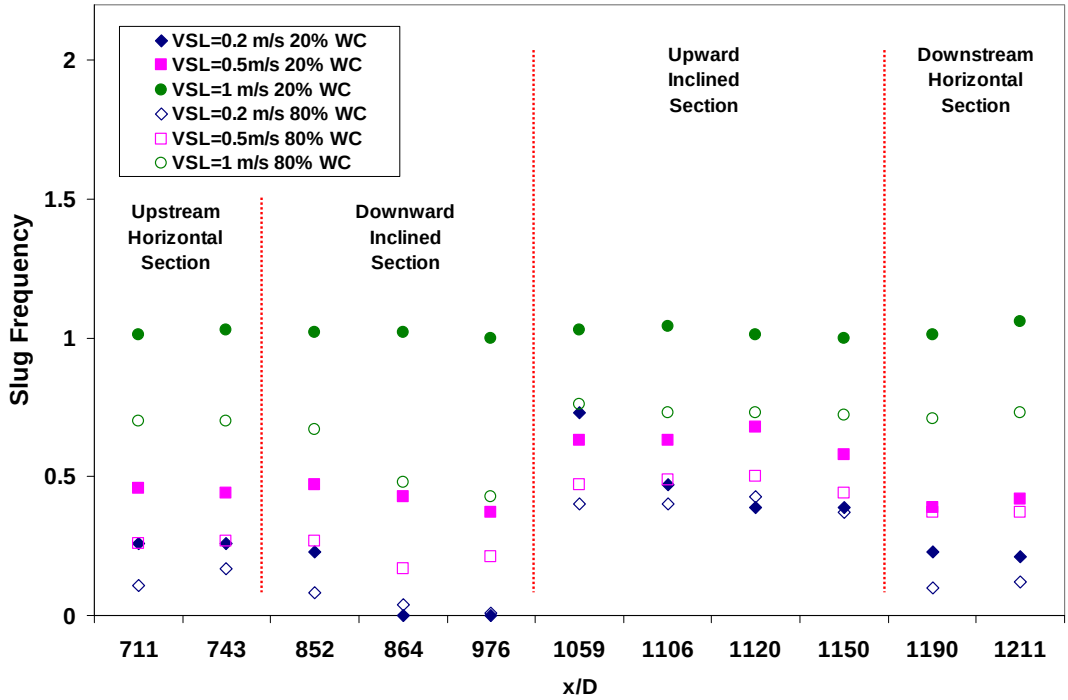

Figure 28: Slug Frequency for v_{Sg} = 3 m/s for 20 and 80% Water Cuts

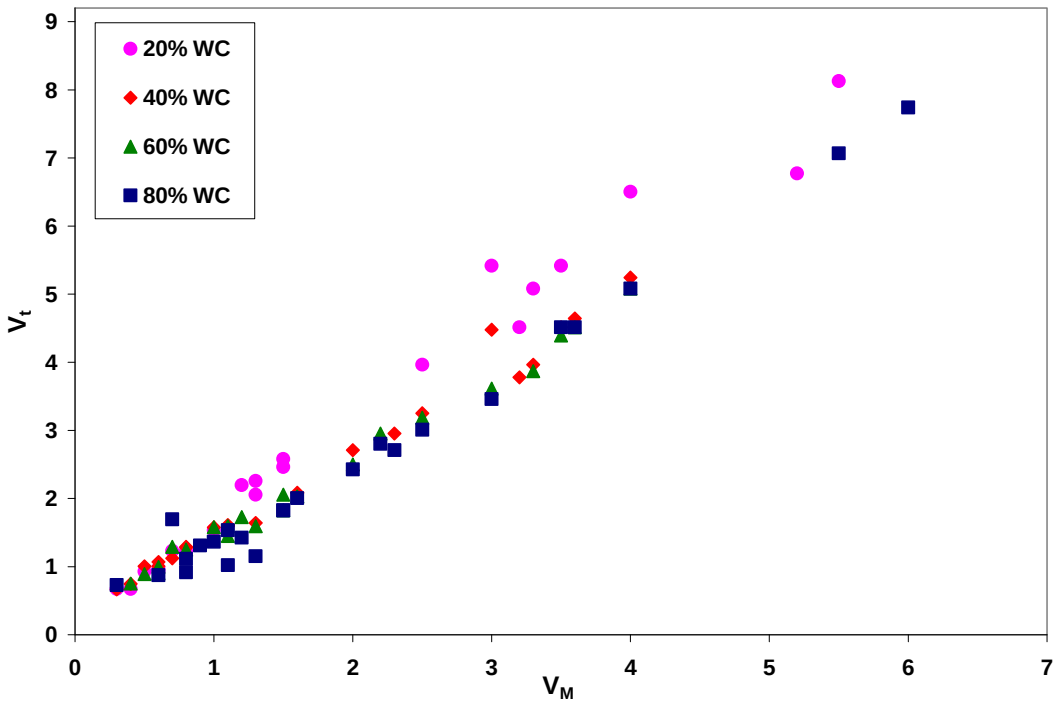

Figure 29: Translational vs. Mixture Velocity at Upstream Horizontal Section (LSR3/4)

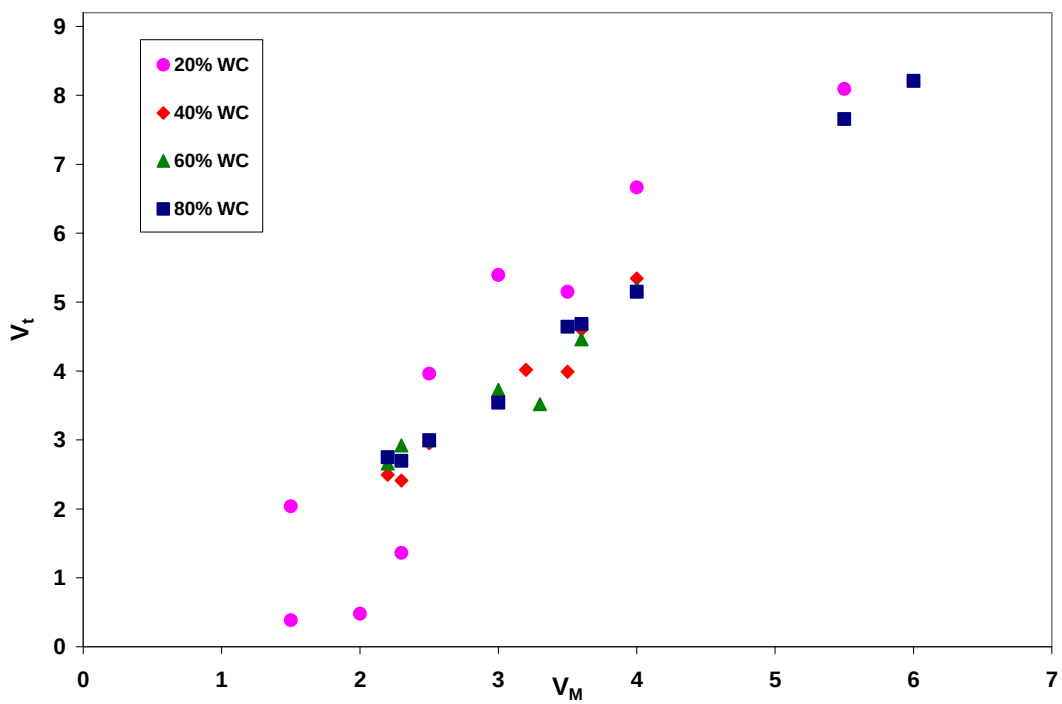

Figure 30: Translational vs. Mixture Velocity at Downward Section (LSR 6/7)

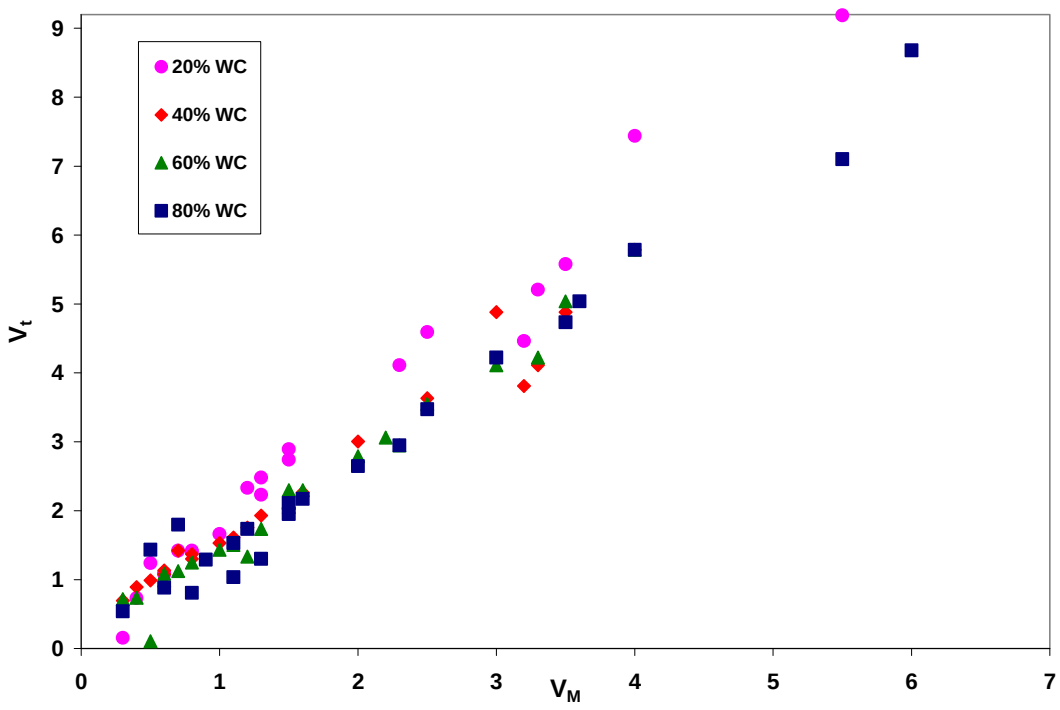

Figure 31: Translational vs. Mixture Velocity at Upward Section (LSR 13/14)

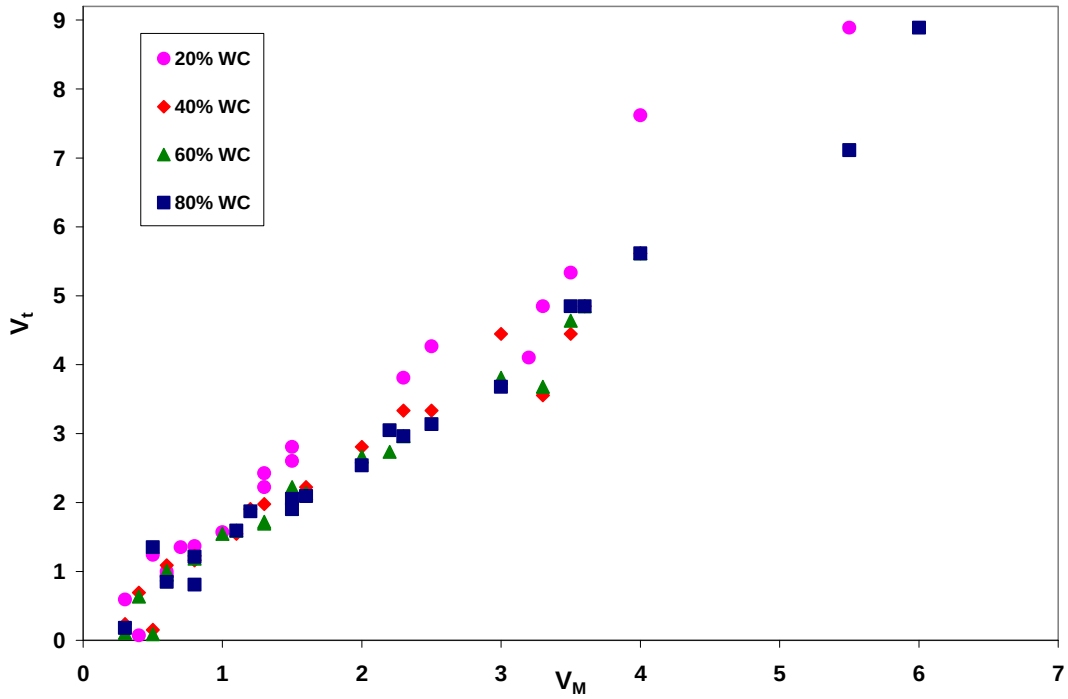

Figure 32: Translational vs. Mixture Velocity at Downstream Horizontal Section (LSR11/12)

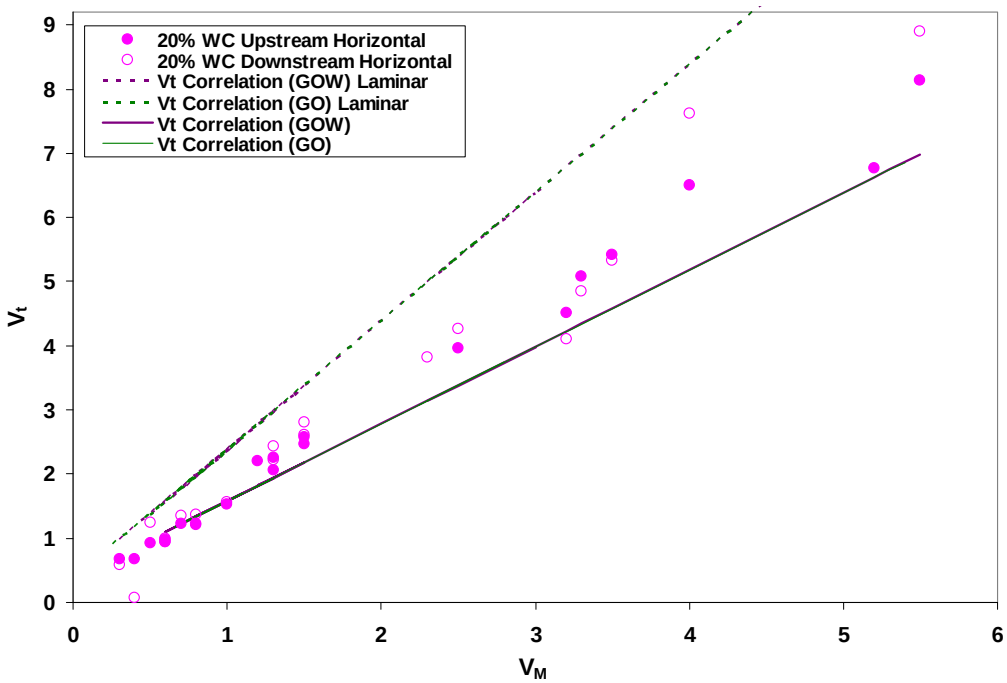

Figure 33: Comparison of Experimental and Calculated Translational Velocities at Upstream and Downstream Horizontal Sections for 20% Water Cut

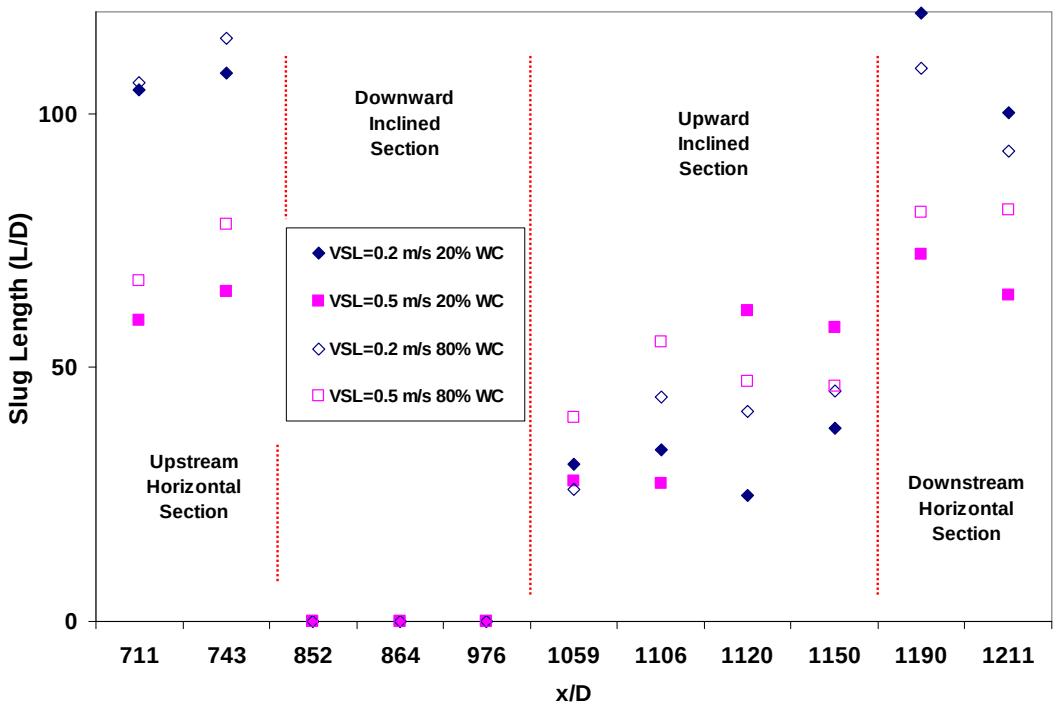

Figure 34: Slug Length for v_{Sg} = 0.1 m/s for 20 and 80% Water Cuts

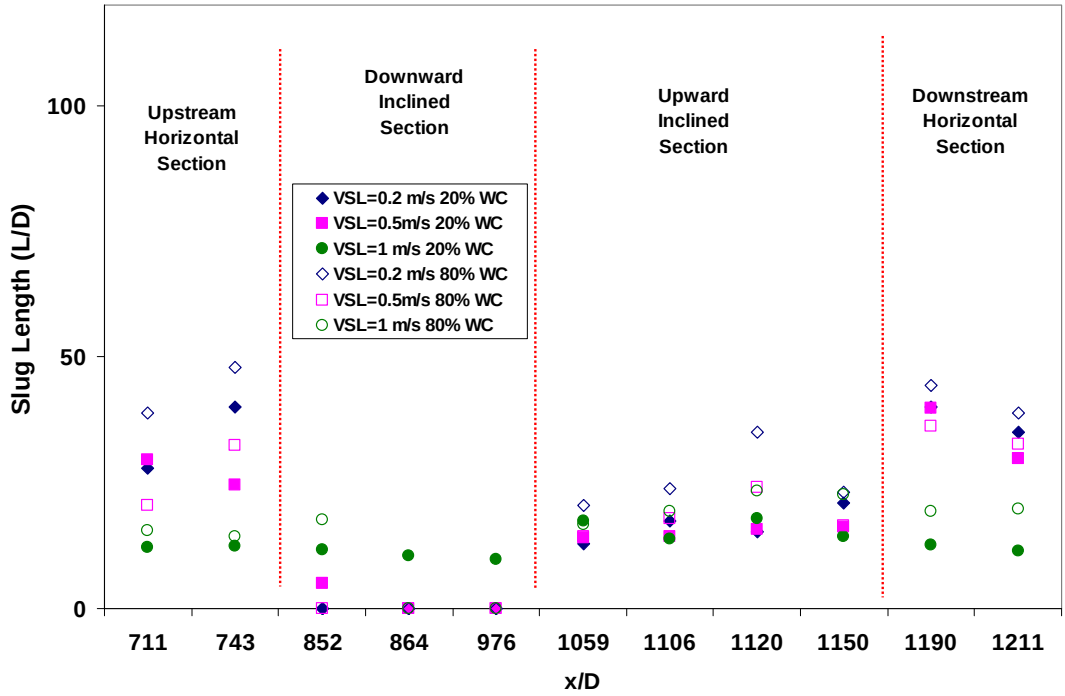

Figure 35: Slug Length for v_{Sg} = 1 m/s for 20 and 80% Water Cuts

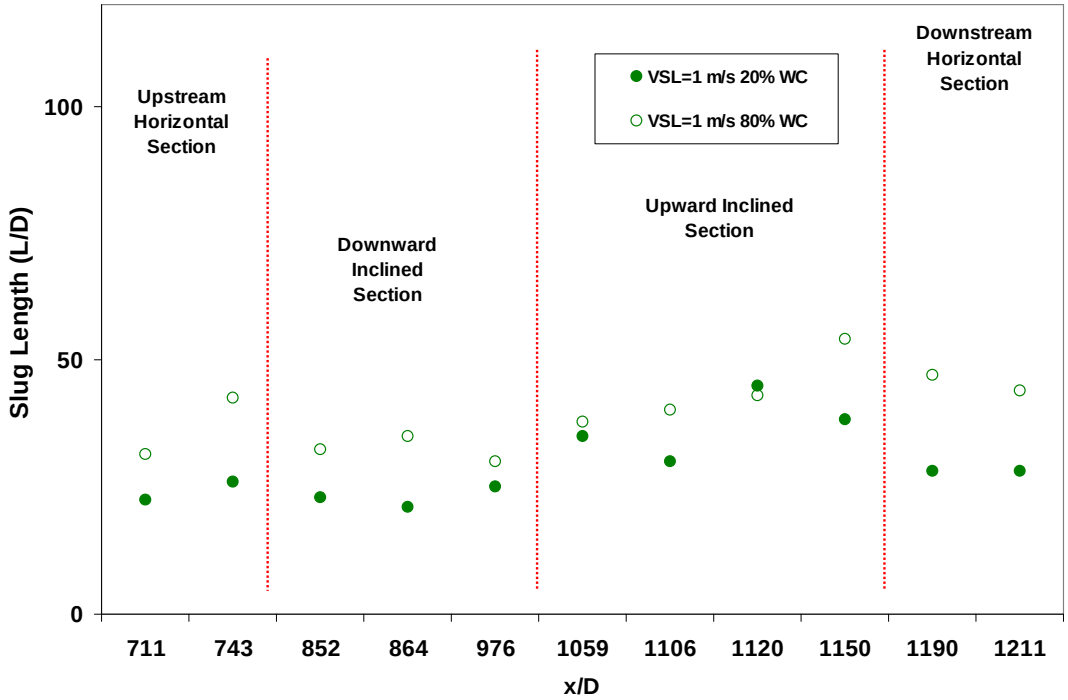

Figure 36: Slug Length for v_{Sg} = 3 m/s for 20 and 80% Water Cuts

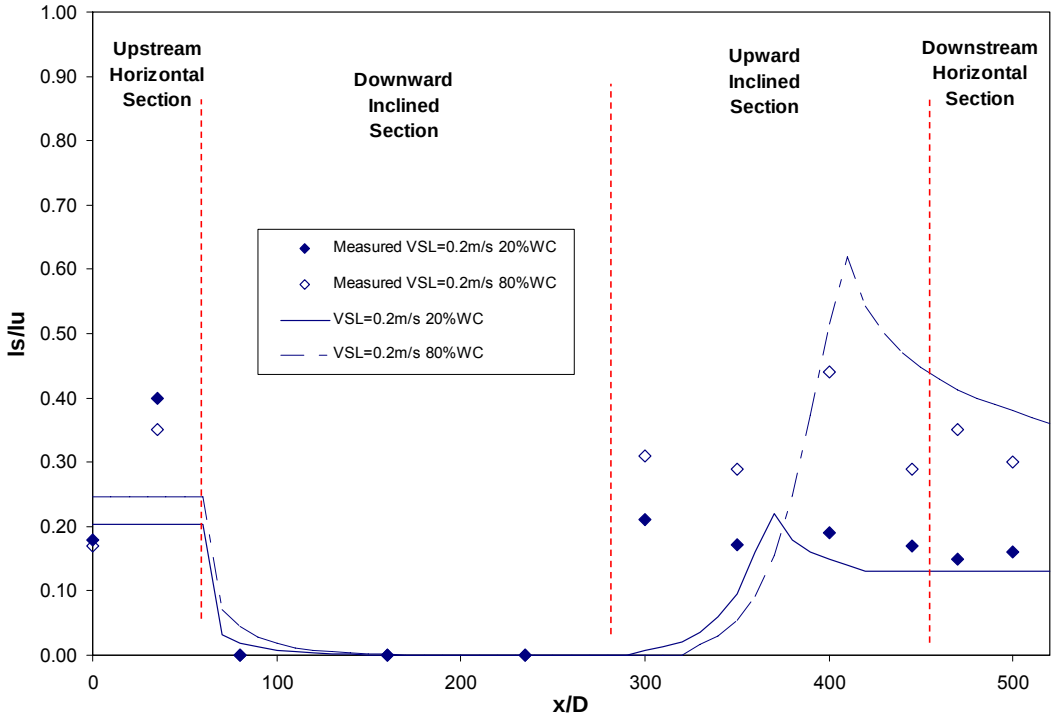

Figure 37: Comparison of Computed Slug Length to Slug Unit Length Ratio with Measurements for v_{Sg} = 1 m/s for 20 and 80% Water Cuts

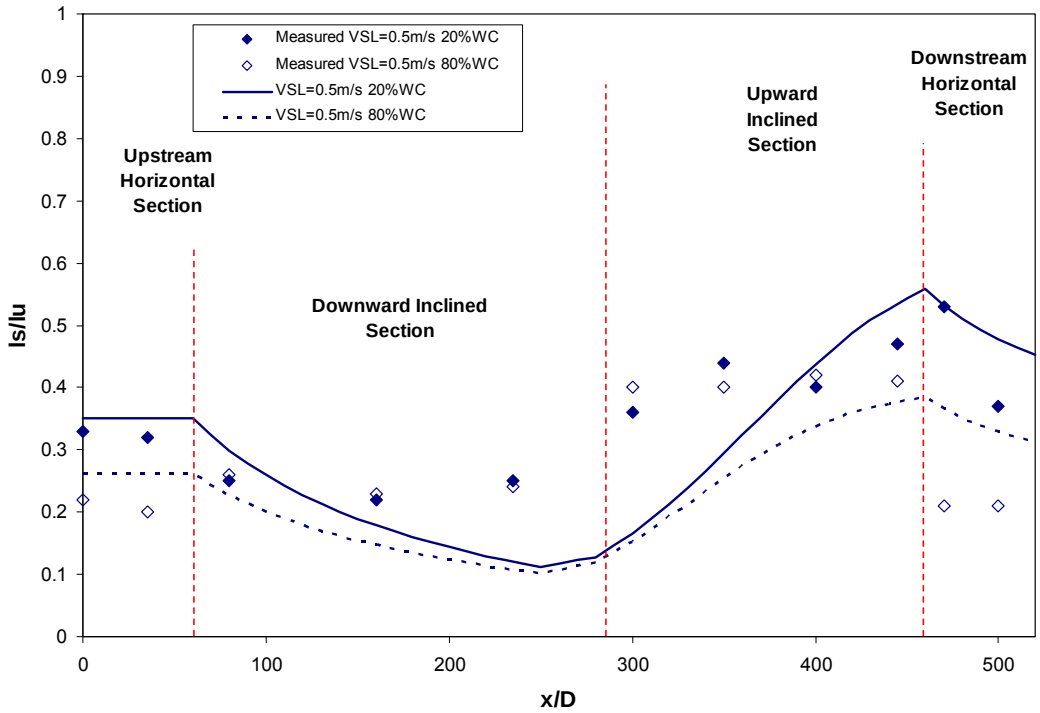

Figure 38: Comparison of Computed Slug Length to Slug Unit Length Ratio with Measurements for v_{Sg} = 2 m/s for 20 and 80% Water Cuts

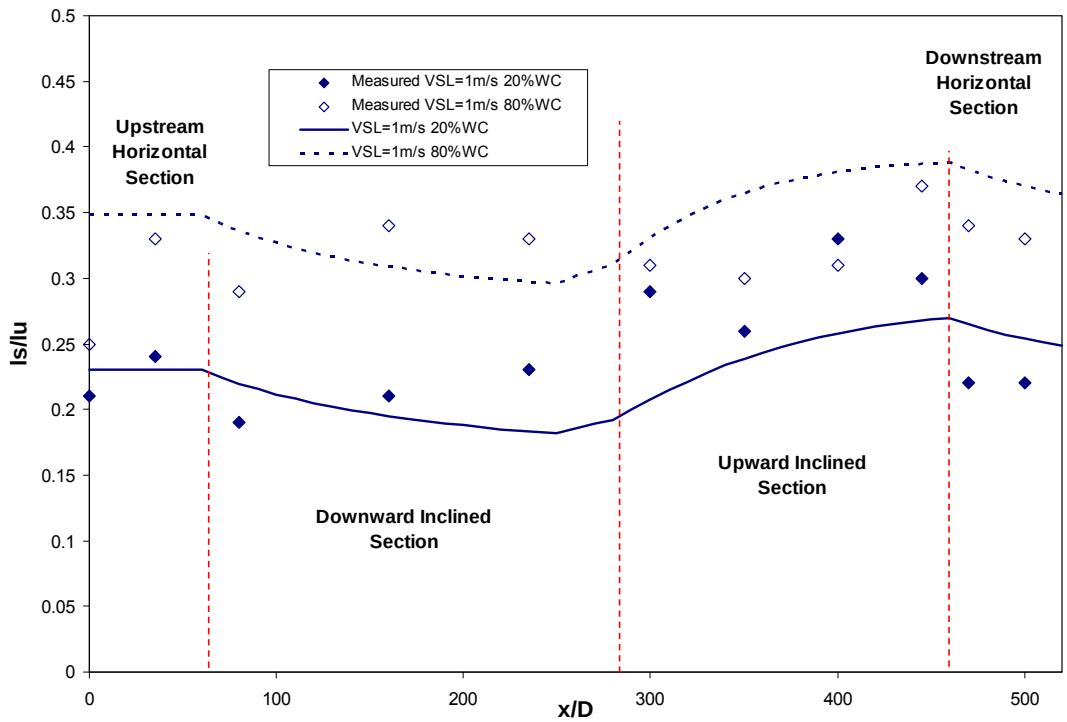

Figure 39: Comparison of Computed Slug Length to Slug Unit Length Ratio with Measurements for v_{Sg} = 3 m/s for 20 and 80% Water Cuts

Fluid Flow Projects

Executive Summary of Research Activities

Cem Sarica

Advisory Board Meeting, May 12, 2010

Low Liquid Loading Flow

- Significance
  - Wet Gas Transportation
    - Holdup and Pressure Drop Prediction
    - Corrosion Inhibitor Delivery (Top of the Line Corrosion)
- Objectives
  - Develop Better Predictive Tools

Low Liquid Loading Flow …

- Past TUFFP Studies
  - Two-phase, Small Diameter, Low Pressure
    - Air-Water and Air-Oil
    - 2-in. ID Pipe with ±2° Inclination Angles from Horizontal
  - Two-phase, Large Diameter, Low Pressure
    - Air-Water
    - 6-in. ID and ±2° Inclination Angles from Horizontal

Low Liquid Loading Flow …

- Past TUFFP Studies …
  - Three-phase, Large Diameter, Low Pressure
    - Air-Mineral Oil-Water
    - 6-in. ID, Horizontal Flow
    - Findings
      - Observed and Described Flow Patterns and Discovered a New Flow Pattern
      - Acquired Significant Amount of Data on Various Parameters, Including Entrainment Fraction
    - Remaining Tasks
      - Development of Improved Closure Relationships

Low Liquid Loading Flow …

- Current Study
  - Three-phase, Large Diameter, Low Pressure Inclined Flow
    - Air-Mineral Oil-Water
    - 6-in. ID and ±2° Inclination Angles from Horizontal
    - Objectives
      - Acquire Similar Data as in Horizontal Flow Study
      - Develop Improved Closure Relationships

Low Liquid Loading Flow …

- Status
  - Re-Started in Spring 2009
  - Successful Repeat Tests
  - Various Facility Fixes
  - Oil is Replaced with Lighter Oil
  - Some Two-phase and Three-phase Tests are Conducted
    - Smaller Onset v_{Sg} of Entrainment for Lighter Oil
- Future Studies
  - Two and Three-phase, Large Diameter, High Pressure Horizontal and Inclined Flow
    - Requires New High Pressure Facility

Fluid Flow Projects

Low Liquid Loading Gas-Oil-Water in Pipe Flow

Kiran Gawas

Outline

- Objectives
- Introduction
- Literature Review
- Experimental Study
- Near Future Tasks

Objectives

- Acquire Experimental Data of Low Liquid Loading Gas-Oil-Water Flow in Horizontal and Near Horizontal Pipes Using Representative Fluids
- Check Suitability of Available Models for Low Liquid Loading Three Phase Flow and Suggest Improvements If Needed

Introduction

- Low Liquid Loading Flows Correspond to Liquid to Gas Ratio ≤ 1100 $m^3/MMsm^3$
- Widely Encountered in Wet Gas Pipelines
- Small Amounts of Liquid Influences Pressure Distribution – Hydrate Formation, Pigging Frequency, Downstream Equipment Design etc.
- Transport of Additives

Literature Review

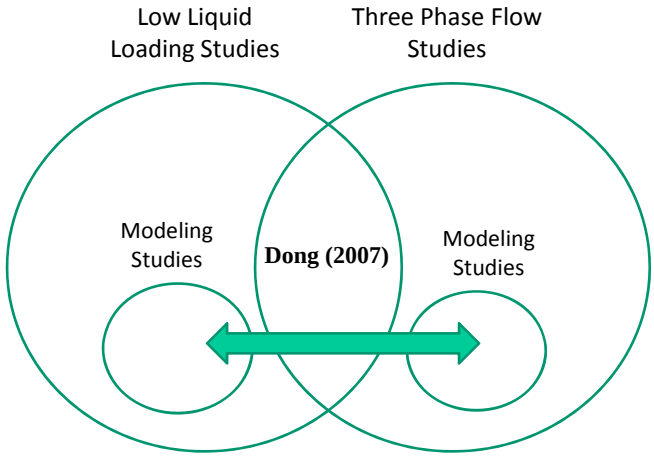

Literature Review …

- Entrainment in Vertical Flow
  - Uniform Across the Cross Section
  - Easier to Study Experimentally
  - Considerable Experimental Data and Correlations
- Entrainment in Horizontal Flow
  - Non-Uniform Across Cross Section
  - Limited Experimental Data and Correlations

Literature Review …

- Wicks and Dukler (1960)
  - Analogy between Momentum and Mass Transfer
  - Mass Transfer per unit Area Correlates with Lockhart-Martinelli Parameter X

$$R = 1.346 \times 10^{-4} X^{2.05}$$

where,

$$R = \frac{q_L We_{cr} W_{LE}}{q_g \left(dP/dL \right)_g}$$

$$R = 4\times10^{-7} \text{ to } 1.6\times10^{-4} \text{ kgm}^3/\text{Ns}$$

Literature Review …

- Paleev and Filippovich (1966)
- Correlation Based on Data Fitting

$$F_E = 0.015 + 0.44 \log\left(\frac{\rho_m}{\rho_L} \left(\frac{\mu_L v_g}{\sigma} \right)^2 10^4 \right)$$

where,

$$\rho_m = \rho_g \left[1 + \left(\frac{\rho_L v_{SE}}{\rho_g v_g} \right) \right]$$

- Effect of Liquid Flow Rate not Considered

Literature Review …

- Pan and Hanratty (2002)
  - Liquid with Viscosities Close to Water

$$R_D = R_A$$

$$\frac{F_E / F_{Em}}{1 - F_E / F_{Em}} = 9 \times 10^{-8} \left(\frac{D v_g^{\,3} \sqrt{\rho_L \rho_g}}{\sigma} \right) \left(\frac{\rho_g^{\,1-m} \mu_g^{\,m}}{d_{32}^{\,1+m} g \rho_L} \right)^{1/(2-m)}$$

where,

$$F_{Em} = 1 - \frac{W_{Fcr}}{W_L}$$

Literature Review …

- Mantilla (2008)
  - Effect of Liquid Film Characteristics on Entrainment Rate
  - Studied Effect of Fluid Properties (Surface Tension and Viscosity) on Entrainment and Wave Characteristics

$$F_E = \frac{1 - \dfrac{4}{v_{SL} \pi d^2} \displaystyle\int_0^{A(h_{Lb})} \overline{u} dA}{1 + \dfrac{k_D}{v_{Sg}} \dfrac{4 S_I L_w}{\phi \pi d^2}}$$

Literature Review …

- Kyle Magrini (2009)
  - Variation of Liquid Entrainment in Air-Water Annular Flow with Inclination
  - Checked suitability of Available Correlations at Different Inclinations
  - Horizontal Annular Flow – Pan and Hanratty (2002)

Experimental Study

- Experimental Facility
- Test Section
- Test Fluids
- Instrumentation and Data Acquisition
- Preliminary Tests
- Experimental Program
- Experimental Results

Facility

- 6 in. ID Low Pressure Flow Loop
- Previously Used by Dong (2007)
- Re-commissioned During Summer 2009 for Current Study
- Modified to Achieve Higher Gas Flow Rates

Facility ...

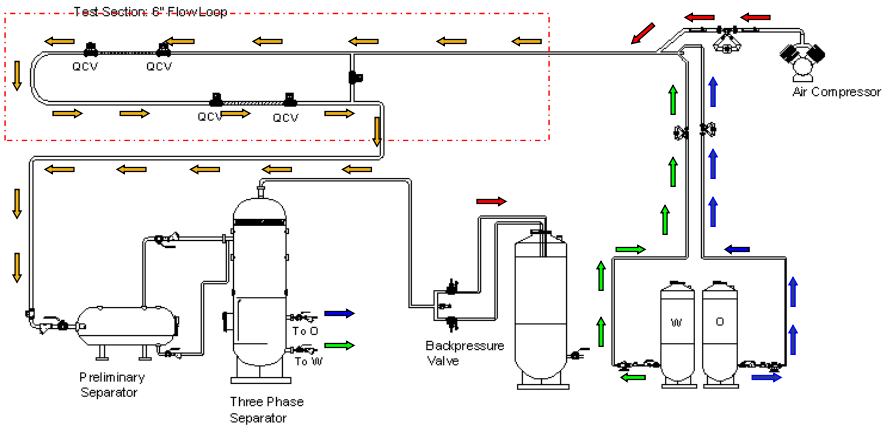

Test Section

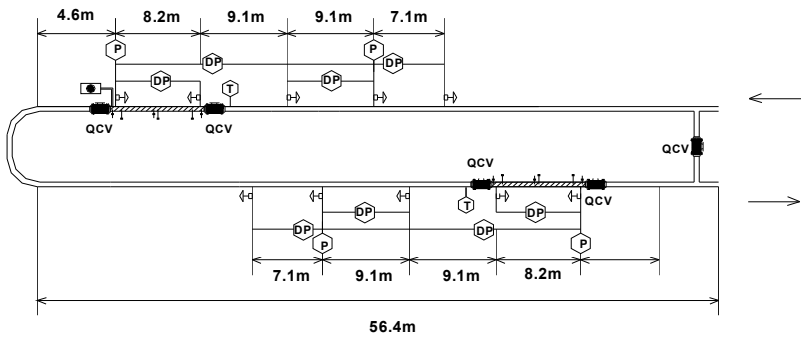

Test Fluids

- Test Fluid
  - Gas – Air
  - Water – Tap Water
  - Oil - ?
- Selection of Test Fluids is Very Important
- Properties Resembling Those of Wet Gas Condensate
  - Low Viscosity and Specific Gravity

Test Fluids …

Oil	Specific gravity	Viscosity (cP)	Surface tension (dynes/cm)	Liquid-water interfacial tension (dynes/cm)	Composition
Kerosene	0.775-0.81	2.1-2.2	23-32	47-49	Mainly C9 - C16
Tulco Tech 80 (Dong 2007)	0.86	13.5	29.14	16.38	Contains Mainly C14+
Lubsnap 40 (Meng 1999)	0.877	5.66	30	Not Available	Hydrotreated Naphthenic Oil
Natural Gas – Sweet	0.62-0.76	Comparable to Water	Not Available	Not Available	Mainly C7-C12
Norpar 12	0.749	1.22	25	Not Available	C12
Isopar L	0.748	1.3	23	45	iC12
Isopar K	0.762	1.14	24	Not Available	iC10

Instrumentation/Data Acquisition

- Pressure and Temperature: PTs and DPs and TTs
- Holdup: Quick Closing Valves and Pigging System
- Wetted Wall Perimeter: Scales on Wall
- Liquid Film Thickness: Conductivity Probes
- Liquid Velocity: Cold/Hot Liquid Injection
- Liquid Entrainment: Iso-kinetic Sampling System
- Data Acquisition: DeltaV

Holdups: QCVs & Pigging System

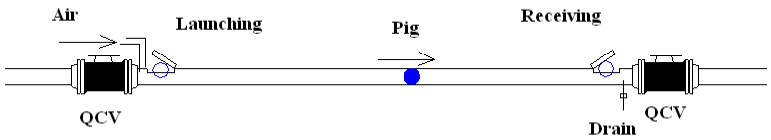

Pigging Efficiency Tests

	Water Test (ml)	Oil Test (ml)	Water + Oil (1:1)	
			Water (ml)	Oil (ml)
1st Pigging	60	70	30	50
2nd Pigging	35	40	10	30
3rd Pigging	15	20	0	15
Percentage Left after Third Pigging	0.5	0.67	0	0.5

Wetted Perimeter

- Scales Attached to the Pipe
- At High Gas Flow Rates Large Fluctuations due to Film Waviness

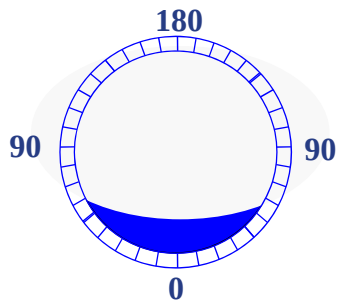

Film Thickness & Phase Continuity: Conductivity Probes

- Principle: Conductivity Difference
- Traverse Across Pipe

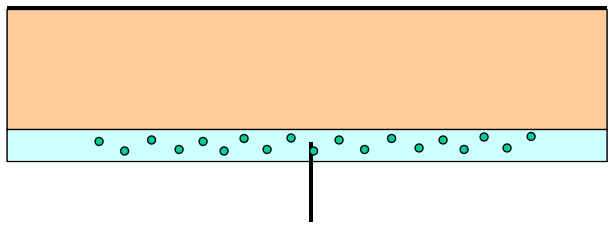

Film Velocity: Cold Liquid Injection

- Detect Temperature Variation
- $\text{Velocity} = \dfrac{\text{Distance}}{\text{Time}}$
- High Flow rates – Uncertainty

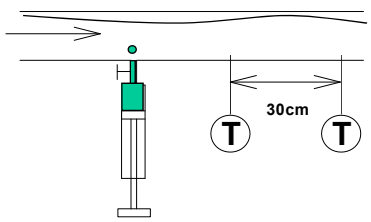

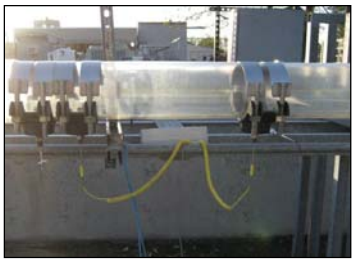

Liquid Entrainment: Iso-kinetic Probe

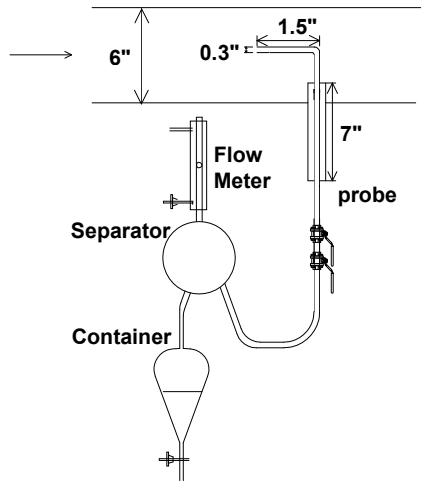

Experimental Program

- Preliminary Tests
  - Reproduce Dong's (2007) Results
- Entrainment Studies with New Test Fluid
  - Gas-Oil Two-phase Tests
  - Gas-Oil-Water Three-phase Tests

Experimental Program …

- Test Ranges for Entrainment Studies
  - Superficial Gas Velocity:
    15 to 22.5 m/s
  - Liquid Loading Level:
    50 to 1200 m^3/MMsm^3
  - Water Cut:
    0 to 0.5
  - Inclination Angles:
    0º, +2º, -2º

Preliminary Test

Test Matrix for Preliminary Test

Gas-liquid flow pattern	Oil/Water Flow Pattern	v_{Sg} (m/s)	Liquid Loading	Water Cut
Stratified smooth	Oil with discontinuous water strip	5	600	0.1
Stratified wavy	Stratified with channel water and water in oil dispersion	10	600	0.1
Stratified wavy	Stratified wavy with water in oil dispersion	15	300	0.1
Stratified wavy with droplet entrainment	Stratified with channel water and dual dispersion	15	900	0.5

Flow Pattern Identification

Gas-Liquid-Stratified Smooth/Oil-Water-Oil with Discontinuous Water Strip

Side View

Bottom View

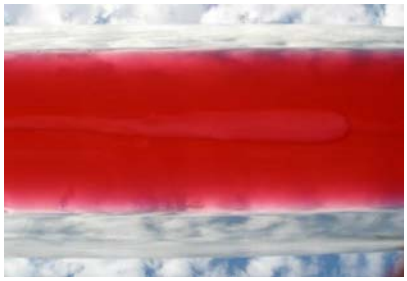

v_{Sg} = 5 m/s, LL = 600 m^3/MMsm^3, WC = 0.1

Flow Pattern Identification …

- Gas-Liquid-Stratified Wavy/Oil-water-Oil with Channel Water and Dispersion of Water in Oil

Side View

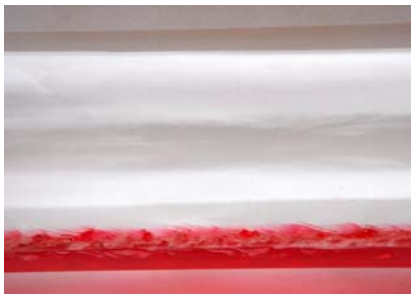

Bottom View

v_{Sg} = 10 m/s, LL = 600 m^3/MMsm^3, WC = 0.1

Flow Pattern Identification …

- Gas-Liquid-Stratified Wavy/Oil-Water-Water in Oil Dispersion

Side View

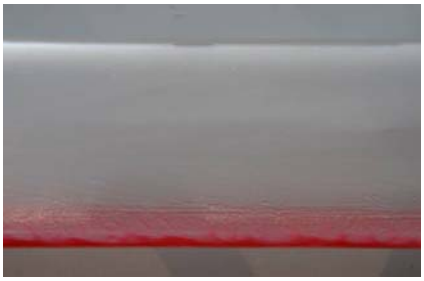

Bottom View

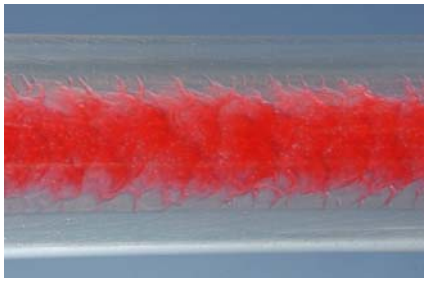

v_{Sg} = 15 m/s, LL = 300 m^3/MMsm^3, WC = 0.1

Flow Pattern Identification …

- Gas-Liquid-Stratified Wavy/Oil-Water-Channel Water and Dual Dispersion

Side View

Bottom View

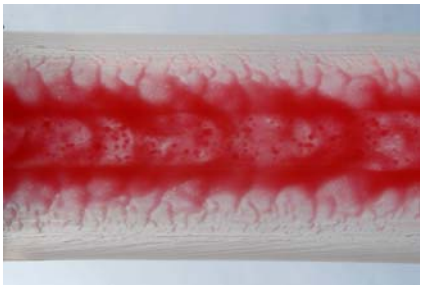

v_{Sg} = 15 m/s, LL = 900 m^3/MMsm^3, WC = 0.5

Entrainment Studies

- Test Matrix for Entrainment Studies

Superficial Gas Velocity (m/s)	Superficial Liquid Velocity (m/s) Water Cuts : 0, 5%, 10%, 20%, 50%				
16.5	0.004	0.006	0.008	0.01	0.012
18.5	0.004	0.006	0.008	0.01	0.012
20.5	0.004	0.006	0.008	0.01	0.012
22.5	0.004	0.006	0.008	0.01	0.012

Entrainment Studies …

- Onset of Entrainment
- Vertical Flow – Entrainment Uniform Across the Cross Section
- Entrainment Profile Across the Pipe Cross Section
  - Iso-kinetic Probe at Different Positions Across the Pipe Cross Section

Entrainment Studies …

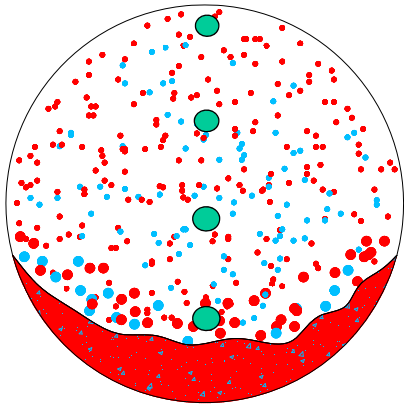

Total Liquid Entrainment Rate Profile (v_{Sg} = 16.5 m/s and WC = 0 %)

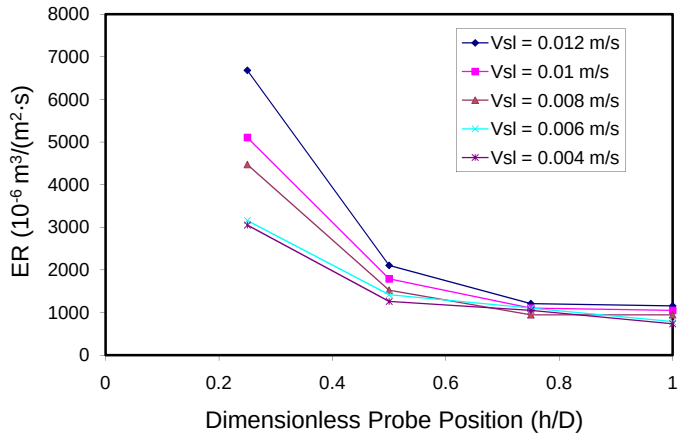

Fluid Flow Projects

Advisory Board Meeting, May 12, 2010

Total Liquid Entrainment Rate Profile (v_{Sg} = 18.5 m/s and WC = 0 %)

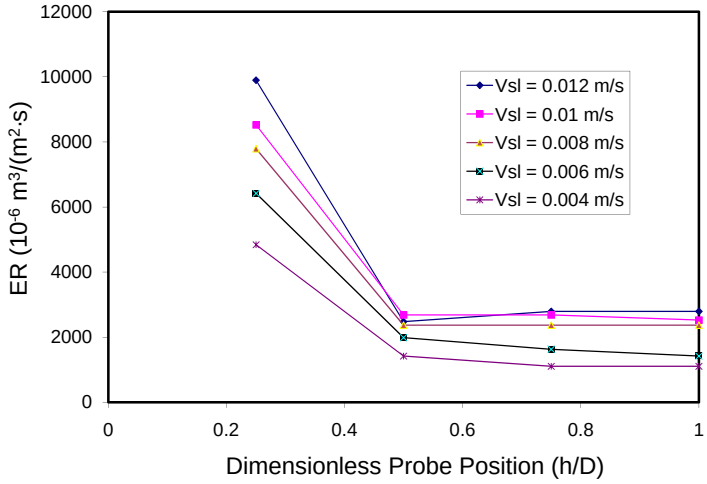

Fluid Flow Projects

Advisory Board Meeting, May 12, 2010

Total Liquid Entrainment Rate Profile (v_{Sg} = 16.5 m/s and WC = 5 %)

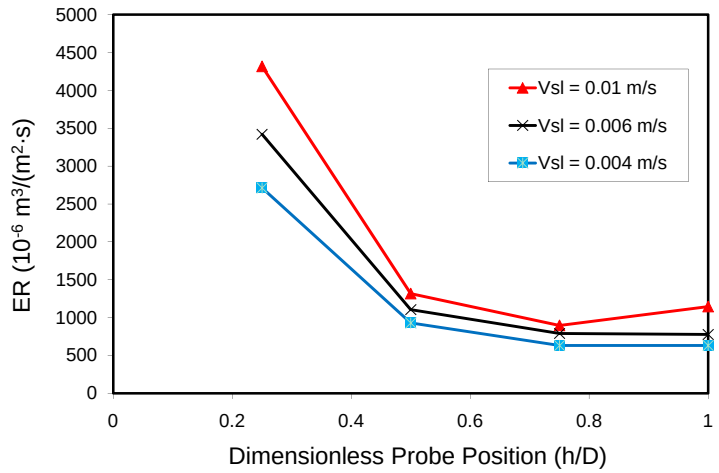

Fluid Flow Projects

Advisory Board Meeting, May 12, 2010

Total Liquid Entrainment Rate Profile (v_{Sg} = 18.5 m/s and WC = 5 %)

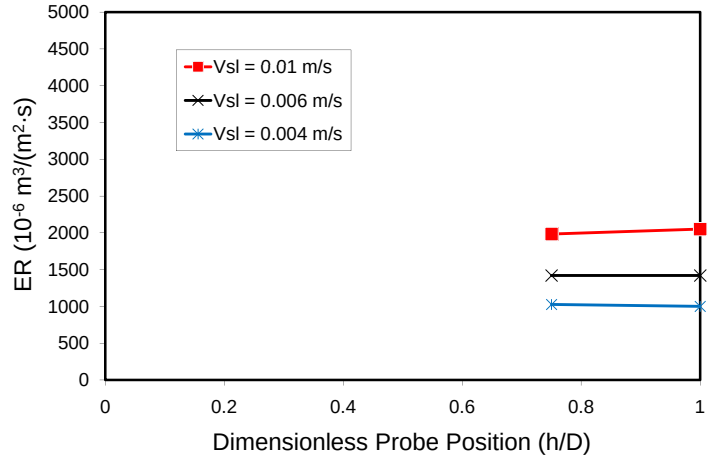

Fluid Flow Projects

Advisory Board Meeting, May 12, 2010

Variation of Liquid Entrainment Rate with v_{SL} (v_{Sg} = 16.5 m/s and WC = 0 %)

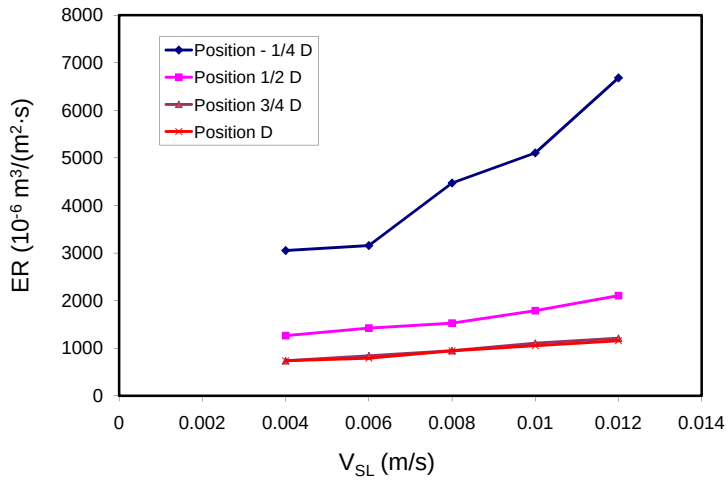

Fluid Flow Projects

Advisory Board Meeting, May 12, 2010

Variation of Liquid Entrainment Rate with v_{SL} (v_{Sg} = 18.5 m/s and WC = 0 %)

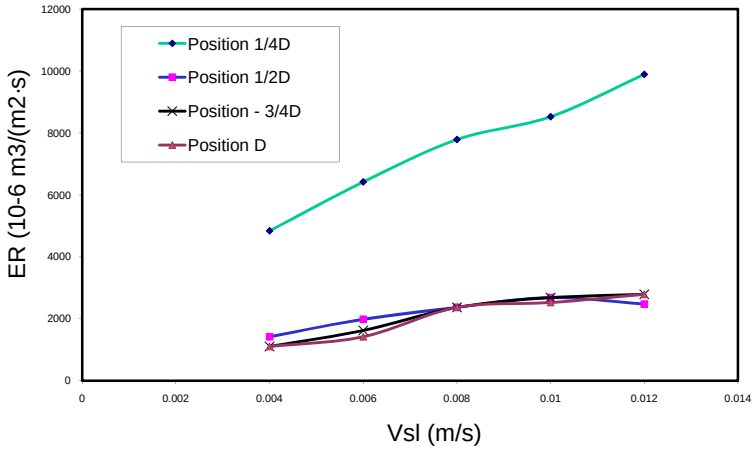

Fluid Flow Projects

Advisory Board Meeting, May 12, 2010

Variation of Liquid Entrainment Rate with v_{SL} (v_{Sg} = 16.5 m/s and WC = 5 %)

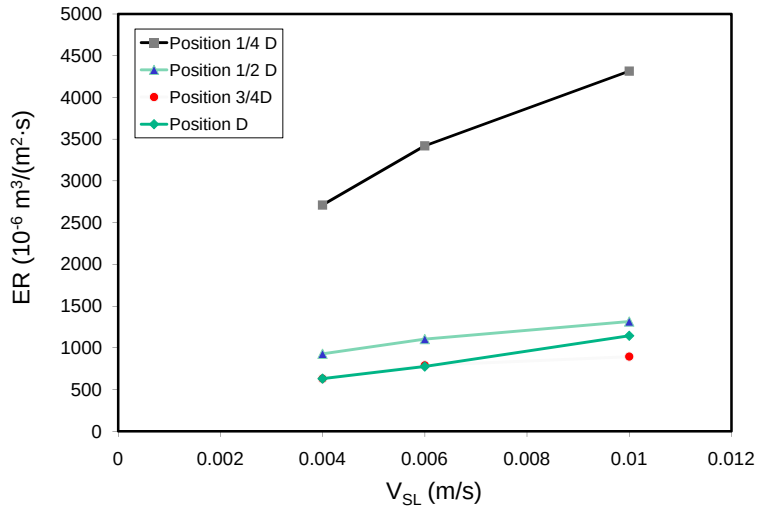

Fluid Flow Projects

Advisory Board Meeting, May 12, 2010

Variation of Liquid Entrainment Rate with v_{SL} (v_{Sg} = 18.5 m/s and WC = 5 %)

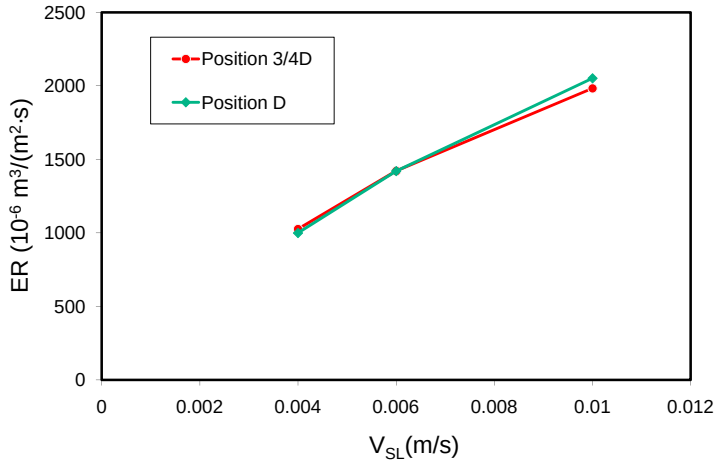

Fluid Flow Projects

Variation of Liquid Entrainment Rate with v_{SL} (V_{Sg} = 16.5 m/s and WC = 0 % and 5 %)

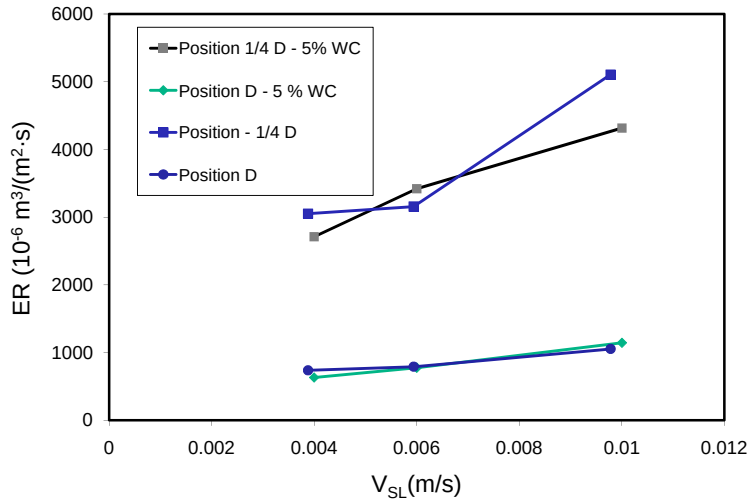

Fluid Flow Projects

Variation of Liquid Entrainment Rate with v_{SL} (v_{Sg} = 18.5 m/s and WC = 5 %)

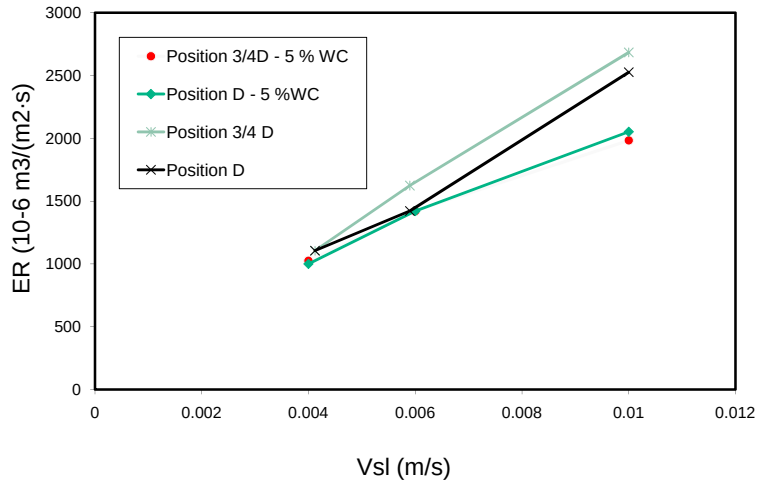

Fluid Flow Projects

Water Fraction Profile in Total Liquid Entrainment (v_{Sg} = 16.5 m/s and WC = 5 %)

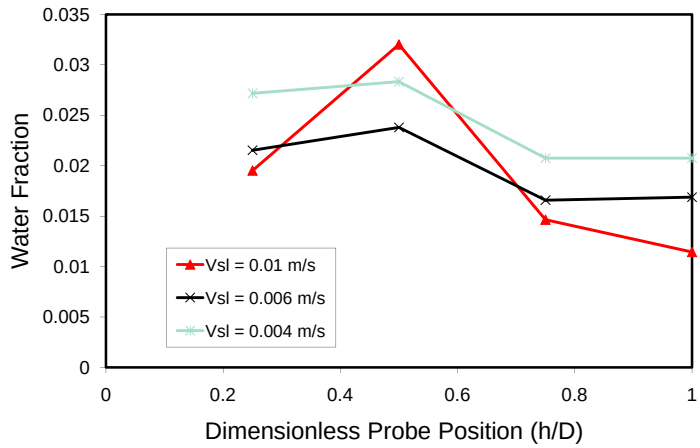

Fluid Flow Projects

Advisory Board Meeting, May 12, 2010

Water Fraction Profile in Total Liquid Entrainment (v_{Sg} = 18.5 m/s and WC = 5 %)

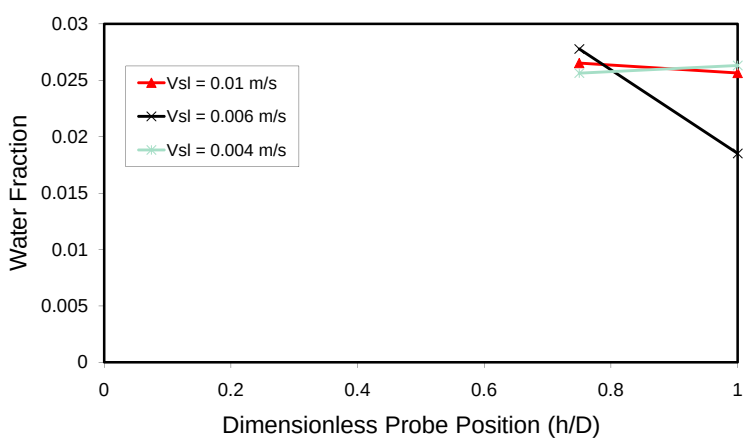

Fluid Flow Projects

Advisory Board Meeting, May 12, 2010

Future Work

- Check the Suitability of Available Correlations for Entrainment Fraction in Three-phase Flow
- Develop a Model for Three-phase Flow with Low Liquid Loading and Compare it with Experimental Results

Near Future Tasks

Literature Review	Ongoing
Ph.D. Qualifying	August 2010
Testing Phase-1	October 2010
Data Analysis and Model Comparison	December 2010
Testing Phase-2	April 2011
Model Development	December 2011
Final Report	May 2012

Questions

Low Liquid Loading in Gas-Oil-Water Pipe Flow

Kiran Gawas

PROJECT COMPLETION DATES:

Literature Review	Ongoing
Ph.D. Qualifying Exam	August 2010
Testing Phase 1	October 2010
Data Analysis and Model Comparison	December 2010
Testing Phase 2	April 2011
Model Validation	December 2011
Final Report	May 2012

Introduction

Low liquid loading gas-oil-water flow is widely encountered in wet gas pipelines. Even though the pipeline is fed with single phase gas, the condensation of the heavier components of the gas along with traces of water results in three-phase flow. The presence of these liquids can result in significant changes in pressure distribution. Many issues like hydrate formation, pigging frequency, and downstream facility design dependent on the pressure and holdup are thus also affected. Similarly the transport of contaminants and additives such as corrosion inhibitors is of great significance since most of these additives are observed in the liquid phase. Therefore, understanding of the flow characteristics of low liquid loading gas-oil-water flow is of great importance in transportation of wet gas. However, very few studies have been conducted on low liquid loading especially in three-phase flow.

Several authors have published papers on three-phase flow pattern and modeling of three-phase flow. However, most of them do not cover the range of low liquid loading flow. In this study, low liquid loading gas-oil-water flow experiments will be conducted in a 6 in. ID flow loop. The flow pattern, pressure drop, volumetric fractions of the three phases, liquid film thickness, wetted wall fractions and entrainment fractions will be observed and measured at different flow rates, liquid loading levels and water cuts.

Literature Review

Although significant research has been conducted in the field of two phase gas liquid flow much fewer studies have been conducted in the domain of low liquid loading. Some of these studies were presented at the fall 2009 ABM meeting. The literature review is still an ongoing task. The literature search is focused on the droplet entrainment during this period.

Chen (2005) conducted a study to investigate the influence of individual closure relationships on predictions of mechanistic models for multiphase flows. The study concluded that the variation in droplet entrainment fraction substantially affects the pressure gradient and liquid holdup predictions. Thus better understanding of the entrainment phenomena is very important. Entrainment in vertical flow is symmetrical and thus is easier to study experimentally. Consequently, there are several studies and correlations developed for predictions of entrainment fraction in vertical flow as compared to horizontal flow. Wicks and Dukler (1960) developed a model for the mass flow rate of droplets, W_{LE}, based on the assumption of analogy between momentum and mass transfer. Based on the assumption that ratio of mass transfer per unit area correlates with Lockhart-Martinelli parameter X, in a similar way as the ratio of momentum transfer (pressure gradient) with entrainment group R as,

$$R = \frac{q_L We_{cr} W_{LE}}{q_g \left(dP/dL \right)_g} \qquad (1)$$

The following correlation was obtained between R and X which is valid in the range of R = 4×10^{-7} to 1.6×10^{-4} kgm^3/N-s.

$$R = 1.346\times10^{-4}\, X^{2.05}\,. \qquad (2)$$

Paleev and Filippovich (1966) developed a correlation by data fitting to their experiments and database from other researchers. The effect of liquid rate was not considered. The entrainment fraction was given by,

$$F_E = 0.015 + 0.44\log\left(\frac{\rho_m}{\rho_L}\left(\frac{\mu_L v_g}{\sigma}\right)^2 10^4\right). \qquad (3)$$

where,

$$\rho_m = \rho_g\left[1+\left(\frac{\rho_L v_{SE}}{\rho_g v_g}\right)\right]. \qquad (4)$$

Pan and Hanratty (2002) developed a correlation for liquids with viscosities close to that of water, based on balance between rates of atomization and deposition and considering both gravity and droplet size effect,

$$\frac{F_E/F_{Em}}{1-F_E/F_{Em}} = 9\times10^{-8}\left(\frac{D v_g^{\,3}\sqrt{\rho_L\rho_g}}{\sigma}\right)\left(\frac{\rho_g^{\,1-m}\mu_g^{\,m}}{d_{32}^{\,1+m} g\rho_L}\right)^{1/(2-m)} \qquad (5)$$

where the maximum entrainment, F_{Em} is given by

$$F_{Em} = 1-\frac{W_{Fcr}}{W_L} \qquad (6)$$

Where W_{Fcr} is the liquid critical flow rate, i.e. the minimum flow rate at which entrainment begins and is given by

$$W_{Fcr} = \frac{1}{4}\mu_L \pi D\,\mathrm{Re}_{Fcr}\,. \qquad (7)$$

Where

$$\mathrm{Re}_{Fcr} = 7.3(\log w)^3 + 44.2(\log w)^2 - 263\log w + 439\,. \qquad (8)$$

and

$$w = \frac{\mu_L}{\mu_g}\sqrt{\frac{\rho_g}{\rho_L}}\,. \qquad (9)$$

Mantilla (2008) developed a mechanistic model for liquid entrainment based on wave characteristics and also studied the effect of surface tension and viscosity on the entrainment phenomenon. The entrainment fraction according to the model is

$$F_E = \frac{1-\dfrac{4}{v_{SL}\pi d^2}\displaystyle\int_0^{A(h_{Lb})} u\,dA}{1+\dfrac{k_D}{v_{Sg}}\dfrac{4S_I L_w}{\phi\pi d^2}}\,. \qquad (10)$$

Kyle Magrini (2009) studied liquid entrainment in annular air-water flows in 3" pipe for different inclinations. The effect of inclination on wave characteristics and liquid entrainment was studied. He also checked the suitability of the available correlations for different inclinations and found that Pan and Hanratty (2002) correlation was most accurate in predicting entrainment fraction for horizontal annular flow.

Thus, current state of literature indicates that more work related to liquid entrainment is required especially in case of three-phase flow. Closure relationships must be examined based on experimental results so that improvements or new developments can be achieved.

Experimental Study

Experimental Facility

The experimental facility for this study is the 6 in. flow loop which has been used to conduct research on low liquid loading flow for several years. The flow loop was re-commissioned in summer 2009 to ensure that it is in working order. This involved checking all the pumps, air compressor, calibration of the instruments, removal of all leaks, and replacement of pipe sections where necessary.

As suggested by member companies at the last ABM, it was decided to focus on studies at high gas velocities to obtain entrainment data. Due to limitations of the earlier facility tests could only be done up to gas superficial velocity of 18.5 m/s. However, the facility has now been modified to reduce back pressure of the loop, and higher gas flow rates can now be attained. Also the current

modification enables better control over back pressure. Fig. 1 shows a schematic of the modified flow loop. The test section consists of two runs of 6-in. ID pipes, each run being 56.4 m in length. Acrylic visualization sections are provided at the end of each run. The inclination angle of the test section can be changed from 0° to 2° in upward and downward directions.

Test Fluids

As shown by Utvik *et al.* (2001) the choice of test fluids play a very important role in the results of the experiments. Since the phenomenon of low liquid loading is observed mainly in wet gas pipelines, the test fluid selected should resemble the gas condensates as much as possible. Table 1 represents comparative study of the properties of different oils considered for the selection of test oil. The selected oil should have low viscosity (comparable to that of water), low specific gravity and high interfacial tension with water. Based on these criteria the test fluids selected are Isopar L, air and water. Since the last ABM (Tulco Tech 80) used for earlier studies has been replaced with isopar L.

Instrumentation and Data Acquisition

The DeltaV^{TM} digital automation system is used as the data acquisition software. Gas flow rate is measured using the micro motion flow meter CMF300 while two micro motion flow meters CMF100 and CMF050 are used to measure oil and water flow rates, respectively. The flow meters are calibrated by the manufacturer and have a mass flow rate uncertainty of ±0.1% and density measurement uncertainty of ±0.5%.

Pressure, temperature and pressure gradients are measured using Rosemount pressure, temperature transmitters and Rosemount differential pressure transducers, respectively.

Liquid holdup is measured by trapping liquid between the two quick-closing valves (QCV) installed on the first run of the test section and then pigging out the entrapped liquid into graduated cylinders. The results of the pigging efficiency tests are as shown in Table 2.

Wetted wall perimeter is measured using grades on pipe circumference. Liquid entrainment fraction is measured using iso-kinetic sampling system. The working principle of which is shown in Fig. 2. Liquid entrainment is not uniform in horizontal stratified flow. The entrainment rate is higher near the gas-liquid interface and decreases from bottom to top. Hence the iso-kinetic sampling probe is inserted into the pipe at four different radial locations (1/4D, 1/D, 3/4D and D; where D is diameter of the pipe) as shown in the Fig. 3. The liquid sampled from the gas core is separated in a gas-liquid separator and collected in a graduated cylinder. Entrainment rate is calculated using these measurements, and is then integrated over the gas core area to give entrainment fraction.

Liquid film thickness can be measured using conductivity probe. The probe consists of a single wire which traverses across the pipe cross section. The oil water interface is indicated by change in conductance and hence a change in voltage across the probe. This method is time consuming and relies on visual observation and manually traversing the probe which can introduce considerable error in the measurement. Hence there is a need to devise a method which can provide real time data on liquid film thickness.

Cold liquid injection technique is used to determine liquid velocity. A cold liquid injector is placed at a point in the test section to inject cold oil or water into the test section. Two thermal probes are installed 0.5 ft after the injector with a 1 ft interval between them. The time required for the cold liquid to travel between the two probes is measured which gives the velocity of the liquid. However, at higher gas flow rates the results showed significant variation and hence this method was not used for the entrainment studies.

Preliminary Tests

Preliminary tests were carried out to check the facility and the instruments. This is necessary to ensure that facility works properly and the instruments give reliable measurements. The conditions selected for preliminary tests are shown in Table 3. The flow patterns indicated in Table 3 are as shown in Figs. 4 - 7. This confirms the observations made by Dong (2007).

Experimental Program

Experiments are being performed for oil-gas and oil-water-gas three phase flows. The proposed test matrix is shown in Table 4. The proposed test matrix is designed based on the gas velocities of 16.5-22.5 m/s and liquid loading levels of 200-1000 for water cuts of 0, 5%, 10%, 20% and 50%.

Experimental Results

The liquid entrainment onset points were observed visually. The entrainment onset point is the lowest superficial gas velocity at which droplets can be observed on the pipe surface. In the previous work, Dong (2007), the entrainment onset point for Tulco Tech 80 (μ=13.5 cP @ 40^0C) was observed at superficial gas velocity of 15 m/s. In the current study the oil used is Isopar L (μ=1.23 cP @ 40^0C) and the onset of entrainment was observed at 12.5 m/s. The entrainment onset point did not vary with superficial liquid velocity. Entrainment rate is calculated using the following formula

$$ER = \frac{V_E}{A_{probe} t_s} \qquad (10)$$

Where, ER is the local liquid entrainment flux, V_E is the collected liquid entrainment volume, A_{probe} is the area of probe opening and t_s sampling duration which is 10 minutes in the current study. The results of the experiments for two-phase are shown in Table 5 and three-phase flow in Table 6. Entrainment rates become measurable only for gas superficial velocity above 15.5 m/s. Figs. 8 and 9 show that the entrainment rate increases with liquid loading level. Also from Figs. 10 and 11 it is clear that the entrainment rate is very high near the gas-liquid interface and tends to level off towards the top of the pipe. Gas-oil-water three-phase studies are in progress. Figs. 12 and 13 show the variation of total liquid entrainment rate with liquid loading and for water cut of 5 %. Also Figs. 14 and 15 show the total liquid entrainment rate profile for water cut of 5 %. Figs. 16 and 17 indicate that the total liquid entrainment rate decreases with an increase in water cut. This could be due to increase in viscosity of the liquid phase. Moreover, water being heavier would be entrained less than oil which could decrease the liquid entrainment rate. Figs. 18 and 19 indicate the variation of water fraction in the entrained liquid with position of the iso-kinetic probe. The results indicate that the water fraction in the entrained liquid is less than the inlet water fraction. The fraction of water entrained seems to remain constant with position of the probe. However, more experiments need to be performed to ascertain the results and draw conclusions.

Near Future Tasks

- Complete the proposed test matrix.
- Ph.D. qualifying exam
- Analyze experimental data.
- Carry out comparison with existing models
- Development of new model

Nomenclature

A = area [m^2]

C = droplet concentration [kg/m^3]

d = pipe diameter [m]

F_E = entrainment group [kgm^3/N-s]

k = empirical entrainment and deposition coefficients [m/s]

R = entrainment group [kg/m^2s]

Re = Reynolds number

S_I = interfacial perimeter [m]

v = velocity [m/s]

We = Weber number

X = Lockhart-Martinelli parameter

Greek Letters

μ = viscosity [kg/ms]

θ = pipe inclination angle [degree]

ρ = density [kg/m^3]

σ = surface tension [N/m]

Subscripts

C = gas core

cr = critical

D = deposition

d = Droplet

E = entrainment

g = gas phase

I = interface

L = liquid phase

LF = liquid film

m = maximum

probe = isokinetic probe

s = sampling time

Sg = superficial gas

SL = superficial liquid

References

Chen, X.: "Droplet-Homophase Interaction Studies," TUFFP ABM March 2005, pp. 135-186, (2005).

Dong, H.-K.: "Low Liquid Loading Gas-Oil-Water Flow in Horizontal Pipes," M.S. Thesis, U. Tulsa. Tulsa, OK. (2007).

Magrini, K. L.: "Liquid Entrainment in Annular Gas-Liquid Flow in Inclined Pipes," M.S. Thesis, U. Tulsa, Tulsa, OK (2009).

Mantilla, I.: "Mechanistic Modeling of Liquid Entrainment in Gas in Horizontal Pipes," Ph.D. Dissertation, U. Tulsa, OK, (2008).

Paleev, I. I., and Filippovich, B. S., "Phenomena of Liquid Transfer in Two phase Dispersed Annular Flow," *Intl. J. Heat and Mass Transfer*, Vol. 9, pp. 1089-1093, (1966).

Pan, L. and Hanratty, T. J., "Correlation of Entrainment for Annular Flow in Horizontal Pipes," *Intl. J. Multiphase Flow*, Vol. 28, pp. 363-384, (2002).

Wicks, M and Dukler, A. E., "Entrainment and Pressure Drop in Concurrent Gas-Liquid Flow: I. Air-Water in Horizontal Flow," *AIChE J*, Vol. 6, pp. 463-468, (1960).

Utvik, O. H., Rinde, T., and Valle, A.: "An Experimental Comparison Between a Recombined Hydrocarbon-Water Fluid and a Model Fluid System in Three-Phase Pipe Flow," *ASME, J. Energy Res. Tech.*, Vol. 123, pp. 253-259 (2001).

Table 1: Physical Properties of Test Oil

Oil	Specific gravity	Viscosity (cP)	Surface tension (dynes/cm)	Liquid-water interfacial tension (dynes/cm)	Composition
Kerosene (Chen *et al.* , 1997)	0.775-0.81	2.1-2.2	23-32	47-49	Mainly C9 - C16
Tulco Tech 80 (Dong 2007)	0.86	13.5	29.14	16.38	Contains mainly C14+
Lubsnap 40 (Meng 1999)	0.877	5.66	30	NA	Hydro-treated naphthenic oil
Natural gas - sweet	0.62-0.76	Comparable to water	NA	NA	Mainly C7-C12
Norpar 5s	0.626			NA	C5
Norpar 12	0.749	1.22	25	NA	C12
Norpar 13	0.762	2.36	26	NA	C13
Norpar 15	0.772	3.27	27	NA	C15
Exxsol D80	0.8	1.4-1.8	NA	NA	contains C11-C15 - 99%,
Isopar L	0.769	1.3	23	45	i-C12
Isopar K	0.762	1.14	24	NA	NA

Table 2: Pigging Efficiency Test Results

	Water Test (ml)	Oil Test (ml)	Water + oil (1:1)	
			Water (ml)	Oil (ml)
1st pigging	60	70	30	50
2nd Pigging	35	40	10	30
3rd Pigging	15	20	0	15
Percentage liquid left at the end of 3rd pigging	0.5	0.67	0	0.5

Table 3: Conditions for Repeat Tests

Gas-liquid flow pattern	Oil/Water flow pattern	v_{Sg} (m/s)	Liquid Loading	Water Cut
Stratified smooth	Oil with discontinuous water strip	5	600	0.1
Stratified wavy	Stratified with channel water and water in oil dispersion	10	600	0.1
Stratified wavy	Stratified wavy with water in oil dispersion	15	300	0.1
Stratified wavy with droplet entrainment	Stratified with channel water and dual dispersion	15	900	0.5

Table 4: Test Matrix for Entrainment Studies

Superficial Gas Velocity (m/s)	Superficial Liquid Velocity (m/s) Water cuts : 0, 5%, 10%, 20%, 50%				
16.5	0.004	0.006	0.008	0.01	0.012
18.5	0.004	0.006	0.008	0.01	0.012
20.5	0.004	0.006	0.008	0.01	0.012
22.5	0.004	0.006	0.008	0.01	0.012

Table 5: Results of Entrainment Tests for Two-phase Flow

v_{Sg} (m/s)	v_{SL} (cm/s)	ER (10^{-6} $m^3/(m^2 \cdot s)$)					
		P2 (1/4D)	P3 (1/2D)	P4 (3/4D)	P5 (D)	P (kPa)	T(°K)
	0.6	142.1	NA	NA	NA	139	289
	0.8	263.1	NA	NA	NA	138	289
	1	342	NA	NA	NA	138	288
15.5	1.2	368.34	NA	NA	NA	139	288
	0.4	3052	1262.88	736.68	736.68	172	316
	0.6	3157	1420.7	841.92	789.93	170	311
	0.8	4473	1526	947.16	947.16	172	306
	1	5104	1789.1	1105	1052.4	172	306
16.5	1.2	6683	2104.9	1210.3	1157.64	172	306
	0.4	4841	1420.76	1105	1105.03	208	304
	0.6	6419.7	1983	1623.5	1420.76	209	304
	0.8	7787.9	2367.93	2367.9	2367.9	210	303
	1	8524.5	2683.6	2683.6	2525.8	211	303
18.5	1.2	9892.69	2473.2	2788.9	2788.9	212	302

Table 6: Results of Entrainment Tests for Three-phase Flow

v_{Sg}	v_{SL}			ER (10^{-6} $m^3/(m^2 \cdot s)$)											
	T	O	W	P1(1/4D)			P2(1/2D)			P3(3/4D)			P4(D)		
m/s	cm/s	cm/s	cm/s	T	O	W	T	O	W	T	O	W	T	O	W
	0.4	0.38	0.02	2710.7	2637.03	73.67	928.6	902.29	26.31	631	617.9	13.1	631	617.9	13.1
	0.6	0.57	0.03	3420	3346.33	73.67	1105.2	1078.71	26.31	789.93	776.83	13.1	776	762.9	13.1
16.5 m/s	1	0.95	0.05	4314.84	4320.65	84.192	1315	1272.9	26.31	894.54	881.44	13.1	1144.4	1131.3	13.1
	0.4	0.38	0.02							1026	999.7	26.3	999.78	973.5	26.3
	0.6	0.58	0.03							1420.7	1381.23	39.465	1420.7	1394.4	26.31
18.5	1	0.95	0.05							1983	1930.4	52.62	2052	1999.4	52.62

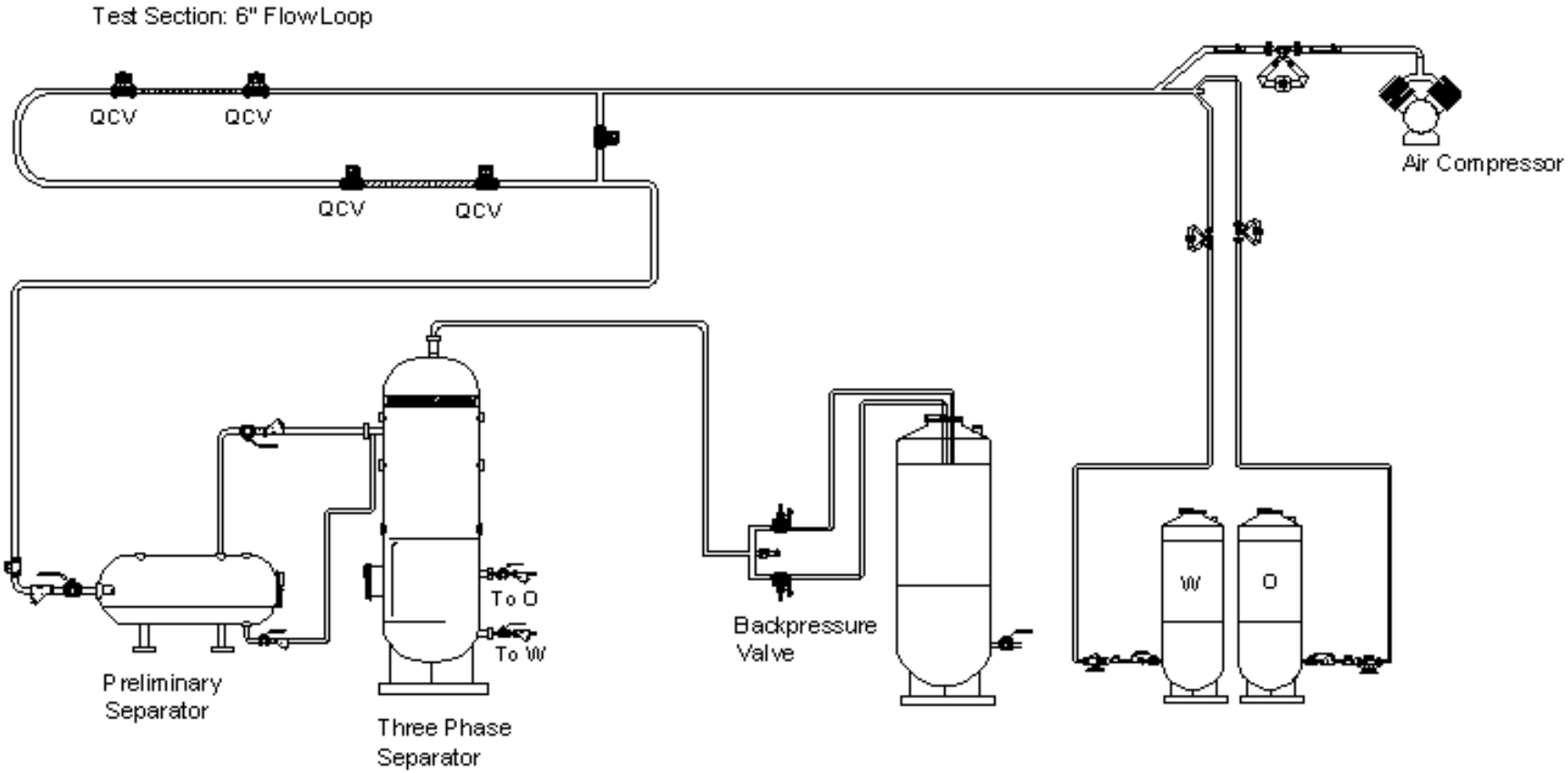

Figure 1: Schematic of Modified Flow Loop

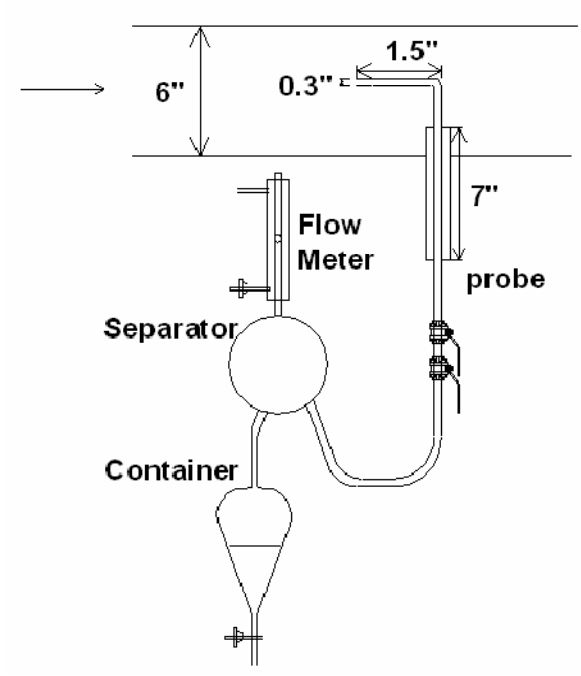

Figure 2: Iso-kinetic Sampling Probe.

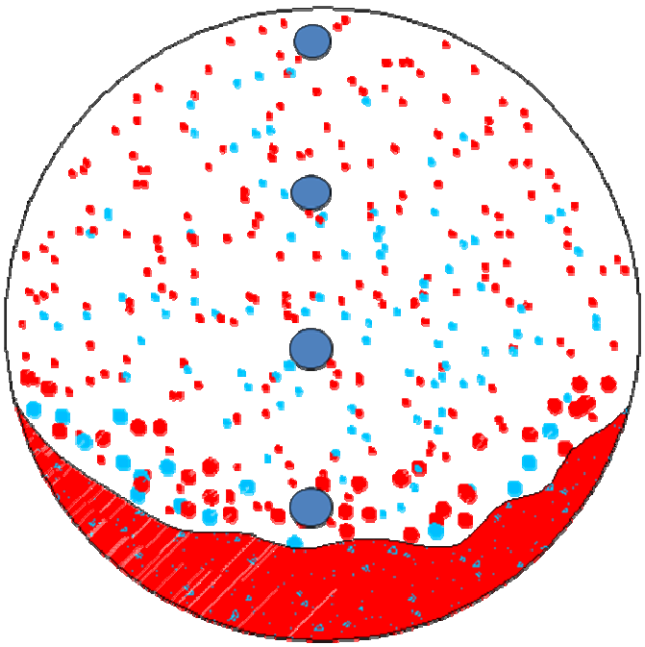

Figure 3: Positions of Iso-kinetic Probe

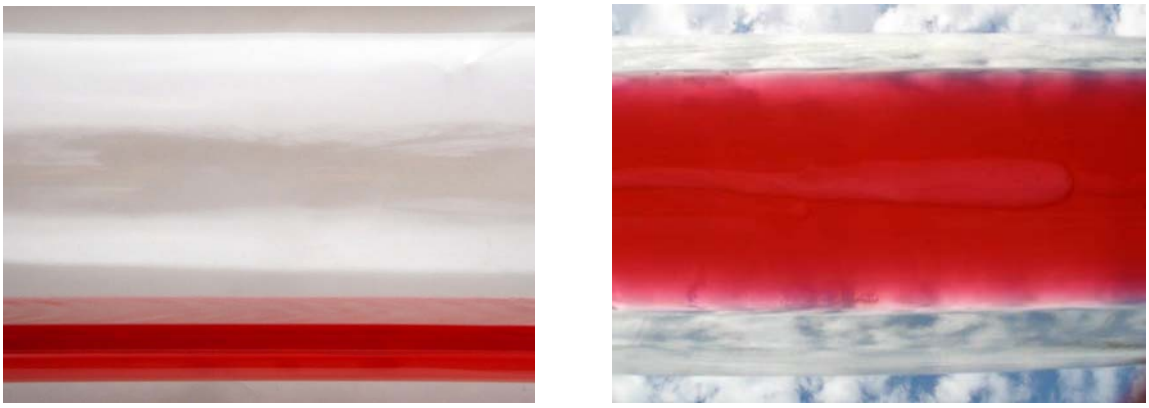

(a) (b)

Figure 4: Gas-Liquid-Stratified Smooth/Oil-Water- Oil with Discontinuous Water Strip. (a) Side View. (b) Bottom View

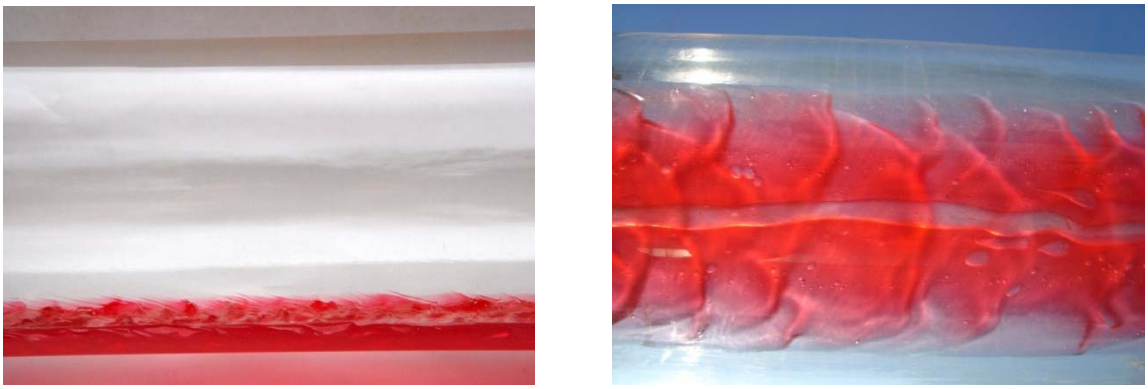

(a) (b)

Figure 5: Gas-Liquid-Stratified Wavy/Oil-Water- Oil with Channel Water and Dispersion of Water In Oil. (A) Side View. (B) Bottom View.

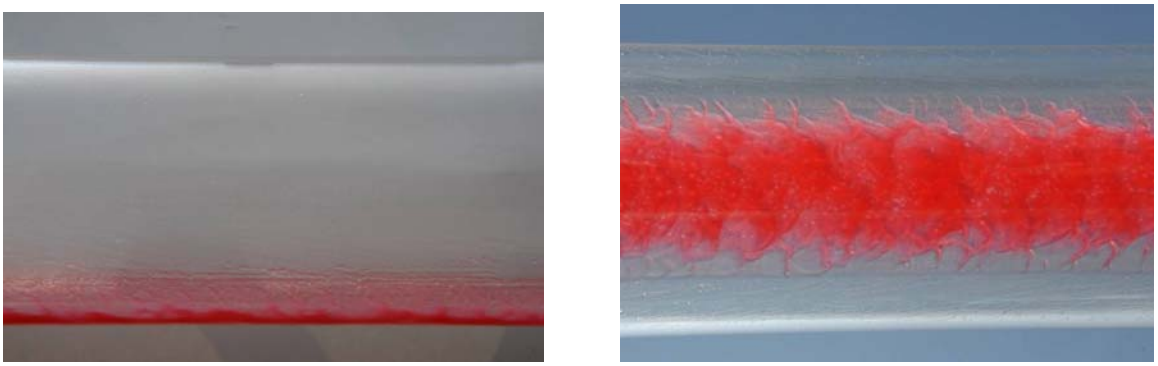

(a) (b)

Figure 6: Gas-Liquid-Stratified Wavy/Oil-Water- Water in Oil Dispersion. (A) Side View. (B) Bottom View.

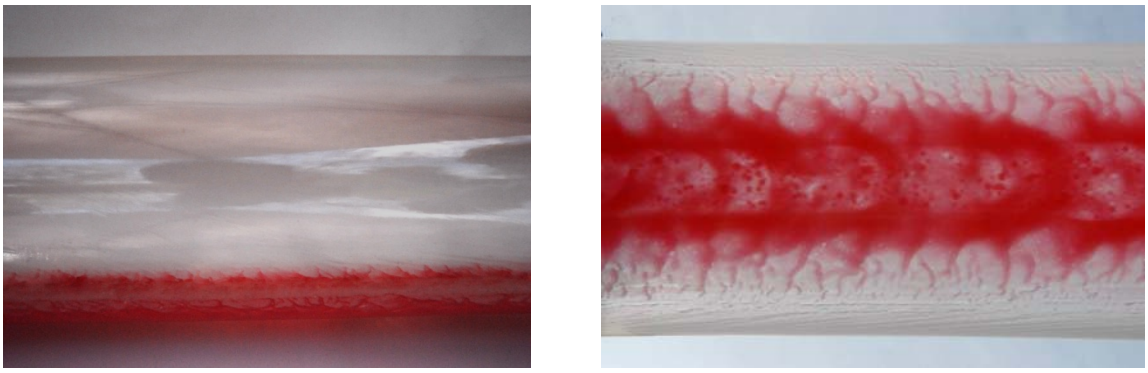

(a) (b)

Figure 7: Gas-Liquid-Stratified Wavy/Oil-Water-Channel Water and Dual Dispersion. (A) Side View. (B) Bottom View.

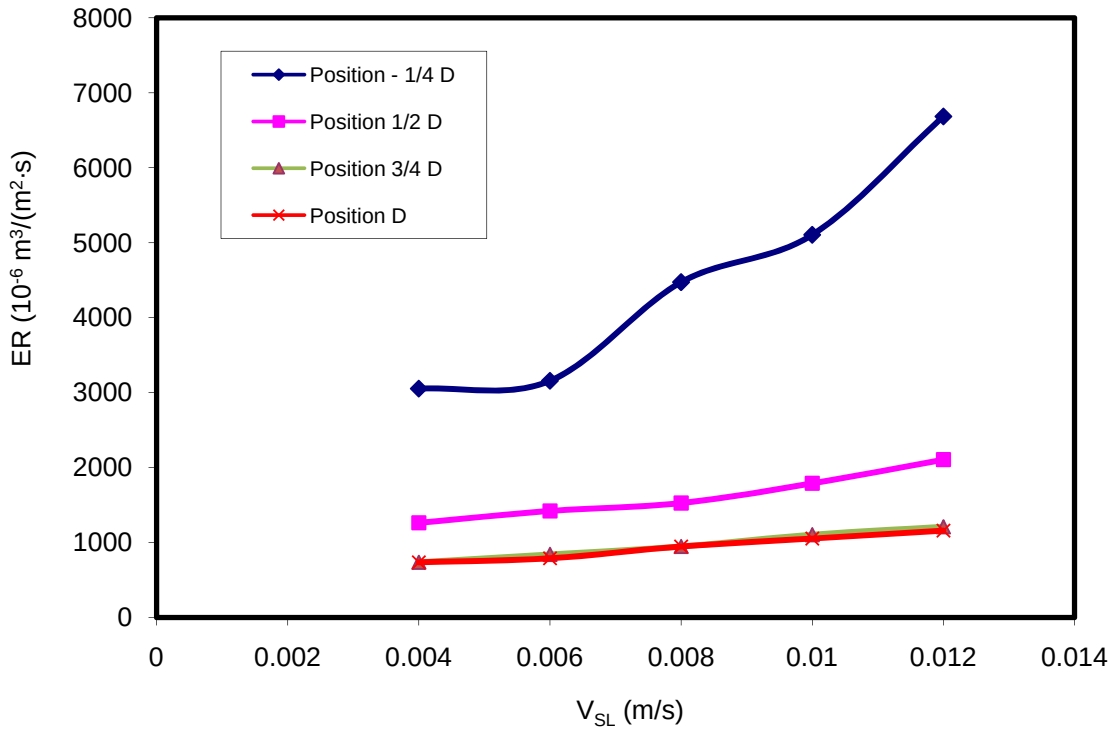

Figure 8: Variation of Liquid Entrainment Rate with Superficial Liquid Velocity (v_{Sg} = 16.5 m/s and WC=0 %)

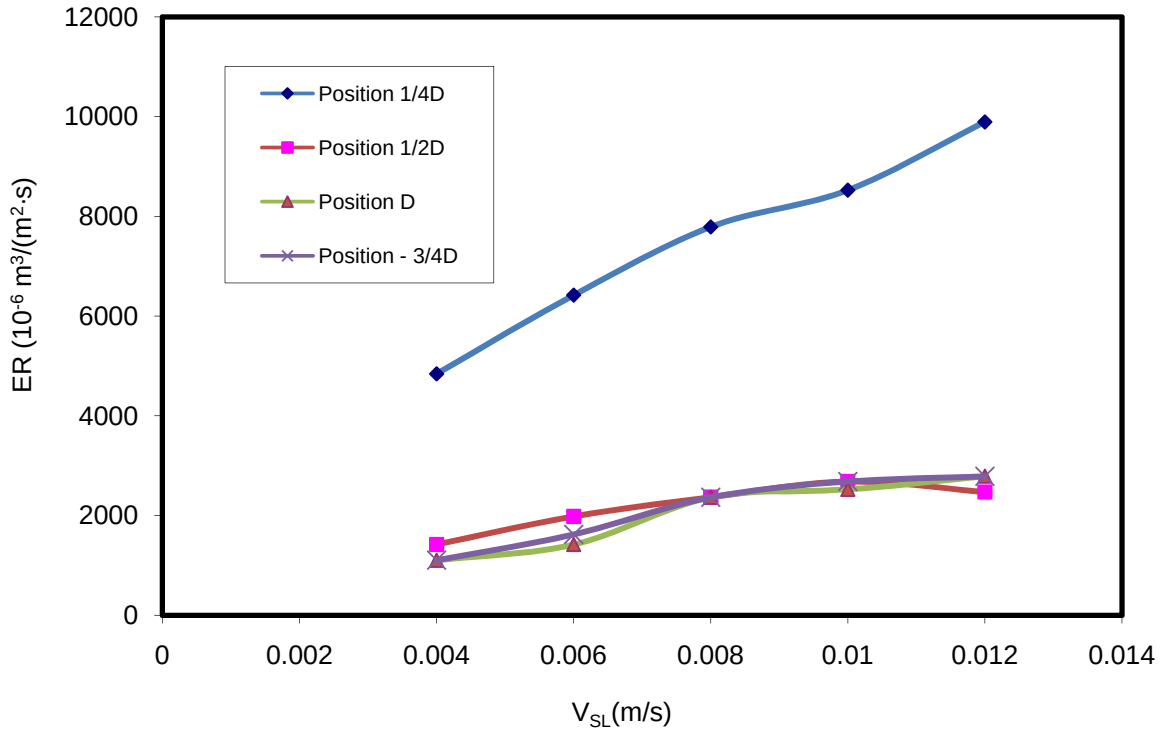

Figure 9: Variation of Liquid Entrainment Rate with Superficial Liquid Velocity (v_{Sg} = 18.5 m/s and WC=0 %)

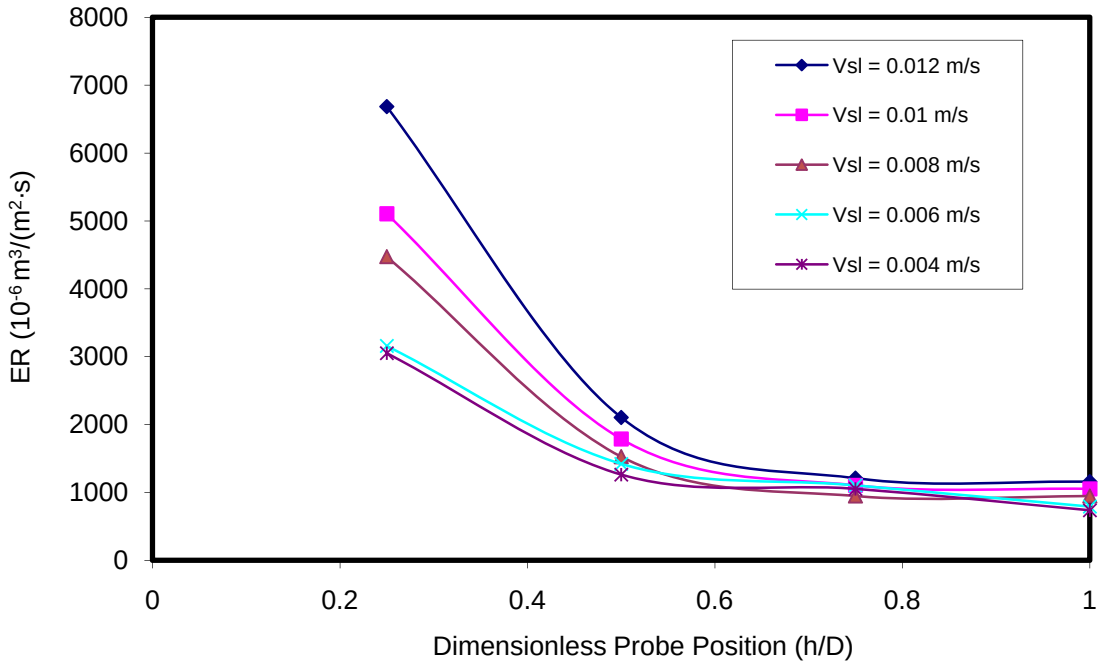

Figure 10: Total Liquid Entrainment Rate Profile (v_{Sg} = 16.5 m/s and WC = 0%)

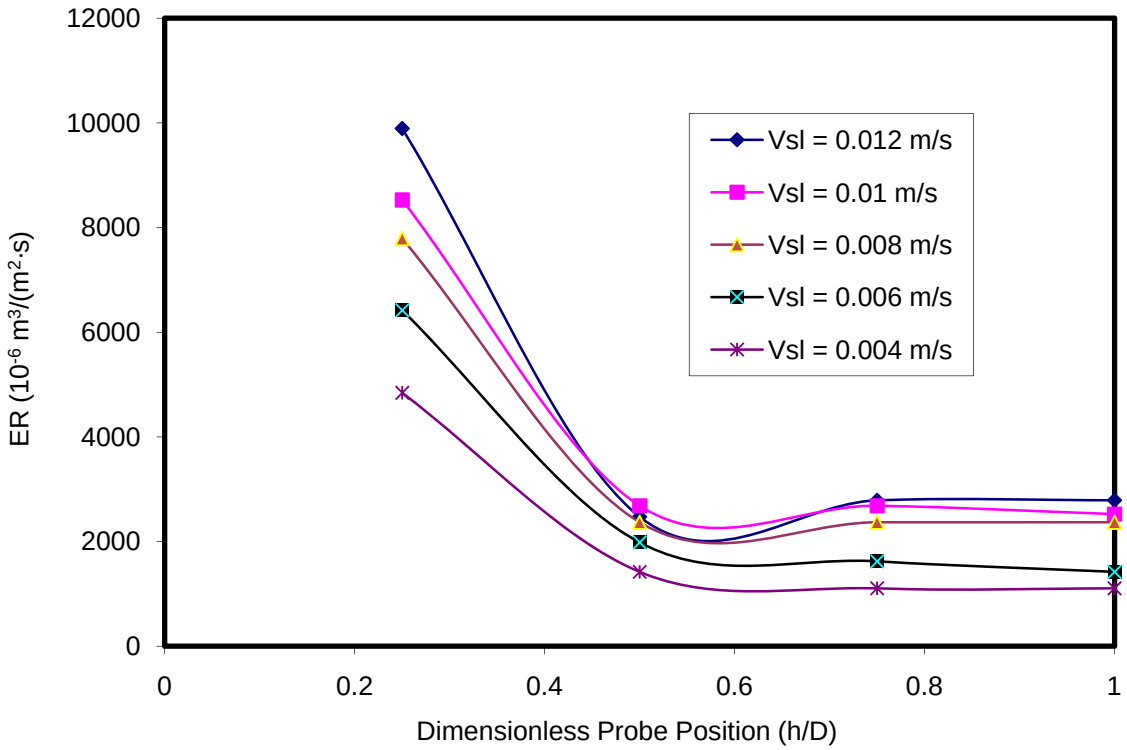

Figure 11: Total Liquid Entrainment Rate Profile (v_{Sg} = 18.5 m/s and WC = 0%)

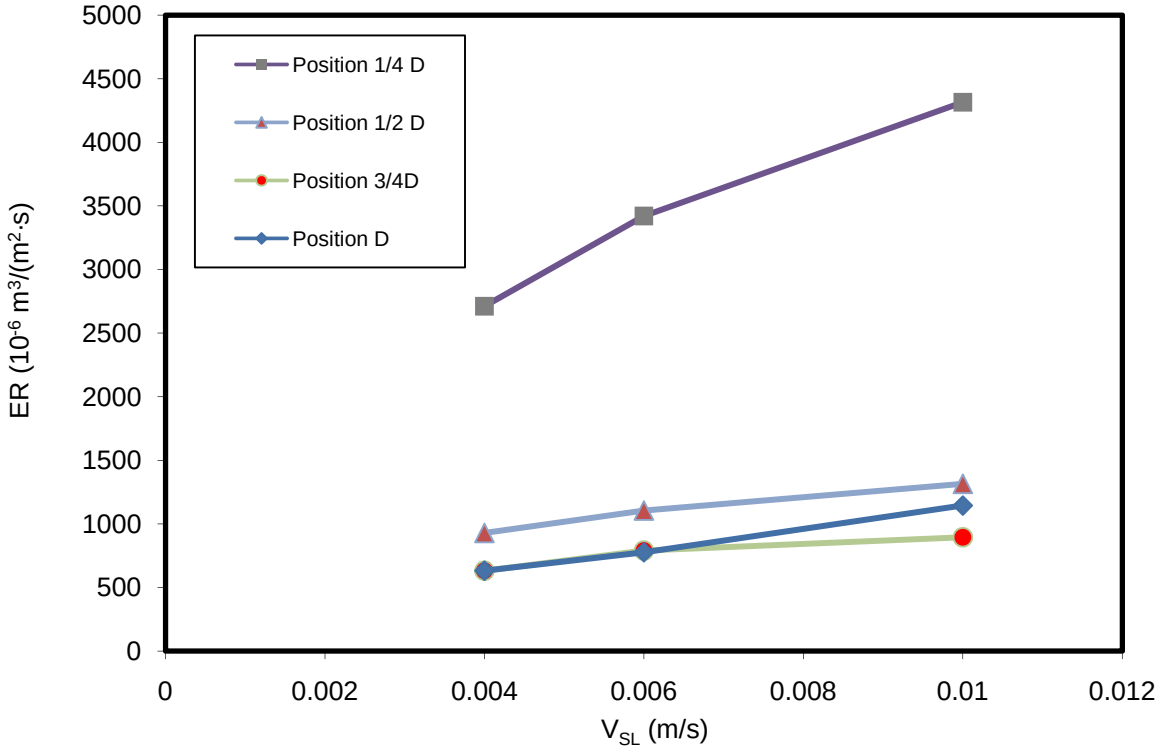

Figure 12: Variation of Liquid Entrainment Rate with Superficial Liquid Velocity (v_{Sg} = 16.5 m/s and WC= 5%)

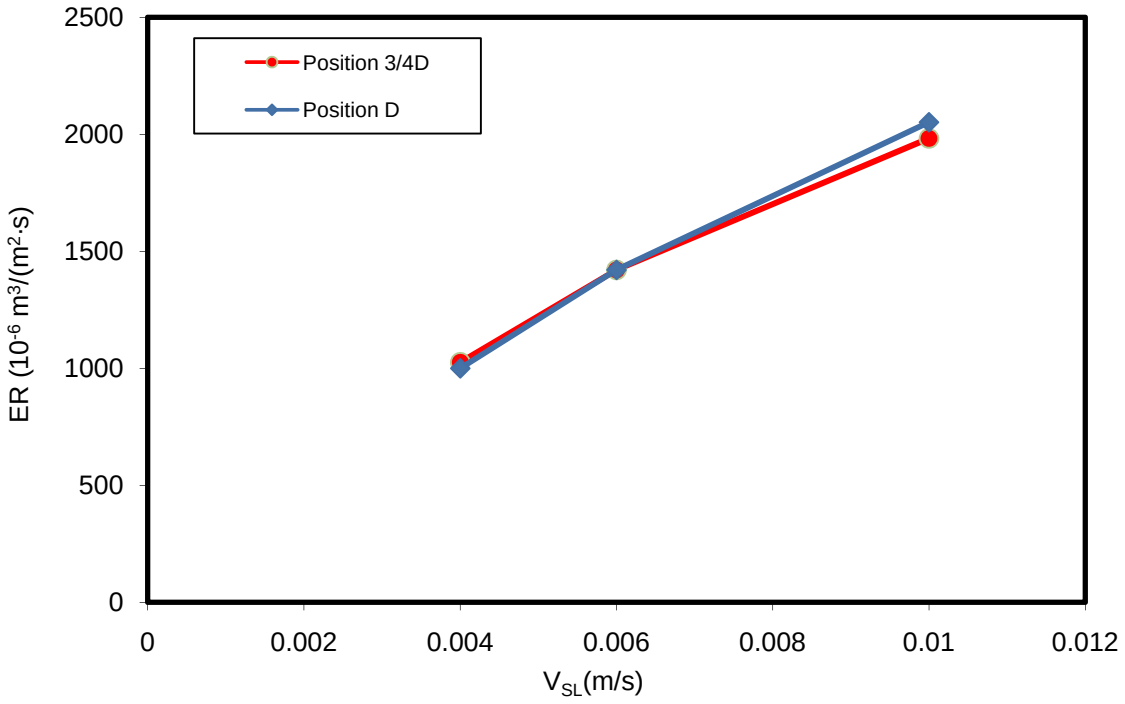

Figure 13: Variation of Liquid Entrainment Rate with Superficial Liquid Velocity (v_{Sg} = 18.5 m/s and WC = 5%)

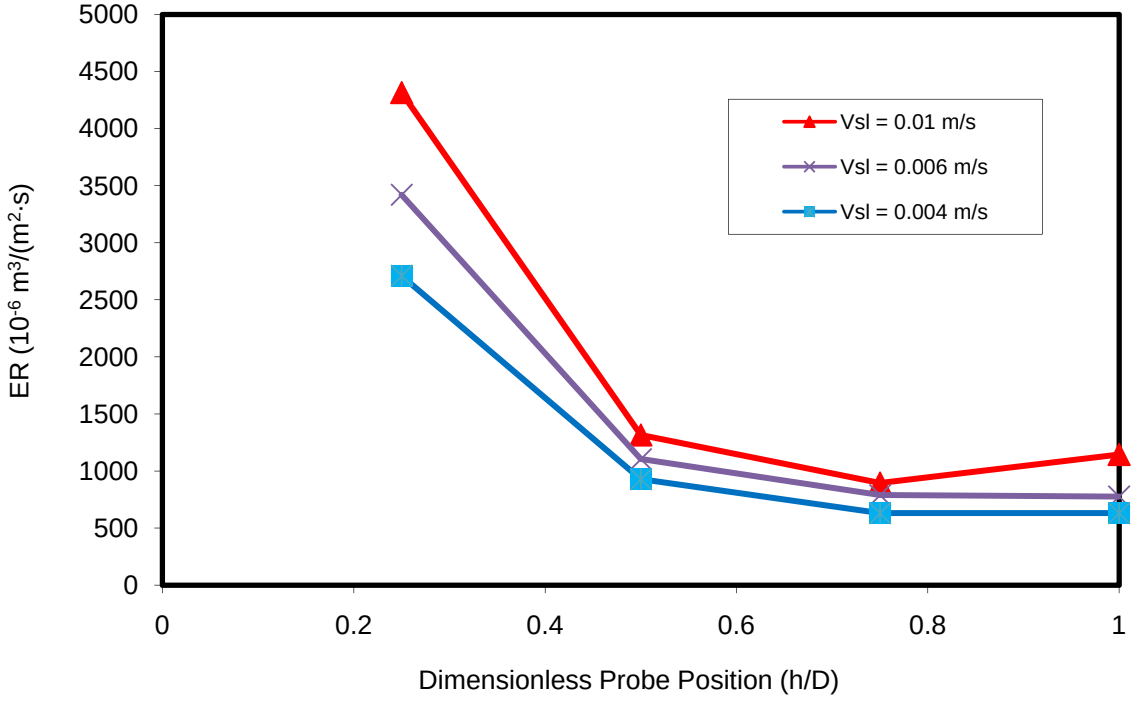

Figure 14: Total Liquid Entrainment Rate Profile (v_{Sg} = 16.5 m/s and WC = 5%)

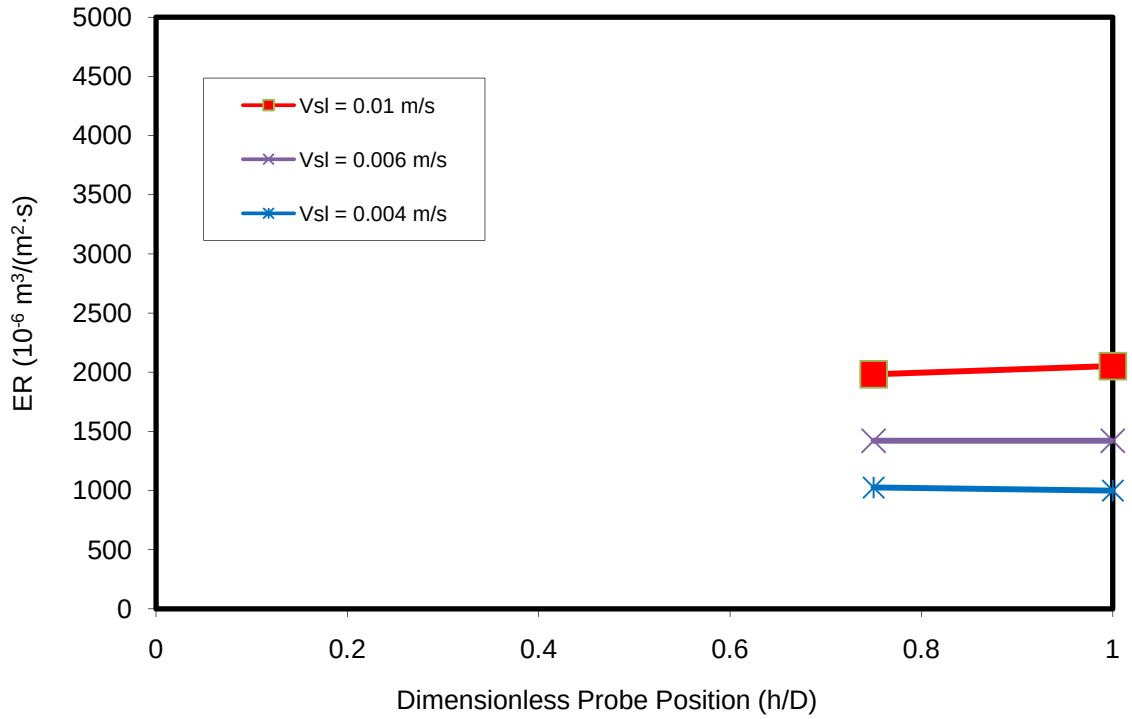

Figure 15: Total Liquid Entrainment Rate Profile (v_{Sg} = 18.5 m/s and WC = 5%)

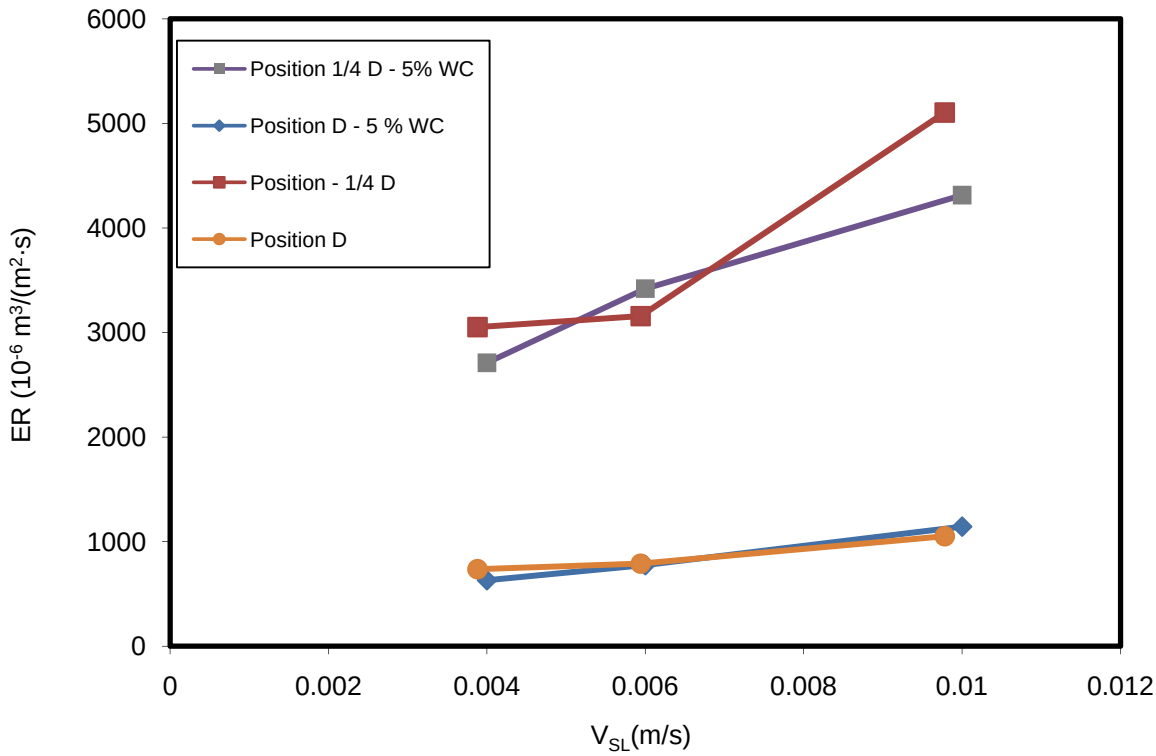

Figure 16: Variation of Total Liquid Entrainment Rate with Superficial Gas Velocity (v_{Sg} = 16.5 m/s WC = 0% and 5 %)

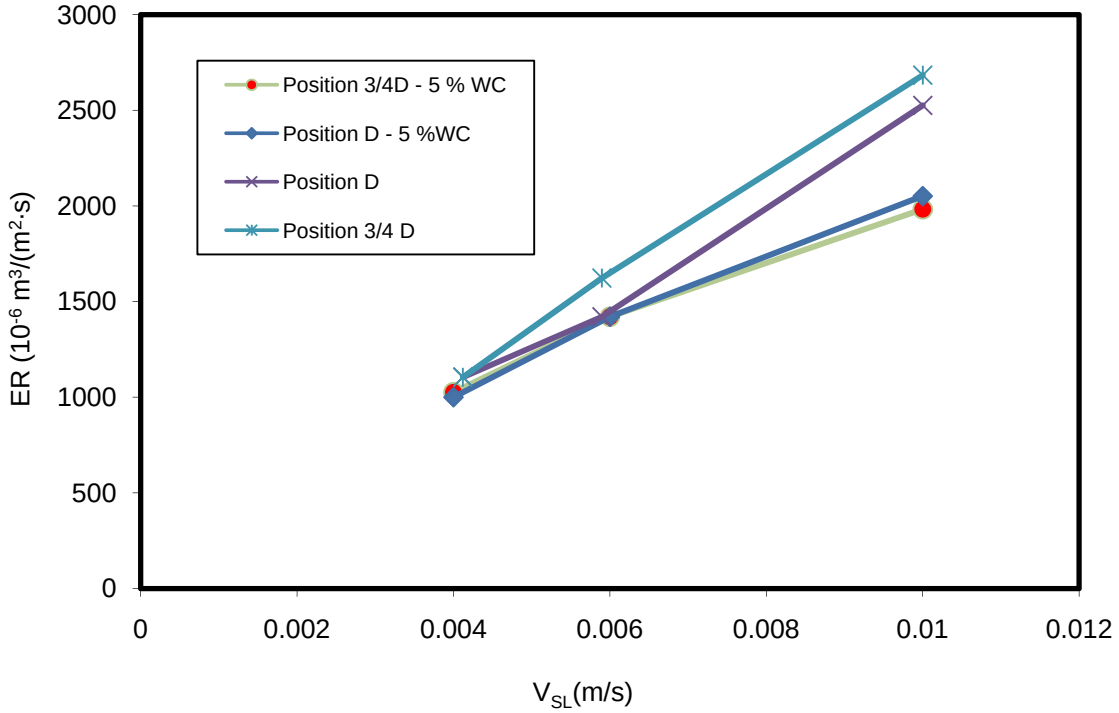

Figure 17: Variation of Total Liquid Entrainment Rate with Superficial Gas Velocity (v_{Sg} = 18.5 m/s WC = 0% and 5 %)

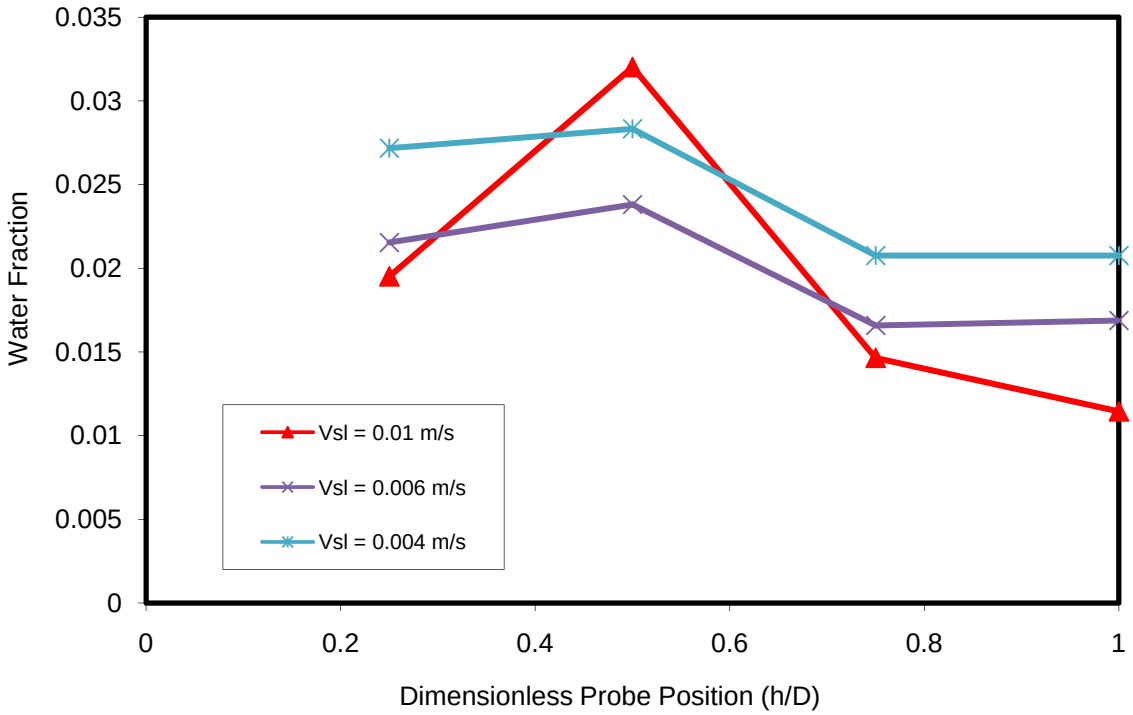

Figure 18: Water Fraction Profile in Total Liquid Entrainment (v_{Sg} = 16.5 m/s and WC = 5 %)

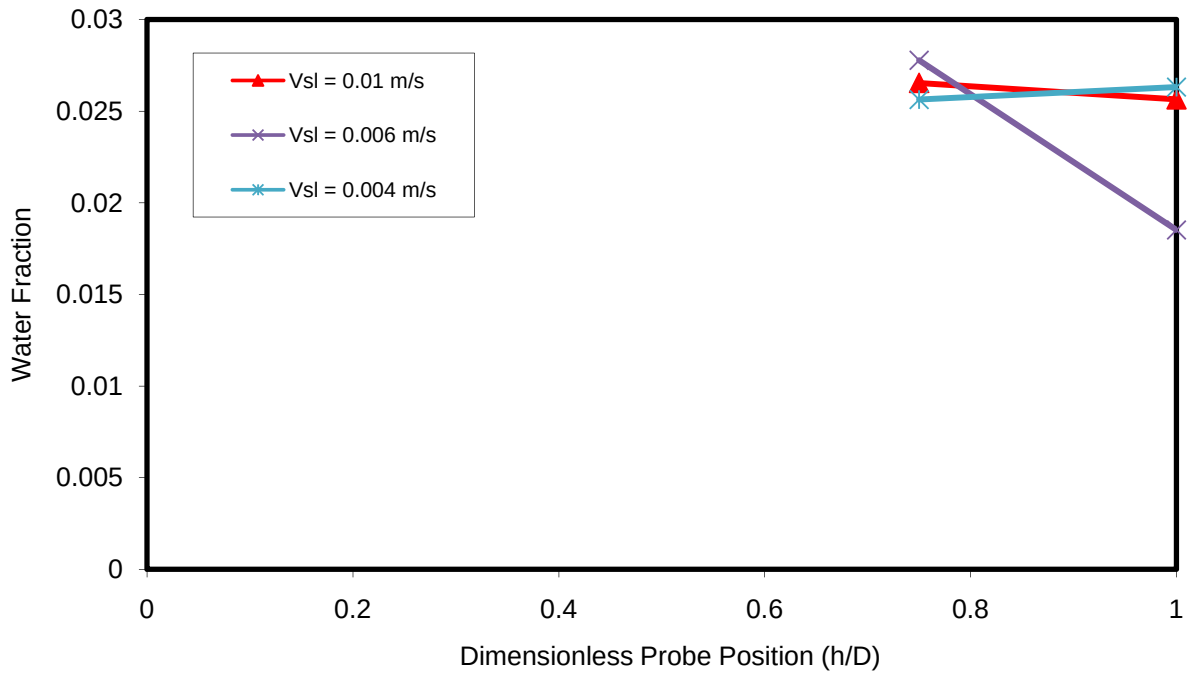

Figure 19: Water Fraction Profile in Total Liquid Entrainment (v_{Sg} = 18.5 m/s and WC = 5 %)

Fluid Flow Projects

Executive Summary of Research Activities

Cem Sarica

Advisory Board Meeting, May 12, 2010

High Viscosity Multiphase Flow

- Significance
  - Discovery of High Viscosity Oil Reserves
- Objective
  - Development of Better Prediction Models
- Past Studies
  - First TUFFP Study by Gokcal (2005)
    - Existing Models Perform Poorly for Viscosities Between 200 and 1000 cp
    - Significantly Different Flow Behavior
      - Dominance of Slug Flow
  - Recent Study by Gokcal (2008)
    - New Drift Velocity and Translational Velocity Closure Models
    - New Slug Frequency Correlation

High Viscosity Multiphase Flow …

- Current Study (Status)
  - Slug Liquid Holdup Closure Relationship Development
  - Drift Velocity Study
  - Slug Length Closure Relationship Development

High Viscosity Multiphase Flow …

- Slug Liquid Holdup
  - Literature Review Complete
  - Liquid Holdup Measurement Methods
    - Quick Closing Valves
    - Capacitance Sensor
  - Data Analysis and Testing of Existing Correlations and Models are Performed for One Oil Viscosity
  - Tests will Continue in Summer

High Viscosity Multiphase Flow …

- Drift Velocity Study
  - 6 in. ID Tests are Completed
  - Drift velocity
    - Decreases with Increase in Liquid Viscosity
    - Increases with Increase in Pipe Diameter
  - Need a Unified Drift Velocity Closure Relationship

High Viscosity Multiphase Flow …

- Slug Length Study
  - Shorter Slug Lengths are experimentally Observed
  - Significant Progress in Probabilistic/Deterministic Modeling of Slug Length Study

High Viscosity Multiphase Flow …

- Continuation Study
  - Inclination Angle Effects
  - Higher Viscosity Oils (1,000 – 10,000 cp)

Fluid Flow Projects

Effects of High Oil Viscosity on Slug Liquid Holdup in Horizontal Pipes

Ceyda Kora

Advisory Board Meeting, May 12, 2010

Outline

- Objectives
- Introduction
- Literature Survey
- Experimental Study
- Model Comparison
- Near Future Tasks
- Project Schedule

Objectives

- Investigate Slug Liquid Holdup for High Viscosity Oil and Gas Flow
- Develop Closure Models for Slug Liquid Holdup

Introduction

- Increase in Consumption of Hydrocarbon Resources
- Decline in Discoveries of Low Viscosity Oils
- Previous Studies Based on Low Viscosity Oils

Introduction

- Gokcal (2005, 2008) Studies
  - Intermitted Flow Observed as Dominant Flow Pattern
  - Significant Effect of High Viscosity Oil on Slug Flow Characteristics Observed
  - TUFFP Unified Model Modified for High Viscosity Oil-Gas Flow

Literature Review Summary

- Available Multiphase Flow Models Developed for Low Viscosity Liquids
- Few Studies Include Liquid Viscosity Effect on Slug Characteristics
- Limited Experimental Data on High Viscosity Oil Multiphase Flow

Experimental Facility

Fluid Flow Projects

Advisory Board Meeting, May 12, 2010

Experimental Facility …

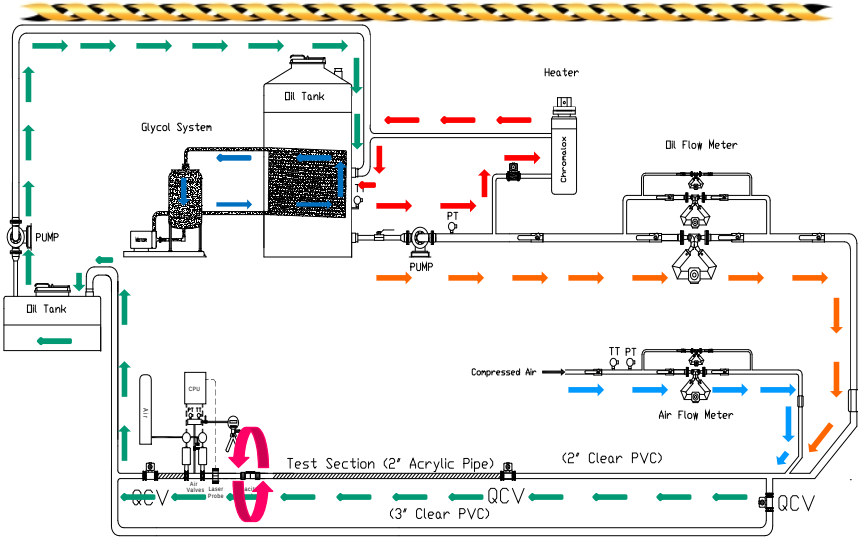

Fluid Flow Projects

Advisory Board Meeting, May 12, 2010

Test Fluids

- Citgo Sentry 220
  - Mineral Oil
  - API Gravity: 27.6 °
  - Viscosity: 0.22 Pa·s @ 40 °C
  - Specific Gravity: 0.89 @ 25 °C
- Air

Testing Range

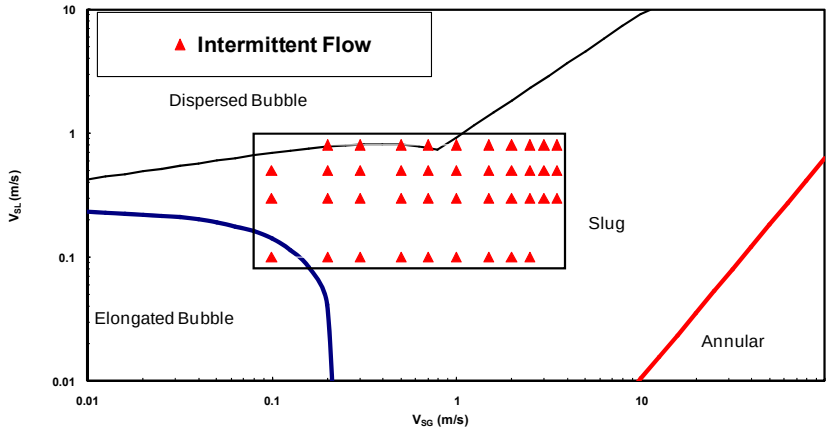

Testing Range …

- Superficial Liquid Velocity
  - 0.1 – 0.8 m/s
- Superficial Gas Velocity
  - 0.1 – 3.5 m/s
- Temperatures
  - 21.1 – 37.8 °C (70 – 100 °F)
  - 0.587 – 0.181 Pa·s
- Inclination
  - Horizontal

Experimental Study

- Quick-Closing Valve
- Capacitance Sensor
- Differential Pressure Transducer

Quick-Closing Valves System

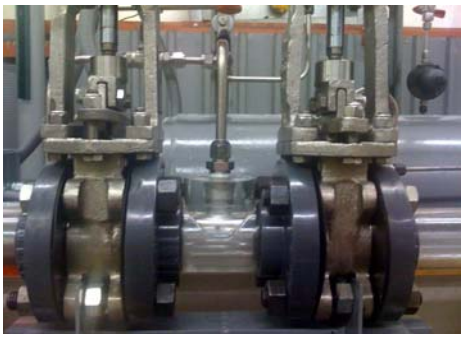

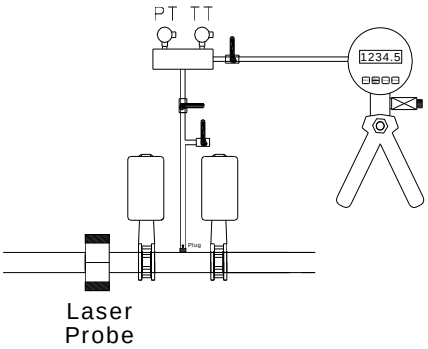

Quick-Closing Valves System …

- Challenges
  - Axial Variation of Holdup in Liquid Slug
  - Slug Length
  - Velocity of Slugs
  - Time

Capacitance Sensor

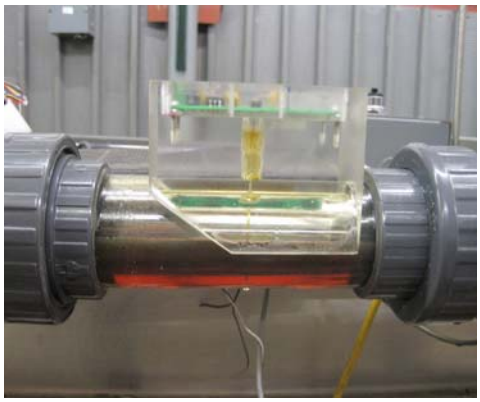

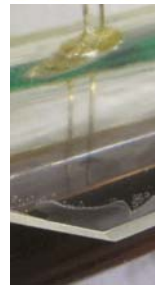

Capacitance Sensor …

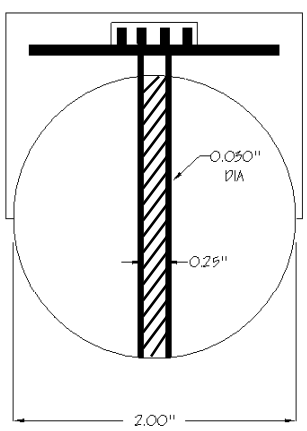

- **Dimensionless Voltage**

$$V^* = \frac{V_{read} - V_{\min}}{V_{\max} - V_{\min}}$$

- **Liquid Holdup**

$$H_{Ls} = \frac{A_{liquid}}{A_{total}}$$

Capacitance Sensor …

- Static Calibration

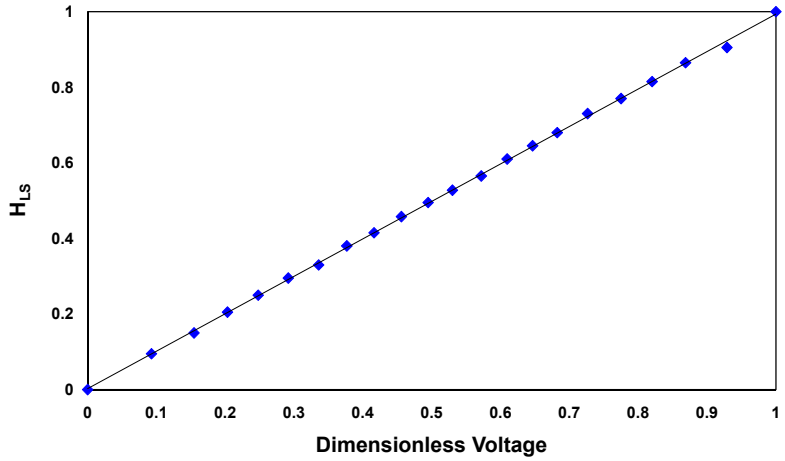

Capacitance Sensor …

- Dynamic Calibration

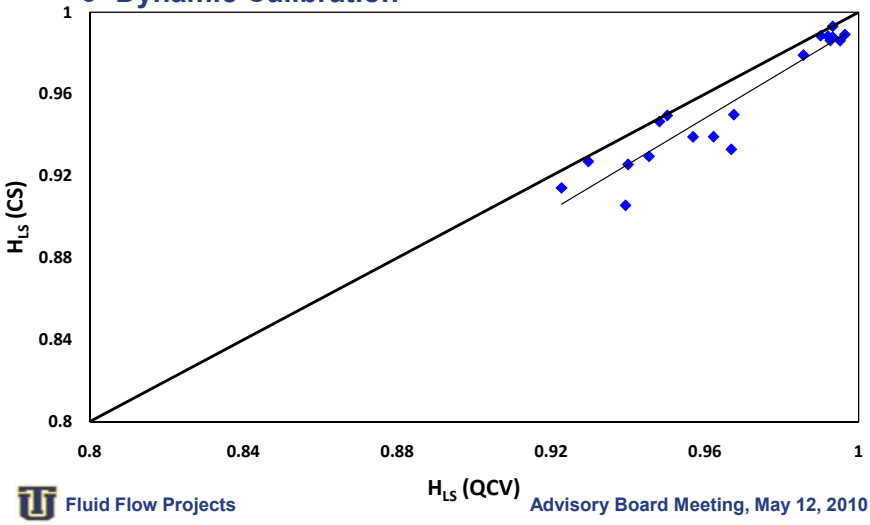

Capacitance Sensor …

- Provide Information About Slug Characteristics
  - Slug Liquid Holdup
  - Bubble Sizes
  - Large Bubble Locations
  - Number of Large Bubbles
  - Liquid Film Holdup (H_{LF})

Capacitance Sensor …

- Liquid Film Holdup (H_{LF})
  - Low Flow Rates
    - Slight Decrease in H_{LF} Along Liquid Film due to Velocity Decrease from Beginning to End
  - Higher Flow Rates
    - After Slug Passed, Slight Increase in H_{LF} due to Top Oil Film Drainage
    - Slight Decrease in H_{LF}

Capacitance Sensor …

- v_{SL} = 0.1 m/s & v_{SG} = 0.1 m/s

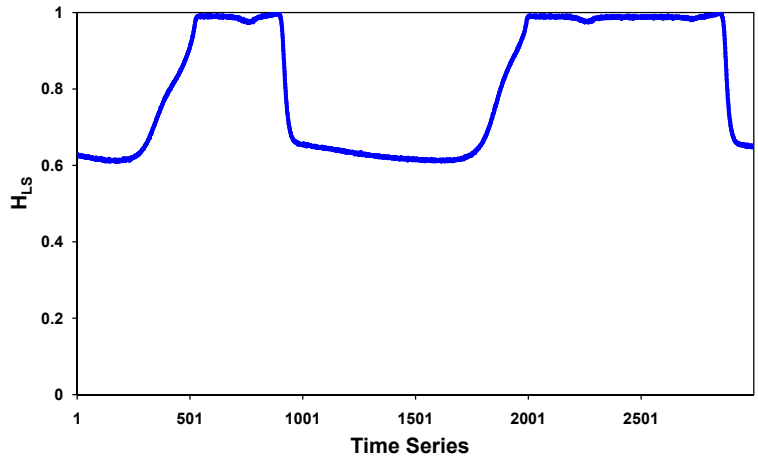

Capacitance Sensor …

- v_{SL} = 0.1 m/s & v_{SG} = 0.1 m/s Video

Capacitance Sensor …

- v_{SL} = 0.5 m/s & v_{SG} = 1 m/s

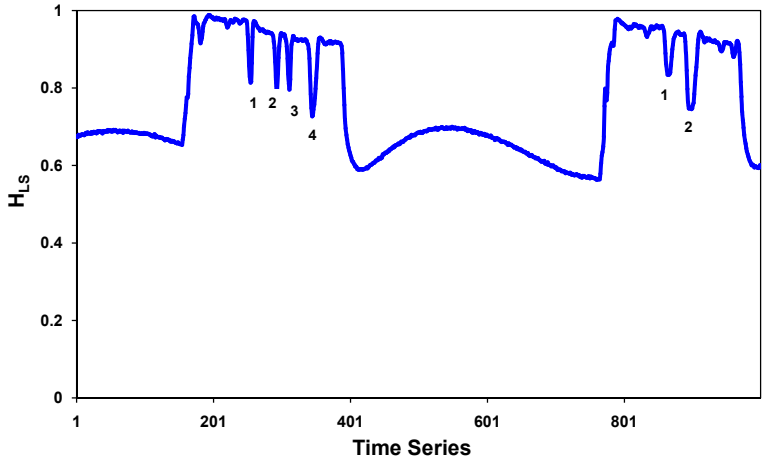

Capacitance Sensor …

- v_{SL} = 0.5 m/s & v_{SG} = 1 m/s Video

Differential Pressure Sensor

- Existing Differential Pressure Transducers Modified to Prevent Gas Bubble Penetration and Oil Drainage Problem into the Transmission Line
- Flush Diaphragm Pressure Transducers Utilized
- Slow to Detect the Pressure Change
- Abandoned

Experimental Results

- Quick-Closing Valve
- Capacitance Sensor

Experimental Results (QCV) …

- Slug Liquid Holdup
  - 98 Tests, 17 Data Points
    - μ_{oil} = 0.587 Pa·s (70 ºF)
    - v_{SL} = 0.1 - 0.8 m/s
    - v_{SG} = 0.1 - 2 m/s

Experimental Results …

- Quick-Closing Valve (H_{LS})

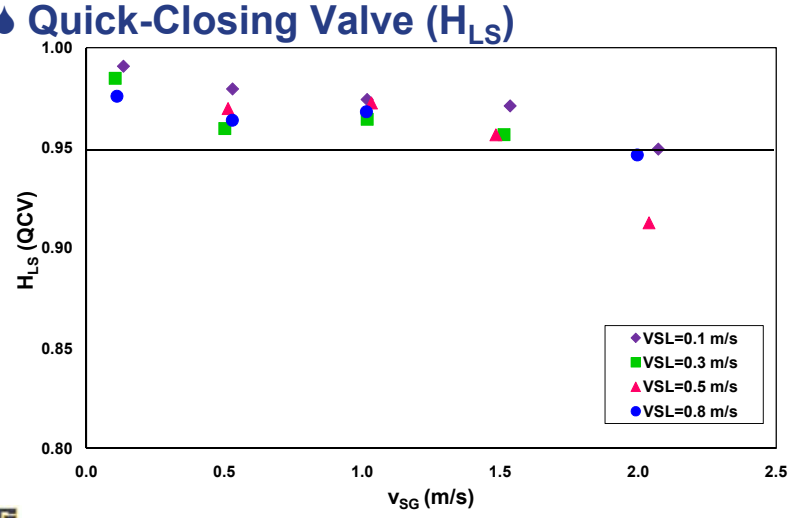

Experimental Results (QCV) …

- Liquid Film Holdup
  - 53 Tests, 19 Data Points
    - μ_{oil} = 0.587 Pa·s (70 ºF)
    - v_{SL} = 0.1 - 0.8 m/s
    - v_{SG} = 0.1 - 2 m/s

Experimental Results …

- Quick-Closing Valve (H_{LF})

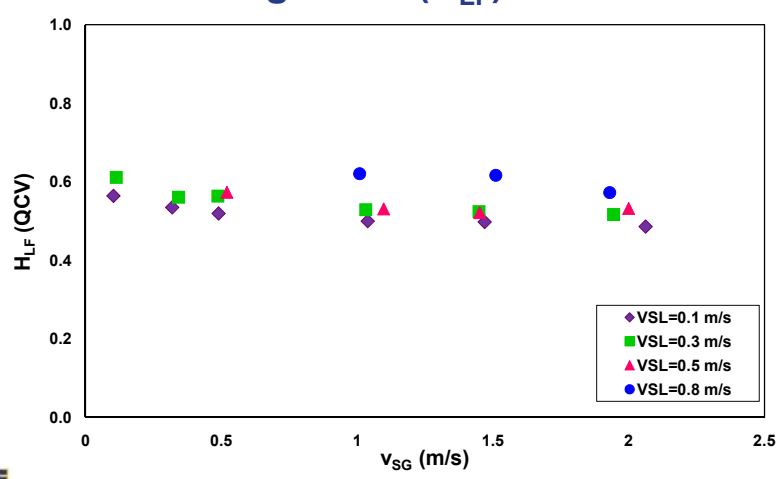

Experimental Results (CS) …

- Slug Liquid Holdup
  - 77 Tests, 36 Data Points
    - μ_{oil} = 0.587 Pa·s (70 ºF)
    - v_{SL} = 0.1 - 0.8 m/s
    - v_{SG} = 0.1 – 3.5 m/s

Experimental Results …

- Capacitance Sensor (H_{LS})

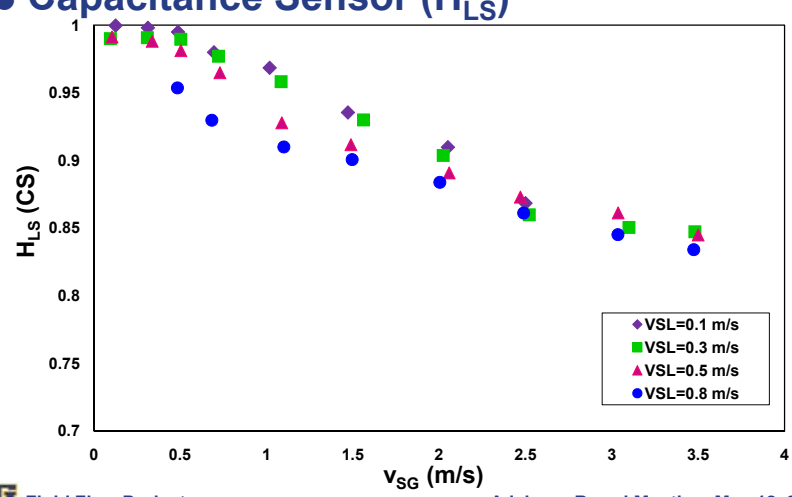

Experimental Results …

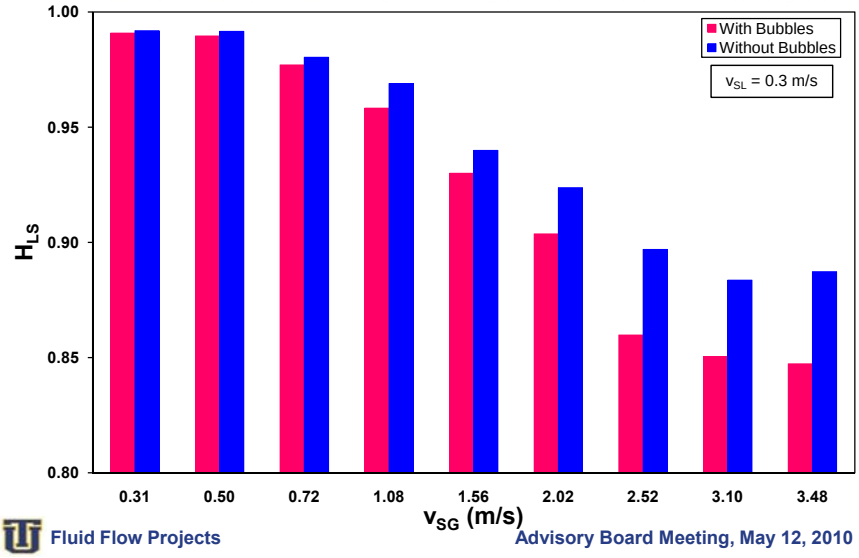

Fluid Flow Projects

Advisory Board Meeting, May 12, 2010

Experimental Results …

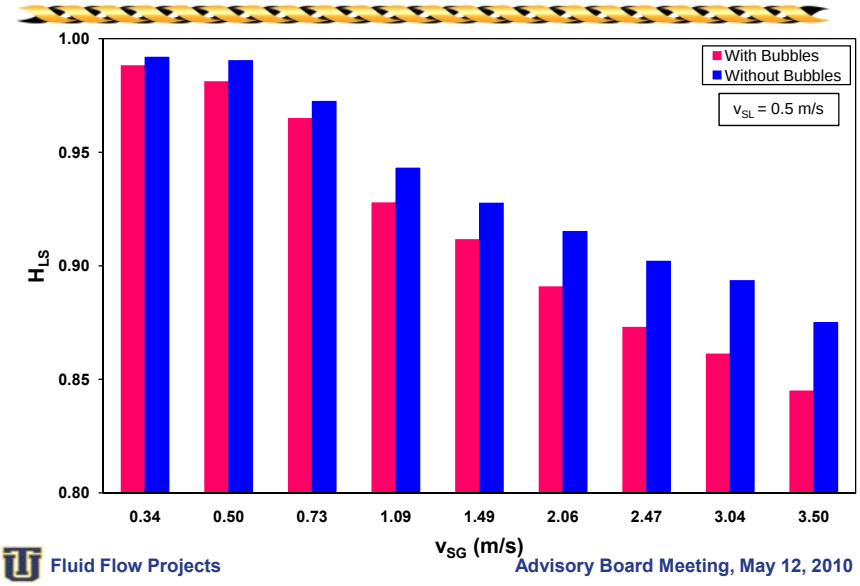

Fluid Flow Projects

Advisory Board Meeting, May 12, 2010

Experimental Results …

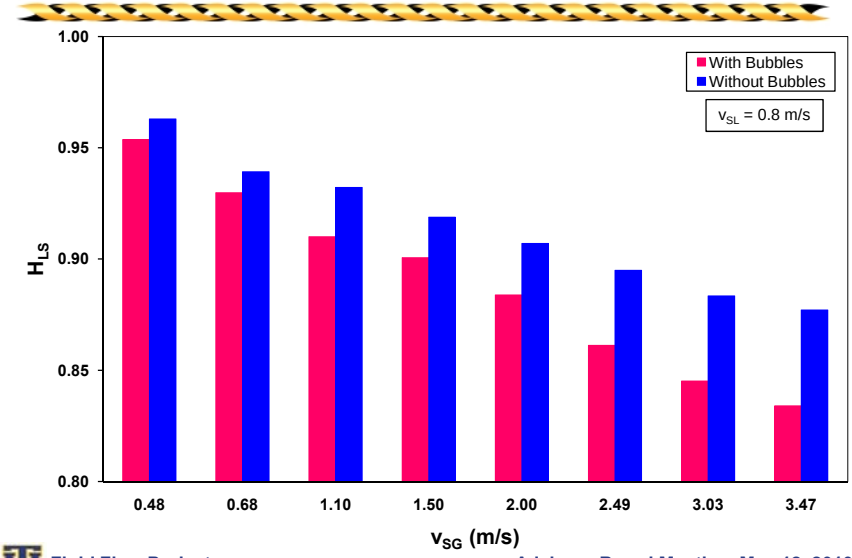

Fluid Flow Projects

Advisory Board Meeting, May 12, 2010

Model and Correlation Evaluation

- Capacitance Sensor (H_{Ls}) $v_{SG} \leq 1$ m/s

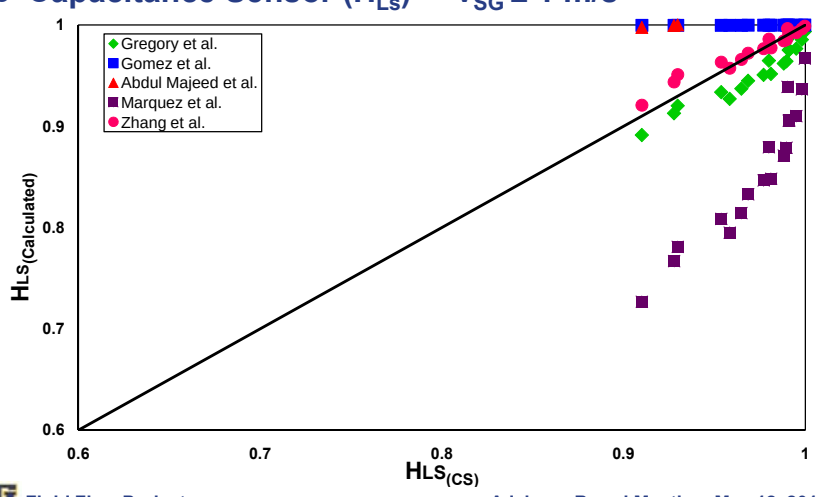

Fluid Flow Projects

Advisory Board Meeting, May 12, 2010

Model and Correlation Evaluation

- Capacitance Sensor (H_{Ls}) $v_{SG} \leq 1$ m/s

Correlation/Model	ε_1 (%)	ε_2 (%)	ε_3 (%)	ε_4 (-)	ε_5 (-)	ε_6 (-)
Gregory *et al.*	-1.95	1.95	0.82	-0.02	0.02	0.01
Gomez *et al.*	2.95	2.95	2.88	0.03	0.03	0.03
Abdul-Majeed	3.29	3.29	2.63	0.03	0.03	0.02
Marquez *et al.*	-12.00	12.00	4.62	-0.12	0.12	0.04
Zhang *et al.*	0.35	0.55	0.77	0.00	0.01	0.01

Model and Correlation Evaluation

- Capacitance Sensor (H_{Ls}) $v_{SG} > 1$ m/s

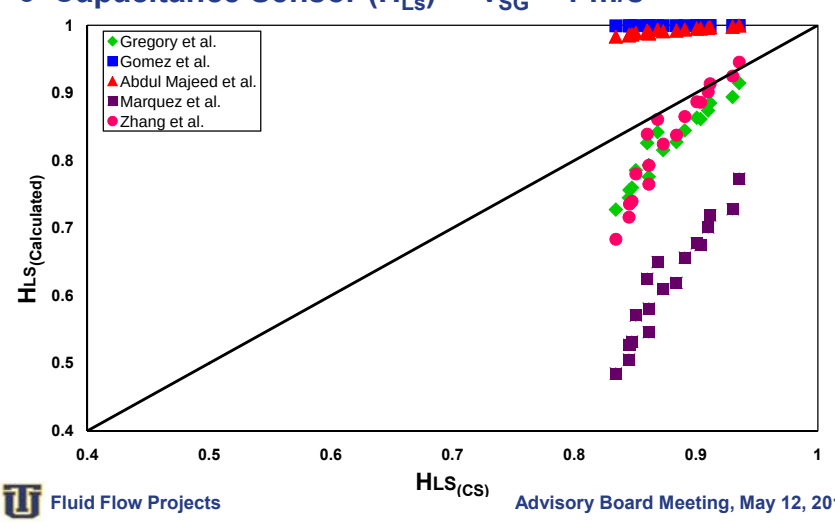

Model and Correlation Evaluation

- Capacitance Sensor (H_{Ls}) v_{SG} > 1 m/s

Correlation/Model	ε_1 (%)	ε_2 (%)	ε_3 (%)	ε_4 (-)	ε_5 (-)	ε_6 (-)
Gregory *et al.*	-6.57	6.57	3.32	-0.06	0.06	0.03
Gomez *et al.*	13.91	13.91	3.96	0.12	0.12	0.03
Abdul-Majeed	12.99	12.99	3.42	0.11	0.11	0.03
Marquez *et al.*	-29.52	29.52	7.11	-0.26	0.26	0.05
Zhang *et al.*	-5.96	6.10	5.89	-0.05	0.05	0.05

Future Tasks

- Conduct Experiments with Capacitance sensor for 0.378, 0.257 and 0.181 Oil Viscosities
- Evaluation of the Acquired Data from Capacitance Sensor
- Collect and Evaluate Data for Liquid Film Holdup with Capacitance Sensor
- Compare Experimental Data with Existing Models
- Develop a New Closure Relationship If Necessary

Project Schedule

Literature Review	Completed
Facility Modifications	Completed
Preliminary Testing	Completed
Testing	June 2010
Data Evaluation	July 2010
Final Report	August 2010

Questions & Comments

Effects of High Oil Viscosity on Slug Liquid Holdup in Horizontal Pipes

Ceyda Kora

PROJECTED COMPLETION DATES:

Literature Review .....Completed
Facility Modifications .....Completed
Preliminary Testing .....Completed
Testing .....June 2010
Data Evaluation .....July 2010
Final Report .....August 2010

Objectives

The main objectives of this study are,

- Investigation of slug liquid holdup for high viscosity oil and gas flow,
- Development of closure models for slug liquid holdup.

Introduction

Heavy oils are produced and transported from many places around the world. Because of the increased consumption of hydrocarbon resources and decline in discoveries of low viscosity oils, the importance of heavy oil has increased. It is important to design a proper production system in order to eliminate operational problems for high oil viscosity fields. Available multiphase flow models are primarily developed for low viscosity liquids. TUFFP has been studying the high viscosity oil multiphase flow systematically since 2005, and has made significant progress towards the improvements in high viscosity oil multiphase flow prediction.

The first experimental study at TUFFP on high viscosity oil was completed by Gokcal (2005). The effects of high oil viscosity on oil-gas two-phase flow behavior were investigated and significant changes in flow behavior were observed. Intermitted flow (slug and elongated bubble) is the dominant flow pattern for high viscosity oil and air flow. Slug characteristics need to be examined in detail for better understanding of high liquid viscosity effect.

An experimental and theoretical investigation of slug flow for high oil viscosity in horizontal pipes was completed by Gokcal in 2008. He developed models for drift velocity, transitional velocity and slug frequency by taking into account the viscosity effect. Slug liquid holdup was not studied due to a lack of proper instrumentation. Only average liquid holdup was measured in his study. Therefore, investigation of slug liquid holdup for high viscosity oil and gas two-phase flow is the focus of this study.

The most challenging part of this study is to measure gas void fraction in liquid slugs. For the measurement of slug liquid holdup, a new capacitance sensor (CS) has been developed, tested and experiments were conducted at 70 °F. Moreover, slug liquid holdup was measured with the quick-closing valve system. High viscosity oil and air two-phase flow experiments will continue to collect slug liquid holdup data at different flow rates and temperatures for horizontal pipe.

Literature Review

Most of the previous studies on slug liquid holdup focused on low oil viscosity. Some investigated the effects of oil viscosity on slug liquid holdup. However, these studies are not adequate to fully understand the effect of high viscosity on slug liquid holdup. Many of these studies were reviewed at the March 2009 TUFFP Advisory Board meeting.

Experimental results are compared with four different liquid holdup correlations and a mechanistic model. Gregory *et al.* (1978) conducted experiments on liquid holdup in slugs with two horizontal pipes with different diameters: 2.58 and 5.12 cm. In their correlation, they assumed the slug to be homogenous.

$$H_L = \frac{1}{1+\left(\frac{v_M}{8.66}\right)^{1.39}} \quad (1)$$

Gomez *et al.* (2000) proposed a dimensionless correlation for liquid holdup in the slug body for horizontal to upward vertical flows. They established their empirical correlation by considering inclination angle and Reynolds number. Although this empirical correlation considers the liquid viscosity through the Reynolds number, it was not validated for high viscosity oils.

$$H_{Ls} = 1.0e^{-\left(0.456\theta R + 2.48\cdot 10^{-6}\,\mathrm{Re}S\right)} \quad (2)$$

$$\mathrm{Re}_S = \frac{\rho_L v_M d}{\mu_L} \quad (3)$$

The empirical correlation of Abdul-Majeed (2000) for slug liquid holdup in horizontal and slightly inclined two-phase flow is a function of mixture velocity, liquid viscosity and inclination angle. He declared that slug liquid holdup is significantly affected by liquid viscosity and inclination angle.

$$H_{Ls} = \left(1.009 - Cv_M\right)A \quad (4)$$

$$C = 0.006 + 1.3377\left(\frac{\mu_G}{\mu_L}\right) \quad (5)$$

$$A = 1.0\left(\theta \le 0\right) \quad (6)$$

Marquez *et al.* (2009) proposed the following correlation for the liquid viscosity greater than 500 cP.

$$H_{Ls} = 1.0046\ e^{-\left(0.0022\ \mathrm{Re}\,s\right)} \quad (7)$$

Zhang *et al.* (2003) developed a mechanistic model for slug liquid holdup. It is based on the slug dynamics. The model was modified in an ad-hoc fashion based on Gokcal (2005) data. If the Reynolds number is less than 5000, the momentum term for gas entrapment is multiplied by Re/5000.

$$H_{Ls} = \frac{1}{1+\frac{T_{sm}}{3.16\left[\left(\rho_L - \rho_G\right)g\sigma\right]^{1/2}}} \quad (8)$$

$$T_{SM} = \frac{1}{C_C}\left[\frac{f_S}{2}\rho_S v_M^2 + \frac{d}{4}\frac{\rho_L H_{LF}(v_T - v_F)(v_M - v_F)}{l_S}\right] \quad (9)$$

$$C_C = \frac{2.5 - \left|\sin(\theta)\right|}{2} \quad (10)$$

Experimental Study

Facility

An existing TUFFP indoor high viscosity facility has been modified for this study (Fig. 1). This facility was previously used by Gokcal (2005 and 2008) to investigate the effects of high oil viscosity on slug flow characteristics.

There are four main parts of the facility: metering section, test section, heating system and cooling system. The test section was designed as an 18.9-m (62-ft) long, 50.8-mm (2-in.) ID pipe consisting of a clear PVC pipe section and a transparent acrylic pipe section. A 9.15-m (30-ft) long transparent acrylic pipe section is used to observe the flow behavior visually. This section is connected to a 76.2-mm (3-in.) ID return pipe with a flexible hose. An oil transfer tank (1.32 m^3) is located at the end of return pipe. Return pipe is connected to this tank with a flexible hose, and +1° inclination from horizontal is given to promote slug flow in the return line before entering the tank. A 3-hp progressing cavity pump is placed to the outlet of the oil transfer tank which sends oil back to the main tank (3.03 m^3) through a riser. From main storage tank, oil is pumped by a 20-hp screw pump to the test section. A dry rotary screw air compressor delivers compressed air to the system. Before entering the test section, two fluids were mixed at a mixing tee. Micro Motion™ mass flow meters are used to meter the mass flow rates and densities of oil and air. There is no special separation system. Air and oil are gravity segregated in the oil tank, and separated air is released to the atmosphere through a ventilation system. The inclination of the test section can be set from -2° to 2° from horizontal by adjusting the heights of the stands.

The test oil viscosity is very sensitive to temperature changes. The temperature measurements are

imperative to determine the viscosity of the oil during experiments. Therefore, it is crucial to conduct experiments at a constant temperature. Existing heating and cooling systems are used to control temperature. Resistance Temperature Detector (RTD) transducers already exist in the facility to measure temperatures during experiments. Pressure transducers and differential pressure transducers are located at various points to monitor the pressure and pressure drop during experiments.

Previously developed data acquisition program is used for the high viscosity facility. Pressure, differential pressure, temperature, flow rates, superficial gas and superficial liquid velocities are monitored on the PC of the facility during the experiments. In addition, the capacitance sensor is connected to a portable data acquisition system using a scan rate of 1000 Hz to measure the resulting voltage signals from the sensor. Data acquisition duration is fixed for 10 seconds. As a result 10,000 data points are collected in one test.

Test Fluids

The previously used high viscosity oil (Citgo Sentry 220) and air were selected again for this study. Following are the typical properties of the oil:

Gravity: 27.6 °API

Viscosity: 0.220 Pa·s @ 40 °C

Density: 889 kg/m^3 @ 15.6 °C

The oil viscosity vs. temperature behavior is shown in Fig. 2.

Testing Range

In this study, experiments will be conducted at various oil and gas velocities and different oil viscosities corresponding to different temperatures. Since the slug characteristics were examined by Gokcal (2008) in the previous project of TUFFP, his test matrix is used as the starting point of this study. Superficial oil velocities range from 0.1 m/s to 0.8 m/s. Superficial air velocities range from 0.1 to 3.5 m/s. The viscosity of Citgo Sentry 220 oil is very sensitive to temperature changes. Experiments will be conducted at four different temperatures: 70, 80, 90, and 100 °F. The correspondent oil viscosities are 0.587, 0.378, 0.257, and 0.181 Pa·s respectively. The test section will be kept horizontal.

Instrumentation

Capacitance Sensor

A new capacitance sensor (CS) had been developed in-house for the measurement of slug liquid holdup. The principle of the capacitance method is based on the differences in the dielectric constants of the gas and liquid phases in the flow. Gokcal (2008) used a concave type capacitance sensor for slug length and slug frequency measurements. Previously, the concave type capacitance sensor was tested for slug liquid holdup measurements. No significant differences in the output data were observed during slug flow. The detailed information was presented at the March 2009 TUFFP Advisory Board meeting.

The new design of the CS provides detailed information across the slug body. A schematic of the capacitance probe is shown in Fig. 3. The sensor consists of two parallel copper wires positioned perpendicular to the flow with a distance in between (0.25 in.), an electronic circuit to filter, amplify and convert the measured capacitance to a voltage, and the housing.

Static calibration of CS was accomplished by placing different amounts of liquid volumes in an acrylic pipe tester with the CS in the middle, and measuring the height of the fluid in the pipe, then recording the corresponding sensor output voltage. The actual voltage reading was then converted to a dimensionless voltage using the following equation:

$$V^* = \frac{V_{read} - V_{min}}{V_{max} - V_{min}} \qquad (11)$$

The corresponding liquid holdup was calculated as the ratio of the cross sectional area of the liquid in between the two wires and the total cross sectional area between the wires (Fig. 4). The calculated liquid holdup values in between two wires are extrapolated to the cross section of the pipe.

Dynamic calibration of CS was conducted using existing quick-closing valve system. CS, quick-closing valve system and high speed video camera were synchronized. CS was placed 1.5-ft before the quick-closing valve system. Shortly before capturing the slug body, data collection process with CS was started; then slug body trapped. High speed video camera was used to verify the trapped part of the slug body for the analysis of the CS reading. The dynamic calibration plot was generated by plotting the actual liquid holdup data (quick-closing valve

system) versus the calculated liquid holdup data (capacitance sensor output) at different test conditions (Fig. 5). The calibration plot shows that a correction on slug liquid holdup should be applied to the experimental data. Finally, in order to calculate the liquid holdup in the slug body, numerical integration is used to estimate the area under the curve, and it is divided by the area as if the liquid slug is pure oil.

Two examples for the response of the CS were plotted after converting the output signals to liquid holdup values in Figs. 6 and 7. In Fig. 6, v_{SL} and v_{SG} are 0.1 m/s while in Fig. 7 v_{SL} is 0.5 m/s and v_{SG} is 1 m/s. In Fig. 6, the calculated liquid holdup values show that liquid slug is almost pure oil, which agrees with high speed video camera videos. On the other hand, in Fig. 7, with the increase in oil and gas flow rates, the effects of large bubbles and also entrained small bubbles on liquid holdup are observed. Furthermore, there is a decline in the liquid holdup towards to the tail of the slug. The possible reason of this behavior is the migration of the small bubbles from front to tail within the slug.

The capacitance sensor can also be used to predict liquid film holdup. In Fig. 6, there is slight decrease in liquid film holdup through the liquid film part of the slug due to the velocity decrease from the beginning to the end of the liquid film. Since the drainage of high viscosity oil is slow, there always exists a liquid film on top of the pipe during the flow. With the increase in superficial liquid and gas velocities, oil drainage becomes significant. After slug passes, significant amount of oil from the top of the pipe drains and liquid film holdup increases. As the drained amount of oil is decreased, there is again a slight decrease in liquid film holdup as it happens for low flow rates (Fig. 7). Due to capillary effect the visual observation or high speed video images does not provide a good comparison with capacitance sensor data.

Differential Pressure Sensor

After the last Advisory Board meeting, two flush diaphragm pressure transducers were tested for measuring differential pressure across the cross section of the pipe to measure slug liquid holdup. Moreover, existing pressure transducers were modified to prevent oil drainage and gas bubbles penetration into the transmission lines. However, the response time of the pressure transducers are not fast enough to detect the change of the differential pressure through the slug unit.

Experimental Results

Slug liquid holdup data were collected by using quick-closing valve system and recently developed in-house capacitance sensor. Moreover, liquid film holdup data were acquired with quick-closing valve system.

Quick-Closing Valve System Results

98 tests were conducted to measure slug liquid holdup at 70 °F corresponding to 0.587 Pa·s oil viscosity. 17 data points were collected for superficial gas velocities from 0.1 to 2 m/s and superficial liquid velocities from 0.1 to 0.8 m/s. With the increase in gas flow rates, slug lengths become shorter. Due to the higher velocity of the slugs trapping process becomes challenging. The test matrix with quick-closing valve system is determined considering these factors. Slight decrease in slug liquid holdup is observed with increasing superficial gas velocity (Fig. 8). There is no significant difference in slug liquid holdup observed with the increase in superficial liquid velocities.

For the liquid film holdup, 53 tests were conducted at 70 °F corresponding to 0.587 Pa·s oil viscosity. 19 data points were collected for superficial gas velocities from 0.1 to 2 m/s and superficial liquid velocities from 0.1 to 0.8 m/s. With the increase in superficial gas velocities, slight decrease in liquid film holdup is observed. The liquid film holdup slightly increases as the superficial liquid velocity increases (Fig. 9).

Capacitance Sensor Results

77 tests were conducted to predict slug liquid holdup at 70 °F corresponding to 0.587 Pa·s oil viscosity with CS. 36 data points were collected for superficial gas velocities from 0.1 to 3.5 m/s and superficial liquid velocities from 0.1 to 0.8 m/s. With the increase of the superficial gas velocity a decrease in liquid holdup is observed. Moreover, with increasing superficial liquid velocity, liquid holdup slightly decreases. This is due to the increase in the number of large bubbles and also entrained small bubbles in the slug body (Fig. 10).

In order to investigate the effect of large bubbles on slug liquid holdup, liquid holdup data was reevaluated after omitting the large bubbles in the slug body. Large bubbles are not observed for v_{SL}=0.1 m/s. The liquid holdup comparisons between slugs with large bubbles and slugs without large

bubbles are plotted in Figs. 11-13. The effect of large bubbles on slug liquid holdup is more pronouncing for higher superficial gas velocities. With the increase in superficial liquid velocity the number of large bubbles increases, however the size of the bubbles gets smaller.

CS provides extensive information through the slug. Even though measuring holdup with quick-closing valve system is a non-intrusive method the results are restricted by the representation of the trapped parts of the liquid slugs. Non-homogenous form of liquid slug is determined from high speed camera videos and CS readings. This is the reason of discrepancy between quick-closing system and CS slug liquid holdup data. Besides liquid holdup, CS can also measure bubble size, the number of large bubbles and location of the large bubbles. Therefore, CS will be used for the measurement of slug liquid holdup.

Model Evaluation

Experimental data for slug liquid holdup are compared with the correlations and a mechanistic model, summarized in literature review section.

Statistical Parameters

Statistical parameters are used to compare the performance of the models. The relative and actual errors are expressed in Eqs. 12 and 13, respectively.

$$e_i = \left[\left(\frac{V_{cal} - V_{\exp}}{V_{\exp}} \right) \times 100 \right] \tag{12}$$

$$e_j = (V_{cal} - V_{\exp}) \tag{13}$$

The subscripts *cal* and *exp* refer to the calculated and experimental values. Based on the relative and actual errors, the following six statistical parameters are defined:

Average Relative Error:

$$\varepsilon_1 = \frac{1}{N} \sum_{i=1}^{N} (e_i) \tag{14}$$

Absolute Average Relative Error:

$$\varepsilon_2 = \left[\frac{1}{N} \sum_{j=1}^{N} \left| e_{rj} \right| \right] \times 100 \tag{15}$$

Standard Deviation about the Average Relative Error:

$$\varepsilon_3 = \sqrt{\frac{\sum_{i}^{N} (e_i - \varepsilon_1)^2}{N-1}} \tag{16}$$

Average Actual Error:

$$\varepsilon_4 = \frac{1}{N} \sum_{j=1}^{N} (e_j) \tag{17}$$

Absolute Average Actual Error:

$$\varepsilon_5 = \frac{1}{N} \sum_{j=1}^{N} \left| (e_j) \right| \tag{18}$$

Standard Deviation about the Average Actual Error:

$$\varepsilon_6 = \sqrt{\frac{\sum_{j}^{N} (e_j - \varepsilon_4)}{N-1}} \tag{19}$$

In the above equations, N is the number of data points. The average relative error, ε_1, and average actual error, ε_4, are an indication of the agreement between the predicted and experimental parameters. Positive values for these average errors indicate overestimation of the parameter. Negative values indicate underestimation of the parameter. The true performance can be masked by these parameters due to the cancellation of the negative and positive values. Therefore, the absolute average relative error, ε_2, and the absolute average actual error, ε_5, better reflect the agreement of the predicted and measured parameters. These parameters denote how large the errors are on the average. The standard deviations, ε_3 and ε_6, indicate the degree of scattering around the corresponding average errors, ε_1 and ε_4.

CS liquid holdup results are compared with the model predictions. The results are divided into two groups for superficial gas velocities higher than 1 m/s and lower than 1 m/s. For the first group, Marquez *et al.* (2009) correlation significantly underestimates slug liquid holdup. On the other hand, the results of Gomez and Abdul-Majeed's correlations are very close to each other, and they slightly overestimate slug liquid holdup. Gregory's correlation and TUFFP Unified model perform better than the other correlations. For Gregory's correlation the values of

ε_2 and ε_5 are 1.95 and 0.02; and for TUFFP Unified Model ε_2 and ε_5 are 0.55 and 0.01, respectively (Fig. 14 and Table-1). For the second group, the behavior of the models are the same, however the error values are increased. Gregory's correlation and TUFFP Unified model still perform better than the other correlations. For Gregory's correlation the values of ε_2 and ε_5 are 6.57 and 0.06; and for TUFFP Unified Model ε_2 and ε_5 are 6.10 and 0.05, respectively (Fig. 15 and Table-2). Previously, in the Unified Model, the slug liquid holdup prediction was based on a turbulent flow assumption. However, laminar flow was mostly observed in the liquid phase for high viscosity oil-air two-phase flow. The momentum term in the slug liquid holdup model was modified considering the high viscosity flow behavior. If the Reynolds number is less than 5000, the momentum term for gas entrapment is multiplied by Re/5000. After this modification TUFFP Unified model worked better for high viscosity oil predictions.

Near Future Tasks

The main future tasks are:

- Conduct experiments with capacitance sensor for 0.378, 0.257 and 0.181 Pa·s oil viscosity,
- Evaluation of the acquired data from capacitance sensor,
- Collect and evaluate data for liquid film height with capacitance sensor, and
- Compare experimental data with existing models.
- Development of a new holdup closure relationship if necessary.

Nomenclature

d	= pipe diameter [m]
e_i	= relative error
e_j	= actual error
f	= friction factor
H	= holdup
Re	= Reynolds number
V	= velocity [m/s]

Greek Letters

μ	= viscosity [kg/ms]
ρ	= density [kg/m3]
σ	= surface tension [N/m]
θ	= inclination angle [º]
ε_1- ε_6	= statistical parameters

Subscripts

G	= gas phase
L	= liquid phase
LS	= liquid slug
M	= mixture
S	= slug
LF	= liquid film
F	= film
C	= gas core
T	= transitional velocity

References

Abdul-Majeed, G.: "Liquid Slug Holdup in Horizontal and Slightly Inclined Two-Phase Slug Flow," *Journal of Petroleum Science and Engineering,* 27, pp. 27–32 (2000).

Al-safran, E.: "Prediction of Slug Liquid Holdup in Horizontal Pipes," *Journal of Energy Resources Technology,* Volume 131, Issue 2 (2009).

Gregory, G.A., Nicholson, M.K., Aziz, K.: "Correlation of the Liquid Volume Fraction in the Slug for Horizontal Gas–Liquid Slug Flow," *International Journal of Multiphase Flow*, 4, 33–39 (1978).

Gokcal, B.: "Effects of High Oil Viscosity on Two-Phase Oil-Gas Flow Behavior in Horizontal Pipes," MSc. Thesis, The University of Tulsa, Tulsa, OK (2005).

Gokcal, B.: "An Experimental and Theoretical Investigation of Slug Flow for High Oil Viscosity in Horizontal Pipes," Ph.D. Dissertation, The University of Tulsa, Tulsa, OK (2008).

Gokcal, B.: "An Experimental and Theoretical Investigation of Slug Flow for High Oil Viscosity in Horizontal Pipes," TUFFP ABM (September 2008a), pp. 47-76 (2008).

Gomez, L.E., Shoham, O., Taitel, Y.: "Prediction of Slug Liquid Holdup: Horizontal to Upward Vertical Flow," *International Journal of Multiphase Flow,* 26, 517–521 (2000).

Marquez J., Manzanilla C., Trujillo J.: "Slug Catcher Conceptual Design as Separator for Heavy Oil," *Society of Petroleum Engineers,* 122829 (2009).

Zhang H., Wang O., Sarica C., Brill J. P.: "Unified Model for Gas-Liquid Pipe Flow via Slug Dynamics—Part 1: Model Development," *Journal of Energy Resources Technology*, Volume 125, Issue 4, 226 (2003).

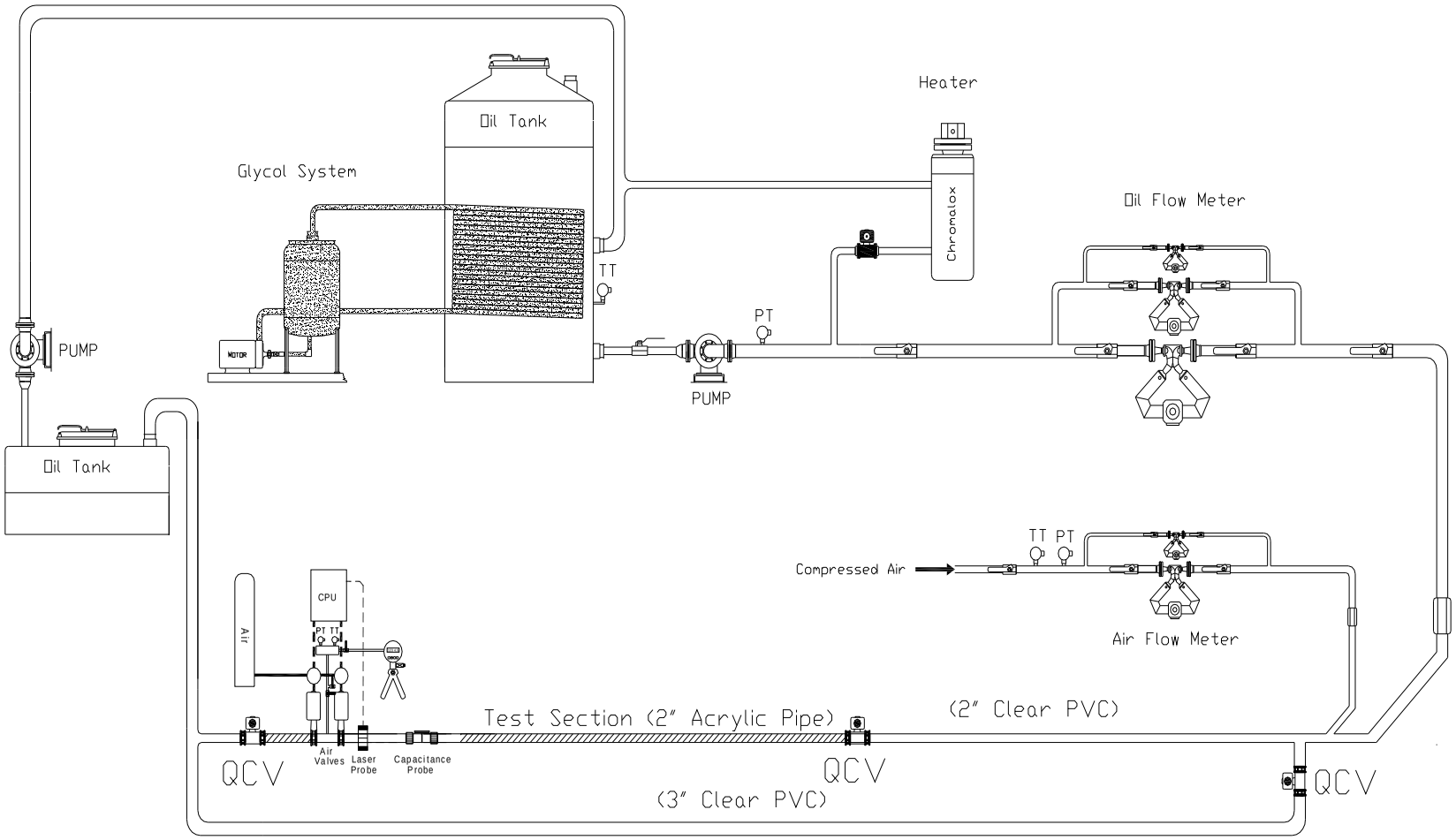

Figure 1: Schematic of High Viscosity Facility of the Tulsa University Fluid Flow Projects (TUFFP)

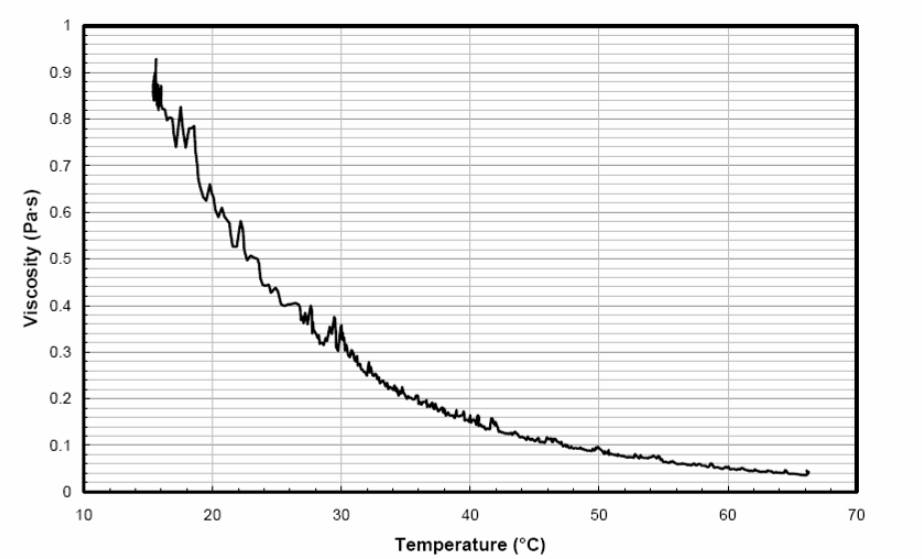

Figure 2: Viscosity vs. Temperature for Citgo Sentry 220 Oil

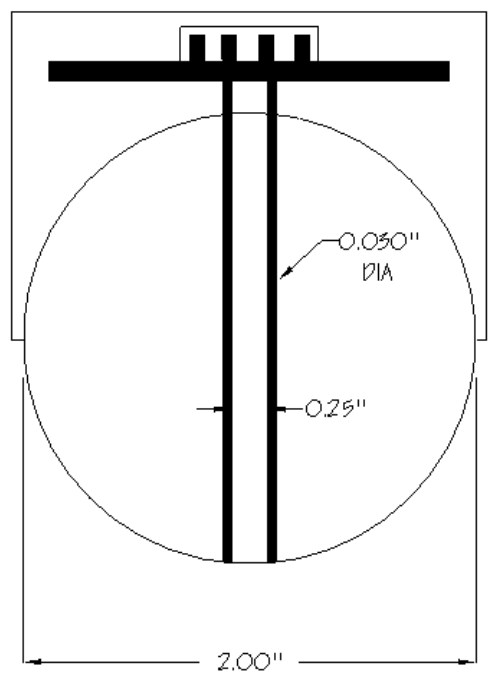

Figure 3: Schematic of New Capacitance Sensor

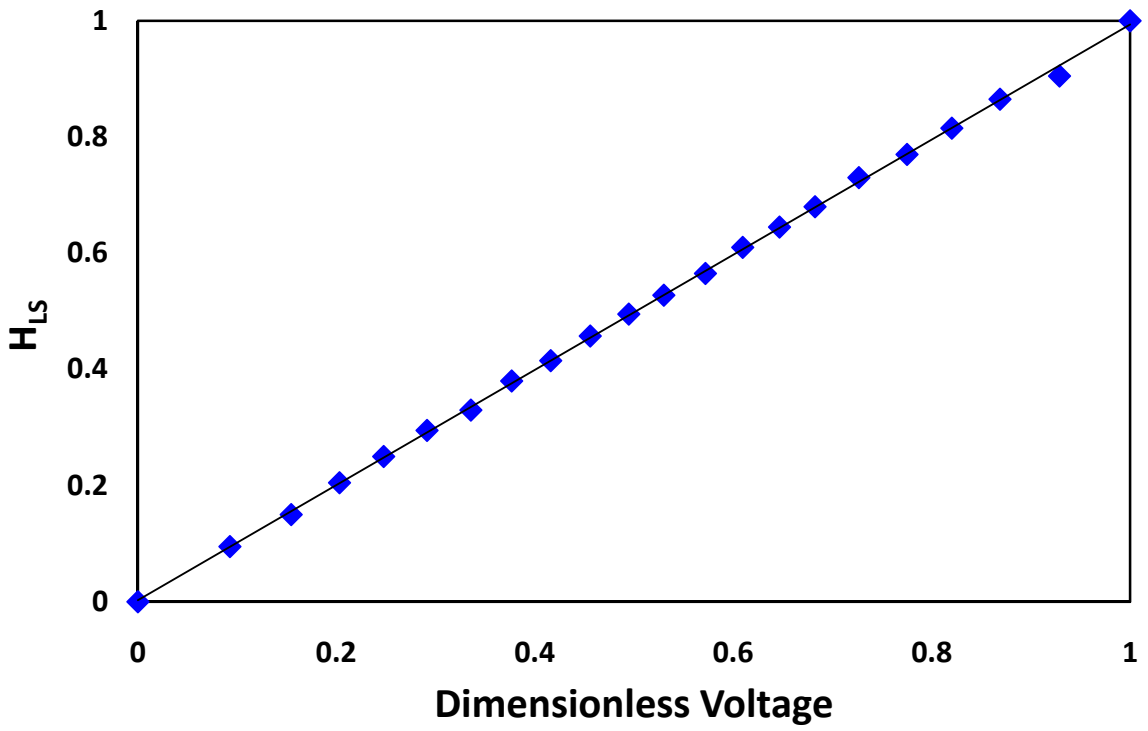

Figure 4: Static Calibration Curve of Capacitance Sensor

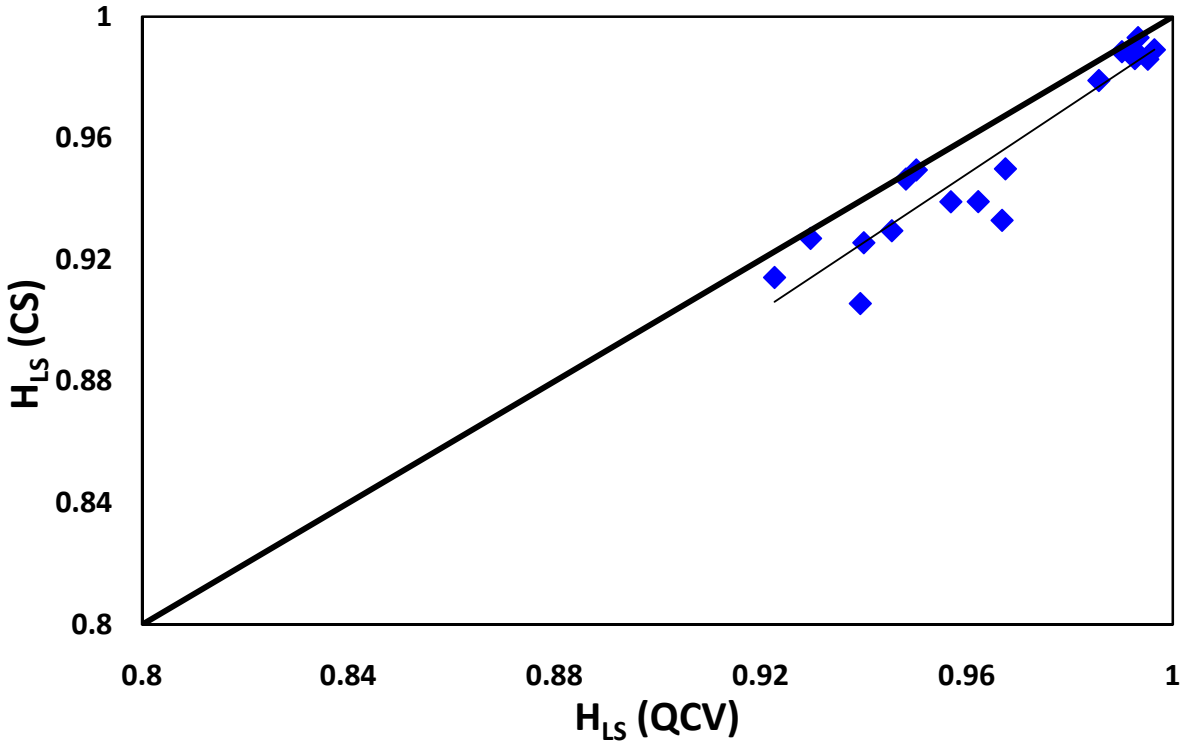

Figure 5: Dynamic Calibration of Capacitance Sensor

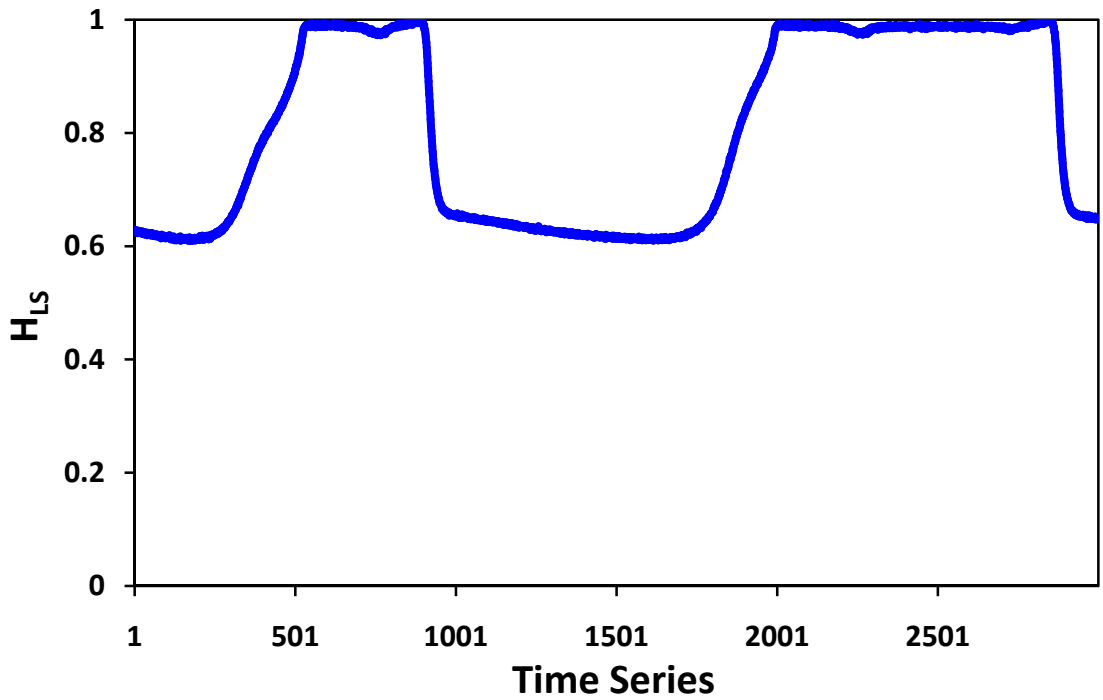

Figure 6: Example of Capacitance Sensor Readings

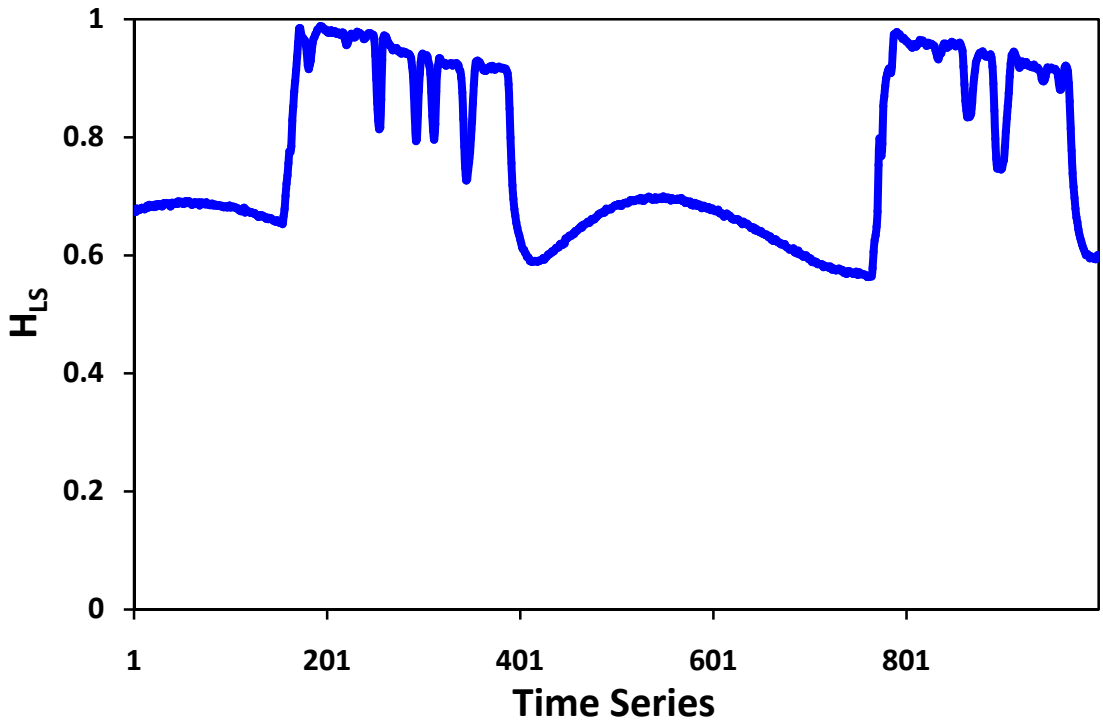

Figure 7: Example of Capacitance Sensor Readings

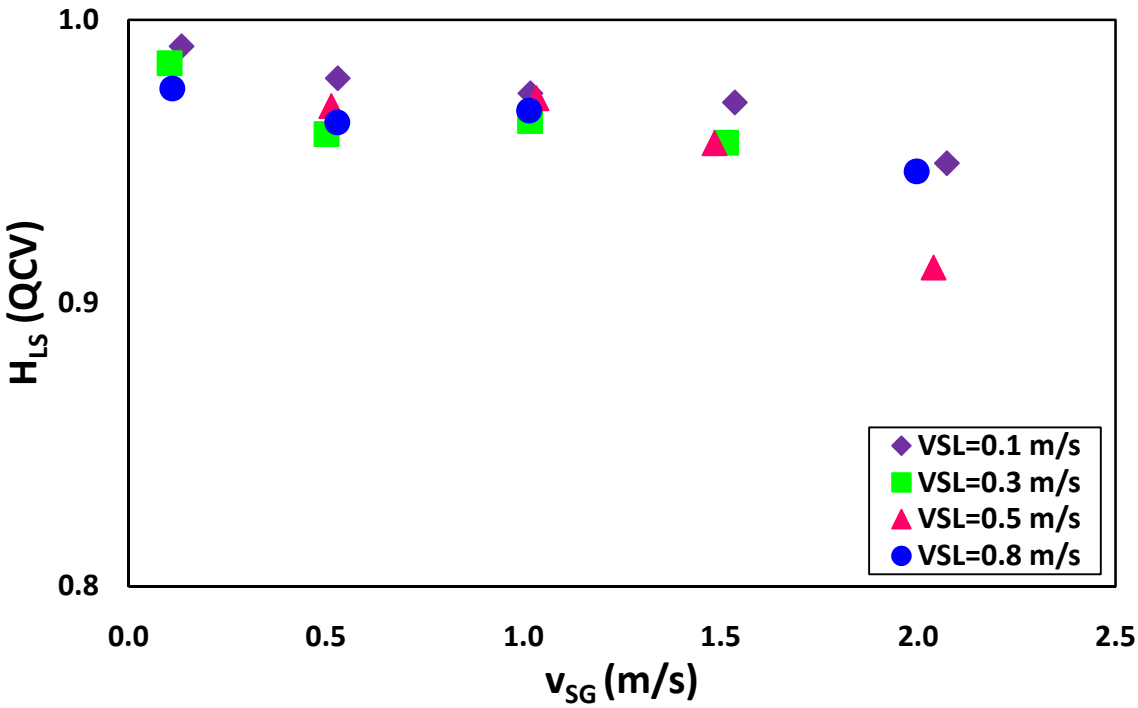

Figure 8: Experimental Results for Slug Liquid Holdup from QCV

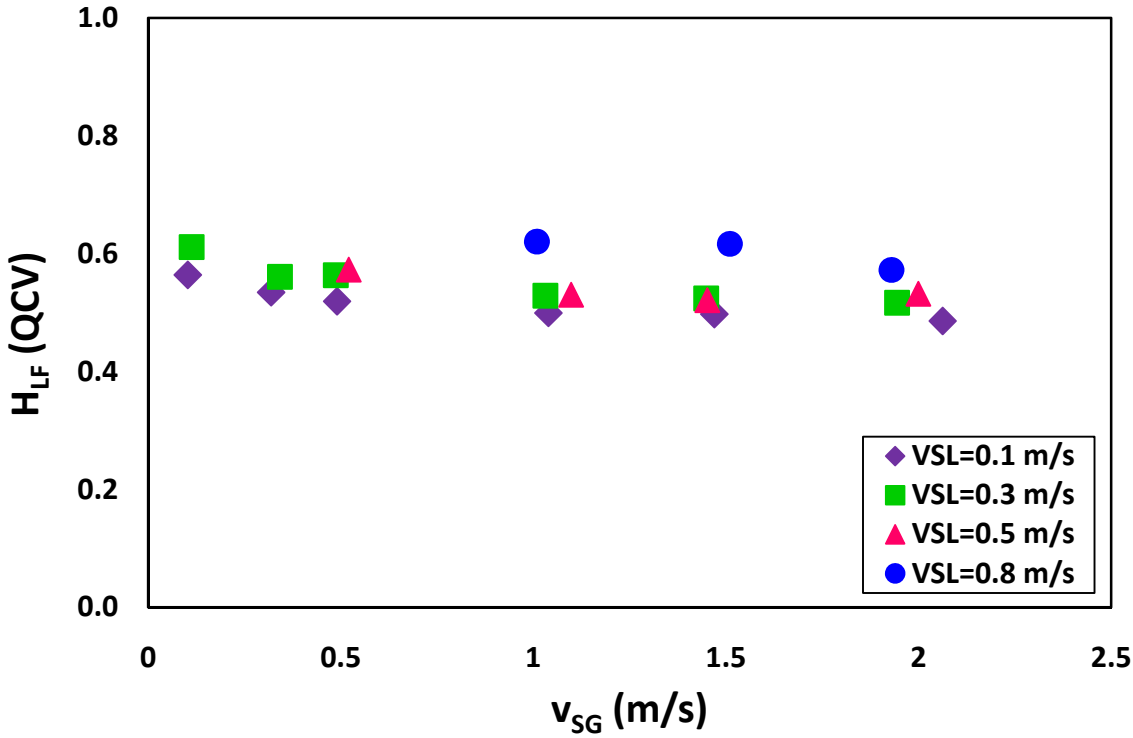

Figure 9: Experimental Results for Liquid Film Holdup from QCV

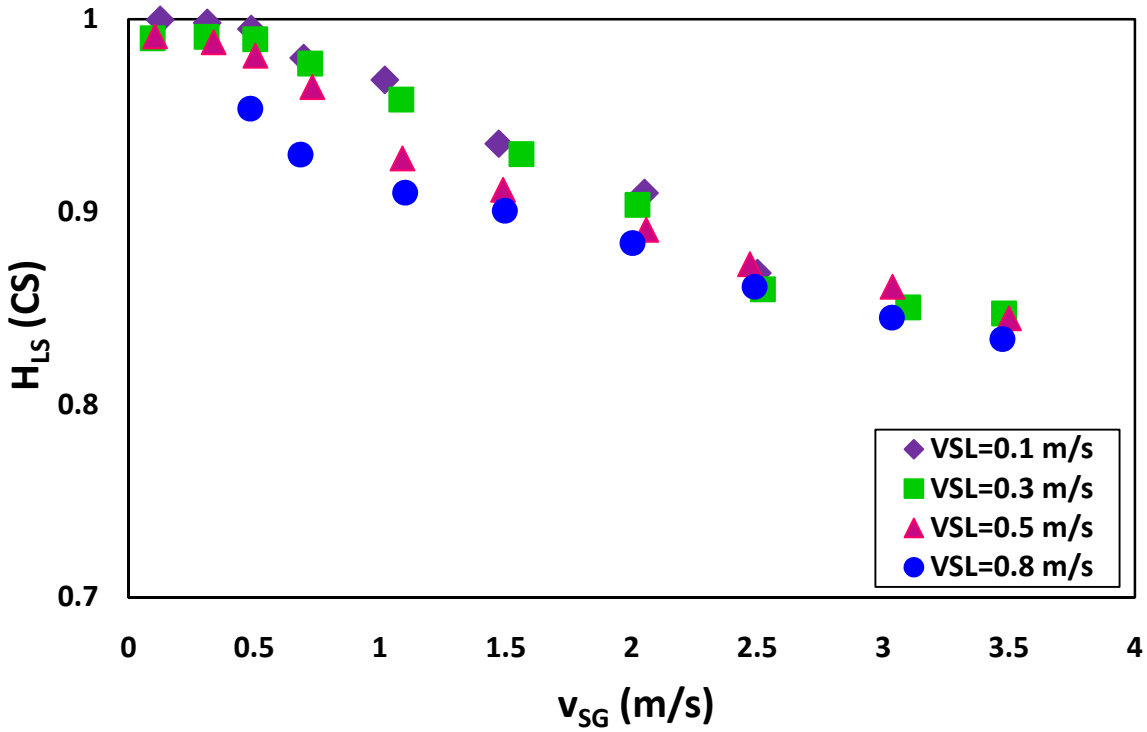

Figure 10: Experimental Results for Slug Liquid Holdup from Capacitance Sensor

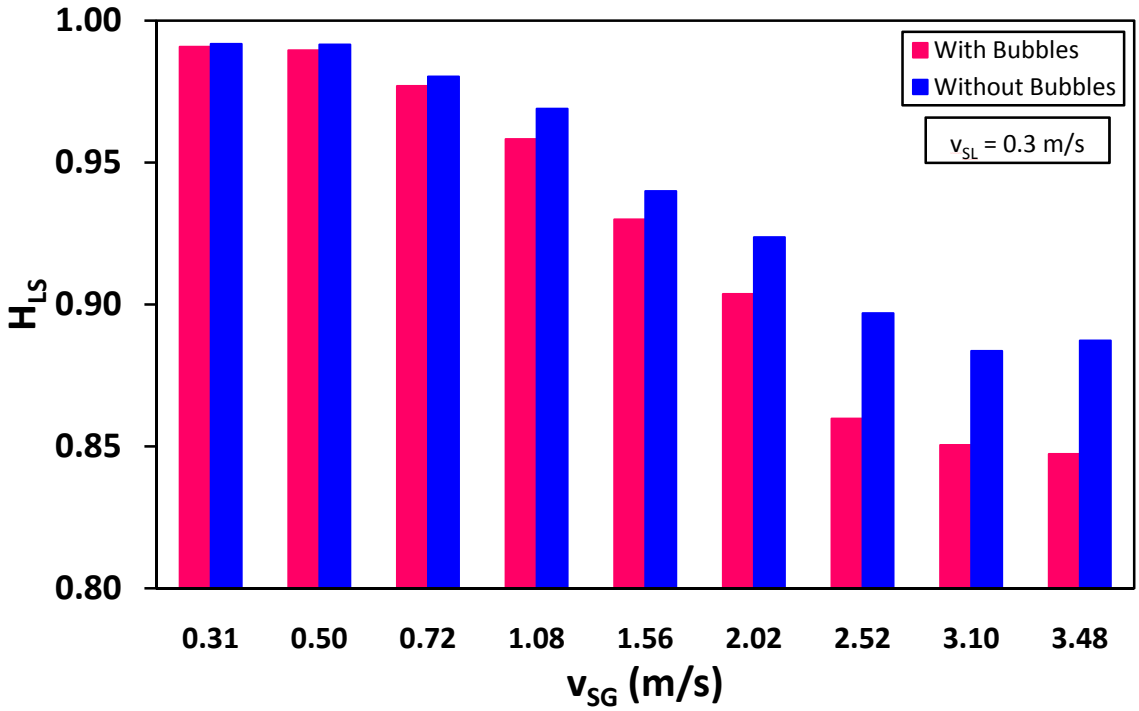

Figure 11: Comparison of Slug Liquid Holdup Measured by CS Experimental Results with Large Bubbles and without Large Bubbles for v_{SL} = 0.3 m/s

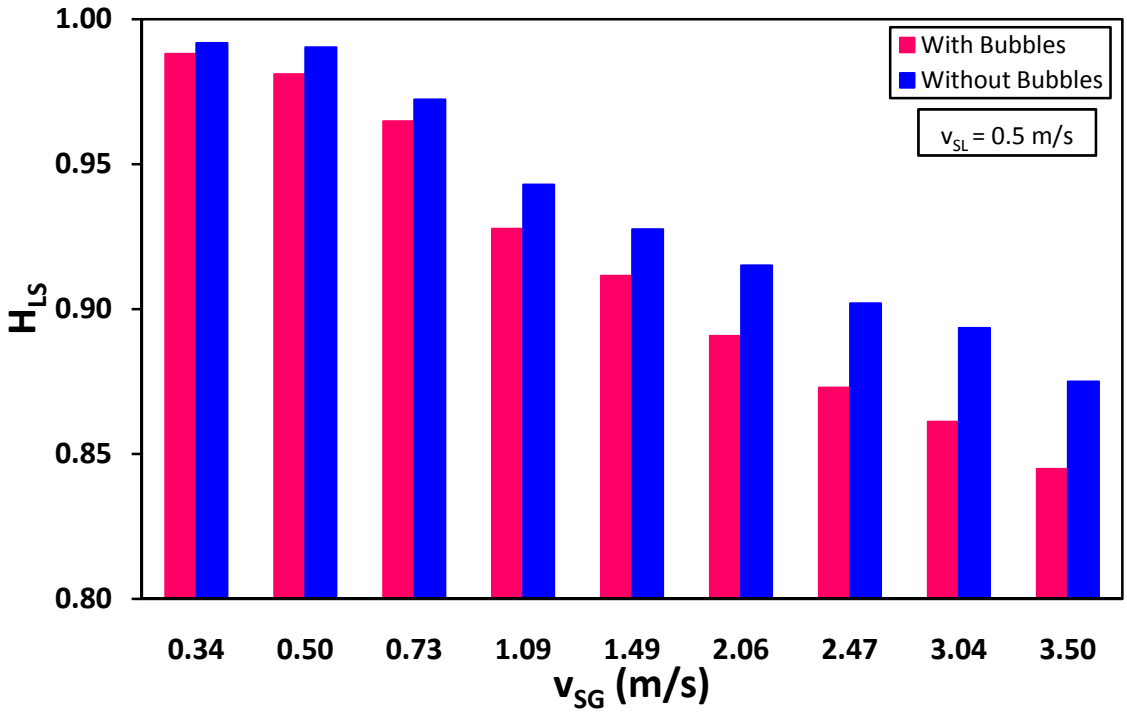

Figure 12: Comparison of Slug Liquid Holdup Measured by CS Experimental Results with Large Bubbles and without Large Bubbles for v_{SL} = 0.5 m/s

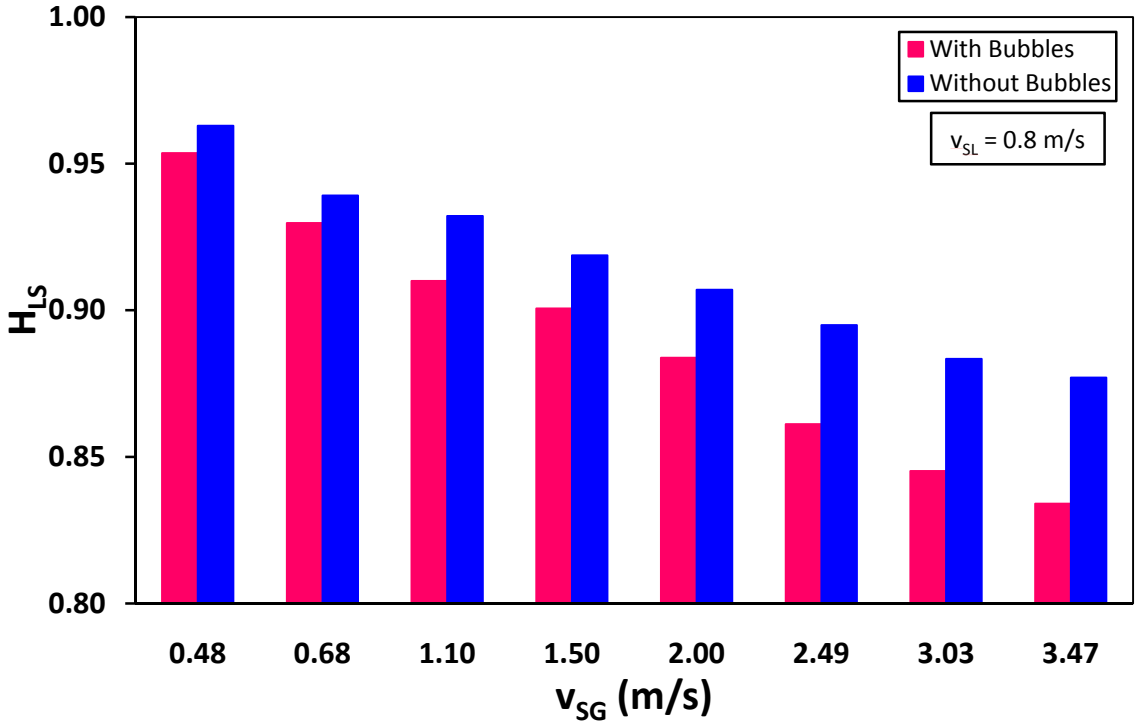

Figure 13: Comparison of Slug Liquid Holdup Measured by CS Experimental Results with Large Bubbles and without Large Bubbles for v_{SL} = 0.8 m/s

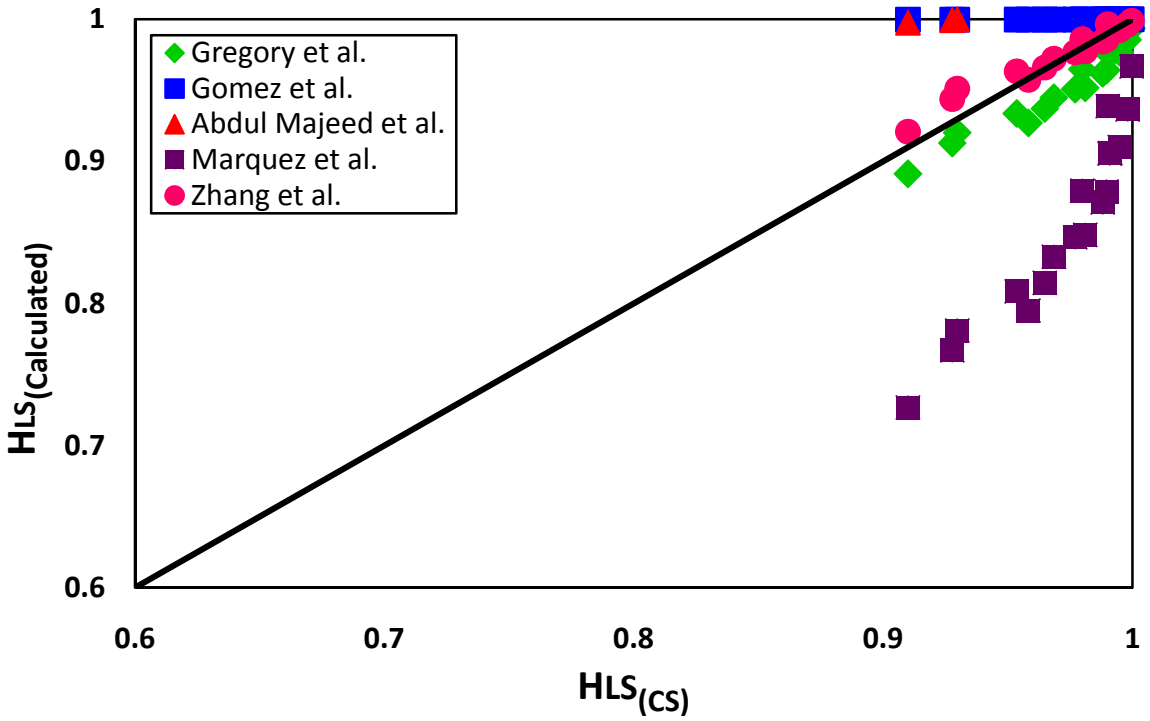

Figure 14: Performance of Gregory *et al.* (1978), Gomez *et al.* (2000) and Abdul-Majeed (2000), Marquez *et al.* (2009) Correlations and Zhang *et al.* CS Slug Liquid Holdup Results for $v_{SG} \leq 1$ m/s

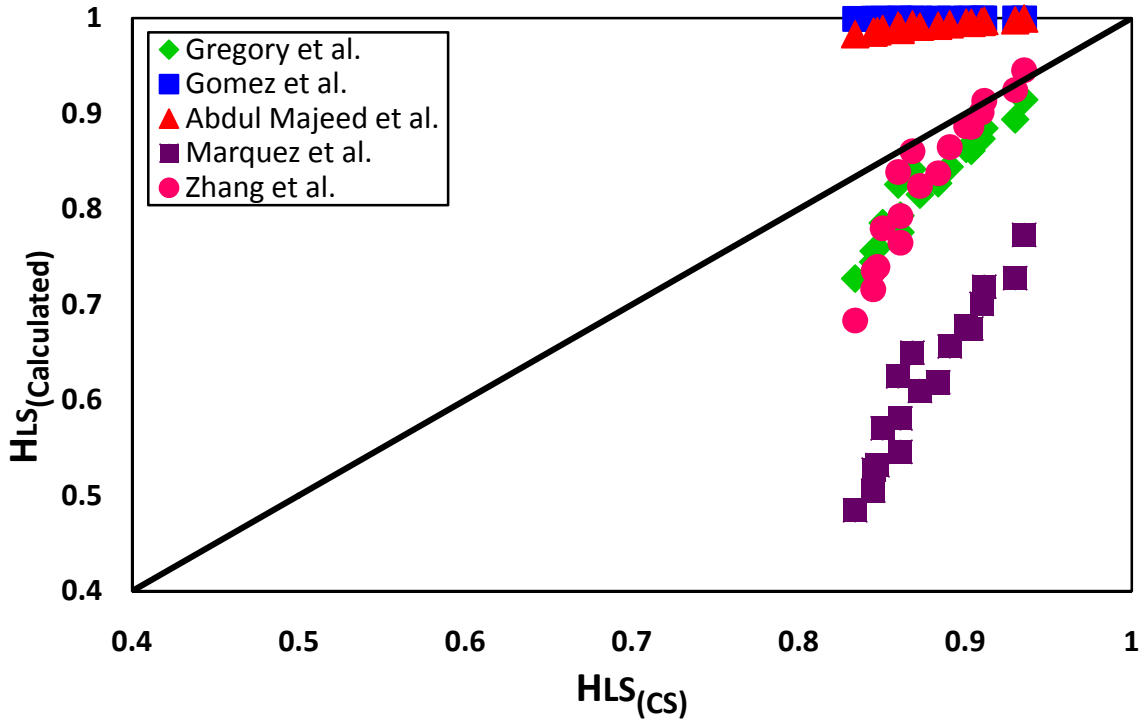

Figure 15: Performance of Gregory *et al.* (1978), Gomez *et al.* (2000) and Abdul-Majeed (2000), Marquez *et al.* (2009) Correlations and Zhang *et al.* CS Slug Liquid Holdup Results for $v_{SG} > 1$ m/s

Table 1: Model Evaluation against Slug Liquid Holdups Measured by CS for for $v_{SG} \leq 1$ m/s

Correlation/Model	ε_1 (%)	ε_2 (%)	ε_3 (%)	ε_4 (-)	ε_5 (-)	ε_6 (-)
Gregory *et al.*	**-1.95**	**1.95**	**0.82**	**-0.02**	**0.02**	**0.01**
Gomez *et al.*	2.95	2.95	2.88	0.03	0.03	0.03
Abdul-Majeed	3.29	3.29	2.63	0.03	0.03	0.02
Marquez *et al.*	-12.00	12.00	4.62	-0.12	0.12	0.04
Zhang *et al.*	**0.35**	**0.55**	**0.77**	**0.00**	**0.01**	**0.01**

Table 1: Model Evaluation against Slug Liquid Holdups Measured by CS for for $v_{SG} > 1$ m/s

Correlation/Model	ε_1 (%)	ε_2 (%)	ε_3 (%)	ε_4 (-)	ε_5 (-)	ε_6 (-)
Gregory *et al.*	**-6.57**	**6.57**	**3.32**	**-0.06**	**0.06**	**0.03**
Gomez *et al.*	13.91	13.91	3.96	0.12	0.12	0.03
Abdul-Majeed	12.99	12.99	3.42	0.11	0.11	0.03
Marquez *et al.*	-29.52	29.52	7.11	-0.26	0.26	0.05
Zhang *et al.*	**-5.96**	**6.10**	**5.89**	**-0.05**	**0.05**	**0.05**

Fluid Flow Projects

Effect of Pipe Diameter on Drift Velocity for High Viscosity Liquids

Benin Chelinsky Jeyachandra

Dr. Abdel Al-Sarkhi

Advisory Board Meeting, May 12, 2010

Outline

- Objectives
- Introduction
- Literature Review
- Experimental Study
- CFD Simulation
- Conclusions
- Future Tasks

Objectives

- Analyze Drift Velocity Data for High Viscosity Oil with Varying Pipe Diameters
- Investigate Effect of Inclination on Drift Velocity for Viscous Oils
- Validate CFD Simulation of Drift Velocity with Experimental Results

Introduction

- High Viscosity Oil
  - Definition
  - Significance of High Viscosity Oil
  - Observed Flow Patterns
  - Discrepancy in Modeling
- Drift Velocity
  - Definition
  - Significance of Modeling Drift Velocity

Literature Review

- Expression for Translational Velocity and Drift Velocity
  - Nicklin *et al.* (1962)

$$v_t = C_o\, v_s + v_d$$

Literature Review …

- Parameters Affecting Drift Velocity
  - Zukoski (1966)
    - Eotvos Number

$$Eo = (\rho_L - \rho_G) g D^2 / \sigma$$

    - Inverse Viscosity Number

$$N_f = D^{3/2} \sqrt{\rho_L (\rho_L - \rho_G) g} / \mu_L$$

    - Inclination Angle

Literature Review …

- Potential Flow Analysis for Drift Velocity
  - Vertical Flow – Dumitrescu (1943), Davies and Taylor (1950)

$$v_d = 0.351\sqrt{gD}$$

  - Horizontal Flow – Benjamin (1968)

$$v_d = 0.542\sqrt{gD}$$

Literature Review …

- Drift Velocity in Inclined Pipes
  - Bendiksen (1984)

$$v_d = v_d^h \cos\theta + v_d^v \sin\theta$$

  - Bonnecase (1971)
    - Increase in Drift Velocity with Increase in Inclination Peaking Around 30-50°
    - After Peak Drift Velocity Decreases

Literature Review …

- Effect of Tube Size, Rheology of Liquid
  - Shosho and Ryan (2001)
    - Experiments with Newtonian and Non-Newtonian Liquids
    - Correlated Drift Velocity with Eotvos Number, Morton Number and Froude Number

$$Mo = \frac{\rho \mu^4}{g \sigma^3}$$

Literature Review …

- Effect of Viscosity
  - Joseph (2003)
    - Model to Predict Bubble Rise Velocity of Spherical Bubbles
    - Considered Effects of Viscosity, Surface Tension
    - Viscosity Slows Bubble Rise Velocity

Experimental Study

- Test Oil Characteristics
- Facility Modifications
- Test Range
- Experimental Results

Test Oil Characteristics

- Test Liquid: Citgo Sentry 220 Oil
  - Gravity: 27.6 °API
  - Viscosity: 0.220 Pa·s @ 40 °C
  - Density: 889 kg/m^3 @ 15.6 °C
  - Surface Tension: 0.02976 N/m
- Test Gas: Air

Facility Modifications

- Replace 3 in. Diameter Pipe with 6 in. Diameter Pipe
- Laser Probes Replaced by Optical Probes
- Aluminum I Beam Used as Support Structure
- Plug Provision at End of Pipe for Horizontal Case

Facility Modifications …

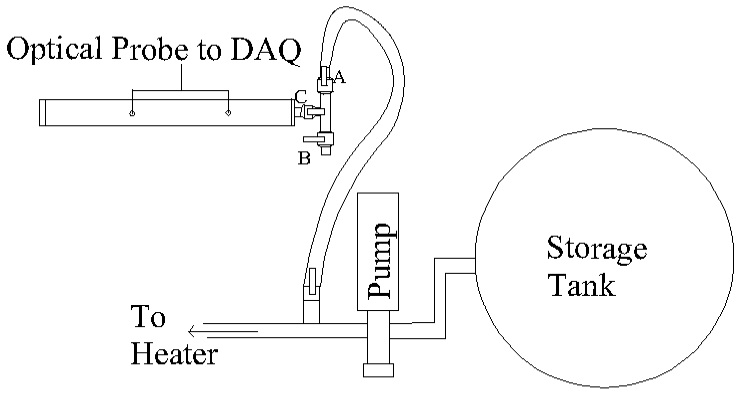

Facility Modifications …

- Optical Probe

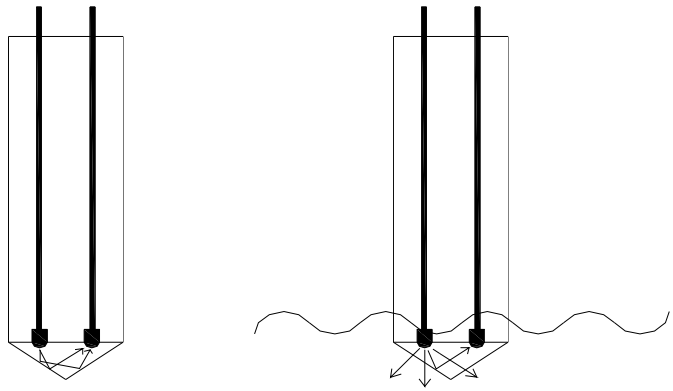

Test Range

- Pipe Diameter
  - 2-in. Data from Gokcal (2008)
  - 3-in. Data from Sharma (2009)
  - 6-in. Data from Jeyachandra (2009-2010)
- Viscosity: 0.574, 0.378, 0.256, 0.105 Pa·s
- Inclinations: 0°,10°,30°,50°,70°,90°

Experimental Results

Froude Number for Water-Air Flow

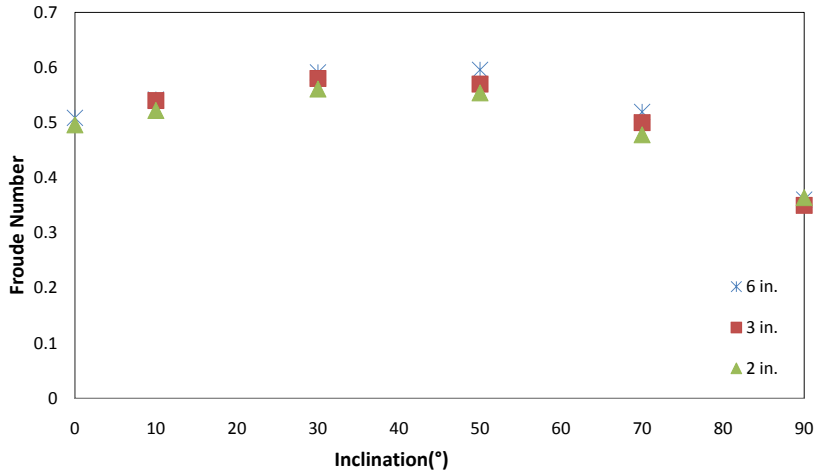

Fluid Flow Projects

Advisory Board Meeting, May 12, 2010

Experimental Results …

Viscosity Effect

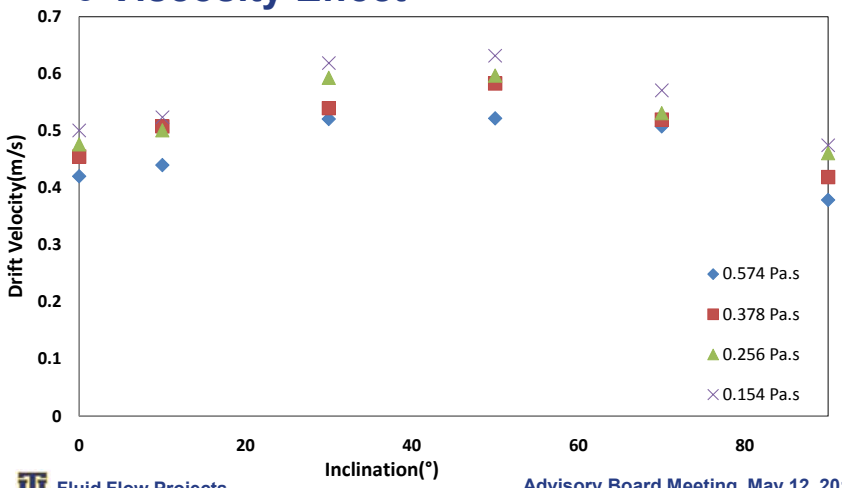

Fluid Flow Projects

Advisory Board Meeting, May 12, 2010

Experimental Results …

Diameter Effect (0.574 Pa·s)

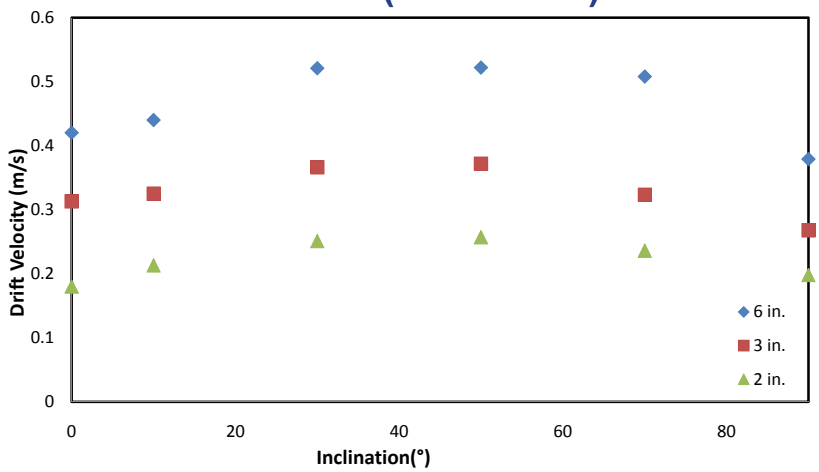

Fluid Flow Projects

Advisory Board Meeting, May 12, 2010

Experimental Results …

Diameter Effect (0.378 Pa·s)

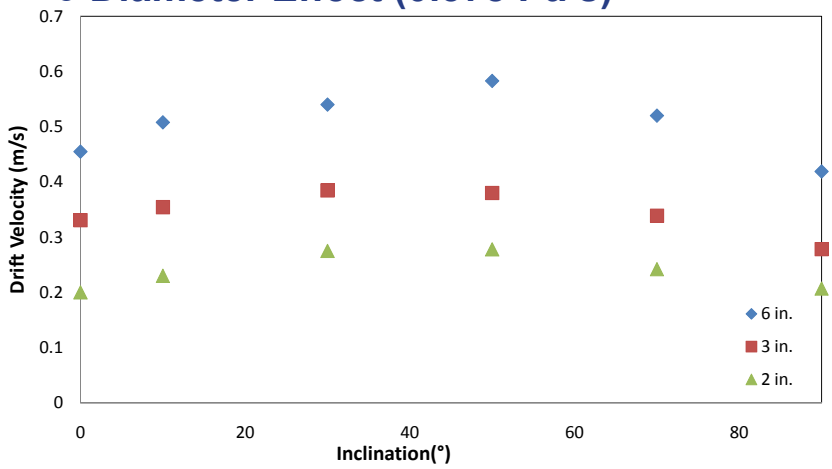

Fluid Flow Projects

Advisory Board Meeting, May 12, 2010

Experimental Results …

Diameter Effect (0.256 Pa·s)

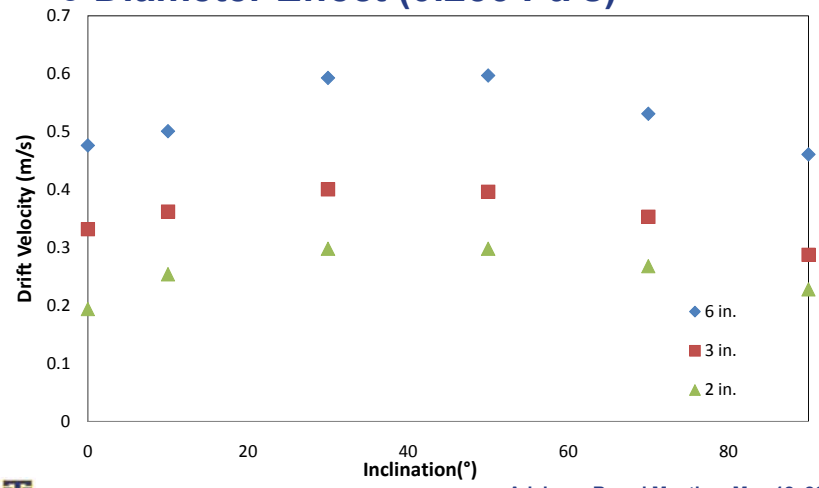

Fluid Flow Projects

Advisory Board Meeting, May 12, 2010

Experimental Results …

Diameter Effect (0.105 Pa·s)

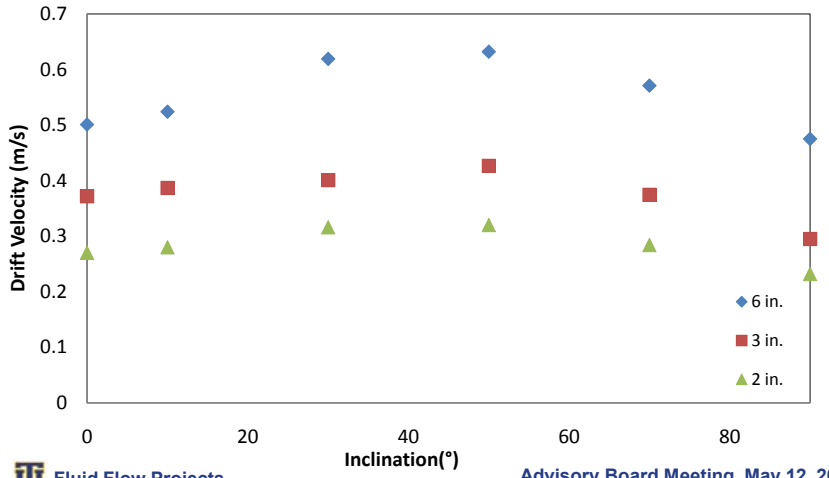

Fluid Flow Projects

Advisory Board Meeting, May 12, 2010

CFD Simulation

- Simulation Software: Fluent 6.1
- Time Dependent Two-phase Flow
- Laminar Flow
- Interface Modeling: Volume of Fluid (VOF) Method
- Horizontal Pipe Filled with Liquid
- A Quick Closing Valve is Opened to Drain Liquid

CFD Simulation …

- Boundary Conditions
  - At x=0, Zero Velocity between Phases
  - At x=L, $P = P_{atm}$ and $\alpha = 1$
  - No Slip Condition at Wall
  - Constant Surface Tension

CFD Simulation …

- Validation
  - Good Agreement with Data

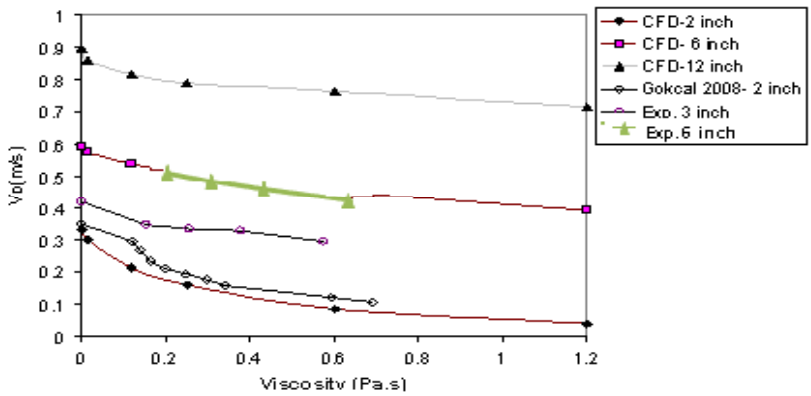

Conclusions

- Drift Velocity
  - Decreases with Increase in Liquid Viscosity
  - Increases with Increase in Pipe Diameter
  - Increases, Reaches Maximum at around 30-50° and then Decreases
- Drift Velocity Data Corroborate with CFD Predictions

Future Tasks

- Develop a Drift Velocity Closure Relationship for Combined Effects of Diameter and Oil Viscosity
- Conduct Experiments with Higher Viscosity Oils
- Compare CFD Simulations for Higher Viscosity Oils with Experiments

Questions/Comments

Effect of Pipe Diameter on Drift Velocity for High Viscosity Liquids

Benin Chelinsky Jeyachandra
Abdel Al-Sarkhi

PROJECTED COMPLETION DATES:

Literature Review	Completed
Facility Modifications	Completed
Preliminary Testing	Completed
Testing	Completed
Data Evaluation	Completed
Final Report	Completed

Objectives

The main objectives of this study are:

- To investigate effect of pipe diameter on drift velocity for high viscosity liquids,
- To identify variation of drift velocity with inclination and liquid viscosity,
- To validate CFD prediction of drift velocity with experimental results.

Introduction

Heavy oil is gaining a center stage in the world energy supply as a promising hydrocarbon energy source. Accurate prediction of flow behavior for high viscosity oil is very important for sizing the production facilities and transport pipelines. Current multiphase flow models are mostly based on experiments conducted with low viscosity as low as 0.02 Pa·s. It is erroneous to use these models for prediction of high viscosity oil multiphase flow. Flow characteristics that are likely to be affected by viscosity include flow patterns, droplet formation, bubble entrainment, slug mixing zones, etc.

The first experimental study at TUFFP on high viscosity oil was completed by Gokcal (2005). The effects of high oil viscosity on oil-gas two-phase flow behavior were investigated and significant changes in flow behavior were encountered. Gokcal (2005) observed intermittent flow (slug and elongated bubble) as the dominant flow pattern for high viscosity oil and air flow. The slug characteristics need be examined in detail for better understanding of high liquid viscosity effect.

Gokcal (2008) investigated the effects of high viscosity on slug flow characteristics. He conducted experiments and theoretical studies on the effect of viscosity on drift velocity, translational velocity, slug frequency and slug length in horizontal pipes. He conducted drift velocity experiments in a 2 in. pipe. Sharma (2009) conducted the same experiments in a 3 in. pipe. Experiments have been carried out in a 6 in. pipe for this study.

Literature Review

Slug translational velocity is one of the key closure relationships in the mechanistic modeling of two phase flow. Translational velocity is defined as the summation of drift velocity and the maximum axial velocity as proposed by Nicklin *et al.* (1962).

$$v_t = C_s v_s + v_d \,. \qquad (1)$$

Drift velocity can be visualized as the velocity with which a bubble travels in a stagnant liquid column. The coefficient C_s is approximately the ratio of the maximum velocity to the average velocity of a fully developed velocity profile. Typical values for C_s are 2 and 1.2 for laminar and turbulent flows, respectively. v_s is the mixture velocity.

Dumitrescu (1943) and Davies and Taylor (1950) conducted potential flow analysis to find the drift velocity for vertical flow. They derived the

dimensionless group Froude number, which has a constant value. Davies and Taylor estimated the constant as 0.328 while Dumitrescu made a more accurate calculation and theoretically determined the value to be 0.351. This value agreed well with the air-water experiment of Nicklin *et al.* (1962).

Drift velocity was thought not to exist for horizontal case by Wallis (1969) and Dukler and Hubard (1975). But Nicholson *et al.* (1978), Weber (1981) and Bendiksen (1984) showed that drift velocity does exist, and its value can exceed the value in vertical flow. The drift velocity for horizontal case results from the hydrostatic pressure difference between the top and bottom of the bubble nose.

Benjamin (1968) used the inviscid potential flow theory to predict the value of horizontal drift velocity coefficient. The drift velocity for horizontal case can be visualized as the penetration of a bubble when liquid is drained out of the horizontal pipe. He obtained with the following correlation,

$$v_d = 0.542\sqrt{gD}\,. \qquad (2)$$

Bendiksen (1984) and Zukoski (1966) supported the study of Benjamin (1968), experimentally.

Zukoski experimentally investigated the effects of liquid viscosity, surface tension, pipe inclination on the motion of single elongated bubbles in stagnant liquid for different pipe diameters. He also found that the effect of viscosity on the drift velocity is negligible for Re ($v_d\rho D/\mu$)>200. The lower values of drift velocity in horizontal pipe were due to changing the pipe diameter and not due to changing the liquid viscosity or surface tension thus the Eotvos number ($Eo=\rho D^2 g/\sigma$) was changed.

Bendiksen (1984) investigated the effect of different inclination angles for velocities of single elongated bubbles. He proposed the following equation for all inclination angles:

$$v_d = v_{d,h}\cos\theta + v_{d,v}\sin\theta\,, \qquad (3)$$

where, $v_{d,h}$ and $v_{d,v}$ are drift velocities for horizontal and vertical flows, respectively. Shosho and Ryan (2000) found that as the inclination angle increases, the bubble shape becomes streamlined and increased the bubble velocity. The force component which tends to reduce the bubble velocity was found as the buoyancy force.

Joseph (2003) modeled the rise velocity of spherical cap bubble and took viscosity effects into consideration. He found that the viscosity slows the bubble rise velocity.

Gokcal (2008) and Sharma (2009) conducted experimental studies on drift velocity of heavy oil at different viscosities corresponding to different temperatures (19.2 to 45°C), in 2 in. and 3 in. pipes, respectively.

Experimental Study

Facility

The experimental facility consists of an oil storage tank, a 20 HP screw pump, a 3.05-m long (10 ft) long acrylic pipe with 152.4-mm (6 in.) ID, heating and cooling loops, transfer hoses and instrumentation (see Fig. 1.). Previous experiments were conducted by replacing the acrylic pipe with 2 in. and 3 in. diameter pipes. The acrylic pipe is located close to the storage tank. The inclination of the pipe can be varied using a pulley arrangement. The pipe inclination can be changed from 0° to 90°. The heating and cooling loops are used to maintain the desired temperature and thereby to control the viscosity of the oil.

The oil pump supplies the pipe with oil. Then, the main inlet valve and the auxiliary inlet valve are closed. The drainage valve is opened to drain the residual oil captured and thereby create a gas pocket. Next, the drainage valve is closed and the main inlet valve is opened to release the gas bubble into the stagnant oil column. The drift velocity is measured by two optical sensors separated by a distance of 0.9144 m (3-ft). The optical sensors work by principle that the light intensity changes when it reflects/refracts the oil or the gas phase. This is stored as voltage readings in a data acquisition system with a frequency of 500 readings/sec. The data is analyzed in a computer and the drift velocity is calculated by dividing the distance between the two sensors (0.9144-m) with time difference between the two voltage peaks. A modification was carried out for the horizontal case. The end plate for the 6 in. pipe was removed and it was replaced with a 6 in. plug. This would facilitate the removal of plug after the pipe is filled and the draining of oil can be modeled as the penetration of gas bubble into the fluid.

Test Fluids

Following are typical properties of the oil:

- Gravity: 27.6 °API
- Viscosity: 0.220 Pa·s @ 40°C
- Density: 889 kg/m3 @ 15.6°C
- Surface tension: 0.03 N/m @ 40°C

The oil viscosity and density vs. temperature are shown in Figs. 2 and 3, respectively.

Experiment with 6 in. ID Pipe

Experiments were conducted with water to find the drift velocity to validate the experimental procedures. The results of the experiments were compared with drift velocity results from Gokcal (2008), Sharma (2009) and Bendiksen (1984) data (Fig. 4). The results are very close to the Bendiksen's prediction and follow the same trend.

Experiments were conducted with heavy oil for for 70, 80, 90 and 105 ^{o}F. The corresponding oils viscosities are 0.574, 0.378, 0.256 and 0.154 Pa·s, respectively. Figure 5 shows the combined effect of both inclination angle and oil viscosity on the drift velocity for 6 in. ID. pipe. Each experiment was carried out for inclination angles of 0°, 10°, 30°, 50°, 70° and 90°. Figures 6-9 show the effect of diameter on the drift velocity of viscous oils.

The results of the experiments were compared with the data of Sharma (2009) and Gokcal (2008). The trend of drift velocity vs. inclination for different diameters was similar.

Validation of CFD Results

The results obtained from the experiments were used to validate the results from the Computational Fluid Dynamics (CFD) simulations by Mansour *et al.* (2010). The CFD simulations were conducted with Fluent 6.1. The process is a time dependent two-phase fluid flow. Since the two phases are not mixed, the volume of fluid method (VOF) is the most suitable method to track the gas-liquid (air-oil) interface during this drainage process. For the range of viscosities studied in the present work the flow in the oil phase is laminar and may be creeping at high viscosity (up to 1.2 Pa·s). Furthermore, the air flow is also laminar as the Reynolds number is expected to stay below 2000 for the cases investigated. The volume fraction of the gas (air) is denoted by α. In the VOF model, given a cell inside the computational domain; three conditions are possible:

- α=0: the cell is full of liquid.
- α=1: the cell is full of gas.
- $0<\alpha<1$: the cell contains an interface between the gas and the liquid.

The local value of the air volume fraction α determines the appropriate properties and variables appearing in the transport equations.

The boundary condition for the above continuity and momentum equations are as follows:

a) At x=0, both phases have zero velocity,
   V(x=0, y, z) = 0;
b) At x=L, a pressure condition is applied and the reverse flow (*rf*) phase to allow air to enter is set to α_a is set to unity:
   P(x=L, y, z) = 1;
   α(x = L+, y, z)=1
c) At all the walls, the no slip condition is set
   $V(0<x<L, y^2+z^2 = D^2/4) = 0$
d) Finally, a constant surface tension value is applied depending on the air-liquid system.

The most robust simulation technique was the implicit time formulation which has guaranteed stability. The simulation for 2 in. ID, 0. 600 Pa·s and 1.2 Pa·s with a 3D grid of 85,200 cells took more than 6 months to finish on a workstation with Pentium 4, 64 bit processor with 2 GHz.

Drift velocity decreases with increasing the viscosity. Larger the pipe diameter is higher the drift velocity. The decrease in the drift velocity with viscosity is sharper in the small pipes than in the large pipes. There was a very good match between the results of CFD and the 6 in. ID. drift velocity results. Figure 10 gives a comparison of CFD simulation of drift velocity to the experimental results.

Conclusion

- Drift velocity decreases with increase in liquid viscosity.
- Drift velocity increases with increase in pipe diameter.
- As the pipe inclination angle increases, the drift velocity increases, reaches a maximum at around 30-50° and then starts decreasing.
- The drift velocity data collected from Gokcal (2008), Sharma (2009) and Jeyachandra (2010) corroborate the CFD predictions.

Future Tasks

The main future tasks are:

- Develop a drift velocity closure relationship for the combined effects of diameter and oil viscosity.
- Conduct experiments with higher viscosity oils.
- Compare the CFD simulations for higher viscosity oils with experiments.

Nomenclature

d = pipe diameter [m]
f = friction factor
H = holdup
Re = Reynolds number
V = velocity [m/s]

Greek Letters

μ = viscosity [kg/ms]
ρ = density [kg/m3]
σ = surface tension [N/m]
θ = inclination angle [º]

Subscripts

G = gas phase
L = liquid phase
M = mixture
S = slug
T = translational velocity
D = drift velocity

References

Ben- Mansour, R., Sharma A. K., Jeyachandra B. C., Gokcal, B., Al Sarkhi, A., Sarica, C.: "Effect of Pipe Diameter and High Oil Viscosity on Drift Velocity for Horizontal Pipes," To be presented, 7th North American Conference on Multiphase Technology, June 2 - 4, 2010, Banff, Canada.

Bendiksen, K.H.: "An Experimental Investigation of the Motion of Long Bubbles in Inclined Tubes," *Int. J. Multiphase Flow (1984),* **10**, 467-483.

Benjamin, T.B.:"Gravity Currents and Related Phenomena," *J. Fluid Mech. (1968),* **31** (2), 209-248.

Carew, P.S, Thomas, N. H., Johnson, A.B.: "A Physically Based on Correlation for the Effects of Power Law Rheology and Inclination on Slug Rise Velocity," Int. J. Multiphase Flow, Vol. 21, pp. 1091-1106 (1995).

Davies, R.M., and Taylor, G.I.: "The Mechanics of Large Bubbles Rising Through Liquids in Tubes," *Proc. Royal Soc. London (1950),* **A 200**, 375-390.

Dumitrescu, D.T.: "Strömung an einer Luftblase im senkrechten," *Rohr. Z. Angew. Mat. Mech.(1943),* **23**, 139-149.

Gokcal, B.: "An Experimental and Theoretical Investigation of Slug Flow for High Oil Viscosity in Horizontal Pipes," Ph.D. Dissertation, The University of Tulsa (2008).

Joseph, D.: "Rise Velocity of a Spherical Cap Bubble," J. Fluid Mech. Vol. 488, pp. 213–223 (2003).

Nicklin, D.J., Wilkes, J.O., Davidson, J.F.: "Two-Phase Flow in Vertical Tubes," *Trans. Inst. Chem. Eng. (1962),* **40**, 61-68.

McNeil, D.A., and Stuart, A.D.: "The Effects of a Highly Viscous Liquid Phase on Vertically Upward Two-Phase Flow in a Pipe," Int. J. Multiphase Flow, Vol. 29, pp. 1523-1549 (2003).

Nadler, M., and Mewes, D.: "Effects of the Liquid Viscosity on the Phase Distributions in Horizontal Gas-Liquid Slug Flow," Int. J. Multiphase Flow, Vol. 21, No. 2, pp. 253-266 (1995).

Table 1: Comparison of 2 in., 3 in. and 6 in. Data for Heavy Oil

			Drift Velocity		
			2 Inch	3 Inch	6 Inch
Temp. (F)	Viscosity. (Pa·s)	Inclination	V_d(m/s)	V_d(m/s)	V_d (m/s)
70.14	0.574	0	0.18	0.313	0.4204
		10	0.21	0.325	0.44
		30	0.251	0.366	0.521
		50	0.257	0.372	0.522
		70	0.236	0.324	0.508
		90	0.198	0.268	0.379
80.14	0.378	0	0.2	0.331	0.4549
		10	0.23	0.354	0.508
		30	0.275	0.385	0.54
		50	0.278	0.380	0.583
		70	0.242	0.339	0.52
		90	0.207	0.278	0.419
90	0.256	0	0.194	0.332	0.47625
		10	0.25	0.362	0.501
		30	0.298	0.401	0.593
		50	0.298	0.397	0.597
		70	0.268	0.353	0.531
		90	0.228	0.288	0.461
105	0.154	0	0.27	0.372	0.501
		10	0.28	0.387	0.524
		30	0.316	0.401	0.619
		50	0.32	0.427	0.632
		70	0.284	0.375	0.571
		90	0.232	0.295	0.475

Table 2: Comparison of 6 in. ID Drift Velocity Data for Water with Bendiksen's Model

Inclination	V_d (m/s)	Bendiksen
0	0.622	0.660
10	0.663	0.723
30	0.723	0.785
50	0.723	0.751
70	0.635	0.627
90	0.44	0.428

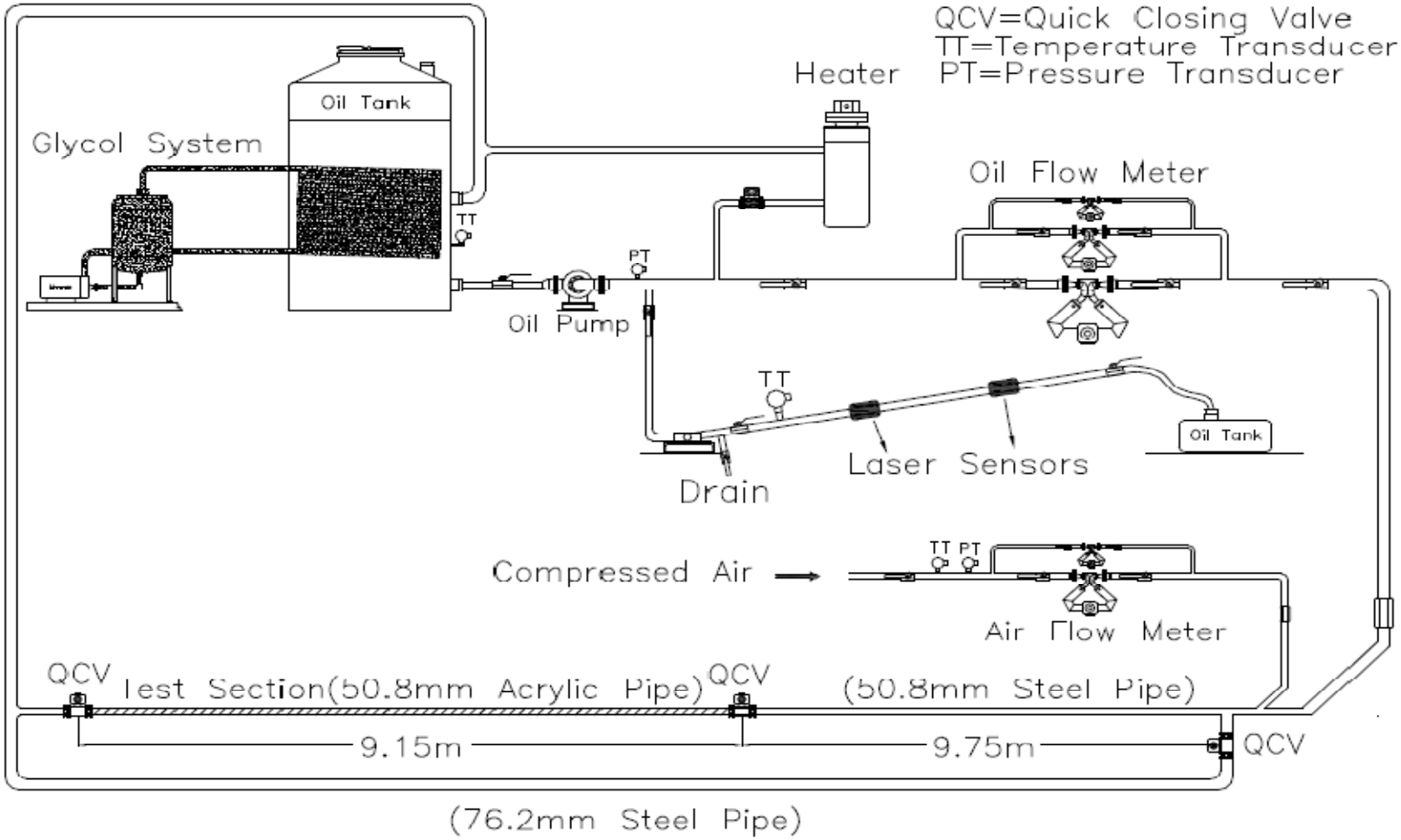

Figure 1: Schematic of High viscosity facility of the Tulsa University Fluid Flow Projects (TUFFP)

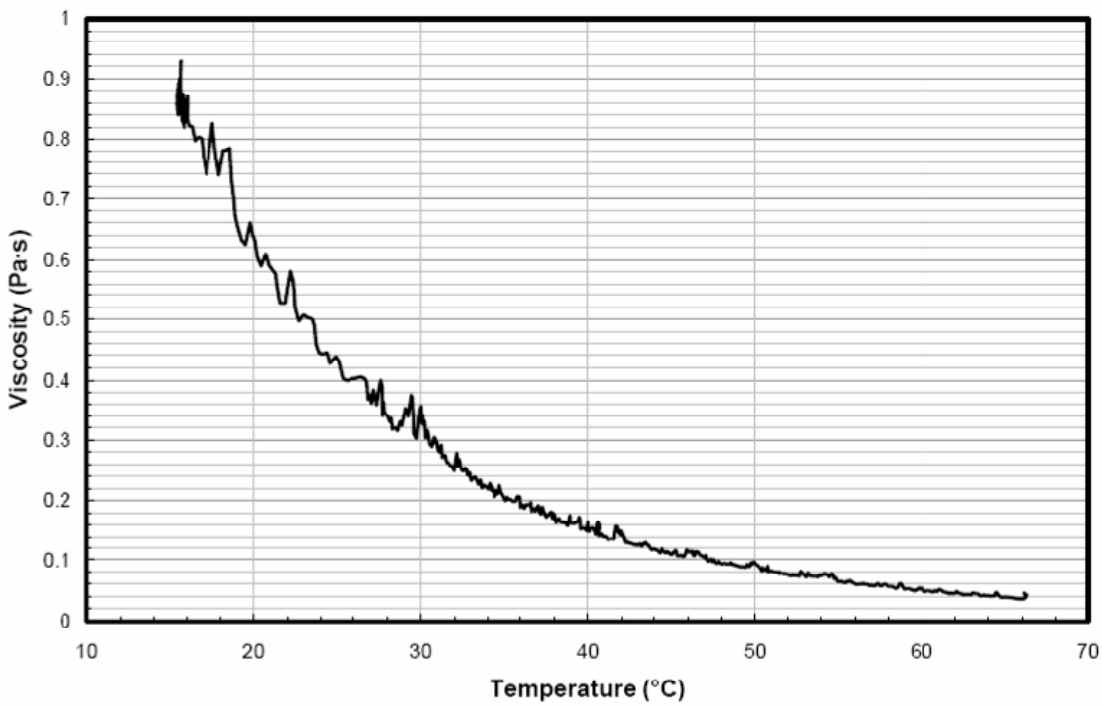

Figure 2: Viscosity vs. Temperature for Citgo Sentry 220

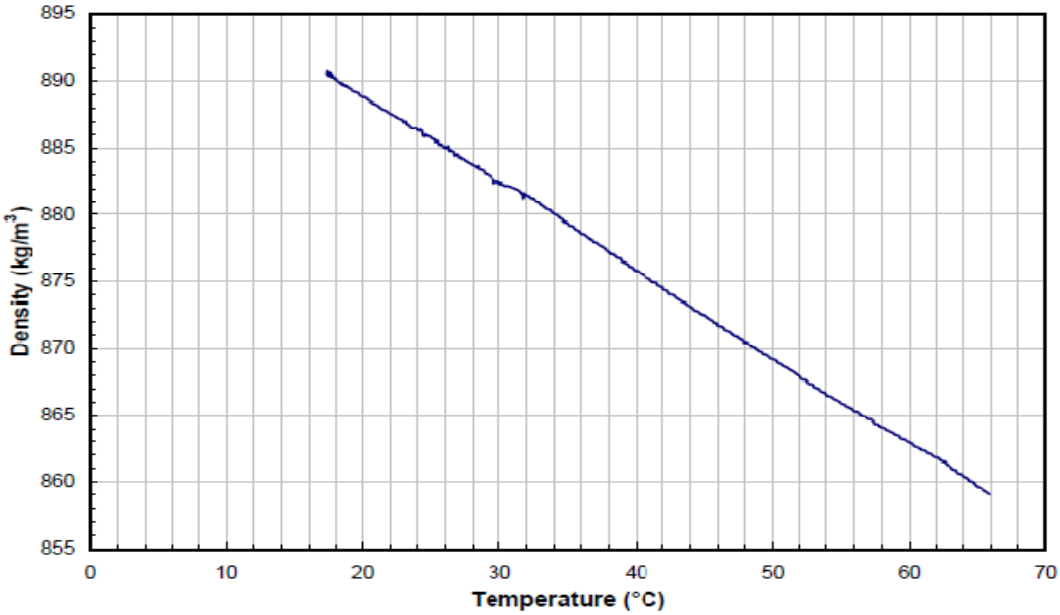

Figure 3: Density vs. Temperature for Citgo Sentry 220

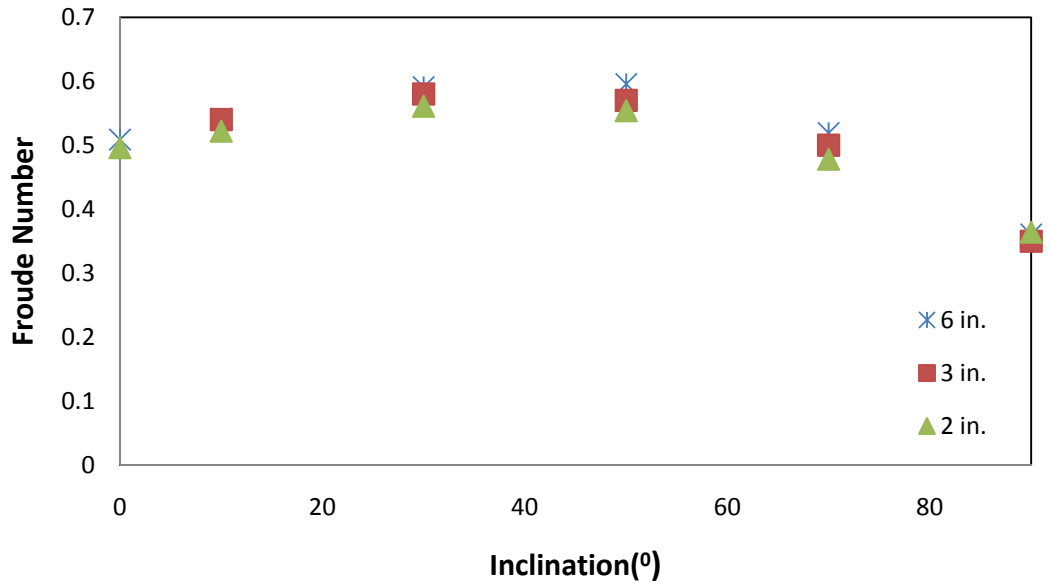

Figure 4: Froude number vs. Inclination for Water

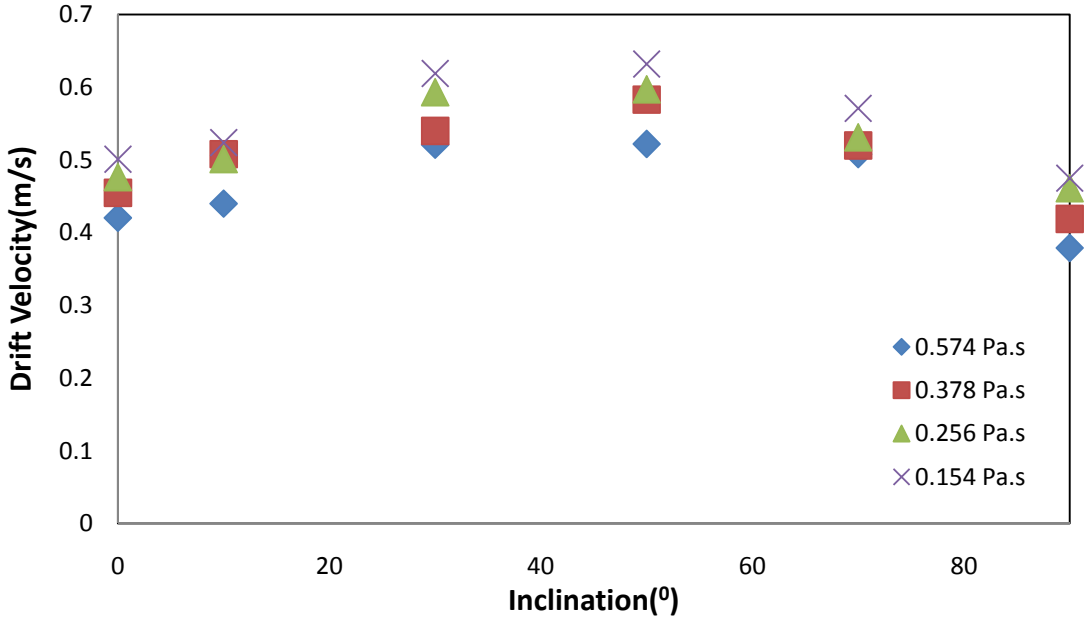

Figure 5: Viscosity and Inclination Effects on Drift Velocity

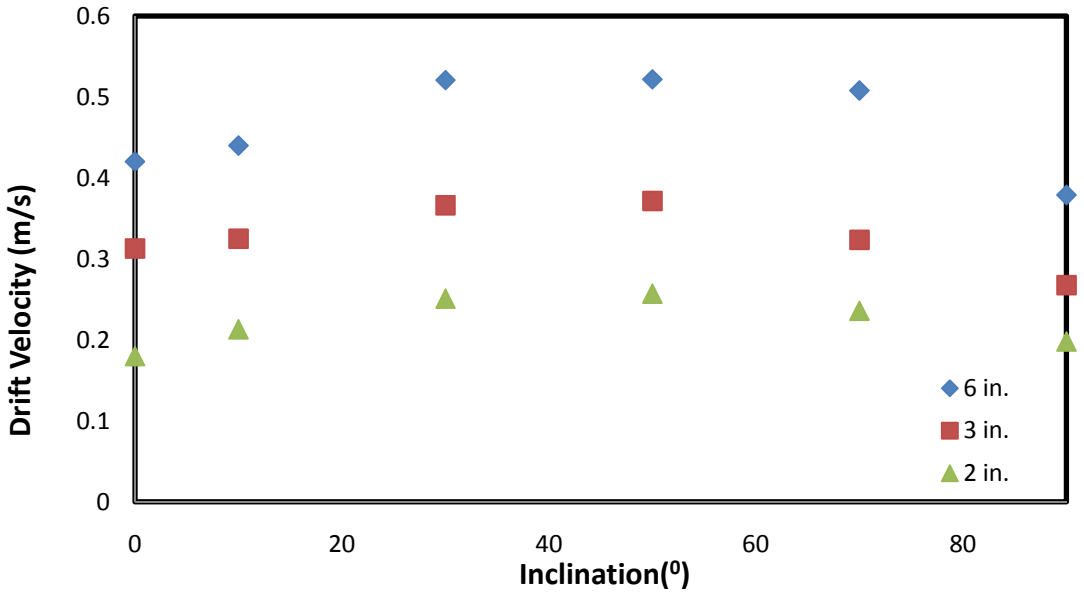

Figure 6: Drift Velocity vs. Inclination for 0.574 Pa·s Viscosity Oil

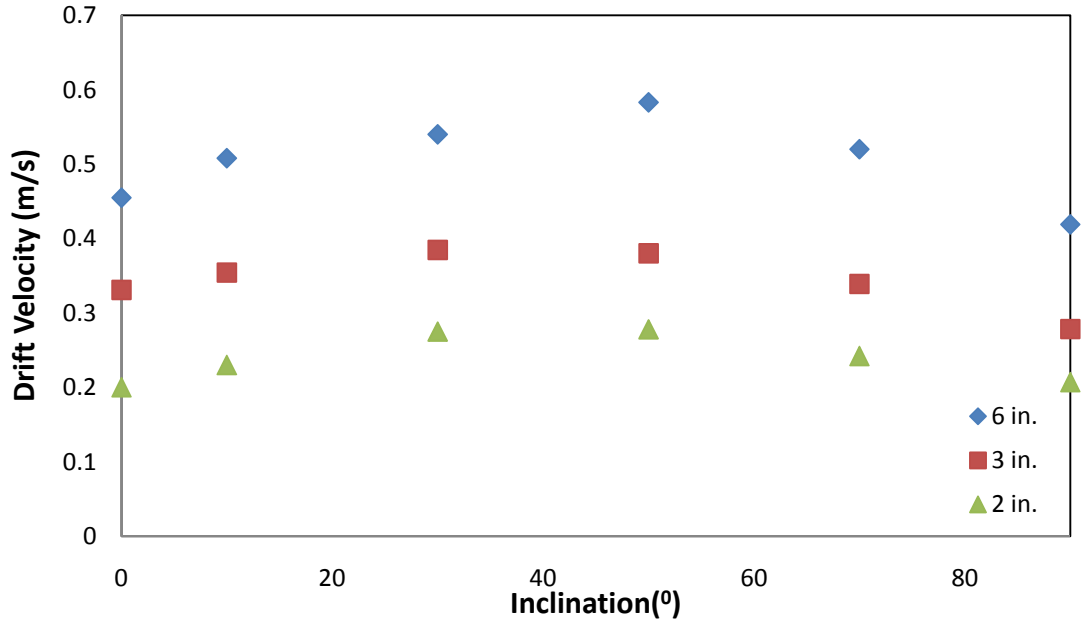

Figure 7: Drift Velocity vs. Inclination for 0.378 Pa·s Viscosity Oil

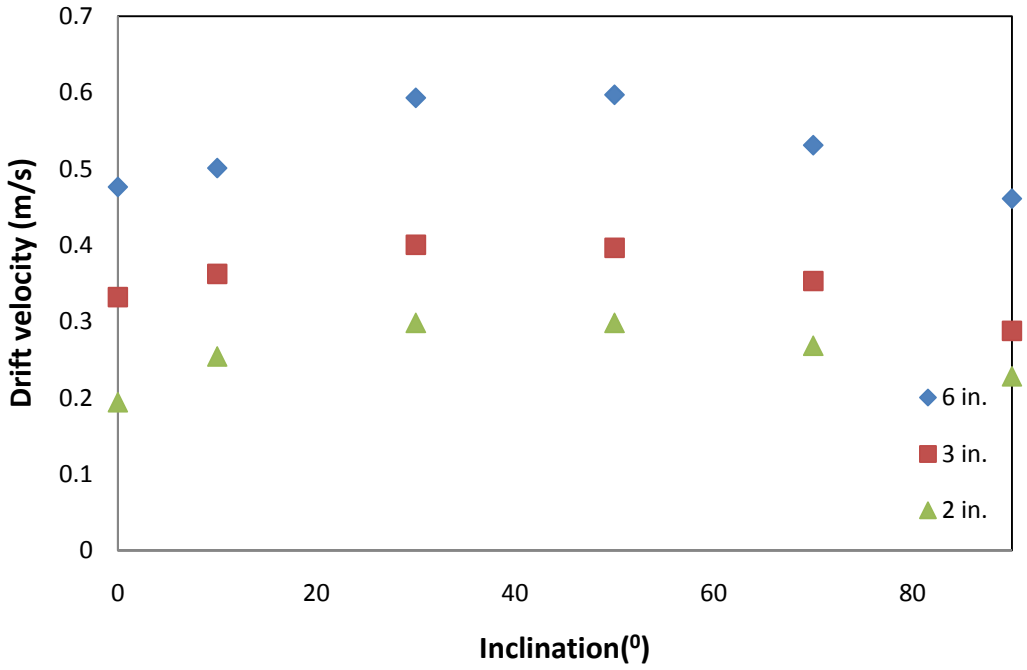

Figure 8: Drift Velocity vs. Inclination for 0.256 Pa·s Viscosity Oil

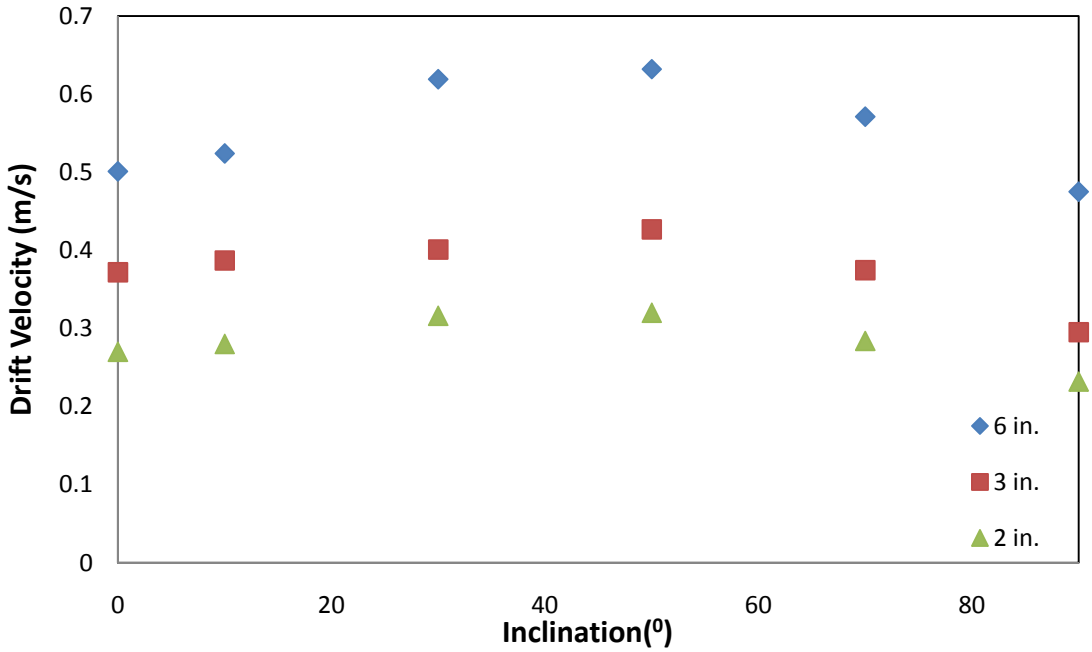

Figure 9: Drift Velocity vs. Inclination for 0.105 Pa·s Viscosity Oil

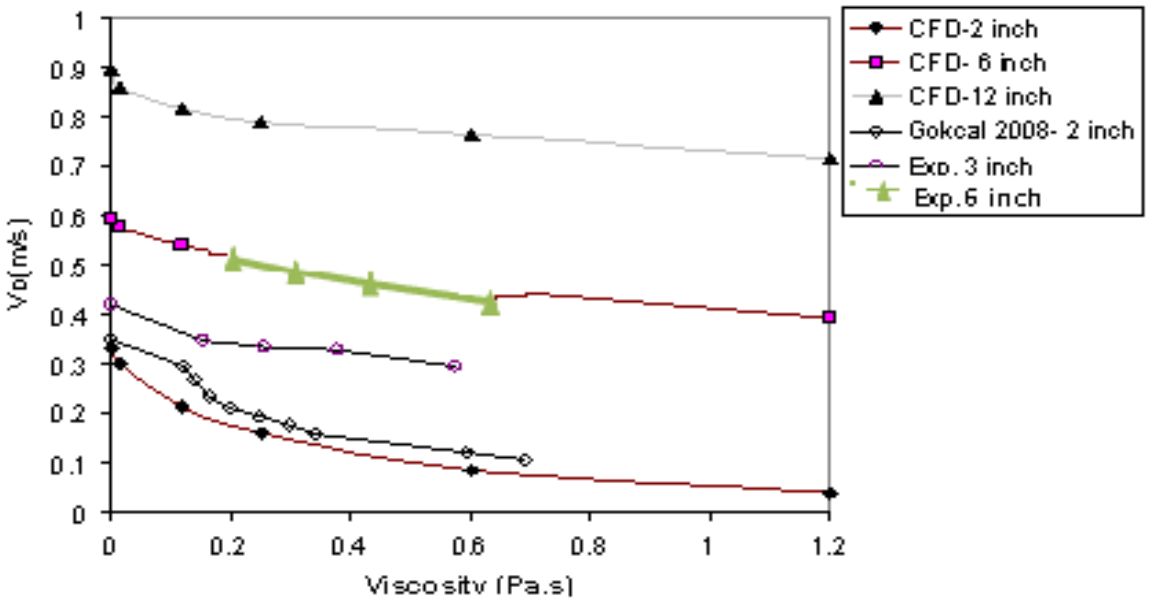

Figure 10: Comparison of Drift Velocity CFD Simulation and Experimental Results

Fluid Flow Projects

Investigation of High Viscosity Oil Two-Phase Slug Length in Horizontal Pipes

Eissa Al-safran (KU/KOC)

Outline

- Introduction
- Flow Visualization
- Data Analysis
- Physical and Theoretical Viscosity Effect
- Modeling
- Future Work

Significance

- Pipeline Design (Sizing and Routing)
  - Pressure Drop
  - Liquid Volume
- Facility/Equipment Design
  - Instantaneous Liquid Rate at Pipe Outlet is 5-20 x Average Rate
  - Slug Catchers
  - Multiphase Pumps
  - Multiphase Meters

Significance …

- Flow Assurance
  - Terrain Slugging
  - Erosion/Corrosion
- Mechanical Integrity
  - Piping System
  - System Components

Literature Review

- No Literature is Found on High Viscosity Oil Two-phase Slug Length
- Low Viscosity Oil Slug Length is Strongly Correlated to Pipe Diameter, and Insensitive to Other Parameters
- Low Viscosity Oil Slug Length
  - Smallest Near the "Center" of Slug Flow Region on Flow Pattern (FP) Map
  - L_s Increases Near Transition Boundaries

Literature Review ...

- High Viscosity Effect on Liquid Holdup in Film and Slug Regions-Direct Relationship
- High Viscosity Effect on Slug Frequency-Inverse Relationship
- Increase of Slug Frequency and Slug Liquid Holdup Results in Short Slugs

Flow Visualization

- Slug Zone (v_{SL}=0.01 m/s, v_{Sg}=1.5 m/s)
  - Slug Front

μ=0.590 Pa.s

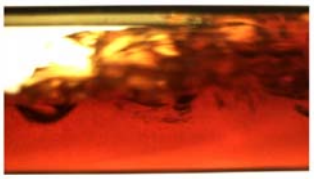

μ=0.182 Pa.s

Flow Visualization ...

- Slug body

μ=0.590 Pa.s

μ=0.182 Pa.s

Flow Visualization ...

- Slug Tail

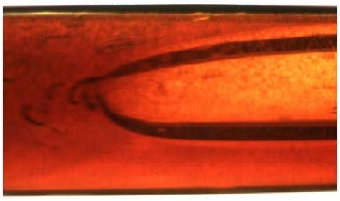

μ=0.590 Pa.s

μ=0.182 Pa.s

Flow Visualization ...

- Film Region (v_{SL}=0.1 m/s, v_{Sg}=2 m/s, μ=0.26 Pa.s)

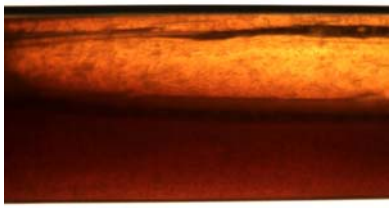

Developing film

Developed film

Data Analysis

- Comparison (Kouba (1986), BP Loop (2001), Alsafran (2003), Gokcal (2008))

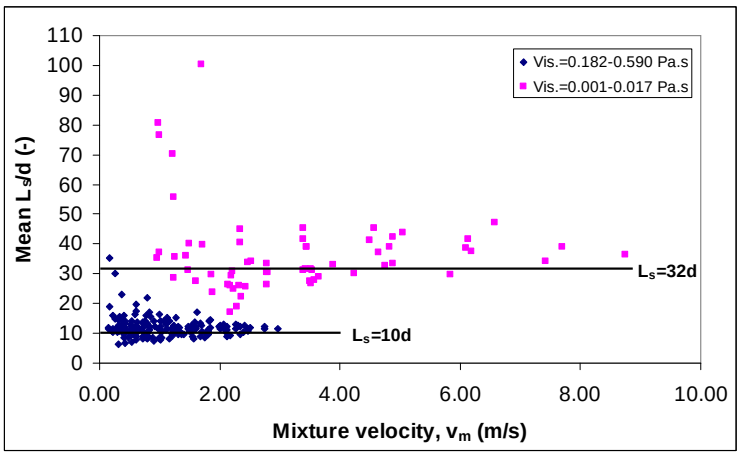

Data Analysis ...

- Slug Length Distribution Comparison (Low Viscosity vs. Moderate vs. High Viscosity)

v_{SL}=0.3 m/s
v_{Sg}=1.5 m/s

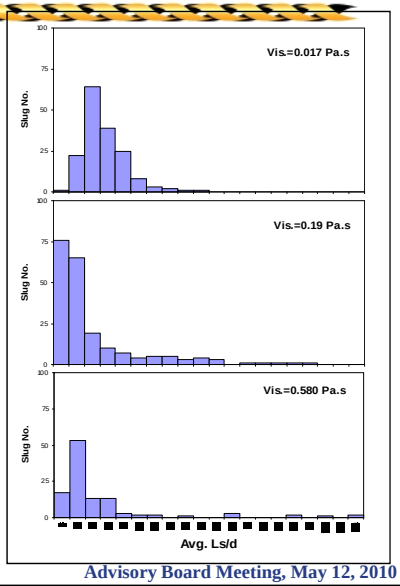

v_{SL}=0.05 m/s, v_{Sg}=2.1 m/s

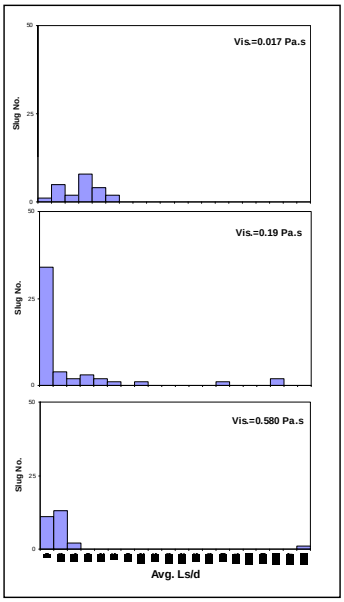

v_{SL}=0.3 m/s, v_{Sg}=2.1 m/s

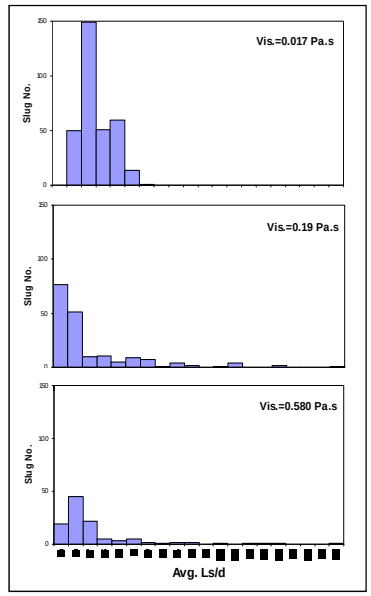

Data Analysis ...

- **Analysis of Variance (ANOVA) to Test the Following Hypothesis:**

$$H_0 : \mu_{low} = \mu_{mid} = \mu_{high}$$

  - **Calculate p-value and Set Significance Level (α=0.10), i.e. 90% Confidence**
  - **Calculated p-value<α, Thus Reject H_0**

Physical Viscosity Effect

- Dukler *et al.* (1985) Proposed Minimum Slug Length Physical Model

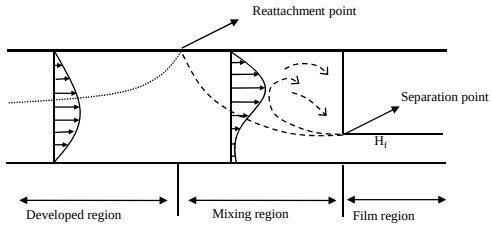

  - Sudden Expansion at Separation Point
  - New Wall Boundary at Reattachment Point
  - Downstream a Fully Developed Velocity Profile is Formed and Flow "Memory" Vanishes

Physical Viscosity Effect ...

- Proposed High Viscosity Liquid Physical Model
  - Thick Film-Less Expansion (Jet Velocity)
  - Less (Short) Front Mixing Intensity
  - Smaller Velocity Profile and Maximum Velocity

$$v_z = \frac{\Delta P \times R^2}{4\mu L}\left[1-\left(\frac{r}{R}\right)^2\right]$$

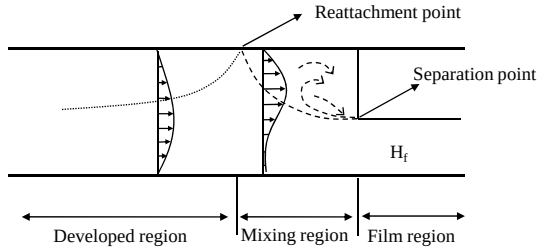

Theoretical Viscosity Effect

$$L_s = \frac{v_s}{\upsilon_s\left(H_{LLS} - H_{LTBe}\right)}\left[\left(\frac{W_L}{\rho_L A_p v_s} - H_{LTBe}\right) + c\left(H_{LLS} - H_{LTBe}\right)\right]$$

First Term: $\left[\frac{v_s \downarrow}{\upsilon_s \uparrow \left(H_{LLS} \uparrow - H_{LTBe} \Uparrow\right)\downarrow}\right]\downarrow$

Second Term: $\left[\left(\frac{W_L \rightarrow}{\rho_L(\rightarrow)A_p(\rightarrow)v_s(\downarrow)}\right)\uparrow - H_{LTBe} \Uparrow\right]\downarrow$

Third Term: $\left[c(\rightarrow)\left(H_{LLS} \uparrow - H_{LTBe} \Uparrow\right)\right]\downarrow$

Thus, Slug Length Decreases with Increasing Liquid Viscosity

Modeling

- **Woods and Hanratty (1996) (Low Viscosity)**

$$\frac{f_s D}{v_{SL}} = 1.2\left(\frac{L_s}{d}\right)^{-1} \quad \text{..... (1)}$$

- **This Study (High Viscosity)**

$$\frac{f_s d}{v_{SL}} = 1.94\left(\frac{L_s}{d}\right)^{-1} \quad \text{..... (2)}$$

Modeling ...

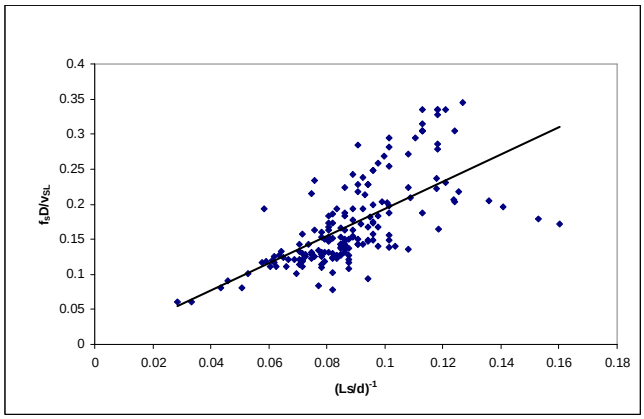

Modeling ...

- Wallis (1969) Presented Dimensional Analysis for Inertia and Viscous Forces

$$F_{rd} = \frac{v_d}{(gd)^{0.5}} \sqrt{\frac{\rho_L}{(\rho_L - \rho_G)}} \quad \text{..... (3)}$$

$$N_\mu = \frac{v_d \mu_L}{gd^2 (\rho_L - \rho_G)} \quad \text{..... (4)}$$

Modeling ...

- Combing Froude and Viscosity Numbers

$$N_f = \frac{F_{rd}}{N_\mu} = \frac{d^{3/2}\sqrt{\rho_L(\rho_L - \rho_G)g}}{\mu_L} \quad \text{..... (5)}$$

- Gokcal *et al.* (2009) showed

$$f_s = 2.623\left(\frac{N_f^{-0.612} v_{SL}}{d}\right) \quad \text{..... (6)}$$

Modeling ...

- Combing Eqs. 2, 5 and 6, and Solving for Dimensionless Slug Length

$$\frac{L_s}{d} = \beta_0 N_f^{\beta_1} \quad \text{..... (7)}$$

- Linearizing and Fitting the Proposed Model against High Viscosity Data

$$\frac{L_s}{d} = 2.63 N_f^{0.321} \quad \text{..... (8)}$$

Modeling ...

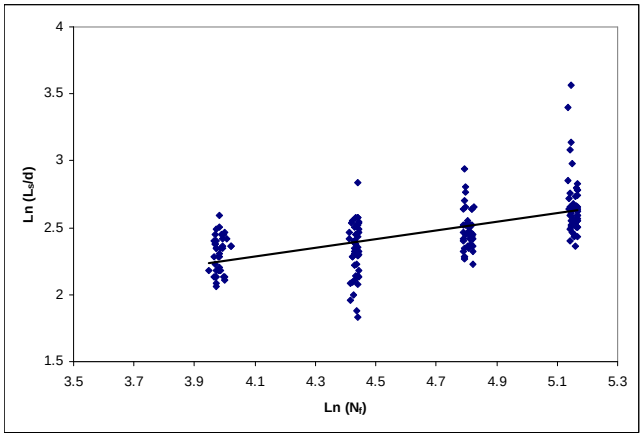

Modeling ...

- Model Statistical Evaluation
  - Overall Model Evaluation

Model df	Error df	SSE	MSE	R^2
1	161	6.43	0.200	0.32

  - Model Coefficient Evaluation

Variable	Coef.	Standard Error	t-statistics	p-value	Lower 95% CI	Upper 95% CI
$Ln(\beta_0)$	0.966	0.170	5.800	0.000	0.650	1.310
β_1	0.321	0.036	8.730	0.000	0.246	0.390

Modeling ...

- Model Validation
  - 10 data points Selected Randomly and Removed From Model Development Process
  - Statistical Error Analysis Results

Stat. Parameter	Value
APE (%)	1.72
AAPE(%)	9.8
SD(%)	13.6

Modeling ...

- Model Validation ...

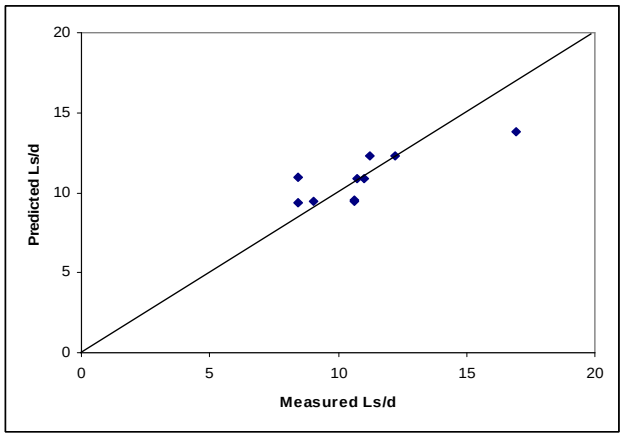

Future Work

- Further Characterize Liquid Behavior in Film Zone to Develop a Physical Model
- Compare Present Model with Existing Slug Length Models and Correlations
- Investigate Best Fit Probabilistic Distribution and Model It for High Viscosity Oil
- Expand Proposed Model to Predict Slug Length Distribution Including Maximum Slug Length and Slug Length Variation

Investigation of High Viscosity Two-Phase Slug Length in Horizontal Pipes

Eissa Al-Safran

Objective

The objectives of this project are as follows:

- Understand the effect of high viscosity liquid on average slug length and slug length distribution.
- Develop a high viscosity two-phase slug length physical and mathematical model.

Background

Gas-liquid two-phase flow in pipes occurs at production and transportation facilities for oil and gas. The most common type of flow patterns in field operation for horizontal and near horizontal pipelines is the slug flow pattern. Slug flow is described by alternating liquid slugs and gas intervals, both of which when combined form what is called slug unit. Among all the slug flow characteristics, slug length is one of the most critical characteristic for system proper design and safe operation. For example, average slug length is important and preferred (over slug frequency) input parameter for mechanistic models to predict liquid holdup and pressure gradient. Furthermore, long slugs often cause operational problems, flooding of downstream facilities, severe pipe corrosion, structural instability of the pipeline, as well as production loss and poor reservoir management due to unpredictable wellhead pressures. Although several investigators studied the average and slug length distribution in pipes for light oil, a recent literature search on high viscosity two-phase slug length revealed no comprehensive study. However, few studies were found on the effect of high viscosity liquid on other two-phase slug flow characteristics such as liquid holdups and frequency, which can be related, implicitly, to slug length.

Nadler and Mewes (1995) experimentally investigated the liquid viscosity effect on liquid holdup in the slug unit, film region and slug zone in the aerated slug flow region. They used three fluid systems, air/light oil (μ_o=17 mPa.s), air/heavy oil systems (μ_o = 34 mPa.s) and air/water systems. In general, their results revealed that by increasing liquid viscosity, a significant increase of liquid holdup in the slug unit and film region is observed, while less significant increase of liquid holdup in the slug zone is observed. The observed directly proportional relationship between film liquid holdup and liquid viscosity is explained by the increase of interfacial and wall shear forces on the liquid film. A significant difference in slug unit and film liquid holdup is observed between air/light oil and air/water systems; which is attributed to the difference in surface tension and densities of the two systems. Abdul-Majeed (2000) developed an empirical correlation for slug liquid holdup as a function of liquid viscosity. He reported that slug liquid holdup is significantly affected by and is directly proportional to liquid viscosity. Brauner and Ullmann (2004) developed a Taylor bubble wake model of gas entrainment from Taylor bubble to slug body to predict the slug liquid holdup in vertical, inclined and horizontal pipes. Their model takes into account the effect of liquid viscosity which predicts that the bubble entrainment decreases (slug liquid holdup increases) with increasing liquid viscosity. Slug frequency was also investigated for the high viscosity two-phase flow. A recent study by Gokcal *et al*. (2009) shows that slug frequency increases with increasing liquid viscosity for which they developed an empirical slug frequency correlation.

The above literature review suggests that under the condition of high liquid viscosity, slugs are less aerated and more frequent. Theoretically, these two characteristics result in short slugs. Furthermore, experimental data (Kouba (1990), Kokal (1987), Marcano (1996), Rothe (1986), Brandt and Fuchs (1989), and El-Oun (1990)) on light oil showed the inverse relationship between slug frequency and slug length, and between the slug liquid holdup and slug length. Therefore, from the limited literature review on high viscosity oil and the previous knowledge and experimental data on the relationships among slug flow characteristics, one can speculate an inverse relationship between liquid viscosity and slug length.

Flow Visualization

The data of this study is acquired by Gokcal (2008) using TUFFP high viscosity two-phase flow loop. In this section, flow visualization using high speed camera is presented for different parts of the slug flow, namely slug back and front, slug body, and film region at different viscosities. The purpose of this visualization is to characterize and better understand the slug flow structure under the effect of high liquid viscosity to be able to relate the slug and film structures to slug length.

Slug Body Zone

Figure 1 shows the slug front, slug body and slug tail for two different liquid viscosities, 0.590 Pa.s, and 0.182 Pa.s at v_{Sg}=1.5 m/s and v_{SL}=0.1 m/s. The low liquid viscosity slug (Slug A) shows turbulence and mixing in the slug front due to the high Reynolds number. On the other hand, the high viscosity slug front (slug B) is less turbulent with a top boundary layer moving faster than the slug body and entraining large bubbles. As oppose to the conventional slug front scooping process, this scooping process does not cause bubble fragmentation and entrainment into slug body; instead, it entrains large bubbles into the slugs under a new mechanism. It is evident from the slug front pictures that viscosity affects the scooping process at the slug front. The middle pictures of Fig. 3 illustrate the slug body for the same slug; which shows the impact of the gas entrainment in the slug front on the slug body. Slug B shows a large gas pocket entrained in the slug front which grows further as small bubbles merge in it. This large bubble is a result of the scooping process at the slug front. As the gas pocket grows, it splits the long slug to two shorter slugs, this is one of the mechanism generating short slugs in high liquid viscosity flows. On the other hand, low viscosity slug body shows relatively smaller entrained bubbles due to the high turbulence and mixing in the slug front which causes bubbles fragmentation generating small bubbles. The lower pictures of Fig. 1 show the slug tail for the same slugs shown previously. The high viscosity slug (Slug A) shows a long bubble nose accelerated by the wake of entrained large gas pocket which leads to short stable slugs. The lower viscosity slug back shows a sharper, less developed and deformed bubble nose. The location of the bubble nose in low viscosity liquid condition with respect to the pipe centerline is asymmetric as oppose to the symmetric geometry in the high viscosity condition. In summary, Fig. 1 shows that liquid viscosity significantly affects the slug structure.

Film (Taylor-bubble) Zone

Similar to the slug zone, high viscosity liquid significantly affects the liquid film characteristics in the Taylor bubble region. Experimental observations, under high liquid viscosity condition, by high speed video recordings show that the film height is significantly large and aerated as oppose to the low liquid viscosity condition. Furthermore, it is observed that the film region has two distinct sub-regions, namely developing and developed regions as shown in Fig. 2. The developing region is observed within 5d-10d from the Taylor bubble nose. As Fig. 2.a shows, the developed film region is characterized by a relatively thick film at the pipe top wall and a secondary tangential film flow in addition to its axial flow which increases the film height in this developing region. The developed section (Fig. 2.b) is far away from the slug zone and can be characterized by a stratified film layer. However, in the case of high liquid viscosity, a thin film layer is observed at the top wall of the pipe similar to annular flow configuration. Under certain condition of high superficial gas velocity, this layer is observed to be wavy with large entrained bubbles. This film characterization under high liquid viscosity may change the conventional modeling approach of the film zone in a slug unit.

Data Analysis

In this section, the average slug length and slug length distributions of high viscosity liquid will be presented and compared with low viscosity liquid slug length. The purpose of this comparison is to illustrate the effect of the liquid viscosity and its magnitude on slug length. Figure 3 illustrates the evolution of the dimensionless average slug length with mixture velocity for high and low viscosity liquids. As observed by Gokcal *et al.* (2008a and 2008b) and Colmenares *et al.* (2001), high viscosity liquid average slug length is shorter than that of low viscosity liquid. Figure 3 further shows a decreasing slug length trend at low values mixture velocity followed by a constant average slug length around 10d for a high viscosity liquid. Similar to the low viscosity liquid slug length trend, high viscosity average slug length shows insensitivity to operational conditions. In addition, the critical mixture velocity beyond which average slug length remains constant for high viscosity liquid is in the order of 0.5 m/s, while it is 1 m/s for light oil condition.

Figures 4-6 investigate the effect of liquid viscosity, superficial gas and superficial liquid velocities on slug length distribution characteristics, namely mean slug length, slug length variation and maximum slug length. As shown in Fig. 4, as the liquid viscosity increases approximately ten folds (from 0.017 Pa.s to 0.19 Pa.s) the slug length distribution changes in the following aspects. The slug length distribution moves from the conventional Inverse Gaussian or Log Normal to a heavily skewed distribution that can not be modeled by any of these probabilistic models. Consequently, the average slug length decreased from approximately 30 to 10 diameters, while the slug length variation increases. As the liquid viscosity further increases by two folds (i.e. 0.580 Pa.s) the central tendency of the data slightly increases moving closer to the average slug length of low viscosity case. In addition, as liquid viscosity, increases the distribution skewness severity decreases, while the slug length variation increases. The distributions show that maximum slug length increases as liquid viscosity increases; which is counter intuitive and theoretically unjustified. Therefore, it is suspected that the long slugs detected by laser props are actually short slugs separated by short gas Taylor bubble. Further investigation is necessary to confirm this observation in the data. To investigate the effect of the superficial gas velocity on slug length statistical parameters, one can inspect the slug length distribution characteristics in Fig. 4 and 5 for the same liquid viscosity condition. For example, although Fig. 5 shows a reduction in slug frequency as superficial gas velocity increases, the effect of liquid viscosity on slug length statistical characteristics stay unchanged. The effect of superficial liquid velocity is investigated by comparing Fig. 5 and 6 for a constant liquid viscosity cases. As the superficial liquid velocity decreases, the slug frequency is decreases, thus the average slug length is increased under all conditions of viscosity. In all of the cases, the effect of liquid viscosity is almost unchanged, indicating insignificant effect of superficial gas and liquid velocities on slug length and on the effect of viscosity of slug length distribution. Conversely, under all the different conditions of operational conditions, the liquid viscosity showed a significant constant effect. These results indicate that liquid viscosity is a significant correlating parameter of slug length, while operational parameters are not.

Inferential Statistical Analysis

Although the above data analysis is carried out on sample data acquired in the experimental study of Gokcal (2008), using probability theory, the analysis can be generalized by extending it to a population with a given confidence interval. Analysis of Variance (ANOVA) is carried out to investigate the existence of a significant difference in the mean slug length of light, medium and heavy liquids. ANOVA tests the following null hypothesis: H_0: $\mu_{low\ vis.}=\mu_{mid.\ vis}=\mu_{high\ vis.}$ (μ is the population mean slug length). The null hypothesis will not be rejected unless the sample data provide convincing evidence that it is false. A significance level has to be selected based on which one decides to reject or accept the null hypothesis. The significance level will be compared with the P-value (calculated by ANOVA) and if the P-value is less than the significant level, the null hypothesis will be rejected; otherwise there is no enough evidence to reject the null hypothesis. In this study, we selected a value of 0.1 significance level (α=0.1) meaning that there is 10% probability that Type I error is committed (Type I error is when true hypothesis is rejected). In other words, we will be 90% confident that our statement about the null hypothesis is true. The value of the significance level depends on how much one can tolerate falling in Type I error.

ANOVA separates the total variation in the data into two groups, namely variation within groups and variation between groups. Then, ANOVA calculates the two variations and compares them. If the variation between the groups is significantly greater than the variation within groups, then the two population means are significantly (to a level of 10%) unequal. A detailed mathematical formulation of ANOVA may be found in Hethea and Rhinehart (1991). The result of the ANOVA analysis is to reject the null hypothesis, indicating that in a population scale the mean slug length of low, medium and high viscosity liquids are significantly different. This emphasizes the effect of liquid viscosity on slug length. Further statistical analysis is under way to conduct Posteriori test to find the relation between each two pairs of averages slug lengths.

Physical and Theoretical Viscosity Effect

Average slug length of low viscosity liquid two-phase flow is found to be more or less constant, approximately, 30D (Dukler and Hubbard (1975), and Nicholson *et al*. (1978)). A fully developed slug is defined as a stable slug with a constant liquid pick-up and shed-back rates. In a stable slug, the velocity

profile at the tail of the slug is fully developed with a maximum velocity close to 1.2 of the slug velocity (Fabre, (1994)). Therefore, if a short slug has a developing velocity profile at its back, the trailing bubble velocity will be accelerated to overtake the leading bubble dissipating the short slug in between. This slug dissipation (bubble overtaking) process will continue until all the slugs in the pipe are long enough to develop a fully developed velocity profile. This process is the one that controls the slug length and establishes stable slug length.

Dukler *et al*. (1985) developed a physical model for the minimum slug length in which the interaction between the film and slug front is simulated as a sudden expansion of a conduit flow into a large reservoir (Fig. 7). As the liquid separates from the film to the slug front it goes into a recirculation process, formed between the separation point and the reattachment point, known as the slug mixing zone and characterized by vortices and high local velocity. At the reattachment point, a new wall boundary layer is developed ending the turbulence structure region. Downstream of the reattachment point, the "memory" of the severe separation effect is vanished and a new developed velocity profile is formed with lower maximum velocity. Dukler *et al*. (1985) found that the minimum stable slug length in horizontal pipe is in the order of 20d; however, experimental slug length data were found to be between 20d-40d.

In another work by Taitel *et al*. (1980) and Barnea and Brauner (1985), the developed slug length is modeled and found equal to a distance in which a jet absorbed by liquid and a fully developed velocity profile is established. According to their approach, a minimum slug length of 32d was obtained in horizontal flow.

According to the above modeling, two hydrodynamic parameters can be deduced which control the minimum stable slug length, namely the film height, which controls the sudden expansion or jet velocity, and the time for the redevelopment of fully developed velocity profile, i.e. the length of slug mixing region. Liquid viscosity affects both parameters as discussed in the flow visualization section and shown in Figs. 1 and 2. Fig. 8 shows a proposed high viscosity liquid slug physical model in which the film height in front of the slug is promoted (thick) indicating shorter mixing zone and reattachment distant which shortens the slug length to achieve a fully developed velocity profile. Furthermore, downstream of the reattachment point, the velocity profile and centerline maximum velocity are smaller because they are inverse functions of liquid viscosity in laminar flow. This can be shown by the laminar velocity profile and maximum velocity in horizontal pipe flow derived from momentum conservation law as follows.

$$v_z = \frac{\Delta P \times R^2}{4\mu L}\left[1-\left(\frac{r}{R}\right)^2\right]. \tag{3}$$

$$v_{z,\max} = \frac{\Delta P \times R^2}{4\mu L}. \tag{4}$$

The proposed physical model in Fig. 8 indicates that the change in slug flow characteristics due to high liquid viscosity result in shorter stable slug lengths.

Theoretically, the slug length can be derived from mass and momentum conservation laws across the slug and film regions (Dukler and Hubbard (1975)) as follows.

$$L_s = \frac{v_s}{f_s\left(H_{LLS} - H_{LTBe}\right)} \times \left[\left(\frac{W_L}{\rho_L A_p v_s} - H_{LTBe}\right) + c\left(H_{LLS} - H_{LTBe}\right)\right] \tag{5}$$

From Eq. 5 the effect of liquid viscosity can be implicitly related to the slug length through the slug flow characteristics, namely v_s, f_s, H_{LLS} and H_{LTBe}. From our experimental observation shown in Fig. 2, the liquid holdup in Taylor bubble, H_{LTBe}, is promoted as well as the slug liquid holdup, H_{LLS}, yet the increase in the film holdup is more significant than in slug zone (Nadler and Mewes (1995)). Thus, the effect on their difference (H_{LLS}-H_{LTBe}) is inversely proportional to liquid viscosity. Furthermore, it is experimentally observed and theoretically investigated by Gokcal (2009) that slug frequency increases with increasing liquid viscosity. If we look at each term of Eq. 5 and its relationship to the LHS term of slug length as liquid viscosity increases, the following is found.

1st term of Eq. 5:

$$\left[\frac{v_s \downarrow}{f_s \uparrow \left(H_{LLS} \uparrow - H_{LTBe} \Uparrow\right)\downarrow}\right]\downarrow$$

2nd term of Eq. 5:

$$\left[\left(\frac{W_L \rightarrow}{\rho_L(\rightarrow)A_p(\rightarrow)v_s(\downarrow)}\right)\uparrow - H_{LTBe} \Uparrow\right]\downarrow$$

3rd term of Eq. 5:
$[c(\rightarrow)(H_{LLS} \uparrow - H_{LTBe} \Uparrow)] \downarrow$

The above analysis shows the significant inverse effect of liquid viscosity on slug length.

Modeling

Woods and Hanratty (1996) presented a relationship between dimensionless slug frequency and the dimensionless slug length as follows.

$$\frac{f_s D}{v_{SL}} = 1.2\left(\frac{L_s}{d}\right)^{-1} \tag{6}$$

In their study, Woods and Hanratty (1996) derived Eq. 6 from light crude experimental slug flow data; thus the 1.2 constant may not be applicable for high liquid viscosity conditions. Therefore, Eq. 6 is fitted against the high viscosity experimental data acquired in this study as shown in Fig. 9.

The data trend in Fig. 9 can be modeled by a simple linear regression model as follows.

$$\frac{f_s d}{v_{SL}} = 1.94\left(\frac{L_s}{d}\right)^{-1} \tag{7}$$

Wallis (1969) presented a dimensional analysis for inertia and viscous forces. As a result, two dimensionless numbers were derived, namely Froude number and viscosity number; which can be defined as in Eq. 8 and 9, respectively.

$$F_{rd} = \frac{v_d}{(gd)^{0.5}}\sqrt{\frac{\rho_L}{(\rho_L - \rho_G)}} \tag{8}$$

$$N_\mu = \frac{v_d \mu_L}{gd^2(\rho_L - \rho_G)} \tag{9}$$

Combining the inertia and viscous forces, the dimensionless inverse viscosity number is found as the ratio of Froude to viscosity numbers as follows.

$$N_f = \frac{F_{rd}}{N_\mu} = \frac{d^{3/2}\sqrt{\rho_L(\rho_L - \rho_G)g}}{\mu_L} \tag{10}$$

Eq. 10 combines the inertia and viscous forces; which are theoretically affect the slug length under high liquid viscosity conditions as shown the previous section. Gokcal *et al.* (2009) showed that slug frequency is correlated to the dimensionless inverse viscosity number as follows.

$$f_s = 2.623\left(\frac{N_f^{-0.612} v_{SL}}{d}\right) \tag{11}$$

Combing Eqs. 7 and 11, the dimensionless inverse viscosity number is related to the dimensionless slug length as follow.

$$\frac{L_s}{d} = \beta_0 N_f^{\beta_1} \tag{12}$$

Eq. 12 is linearized and fitted against the high liquid viscosity data as illustrated in Fig. 10. The two constants, β_0 and β_1, are obtained from the simple linear regression model fitted against the data as the best linear unbiased estimators as follows.

$$\frac{L_s}{d} = 2.63 N_f^{0.321} \tag{13}$$

Model Statistical Evaluation

The model in Eq. 13 overall statistics and the individual coefficient's statistics are calculated and reported in Tables 2 and 3, respectively. Table 2 illustrates the reliability of the regression model and its ability to capture the variability in average slug length. The Sum of Square of Error (SSE) in Table 2 quantifies the deviation of the predicted data from the actual values by the regression model. The square root of the ratio of SSE to error degrees of freedom (df) is the Mean Squared Error (MSE) which quantifies the degree of scatter of the data around the line. The coefficient of variation, R^2, measures the proportion of the variation in the slug length which is explained by the regression model. An R^2 value of 0.32 indicates the capability of the regression model to capture 32% of the variation in slug length, this is a high percent for average dimensionless slug length which is uncorrelated with any of the flow variables.

The second and third columns in Table 3 report the coefficients and standard errors of the model constants, β_0 ($e^{0.966}$) and β_1. The standard error of each coefficient is the square root of the ratio of model variance to its sum of squares of deviations ($x_i = X_i - \overline{X}$). The coefficient's standard error

indicates the scatter of each coefficient value around its mean. When normalized, the estimated regression coefficients follow a t-distribution with the model error degrees of freedom. The P-value in the fifth column is area under the t-probability curve that is used to test the null hypothesis of whether or not the independent parameter is relevant in predicting the slug length (i.e. $H_0: \hat{\beta}_0 or \hat{\beta}_1 = 0$). Using a 5% significance level, one can reject the null hypothesis (H_0) since the p-value is less than the significance level, confirming that the independent variable is significant. The 95% confidence intervals for each independent variable coefficient are also reported in the last two columns. A 95% confidence interval for a coefficient is ($C.I._{(95\%)} = \hat{\beta}_j \pm t_c s_{\hat{\beta}_j}$), where t_c equals 1.96 and corresponds to 95% of the area under the Normal probability t-distribution curve. $\hat{\beta}_j$ is the coefficient and $s_{\hat{\beta}}$ is its standard error. These confidence intervals give the model the flexibility to be tuned when test data is available. Model tuning for a specific system will improve the prediction of slug length for that system.

Model Validation

Because of the lack of independent high liquid viscosity slug length data in the open domain, the validation of the proposed model was a challenge. Alternatively, ten data points of this study were randomly selected and eliminated from the process of model development to be used as independent data set for validation. A statistical error analysis is carried out to test the performance of the proposed correlation on the independent data set. Three statistical parameter are calculated, namely the Average Percent Error (APE), Absolute Average Percent Error (AAPE) and the Standard Deviation (SD), which are summarized in Table 4. The error analysis shows that the model slightly overpredicts experimental data with about 10% absolute error. The analysis further shows that the data dispersion around the model represented by the standard deviation is low, 13.6%. Fig. 11 is a cross plot showing the model performance against the data. Overall the model prediction shows a very good performance, yet more independent data is required to further validate the model performance under different conditions.

Future Work

- Further characterize the liquid behavior in film zone including the developing and developed sections to come up with a physical model.
- Compare the present model with existing slug length models and correlations.
- Investigate the best fit probabilistic distribution and model it for high viscosity oil.
- Expand the proposed model to predict the entire slug length distribution including the maximum slug length and slug length variation in addition to the proposed average slug length.

Nomenclature

A= pipe cross sectional area

c= constant

d= diameter

f= frequency

g= gravitational acceleration

H= liquid holdup, liquid height

L= length

N= dimensionless number

p= pressure

R= pipe radius

v= velocity

W= mass rate

x= arbitrary variable

Subscripts

d= drift

f= film

L= liquid

LS= liquid slug

max= maximum

o= oil

P= pipe

rd= Froude

S= slug

Sg= superficial gas

SL= superficial liquid

TBe= Taylor bubble equilibrium

z= axial direction

Greek

β= coefficient

μ= viscosity, population mean

ρ= density

References

Abdul-Majeed G.: "Liquid Slug Holdup in Horizontal and Slightly Inclined Two-Phase Slug Flow*," J. Pet. Sci. and Eng*. 27, 27-32, (2000).

Brandt, I., and Fuchs, P.: "Liquid Holdup in Slugs: Some Experimental Results from the SINTIF Two-Phase Flow Laboratory," BHRG Multiphase Proceedings, Nice, France (1989).

Brauner, N. and Ullmann, A.: "Modeling of Gas Entrainment from Taylor Bubbles. Part A: Slug Flow," *Int. J. of Multiphase Flow*, 30, 239-272, (2004).

Colmenares,J., Ortega,P., Padino,J., and Trallero, J.L.: "Slug Flow Model for the Prediction of Pressure Drop for High Viscosity Oils in a Horizontal Pipeline," SPE 71111, Presented at SPE International Thermal Operations and Heavy Oil Symposium, Margarita Island, Venezuela, March 12-14 (2001).

Dukler, A.E. and Hubbard, M.G.: "A Model for Gas-Liquid Slug Flow in Horizontal and Near Horizontal Tubes", *I&EC Fundamentals*, 14, pp. 337-347 (1975).

Dukler, A., Moalem-Maron, D., and Brauner, N.: "A Physical Model for Predicting the Minimum Stable Slug Length," Chem. Eng. Sci. 40, 1379-1385 (1985).

El-Oun, Z.: "Gas-Liquid Two-Phase Flow in Pipelines," SPE 20645, Presented at SPE ATCE, New Orleans, LA, (1990).

Fabre, J., Grenier, P. and Gadoin, E.: "Evolution of Slug Flow in Long Pipe," BHRG Production Technology Conference, Cannes, France (1993).

Gokcal, B., Al-Sarkhi, A., Sarica, C. and Al-Safran, E.: "Prediction of Slug Frequency for High-Viscosity Oils in Horizontal Pipes," SPE 124057, Presented in SPE/ATCE, New Orleans, LA, (2009).

Gokcal, B., Wang, Q., Zhang, H. Q., and Sarica, C.: "Effects of High Oil Viscosity on Oil-Gas Flow Behavior in Horizontal Pipes," SPE 102727, *SPE Projects, Facilities & Construction Journal*, June, (2008a).

Gokcal, B.: An Experimental and Theoretical Investigation of Slug Flow for High Oil Viscosity in Horizontal Pipes. Ph.D. Dissertation, The University of Tulsa, Tulsa, Oklahoma, (2008b).

Hethea, R. and Rhinehart, R.: Applied Engineering Statistics, Marcel Dekker Inc., (1991).

Kokal, S.: "An Experimental Study of Two-Phase Flow in Inclined Pipes," Ph.D. Dissertation, The University of Calgary, Calgary, Canada, (1987).

Scott, L. and Kouba, G.: "Advances in Slug Flow Characterization for Horizontal and Slightly Inclined Pipelines," SPE20628, Presented in SPE/ATCE, New Orleans, LA., (1990).

Marcano, R.: "Slug Characteristics for Two-Phase Horizontal Flow," M.S. Thesis, The University of Tulsa, Tulsa, OK, (1996).

Nadler M. and Mewes D.: "Effect of the Liquid Viscosity on the Phase Distribution in Horizontal Gas-Liquid Slug Flow" *Int. J. of Multiphase Flow*, 21, No. 2, 253-266, (1995).

Nicholson, K., Aziz, K., and Gregory, G.: "Intermittent Two Phase Flow in Horizontal Pipes, Predictive Models," *Can. J. Chem. Eng.*, 56, 653-663, (1978).

Rothe, P., Crowley, C. and Sam, R.: "Investigation of Two-Phase Flow in Horizontal Pipes at large Pipe Size and High Gas Density," AGA Pipe Research Committee Project, PR-172-507, (1986).

Taitel, Y., Barnea, D., and Dukler, A.: "Modeling Flow Pattern Transition for Steady Upward Gas-Liquid Flow in Vertical Tube," AIChE J. 26, 345-354 (1980).

Barnea, D., and Brauner, N.: "Holdup of the Liquid Slugs in Two Phase intermittent Flow," Int. J. Multiphase Flow 11, 43-49 (1985).

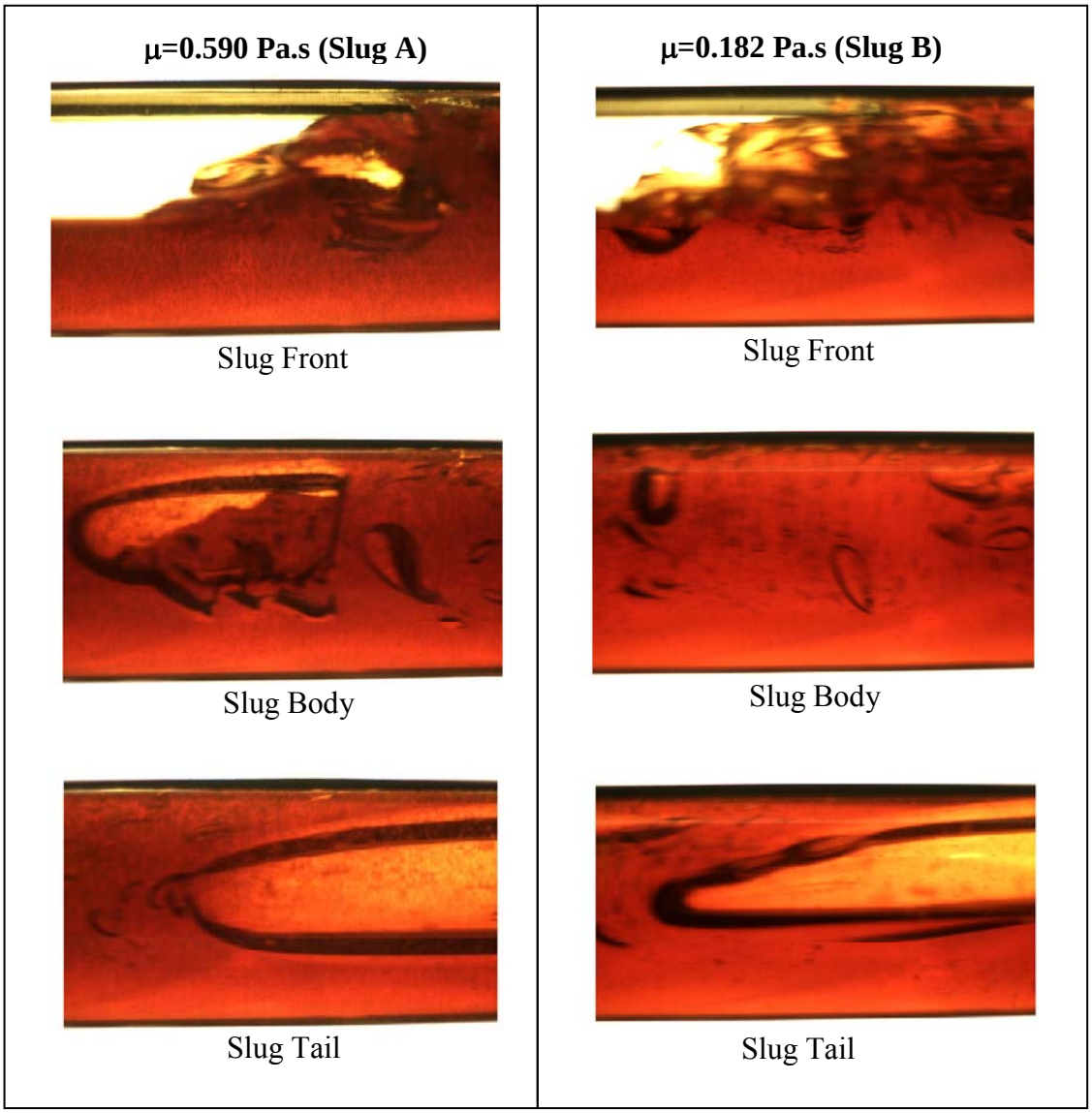

Fig. 1: Comparison of slug front for different viscosities (v_m=1.51 m/s)

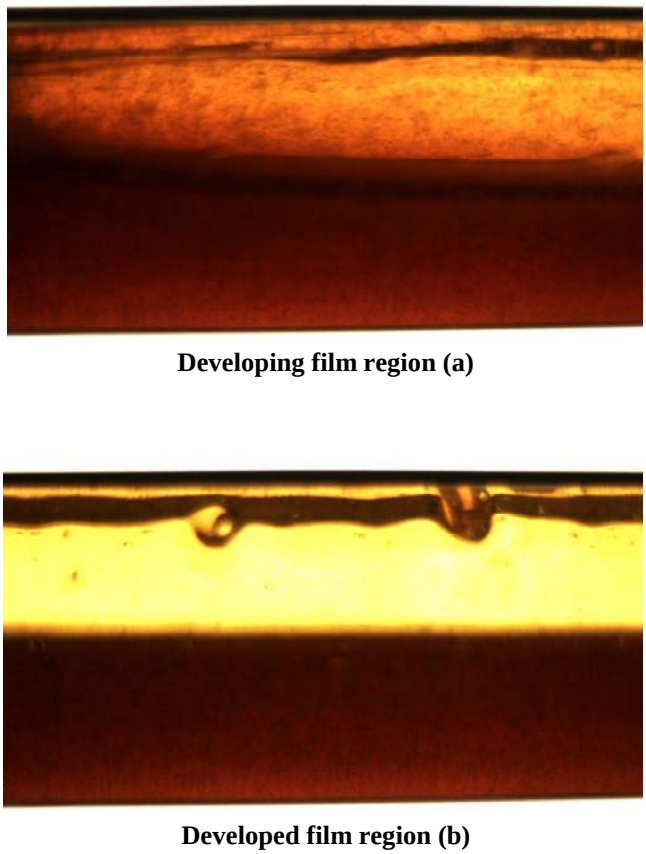

Fig. 2: Developing (top) and developed (bottom) film regions (v_{SL}=0.1 m/s, v_{Sg}=2 m/s, μ=0.26 Pa.s)

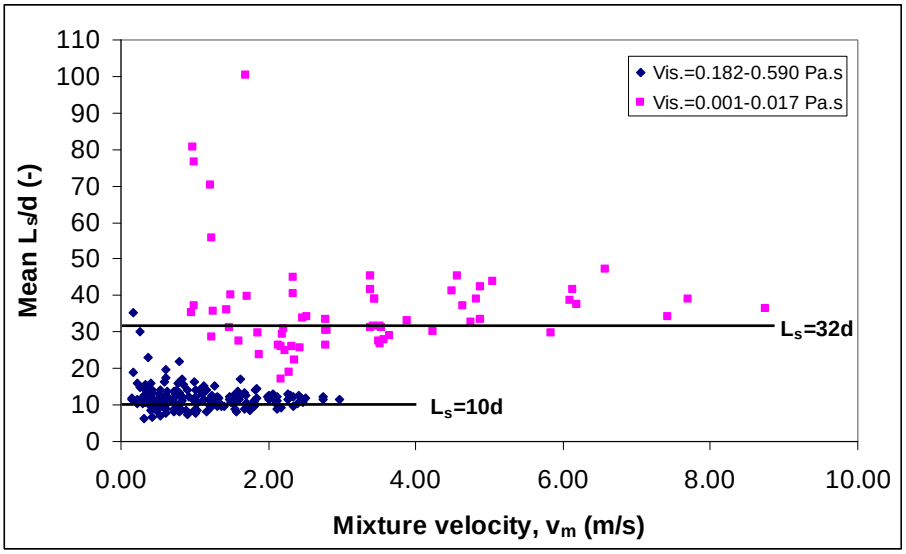

Fig. 3: Evolution of high and low viscosities (Mean slug length vs. Mixture velocity)

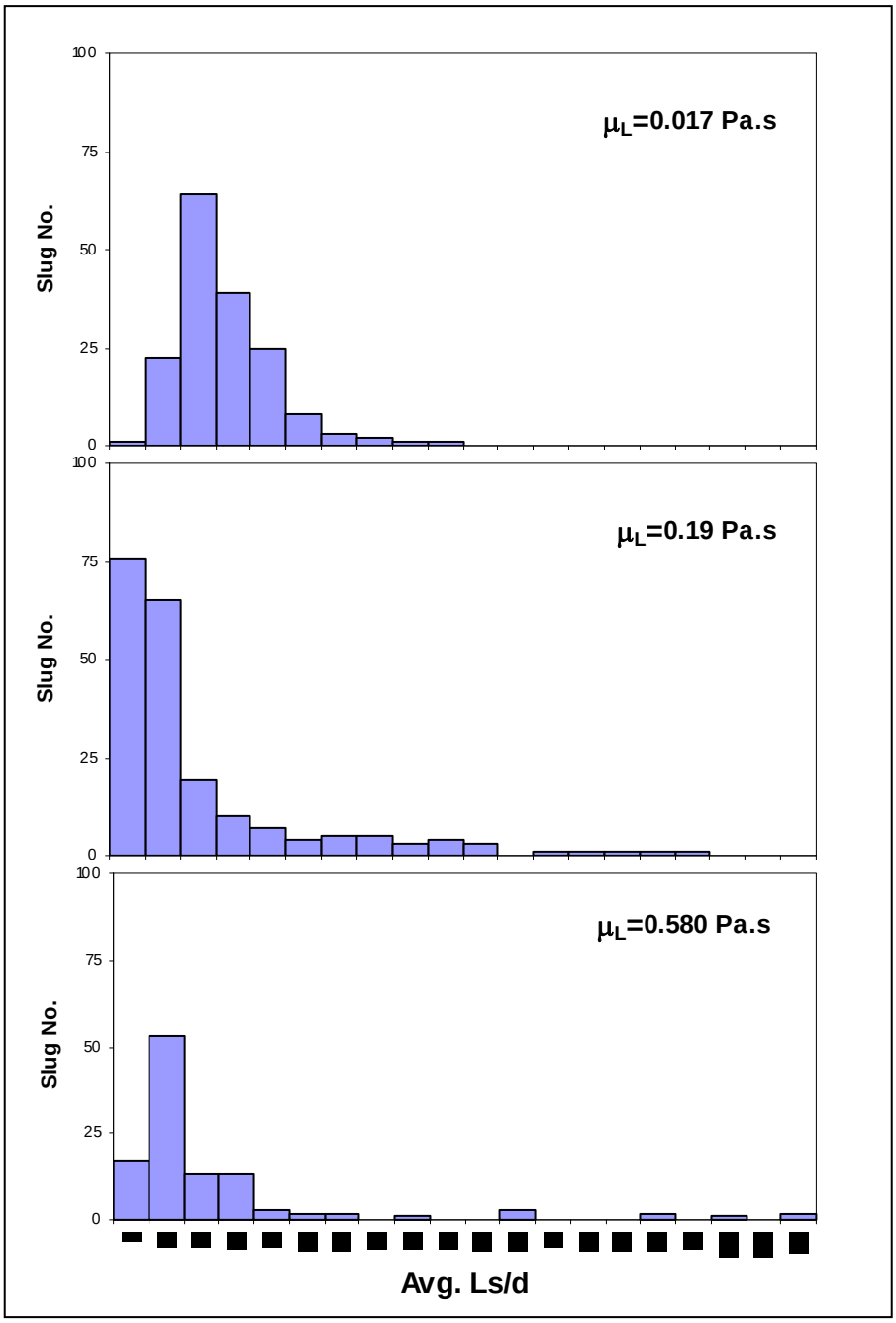

Fig 4: Effect of liquid viscosity on slug length distribution characteristics (v_{SL}=0.3 m/s, v_{Sg}=1.5 m/s)

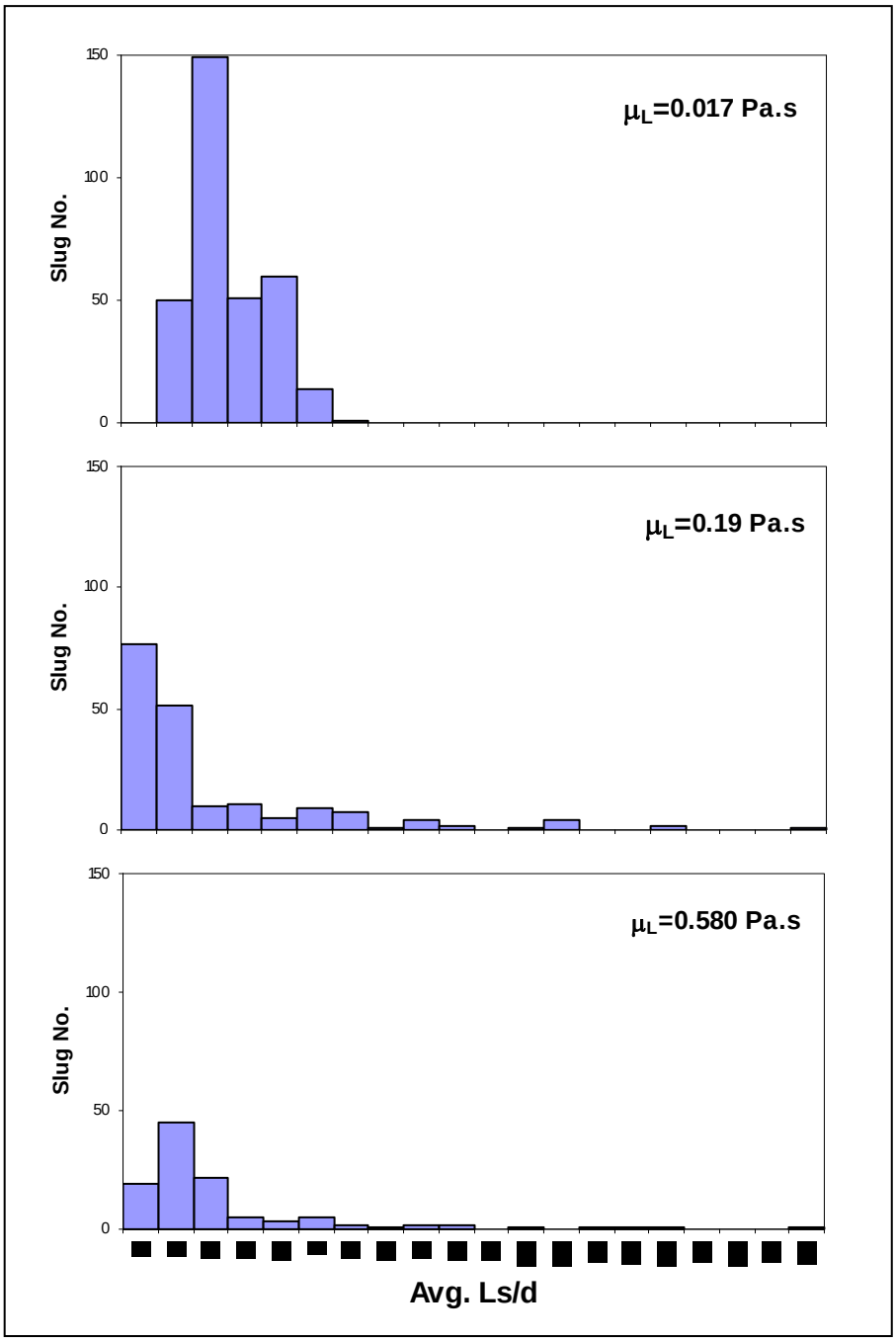

Fig 5: Effect of liquid viscosity on slug length distribution characteristics (v_{SL}=0.3 m/s, v_{Sg}=2.1 m/s)

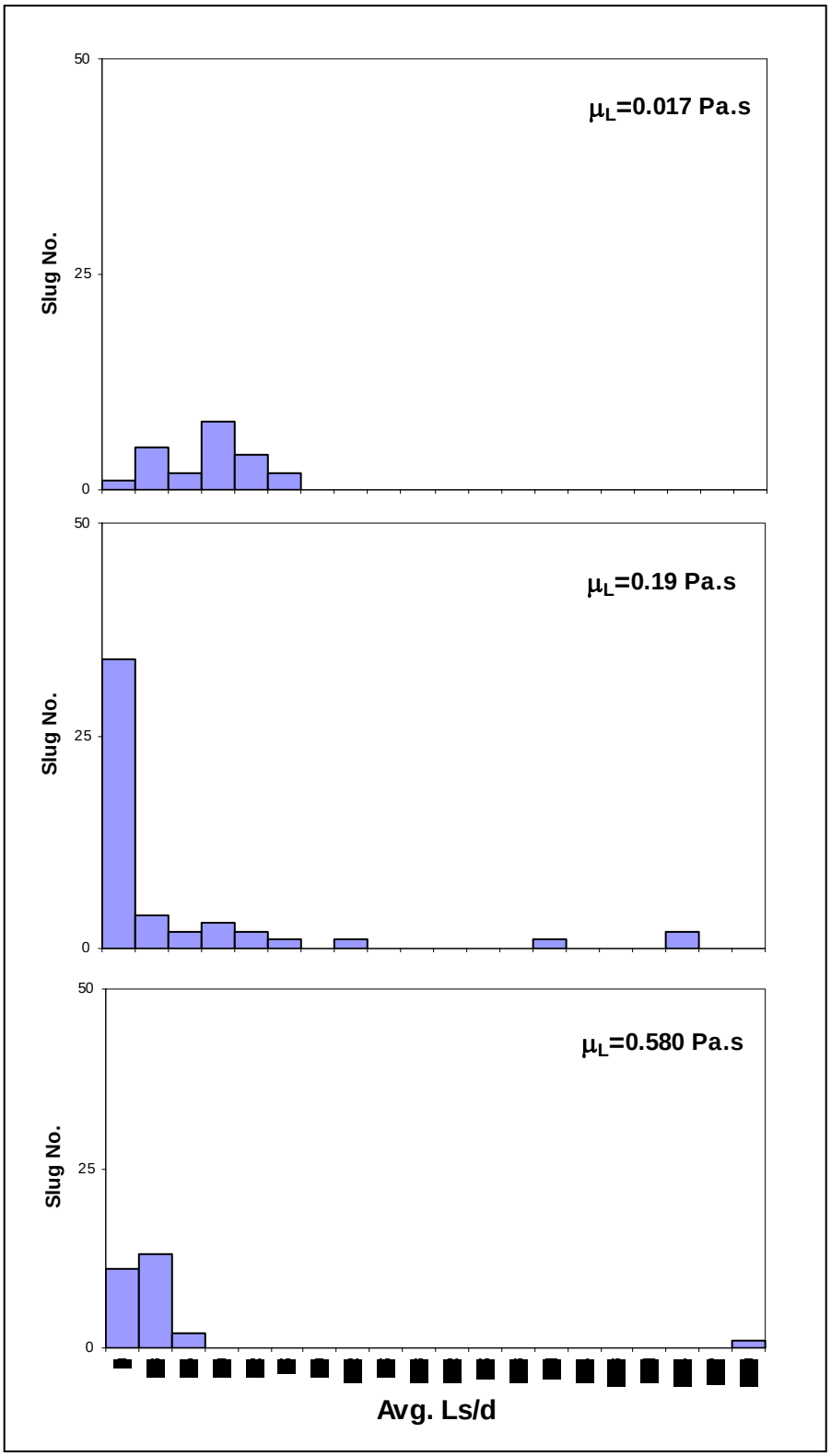

Fig 6: Effect of liquid viscosity on slug length distribution characteristics (v_{SL}=0.05 m/s, v_{Sg}=2.1 m/s)

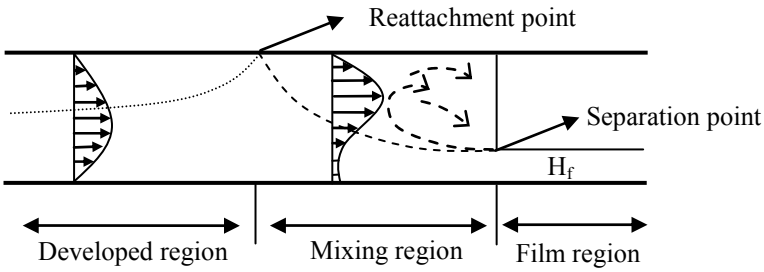

Fig. 7: Light oil minimum slug length physical model (Dukler *et al.* 1985)

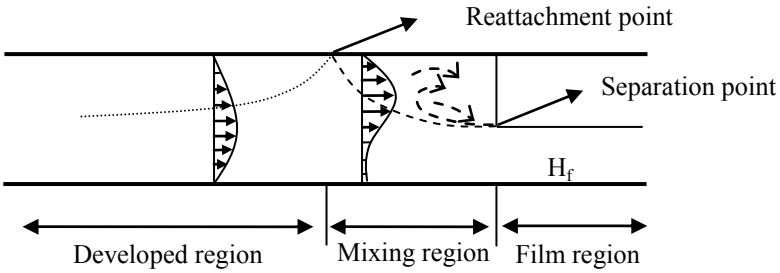

Fig. 8: Proposed high viscosity oil minimum slug length physical model

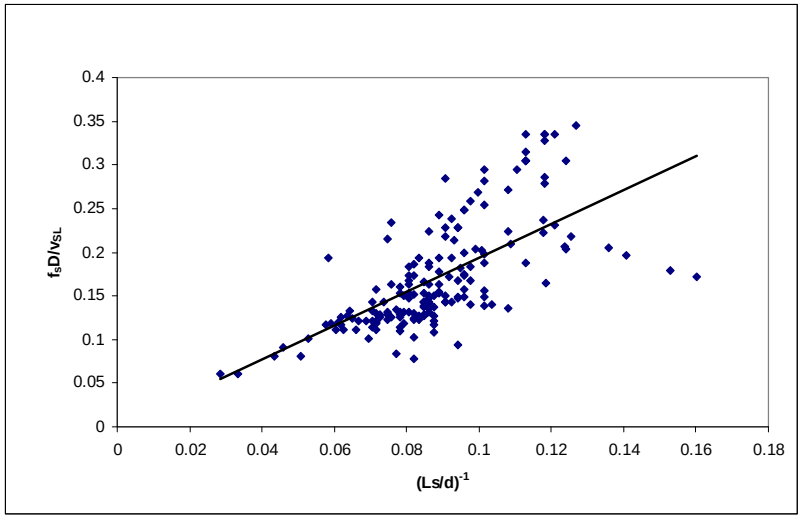

Fig. 9: Dimensionless slug frequency versus the inverse of average slug length

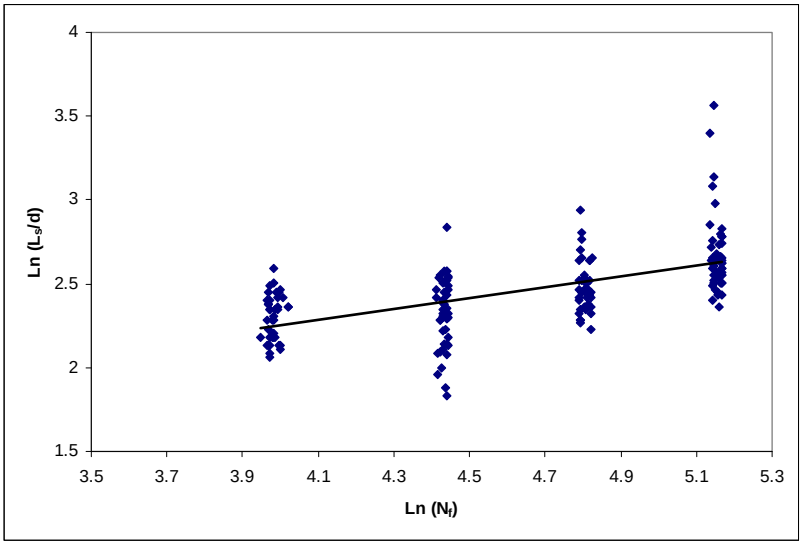

Fig. 10: Simple linear regression fit of the linearized average slug length model

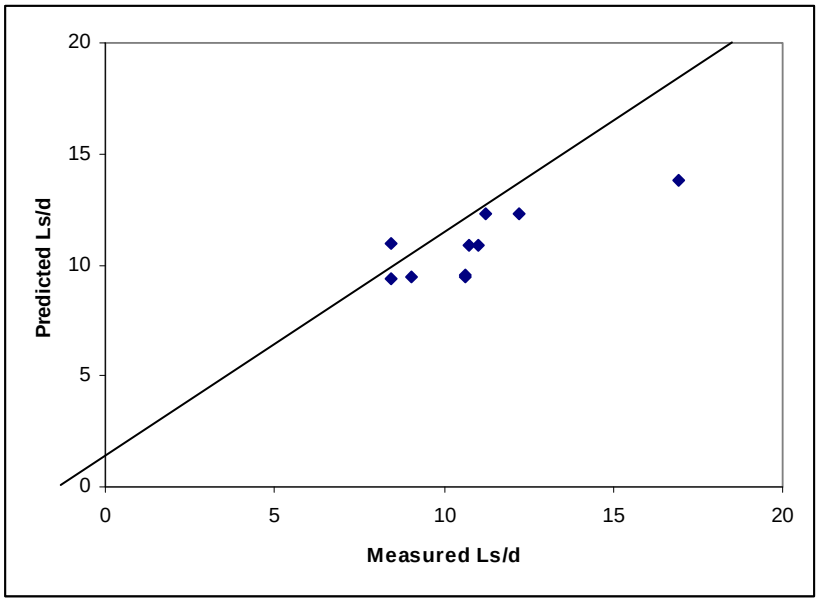

Fig. 11: A cross plot of model prediction vs. measurement

Table 1: Overall Model Evaluation

Model df	Error df	SSE	MSE	R^2
1	161	6.43	0.200	0.32

Table 2: Model Coefficients' Evaluation

Variable	Coef.	Standard Error	t-statistics	p-value	Lower 95% CI	Upper 95% CI
$Ln(\beta_0)$	0.966	0.170	5.800	0.000	0.650	1.310
β_1	0.321	0.036	8.730	0.000	0.246	0.390

Table 3: Proposed Model Validation

Stat. Parameter	Value
APE (%)	1.72
AAPE(%)	9.8
SD(%)	13.6

Fluid Flow Projects

Continuation of High Oil Viscosity Two Phase Flow Research

Benin Chelinsky Jeyachandra

Advisory Board Meeting, May 12, 2010

Outline

- Objectives
- Introduction
- Literature Review
- Feasibility Study on Inclined Pipe Flow
- Feasibility Study on High Viscosity Oil Two Phase Flow
- Design Study
- Conclusion

Objectives

- TUFFP's General Objective is Investigate High Viscosity Multiphase Flow
- Specific Objectives of This Presentation
  - Review and Evaluate Possible Alternatives for Continuation Study
  - Identify the Next Project on High Oil Viscosity Two Phase Flow in TUFFP

Introduction

- Accurate Modeling of High Viscosity Liquid Flow Behavior
- Gokcal (2005) - Modeling of Flow Characteristics for Horizontal Flow
- Options
  - Slightly Inclined Flow
  - High Viscosity (1,000 – 10,000 cp) Oil Two Phase Flow

Literature Review

- Effect of Viscosity
- Slug Flow Characteristics
  - Translational Velocity
  - Slug Length
  - Slug Frequency
  - Slug Liquid Holdup
- Effect of Inclination
- Summary

Literature Review …

- Effect of Viscosity
  - Andritsos *et al.* (1989)
    - Initiation of Slugs
    - Kelvin-Helmholtz Waves
    - Viscosity: 20 – 40 cp
  - Nadler and Mewes (1995)
    - Phase Distribution
    - Slug Liquid Holdup
    - Viscosity: 14 – 37 cp

Literature Review …

- Effect of Viscosity …
  - Colmenares *et al.* (2001)
    - Flow Patterns
    - Effect of Viscosity on Flow Behavior
  - Rosa *et al.* (2004)
    - Viscosity on Gas-Liquid Structures
  - Gokcal (2005)
    - Dominant Flow Pattern: Slug Flow
    - 180 – 580 cp

Literature Review …

- Translational Velocity
  - Jeyachandra and Al-Sarkhi (2010)
- Slug Length
  - Brill *et al.* (1981)
    - Log Normal Distribution
    - Pipe Diameter
    - Mixture Velocity

Literature Review …

- Slug Length
  - Taitel *et al.* (1980), Barnea and Brauner (1985)
    - Wall Jet Entering a Reservoir
    - 16d for Vertical
    - 32d for Horizontal
  - Gokcal (2008)
    - Slug Length Decrease with Viscosity Increase

Literature Review …

- Slug Frequency
  - Hill and Wood (1990)
    - Frequency as Function of Liquid Holdup
  - Al-Safran (2008)
    - Frequency as Function of Pipe Diameter, Actual Liquid Velocity and Ratio of Slip to Mixture Velocity
  - Gokcal (2008)
    - Closure Model for Slug Frequency

Literature Review …

- Effect of Inclination
  - Sevigny (1962)
    - Study on Effect of Inclination Angle on Flow Behavior
  - Mattar and Gregory (1974)
    - Experiments for Slug Velocity, Holdup and Pressure Gradients

Literature Review …

- Effect of Inclination
  - Flanigan (1958)
    - Pressure Drop
  - Bonnecaze *et al.* (1971)
    - Study on Pressure Drop
  - Abduvayt *et al.* (2003)
    - Effect of Pipe Diameter and Inclination
    - Slip Models for Pressure Drop
    - Flow Pattern Transitions

Literature Review …

- Effect of Inclination
  - Xiao *et al.* (1990)
    - Comprehensive Mechanistic Modeling
  - Zhang *et al.* (2003)
    - Unified Hydrodynamic Model
    - Flow Pattern Transitions, Pressure Gradient and Liquid Holdup and Slug Characteristics

Literature Summary

- Most Correlations Ignore the Combined Effect of Viscosity and Inclination Angle
- Literature on Viscosity Effects on Flow Characterization of Two Phase Inclined Flow is Scarce
- Better Closure Relationships can be Obtained After Careful Research

Fluid Flow Projects

Feasibility Study on Inclined Pipe Flow

Advisory Board Meeting, May 12, 2010

Test Fluid

- Test Liquid: Citgo Sentry 220 Oil
  - Gravity: 27.6 °API
  - Viscosity: 0.220 Pa·s @ 40 °C
  - Density: 889 kg/m3 @ 15.6 °C
  - Surface Tension: 0.02976 N/m
- Test Gas: Air

Experimental Setup

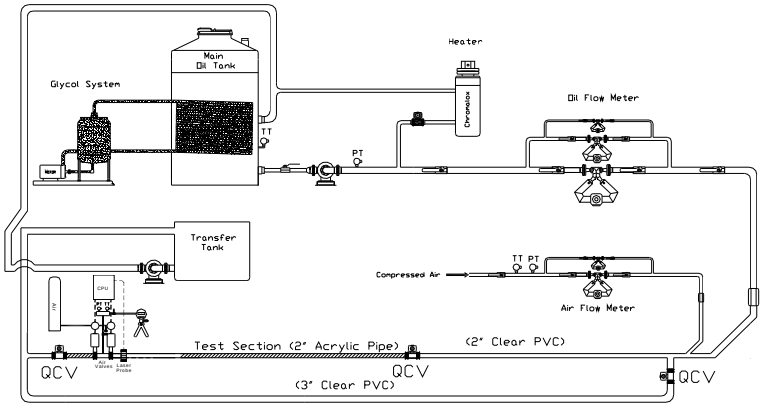

Previous Experiments

- Gokcal (2008) ABM Presentation of Spring 2006
  - 1° Downward Flow
    - Superficial Liquid Velocity 0.01 – 1.75 m/s
    - Superficial Gas Velocity 0.1 – 20 m/s

Experiments – Flow Pattern

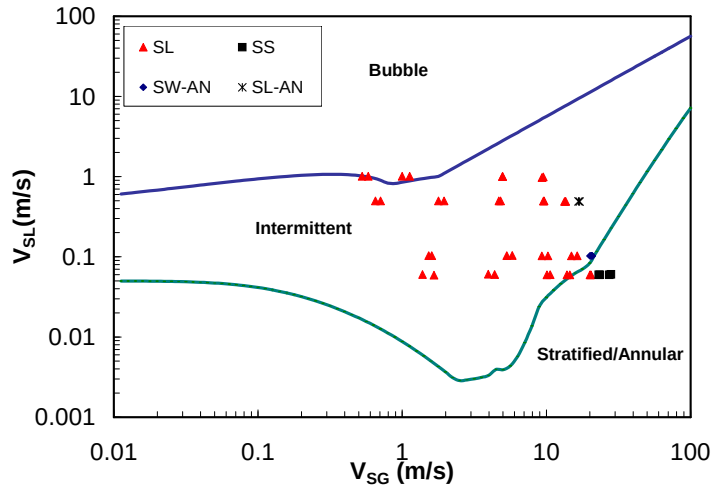

Fluid Flow Projects

Advisory Board Meeting, May 12, 2010

Experiments – Pressure Gradient

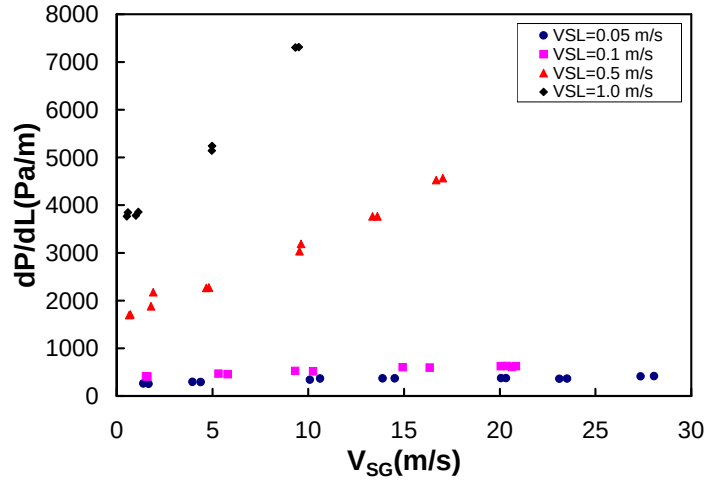

Fluid Flow Projects

Advisory Board Meeting, May 12, 2010

Experiments – Pressure Gradient

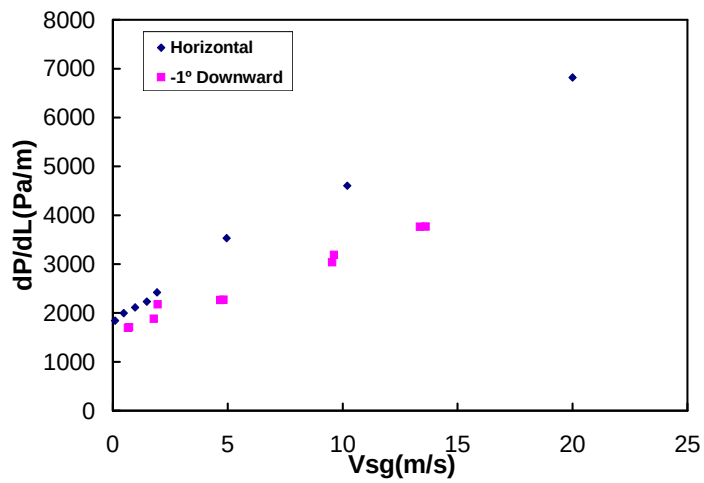

Proposed Experimental Study

- Superficial Liquid Velocity
  - 0.05 – 1.75 m/s
- Superficial Gas Velocity
  - 0.1 – 5 m/s
- Viscosity
  - 0.574, 0.378, 0.256, 0.105 Pa·s
- Inclination
  - -2°, -1°, 1°, 2°

Experimental Parameters

- Flow Pattern
- Pressure Gradient
- Liquid Holdup
- Translational Velocity
- Slug Length
- Slug Frequency
- Film Thickness

Modifications

- Design and Install New Separation System
- New Capacitance and Laser Sensors
- Automate Heating and Cooling Systems
- Install Online Viscometer

Fluid Flow Projects

Feasibility Study on High Viscosity Oil Two Phase Flow (1,000 cp to 10,000 cp)

Advisory Board Meeting, May 12, 2010

Facility Limitations

- Pump
  - Kral Screw Type Pump
    - Max Viscosity: 8.8 Pa·s
    - Max Pressure: 232 psi
- Compressor
  - GD, JOY Compressor
    - Max Pressure: 110 psi
- Pressure Relief Valve Activates at 110 psi
- Pressure Rating Acrylic Pipe - 30 psi

Pressure Calculations

- Viscosity Range: 1, 3, 5, 7 Pa·s
- Single Phase High Viscous Oil Flow
- Liquid Velocity: 0.1, 0.3, 0.5, 0.7 m/s
- Length of pipe:
  - 93.6 ft of 3 in. Steel Pipe
  - 32 ft of 2 in. PVC Pipe
  - 32 ft of 2 in. Acrylic Pipe
  - 65 ft of 3 in. PVC Pipe

Higher Viscosity Single Phase Pressure Calculation

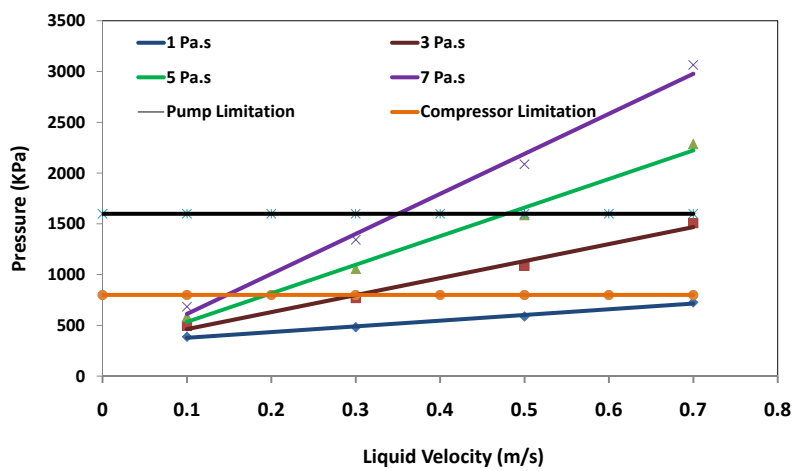

Problem Mitigation

- New Compressor and Pump
- Steel Pipes
- Modify Auxiliary Pump
- New Separator Design with Improved Efficiency

Design Study

- Selection of Pump and Compressor
- Energy Supplied by Pump
- Heater Efficiency
- Selection of Oil
- Online Viscometer
- Separator Design
- Cost Analysis
- Additional Oil Transfer Pump

Conclusions

- Effect of Inclination Can be Studied Without Much Modification
- Significant Modifications are Required for Study on High Viscosity Oil Two Phase Flow

Questions

Immediate Continuation of High Oil Viscosity Two Phase Flow Research

Benin Chelinsky Jeyachandra

PROJECTED COMPLETION DATES:

Literature Review	Completed
Facility Modifications	July 2010
Preliminary Testing	August 2010
Testing	September 2010
Data Evaluation	December 2010
Final Report	May 2011

Objectives

The one of the main objectives of TUFFP is to conduct research, and thereby, further knowledge in high viscosity oil two-phase flow. The specific objectives of this study will be outlined after this Advisory Board meeting based on Advisory Board's decision on the continuation project.

Introduction

Nearly 70% of the oils resources available currently are high viscosity oil reserves. Depletion of lighter hydrocarbon resources has also increased the importance of high viscosity oils. A thorough knowledge on the flow behavior of high viscosity oils is required to optimally design production systems. The existing multiphase flow models were developed using the data collected from experiments on low viscosity oils.

Gokcal (2005) experimentally studied the effects of high viscosity on two phase oil-gas flow. There was marked difference between the experimental results and the model predictions. Intermittent slug and elongated bubble flow were observed to be the dominant flow pattern. Gokcal (2008) conducted experiments and developed correlations for two phase slug flow characteristics, taking into account, the effects of viscosity. The parameters that were studied are pressure gradient, drift velocity, transitional velocity and slug frequency. All tests were conducted for horizontal flow. The range of viscosities studied was from 121 cp to 1,000 cp. Kora (2010) is currently investigating slug liquid holdup for horizontal flow.

The next logical step in the understanding of high viscosity oil-air two-phase flow would be to analyze the effect of inclination on the different flow parameters. An alternate approach for this study would be to conduct the experiments for higher viscosities in the range of 1,000 cp to 10,000 cp. The feasibility of conducting these studies with the restriction of current experimental setup has been undertaken.

Literature Review

The literature review has been presented in three sections a) Effect of Viscosity b) Slug flow characteristics, and c) Effect of inclination.

Effect of Viscosity

Andritsos *et al.* (1989) conducted experiments to study the effect of liquid viscosity on the initiation of gas-liquid slug flow in horizontal 25.2-mm and 95.3-mm ID pipelines. They proposed that, for viscous liquids, slugs arise from small-wavelength Kelvin-Helmhotz (KH) waves. The mechanism showed good agreement with experimental results. They concluded that the new mechanism was applicable to liquids with viscosities above 0.02 Pa·s.

An experimental study conducted by Nadler and Mewes (1995) investigated the effect of liquid viscosity on phase distribution in slug flow for horizontal pipes with other fluid physical properties being kept constant. The viscosity range for their experimental study was 0.014 to 0.037 Pa·s. Experimental results indicated that the average liquid

holdup within the slug unit and the elongated bubble region increased with increasing liquid viscosity.

Colmenares *et al.* (2001) studied pressure drop models for horizontal slug flow for viscous oils. According to their experimental results, the slug flow pattern enlarged when the oil viscosity increased.

Taitel and Barnea (1990) concluded that slug frequency and liquid film height increased, and the slug length decreased as the liquid viscosity increased.

Rosa *et al.* (2004) experimentally investigated the influence of liquid viscosity on gas-liquid structures of horizontal slug flow. Air-water (0.001 Pa·s) and air-glycerin (0.027 Pa·s) were used as the two pairs of test fluids. Bubble shape, velocity and void fraction, bubble and slug lengths, slug frequency and coalescence rate were analyzed in their study. They concluded that the average slug and bubble length and coalescence rate decrease with increasing liquid viscosity. The bubble front velocity and slug frequency increased with an increase in liquid viscosity.

Gokcal (2005) study at TUFFP has investigated a higher viscosity range than Rosa *et al.* covering 0.18 – 0.58 Pa·s range. Moreover, he identified that slug flow was the dominant flow pattern.

Therefore, further efforts were directed towards investigating slug flow pattern.

Slug Flow Characteristics

Translational Velocity

Slug translational velocity is one of the key closure relationships in the mechanistic modeling of two phase flow. A literature review on translational velocity is given in this report by Jeyachandra and Al-Sarkhi.

Slug Length

Based on data taken from the Prudhoe Bay field in Alaska, Brill *et al.* (1981) found that slug lengths could be represented by a log-normal distribution. They proposed a slug length correlation as a function of pipe diameter and mixture velocity.

In order to understand the mechanism of stable slug length formation, the mixing process between the film and slug was simulated by Taitel *et al.* (1980), and Barnea and Brauner (1985) with a wall jet entering a large reservoir. They found that a developed slug length requires a distance for a jet to be absorbed by the liquid. Using this approach, the minimum liquid slug length is 16D and 32D for vertical and horizontal flows, respectively. Moreover, Dukler *et al.* (1985) developed a model to predict the minimum stable slug length in slug flow. The length for reforming of a fully developed velocity profile at the back of a liquid slug is defined as the minimum stable slug length. They found that it is of the order of 20D.

Gokcal (2008) study indicated that average slug lengths decreases with increasing liquid viscosity for horizontal pipes. Further analysis of slug length data has continued as part of high viscosity oil studies in TUFFP. A detailed report on the progress of slug length study for horizontal pipes is presented in this report by Al-Safran.

Slug Frequency

Taitel and Dukler (1977) proposed a mechanistic model for the prediction of slug frequency in horizontal and near-horizontal pipes. They claimed that slug formation is an entrance phenomenon and occurs as a result of solitary waves which grow on unstable equilibrium surfaces. Then, the waves bridge the pipe and block the gas passage. They suggested that slug frequency is the inverse of the time interval needed to rebuild its equilibrium level for a new slug to be formed and solved one-dimensional mass and momentum balances using an open channel flow approach to calculate the time interval. The developed model was validated against data taken by Dukler and Hubbard (1975). However, comparison of the Taitel and Dukler slug frequency model against data gave only fair agreement.

Hill and Wood (1990) developed a slug frequency correlation as a function of equilibrium liquid holdup and relative velocities of the gas and liquid phases.

Zabaras (1999) compared various correlations and mechanistic models for predicting the slug frequency in horizontal and inclined pipes against the data. The data set included both his experimental results and published slug frequency results. He found that performances of existing methods are not sufficiently accurate for inclined slug flow.

Al-Safran (2008) investigated slug frequency in gas-liquid horizontal flow and developed a slug frequency correlation as a function of pipe diameter, actual liquid velocity and ratio of slip to mixture velocities. The slip and actual liquid velocities can

be calculated from the stratified liquid height, assuming stratified flow at the entrance of the pipeline.

Liquid viscosity effect on slug frequency has been investigated by Gokcal (2008) as part of TUFFP. He acquired data for horizontal configuration for liquid viscosities between 181 cp and 0.589 cp. He also developed a frequency closure relationship.

Liquid Slug Holdup

Barnea and Brauner (1985) proposed a mechanistic model to determine liquid holdup in a slug for horizontal and vertical pipes. The parameter that controlled liquid holdup was assumed to be the mixture velocity of the slug.

They also considered that gas in developed liquid slug resembles dispersed bubbles and the liquid slug will have the same liquid holdup as fully dispersed bubble flow moving with the same mixture velocity. The gas carrying capacity of the liquid slug was determined by analyzing the turbulent forces and buoyancy forces due to gravity or surface tension.

Taitel and Barnea (1990) proposed a comprehensive mechanistic model for steady state slug flow. The slug holdup part of this model was based on a mass balance and they stated that liquid and gas velocities in the slug are not the same. An average liquid holdup formula for a slug unit was presented based on the combination of liquid holdup in the slug and the liquid film. Empirical formulas were used to calculate slug liquid holdup. Moreover, they did not consider any fluid property effects in their model.

Gregory *et al.* (1978) conducted experiments on liquid holdup in slugs with two different horizontal diameters pipe: 2.58 cm and 5.12 cm. They proposed an empirical correlation for the liquid slug holdup. In this correlation, they assumed the slug to be homogenous. However, they suggested that the gas fraction in a slug changes with position. Moreover, they mentioned that this correlation has to be modified to include the effects of fluid properties.

Felizola (1992) measured average liquid holdup in the slug for pipe inclinations of 0° to 90° degrees from horizontal. He developed a new empirical correlation for slug liquid holdup which depends on mixture velocity and pipe inclination.

Gomez *et al.* (2000) proposed a new dimensionless correlation for liquid holdup in the slug body for horizontal to upward vertical flows. This correlation included the mixture velocity, liquid viscosity, pipe diameter, and inclination angle. They used the slug liquid holdup experimental data of Kouba (1986).

Zhang *et al.* (2002) developed a unified mechanistic model to predict slug liquid holdup considering the overall dynamics of slug flow. Slug flow characteristics were taken into account while solving momentum and continuity equations for slug flow. In this study, TUFFP data were used to check the validity of the slug liquid holdup model at different inclination angles. In all these experiments, kerosene and air were used as test fluids. The experimental data and the predicted results of the model generally fit well for low viscosity oils. Zhang *et al.* model was later modified arbitrarily based on the Gokcal (2005) data for high viscosity oils.

Effect of Inclination

Most of the early efforts in inclined pipes were concentrated on low viscosity oils. A brief and not all inclusive summary of the multiphase flow studies with inclination effects are given below.

Sevigny (1962) conducted comprehensive study of two phase flow in inclined pipes. He studied air water flow in 2 cm ID pipe with inclinations of varying inclinations. He did not measure the liquid holdup. Beggs (1972) made a detailed study of inclination effects. He used a 5.08 cm (1 in.) and 6.29 cm (1.5 in.) ID pipe. He observed that liquid holdup was strongly affected by the angle of inclination. Flanigan (1958) studied pressure drop in inclines pipes and suggested that the total pressure drop in the system is of two components, a) pressure drop due to friction and b) pressure obtained by multiplying the liquid head with sum of uphill rises. Mattar and Gregory (1974) conducted many experiments to find out the slug velocity, holdup and pressure gradient in upward inclined pipe. Taitel and Dukler (1977) developed a model for slug frequency in near horizontal pipes. Spedding and Chen (1981) studied the pressure drop in two phase flow in inclined pipe and found that the pressure drop is depended on the flow pattern of two phase flow.

Bonnecaze *et al.* (1971) developed a model for two phase flow in inclined pipeline and proposed that the pressure drop is mainly because of the liquid in the slug unit. Abduvayt *et al.* (2003) studied effects of inclination angles (1, 2, and 3°) and pipe diameter on pressure drop. Slip model predictions gave the best fit with experimental results compared to No slip models. Flow pattern transitions were accurately

predicted by Taitel *et al.* criteria and Bendiksen and Espedal criteria.

Xiao *et al.* (1990) developed a comprehensive mechanistic model for slug flow in horizontal and near-horizontal pipelines.

Mass and force balances are applied over a slug unit and a uniform liquid level is assumed in the film zone. The closure relationships of translational velocity, slug length and slug holdup in the slug body are required as inputs to their model.

Zhang *et al.* (2003) developed a unified hydrodynamic model to predict flow pattern transitions, pressure gradient and liquid holdup and slug characteristics in gas liquid pipe flows for all inclination angles from -90° to 90° from horizontal. The model was based on the dynamics of slug flow and is applicable for all pipe geometries and fluid physical properties. Momentum and continuity equations for slug flow were developed by considering the entire liquid film region as the control volume.

Based on Gokcal (2005, 2008) findings, Zhang *et al.* Unified model was modified.

Summary of Literature Review

The above literature review reveals that the available correlations and models do not consider the combined effect of inclination angle and liquid viscosity with the exception of drift velocity closure relationship. The inclined flow needs to be studied thoroughly from flow characterization to closure relationship development.

Experimental Study

Facility

The indoor high viscosity oil-gas facility will be modified to perform experiments to study the inclination effects. The capacity of the oil storage tank is 3.03m^3. A 20 HP screw pump is used to push the liquid through the loop. Air is delivered through a dry rotary screw type compressor. The oil and the air mix in a tee junction before proceeding to the test section.

The facility is comprised of a metering section, a test section, a heating system and a cooling system. The test section is 18.9-m (62-ft) long, 50.8-mm (2-in.) ID pipe. Nearly half of the pipe is made of a clear PVC pipe section and the rest is transparent acrylic pipe section.

A 9.15-m (30-ft) long transparent acrylic pipe section is used to observe the flow behavior visually. A flexible hose connects the test section with the 76.2-mm (3-in.) ID return pipe. An oil transfer tank (1.32 m3) is located at the end of return pipe. Return pipe is connected to this tank with a flexible hose. 3-hp progressing cavity pump is used to pump the oil from the new tank back to the main tank through the riser. The oil flow rates are measured at the inlet of the facility using Micro Motion mass flow meters (CMF025, CMF100, and CMF300). The air is measured at the inlet of the facility using Micro Motion mass flow meters (CMF025 and CMF050).

Separation is accomplished by gravity separation of air and oil. The separated air is removed through the ventilation system. The test section is supported on stands and the inclination of the test section can be set from -2° to 2° from horizontal by adjusting the heights of the stands.

The viscosity of the oil is controlled by controlling the temperature of oil at the tank. A 20 KW Chromalox heater capable of heating the heavy oil from 70°F to 140°F is used. The heating and the cooling section thus play a major part in the experiment to control the viscosities. Resistance Temperature Detector (RTD) transducers measure the temperatures during experiments. Pressure transducers and differential pressure transducers are located at different places to measure pressure and pressure drop in the loop.

TUFFP high speed video system will be used to identify the flow patterns. Two Laser probes and two capacitance probes will be added to the existing system to provide the necessary slug characteristics such as translational velocity, slug frequency, slug length and liquid holdup.

The results obtained from laser probes and capacitance probe can also be validated against each other for consistency of results.

Test Fluids

For the effect of inclination, the viscosity range is kept constant. Therefore the oil which has been used for the previous experiments, CITGO Sentry 220, will be used again. Following are the typical properties of the oil:

Gravity: 27.6 °API

Viscosity: 0.220 Pa·s @ 40 °C

Density: 889 kg/m^3 @ 15.6 °C

Surface tension: 0.03 N/m @ 40 °C

The oil viscosity and density vs. temperature was already discussed by Jeyachandra (2010) in another report given in this brochure.

Study on Effects of Inclination

Testing Range

Inclination, gas and oil flow rates, and oil temperature will be varied. Superficial liquid velocities will be varied from 0.01 m/s to 1.75 m/s and gas superficial velocity will be varied from 0 m/s to 10 m/s, respectively. The lower limits of superficial velocities are due to the accuracy limits of the Micro MotionTM flow meters. The higher limits are determined by the pressure gradient and facility limits. The experiments will be performed at temperatures of 21.1, 26.7, 32.2, and 37.8 °C (70, 80, 90, and 100 °F). The oil viscosities corresponding to the above temperatures are 0.587, 0.378, 0.257, and 0.181 Pa·s, respectively. The pipe inclination values are -2°, -1°, 1°, 2° from horizontal.

Slightly Inclined Flow: Previous Experiments

Gokcal (2006) conducted a series of experiments to determine the flow pattern, pressure drop and liquid hold up for -1° inclination angle and 0.255 Pa·s viscosity oil. The results are briefly discussed.

Flow Patterns

From Fig. 2, the flow patterns that were observed are stratified smooth, slug, and stratified wavy-annular and slug-annular transitions.

Pressure Gradient

From Fig. 3 it can be seen that the pressure gradients increase with increasing superficial gas and oil velocities. The pressure gradient for horizontal and inclined case was compared in Fig. 4. Pressure gradient for inclined pipe is smaller than the pressure gradient for horizontal pipe because of gravitational pressure gradient.

Liquid Holdup

In Fig. 5, the liquid holdup results were tabulated for different oil and superficial gas velocities when the liquid viscosity is 0.255 Pa s for -1º downward flow. Similar trends are observed for liquid holdups when the superficial liquid velocities are 0.05 and 0.1 m/s. However, as the superficial liquid velocity increased from 0.1 to 0.5 m/s, a different trend was observed for the liquid holdup. These tests were preliminary in nature. The tests conducted will be repeated in this study.

Modifications

The proposed experiments can be performed without any major modification to the existing system. Some modification are put forth to improve the quality of the data collected.

- A better separation system can definitely improve the accuracy of the data. Currently, the oil tank is also used as a separator, and opens to the atmosphere. For high gas flow rates, air bubbles can be observed in the viscous oil flow.
- New laser sensors and capacitance sensors should be added to the loop and should be connected to the data acquisition system.
- Automated heating and cooling system can maintain the temperature and thereby control the viscosities to a better degree of accuracy.
- Online viscometer can give in-situ viscosities and this can help in quantifying the results to a better degree.

Study on Effects of High Oil Viscosity

Design Considerations

Capacity of the pump, pressure output from the main pump, auxiliary pump and compressors, pressure rating for acrylic pipes and PVC pipes, the pressure relief valve, the valve operational range and the instrument range are some of the design criteria that may limit the scope of experiments.

The pump is KRAL K-851 screw type pump. The power rating is 20 HP and the viscosity that can be handled is around 9,000 cp. The maximum pump pressure delivery to the oil is 16 bar (232 psi). From

preliminary calculations for single phase flow high viscosity oil flow, the existing pump is an ideal candidate for the higher viscosity oil flow study. System pressure vs. the liquid velocity has been plotted in Fig. 6.

The compressor is a dry rotary screw type compressor. The maximum pressure it can deliver is 110 psi. This is a limitation on the system. Higher superficial gas velocities cannot be reached with the existing compressor system. Moreover, a pressure relief valve is installed before the start of test section to prevent the pressure in the system to reach above 110 psi. Therefore, for higher viscosity flows, the compressor has to be changed to a higher pressure delivery compressor.

The acrylic pipe can handle a pressure of 30 psi. A typical value of pressure before the acrylic pipe, with current viscosities is around 20 psi. If the viscosity is increased, the pressure delivered by the pump will be high to push the liquid through the loop. This might cause cracking of acrylic pipe.

A new separator has to be installed as the efficiency of separation of higher viscosity oil and air will decrease as the viscosity increases.

Modifications

The following modifications have to be done for the system to handle viscosities in the range of 1,000 cp to 10,000 cp.

- A new compressor which can impart higher pressures has to be installed.
- A new separator is a necessity to aid the separation of high viscosity oil and gas.
- The auxiliary pump has to be changed to a pump that can handle higher viscosities.
- The energy which is imparted to the oil by the pump has to be analyzed and necessary corrections should be made for the viscosity calculation.
- The acrylic pipe has to be changed with a pipe with material which can handle higher pressures and be optically transparent at the same time.
- Study on the efficiency of heating and the cooling loop for handling high viscosity has to be done.

Conclusion

From the above studies, it is quite clear that effect of inclination can be studied with the existing system without much modification. The instruments are proven to handle the current viscosities. Significant modifications are required to carry out the study on effect of higher viscosities.

Near Future Tasks

- Modify the experimental setup.
- Conduct experiments for different viscosities.
- Describe and identify the flow behavior.
- Compare experimental data with existing models
- Develop new closure models.

References

Al-safran, E.: “Prediction of Slug Liquid Holdup in Horizontal Pipes,” Journal of Energy Resources TechnologyVolume 131, Issue 2 (2009).

Alves, I.N., Shoham, O., and Taitel Y.: “Drift Velocity of Elongated Bubbles in Inclined Pipes,” Chem. Eng. Sci., Vol.48, pp. 3063-3070 (1993).

Barnea, D., Brauner, N.: “Holdup of the Liquid Slug in Two-Phase Intermittent Flow,” Int. J. Multiphase Flow 11, 43–49 (1985).

Barnea, D.: “On the Effect of Viscosity on Stability of Stratified Gas-Liquid Flow-Application to Flow Pattern Transition at Various Pipe Inclinations,” Chem. Eng. Sc.,Vol. 46, pp. 2123-2131 (1991).

Barnea, D., and Taitel, Y.: “Kelvin-Helmholtz Stability Criteria for Stratified Flow: Viscous versus Non-Viscous (Inviscid) Approaches,” Int. J. Multiphase Flow, Vol.19, No. 4, pp. 639-649 (1993).

Bonnecaze, R. H., Eriskine, W. Jr., and Greskovich, E. J.: “Holdup and Pressure Drop for Two-Phase Slug Flow in Inclined Pipelines,” AIChE J., Vol.17, pp. 1109-1113(1971).

Ben- Mansour, R.,Sharma, A. K., Jeyachandra B. C., Gokcal, B., Al Sarkhi, A., Sarica, C.: “Effect of Pipe Diameter and High Oil Viscosity on Drift Velocity for Horizontal Pipes,” To be presented, 7th North American Conference on Multiphase Technology, June 2 - 4, 2010, Banff, Canada.

Colmenares, J., Ortega, P., Padrino, J., and Trallero, J.L.: “Slug Flow Model for the Prediction of Pressure Drop for High Viscosity Oils in a Horizontal Pipeline,” SPE 71111, Presented at SPE International Thermal Operations and Heavy Oil Symposium, Margarita Island, Venezuela, March 2001.

Dumitrescu, D. T., Strömung an einer Luftblase im senkrechten Rohr. Z. Angew. Mat. Mech. 23, pp. 139-149 (1943).

Furukawa, T. and Fukano, T.: “Effects of Liquids Viscosity on Flow Pattern in Vertical Upward Gas-Liquid Two-Phase Flow,” Int. J. Multiphase Flow, Vol. 27, pp. 1109- 1126 (2001).

Gregory, G.A., Nicholson, M.K., Aziz, K.: “Correlation of the Liquid Volume Fraction in The Slug for Horizontal Gas–Liquid Slug Flow,” International Journal of Multiphase Flow, 4, 33–39 (1978).

Gokcal, B.: “Effects of High Oil Viscosity on Two-Phase Oil-Gas Flow Behavior in Horizontal Pipes,” M.S. Thesis, The University of Tulsa, Tulsa, OK (2005).

Gokcal, B.: “Effects of High Oil Viscosity on Two-Phase Oil-Gas Flow Behavior,” ABM Presentation, The University of Tulsa, Tulsa, OK (2006).

Gokcal, B.: “An Experimental and Theoretical Investigation of Slug Flow for High Oil Viscosity in Horizontal Pipes,” Ph.D. Dissertation, The University of Tulsa, Tulsa, OK (2008).

Gregory, G. A., and Scott, D. S.: “Correlation of Liquid Slug Velocity and Frequency in Horizontal Co-current Gas-Liquid Slug Flow,” AIChE J., Vol. 15, pp. 933-935(1969).McNeil, D.A., and Stuart, A.D.: “The Effects of a Highly Viscous Liquid Phase on Vertically Upward Two-Phase Flow in a Pipe,” Int. J. Multiphase Flow, Vol. 29, pp.1523-1549 (2003).

Nadler, M., and Mewes, D.: “Effects of the Liquid Viscosity on the Phase Distributions in Horizontal Gas-Liquid Slug Flow,” Int. J. Multiphase Flow, Vol. 21, No. 2, pp.253-266 (1995).

Nicklin, D. J., Wilkes, J. O., Davidson, J. F.: “Two-Phase Flow in Vertical Tubes,” Trans. Inst. Chem. Eng., Vol. 40, pp. 61-68 (1962).

Nicholson, M. K., Aziz K., and Gregory G. A.: “Intermittent Two-Phase Flow in Horizontal Pipes: Predictive Models,” Can. J. Chem. Eng., Vol. 56, pp. 389-399(1978).

Petalas, N., and Aziz, K.: “A Mechanistic Model for Multiphase Flow in Pipes,” Presented at 49th Annual Technical Meeting of Petroleum Society of the Canadian Institute of Mining, Metallurgy and Petroleum, Paper 98-39, Calgary, Alberta, June 8-10, 1998.

Rosa, E.S., and Netto, J.R.F.: “Viscosity Effect and Flow Development in Horizontal Slug Flows,” Paper No.306, Presented at 5th International Conference on Multiphase Flow, Yokohama, Japan, June 2004.

Shosho, C. E., and Ryan, M. E.: “An Experimental Study of the Motion of Long Bubbles in Inclined Pipes,” Chem. Eng. Sci., Vol. 56, pp. 2191-2204 (2001).

Taylor, G. I.: “Deposition of A Viscous Fluid on the Wall of A Tube,” J. Fluid Mech., Vol. 10, pp. 161-165(1961).

Zhang, H.-Q., Wang, Q., Sarica, C., and Brill, J.P.: “Unified Model for Gas-Liquid Pipe Flow via Slug Dynamics - Part 1: Model Development,” ASME, J. Energy Res. Tech., Vol. 125 (2003).

Zukoski, E. E.: “Influence of Viscosity, Surface Tension, and Inclination Angle on Motion of Long Bubbles in Closed Tubes,” J. Fluid Mech., Vol. 25, pp. 821-837(1966).

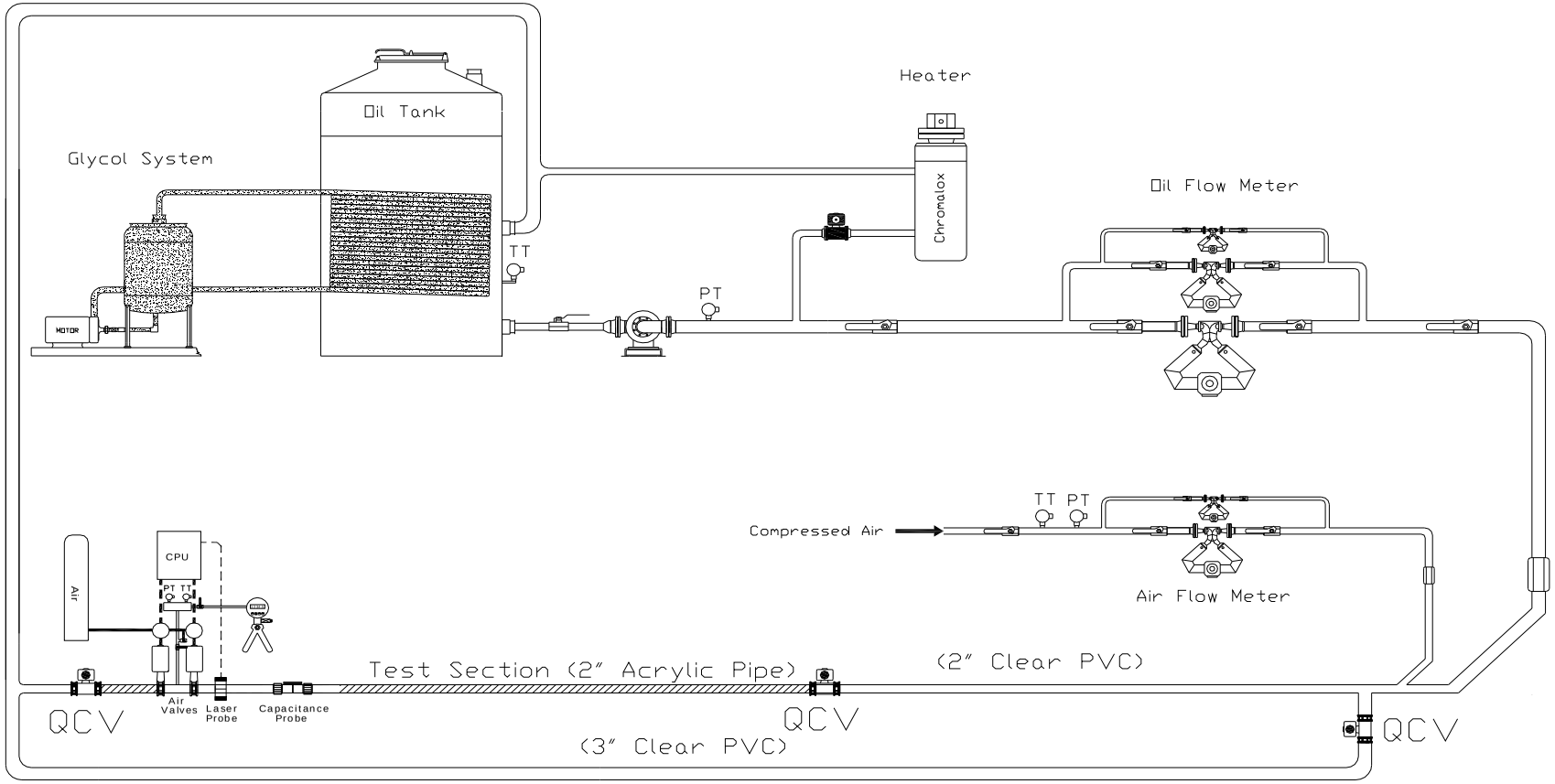

Figure 1: Schematic of High viscosity facility of the Tulsa University Fluid Flow Projects (TUFFP)

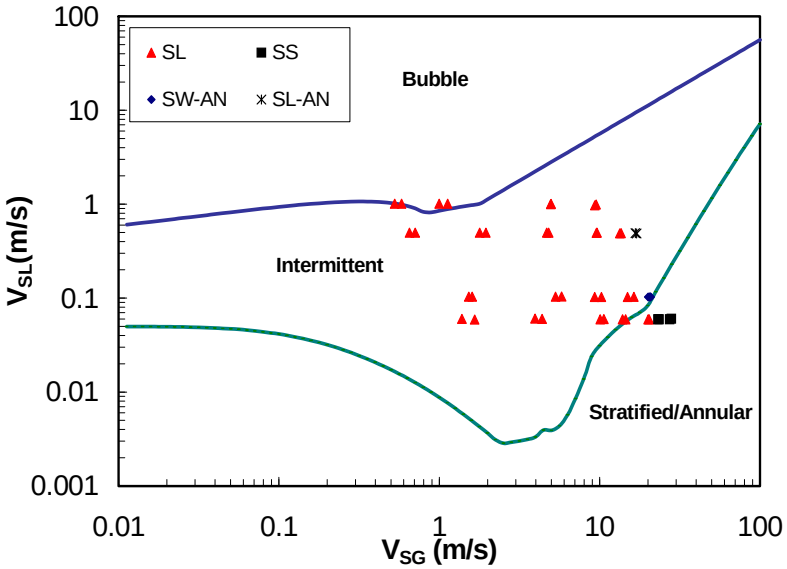

Figure 2: Flow Patterns for Citgo Sentry 220 with Inclination -1°

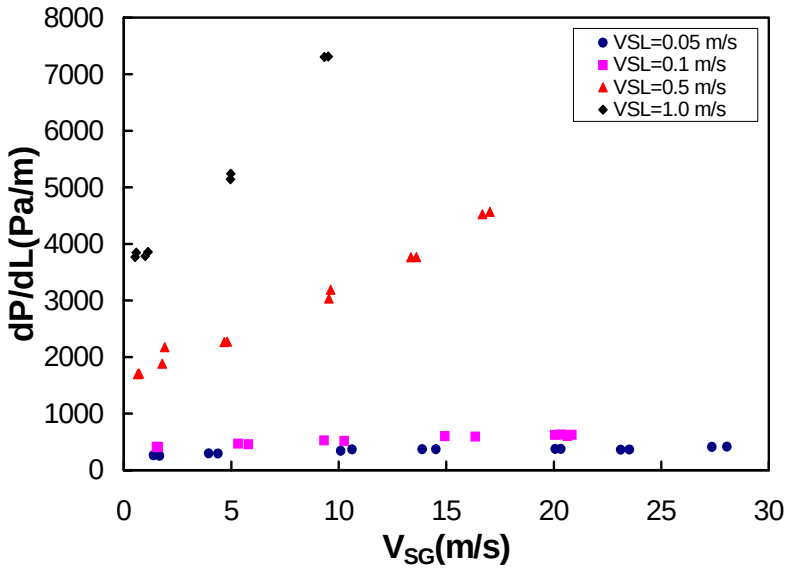

Figure 3: Pressure Gradient vs. Superficial Gas Velocity with Inclination -1°

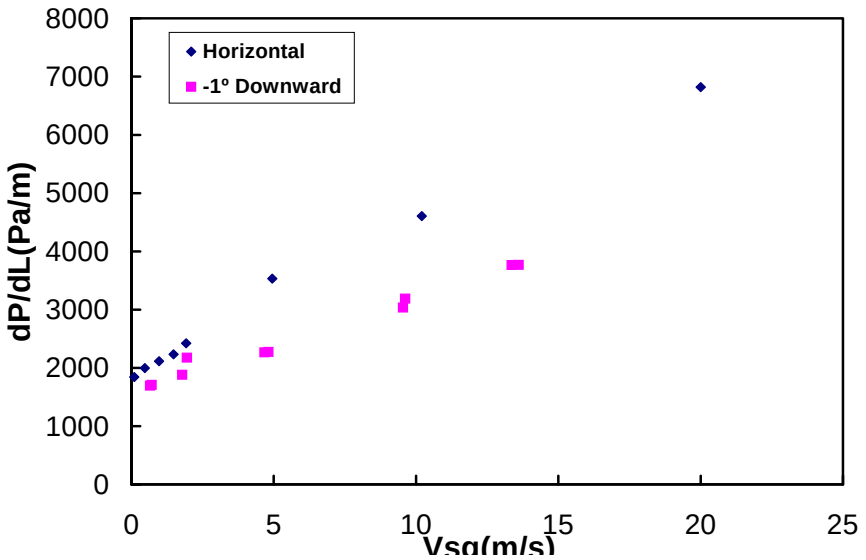

Figure 4: Comparison of Pressure Gradient between -1 ° Inclined Case and Horizontal Case (v_{SL}= 0.5 m/s)

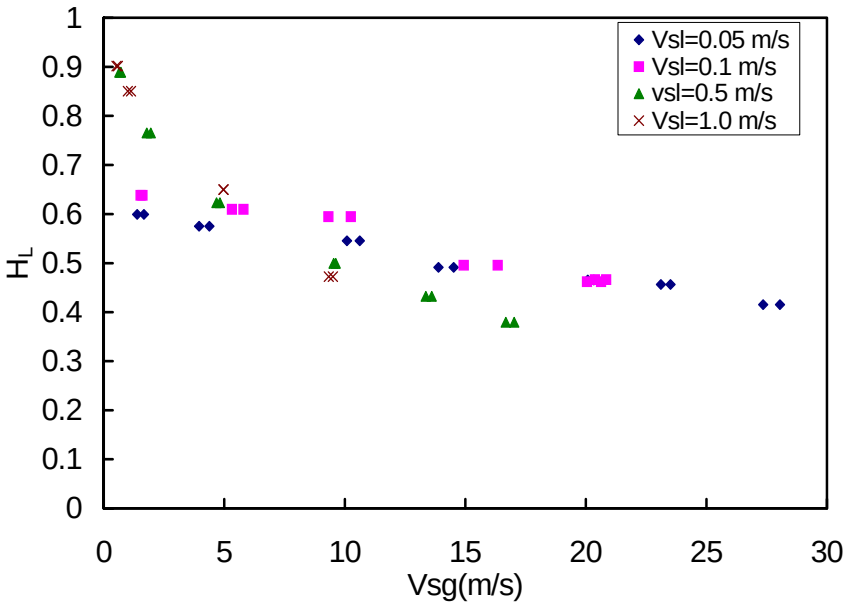

Figure 5: Liquid Holdup vs. v_{Sg} with Inclination -1 °

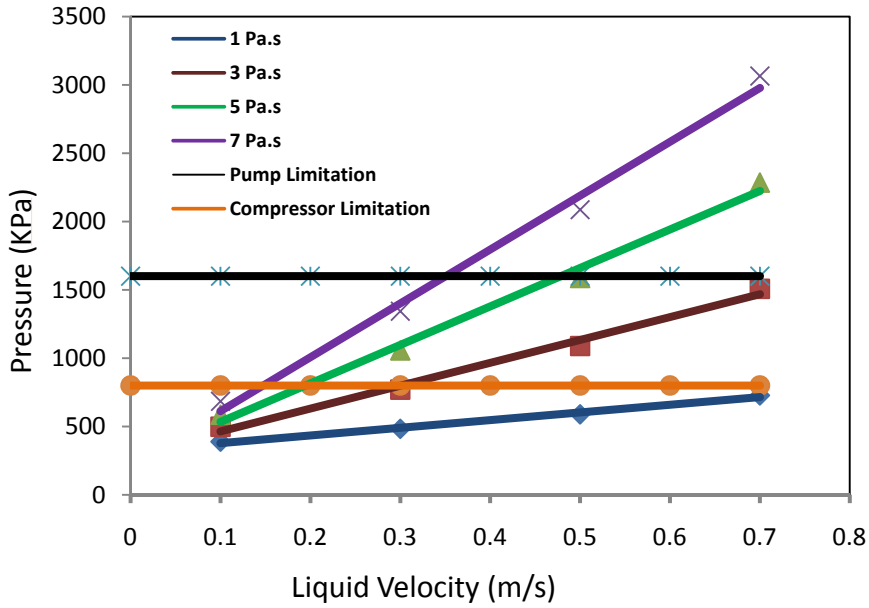

Figure 6: Pressure vs. Liquid Velocity for Single Phase High Viscosity Oil Flow

Fluid Flow Projects

Executive Summary of Research Activities

Cem Sarica

Advisory Board Meeting, May 12, 2010

Up-Scaling Studies

- Significance
  - Better Design and Operation
- Objective
  - Testing and Improvement of Existing Models for Large Diameter and Relatively High Pressures
- Past Studies
  - Low Pressure and 6-in. ID Low Liquid Loading (Fan and Dong)
  - High Pressure 2-in. ID (Manabe, 2002)

Up-Scaling Studies …

- Current Project
  - Construction of a New High Pressure, Large Diameter Facility
  - Extension of Low Liquid Loading Study to High Pressures is Envisioned as the First Study

Up-Scaling Studies …

- Status
  - Equipment Purchases
    - Most of the Equipment are either Purchased or Ordered
  - Construction is Underway

Up-Scaling Studies …

- Near Future Activities
  - Completion of Support Structures
  - Assembly of All of the Available Components
  - Commissioning by Early 2011

Fluid Flow Projects

High Pressure – Large Diameter Multiphase Flow Loop

Scott Graham and Cem Sarica

Outline

- Introduction
- Objectives
- Facility Design and Construction
- Capital Cost

Introduction

- Pressure and Pipe Diameter Affect Flow Behavior in Multiphase Flow Significantly
- Limited Study of Multiphase Flow in Large-Diameter Pipes at Pressure Conditions Higher than 2,000 kpa (290 psi)
- Need
  - Investigation of Diameter and Pressure Effects on Multiphase Flow
  - Experimental Data
- Requires a Proper Facility

Objectives

- Design and Construct a 6 in. ID High Pressure Multiphase Facility
- Conduct Research Projects to Better Understand Multiphase Flow
- Upscale Available Predictive Tools

Facility Design and Construction

- Design
  - Fluids
  - Operating Range
  - Facility Layout
  - Instrumentation
- Construction Activities

Fluids

- Gas Phase
  - Nitrogen
  - Natural Gas
- Oil Phase
  - Tulco Tech-80 Mineral Oil

Operating Range (Flow Pattern Map)

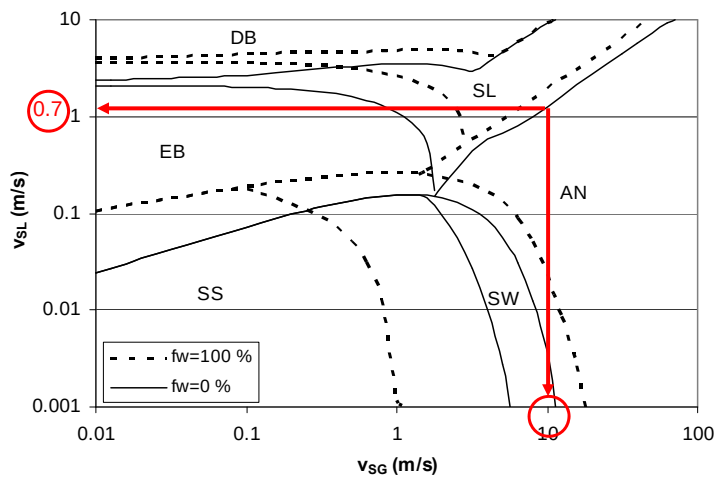

Operating Range …

- Operating Pressure = 500 psig
- $v_{SL,\ max}$=0.7 m/s; $v_{Sg,\ max}$=10 m/s
- f_w Between 0 and 100 %
- $q_{G,\ max}$ = 18 MMSCFD
- $q_{L,\ max}$ = 200 GPM
- Separator 54" x 10' @ 600 psig

Facility Diagram

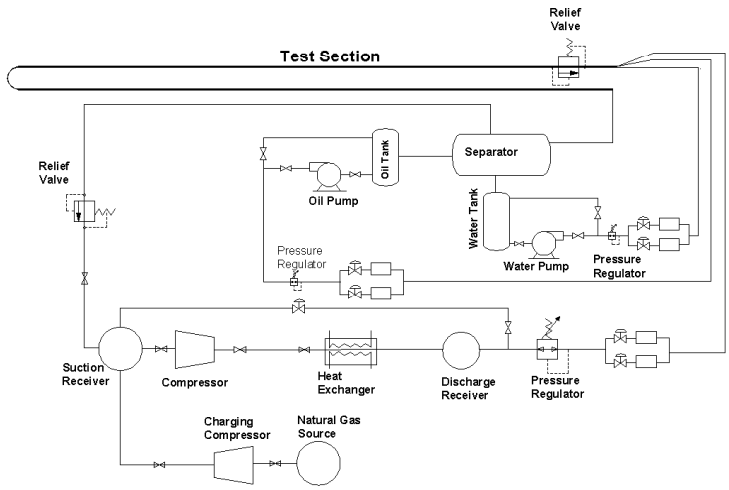

Facility Layout

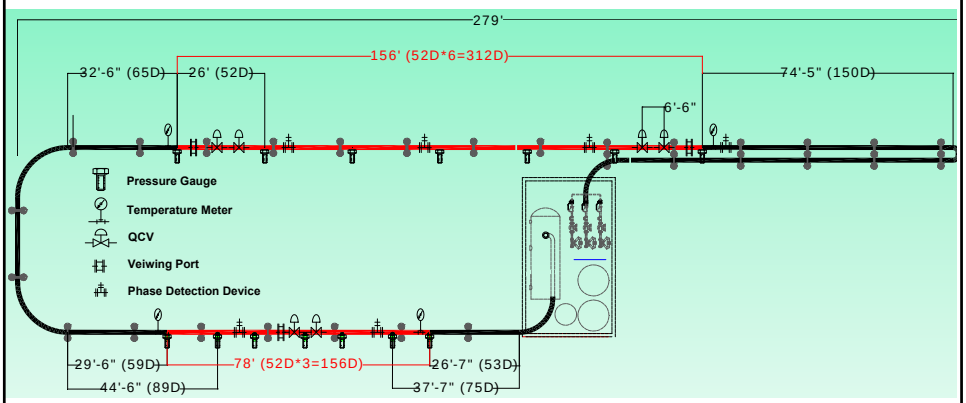

Facility Layout …

- 6 in. ID Stainless Steel Pipe
- Test Section-1
  - 156 ft (312D) Long and $-3° < \theta < +3°$
- Test Section-2
  - 78 ft (156D) Long and Horizontal
- Flow Development Sections with Sufficient Lengths

Facility Layout …

- Test Section-1
  - Six 26 ft (52D) Long Pressure Drop Sections
  - Two 6.5 ft Long Trap Sections
  - Two Viewing Ports
  - Two Temperature Transducers
  - Four Phase Detection Devices (TBD)
- Test Section-2
  - Six Pressure Drop Sections
  - One 6.5 ft Trap Section
  - One Viewing Port
  - Two Phase Detection Devices (TBD)
  - Two Temperature Transducers

Basic Instrumentation

	Pressure (psig)	Capacity
Gas Flow Rate	600	18 MMSCFD
Water Flow Rate	600	200 GPM
Oil Flow Rate	600	200 GPM
Differential Pressure	500	0 – 50 in H_2O
Pressure	600	0 – 800 psi
Temperature	500	0-100 °C
Quick Closing Valves	600	6 in. ID

Specific Instrumentation

- Trap Sections
  - Test Section-1
    - Located at Upstream and Downstream
  - Test Section-2
    - Located at Center

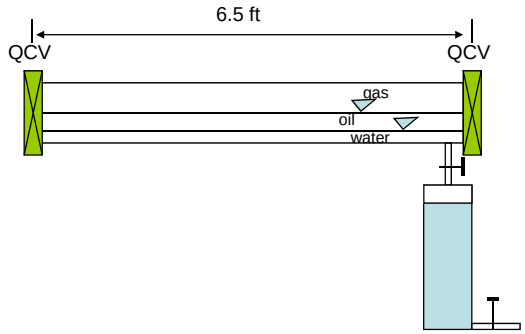

Special Instrumentation ..

- **Whole Perimeter Viewing Section**
  - **Visual Flow Observation**

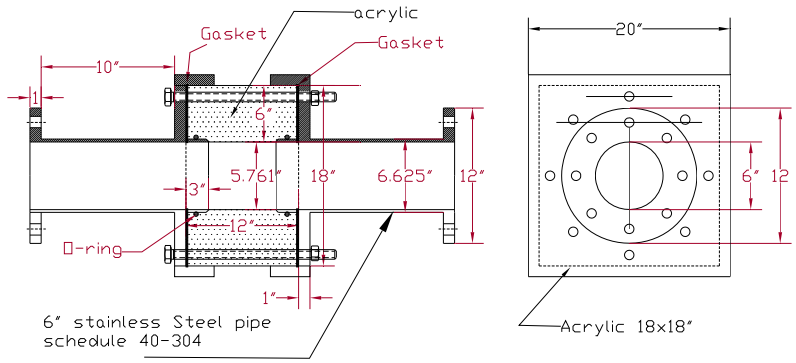

Special Instrumentation …

- **Boroscope**
  - **Visual Flow Observation**

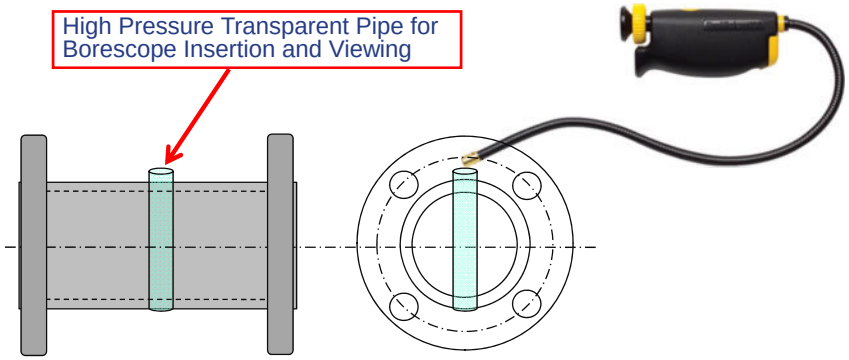

Construction Activities

- Equipment Pad
- Piers
- Structure

Equipment Pad

Rebar Detail

Pad & Equipment

Gas Compressor

Structure …

- Support Detail

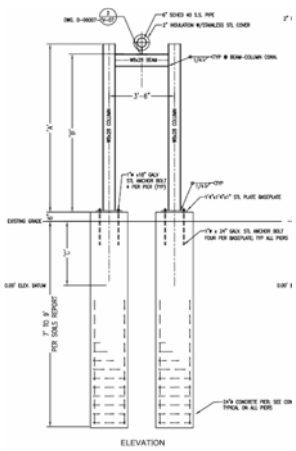

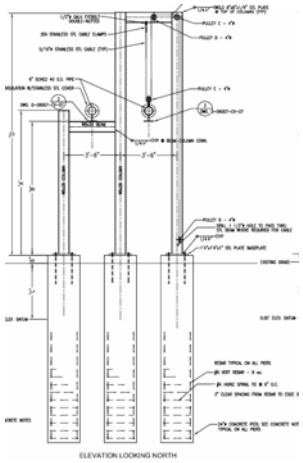

Piers …

Pouring

Pipe Supports

Pipe Supports

Structure

- Mechanical Pivot

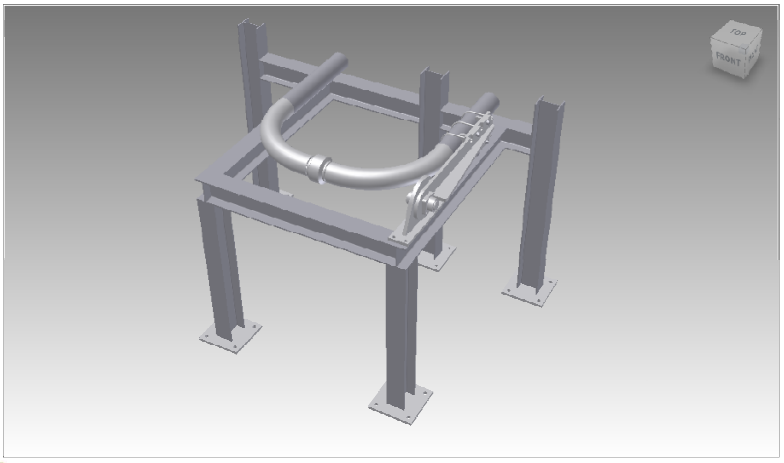

Pivot Mechanism

View from Above

View from Above

View from Above

Fluid Flow Projects

Advisory Board Meeting, May 12, 2010

Capital Cost Analysis

Equipment	Purchased	Budgeted for 2010	To Be Purchased Later
Oil Tank	35,000.00		
Air Exchanger	70,000.00		
Moyno Pump	23,500.00		
2phase Separator	39,000.00		
3phase Separators	30,000.00		
Transmitters	33,000.00		
Instrumentation	39,075.00		
Compressor	243,980.00		
P&ID, Permit Review, Civil/Structural Desig	84,888.62		
Generator	64,965.00		
Concrete	93,596.07		
Steel Structure	74,378.00		
Commercial Steel	36,068.00	52,168.00	
Quick Closing Valves	36,764.00	-	
Surge Control Package	56,000.00		
Valves	19,000.00	11,000.00	
Instrumentation		17,000.00	
Suction Control Valve	7,300.00	2,700.00	
DAQ	8,000.00		
Misc. (switches, motors)		50,000.00	
Fittings		10,000.00	
Welding Process Area		40,000.00	
Speciality Instrumentation		75,000.00	
Water Phase			
Tank			35,000.00
Meters			33,000.00
	$ 994,514.69	$ 257,868.00	$ 68,000.00

Fluid Flow Projects

Executive Summary of Research Activities

Cem Sarica

Advisory Board Meeting, May 12, 2010

Transient Modeling

- Project Proposal Rated High in a Recent TUFFP Questionnaire
- Significance
  - Industry has Capable All Purpose Transient Software
    - OLGA, PLAC, TACITE
  - Efforts are Well Underway to Develop Next Generation All Purpose Transient Simulators
    - Horizon, LEDA
  - Need for a Simple Transient Flow Simulator

Transient Modeling …

- Objective
  - Development and Testing of a Simple and Fast Transient Flow Simulator That Can Be Used as a Screening Tool
- Past Studies
  - TUFFP has Conducted Many Transient Multiphase Studies
    - Scoggins, Sharma, Dutta-Roy, Taitel, Vierkandt, Sarica, Vigneron, Minami, Gokdemir, Zhang, Tengesdal, and Beltran

Transient Modeling …

- Status
  - Significant Progress Since Last ABM
  - Two Models Developed
    - Two-Fluid
    - Drift Flux
  - Compared with TUFFP Transient Flow Data

Fluid Flow Projects

Transient Two-Phase Flow Modeling

Michelle Li

Advisory Board Meeting, May 12, 2010

Outline

- Objectives
- Significance
- Past Studies on Transient Multiphase Flow Modeling
- Current Approach
  - Two Fluid Model
  - Drift Flux Model
- Further Work

Objectives

- Develop a Simplified Simulator for Gas-Liquid Two-Phase Flow in Pipelines
- Test Model Against Available Experimental Data

Significance

- Oil and Gas Pipelines Rarely Operate under Steady State
- Transient Phenomena can be Induced due to Boundary Conditions, or Geometry of the Pipe
- Currently, Most Two-Phase Flow Pipelines Still Designed Under Steady Condition

Significance …

- All Purpose Transient Software Packages Available: OLGA, PLAC, TACITE
- Further Efforts Underway to Develop Next Generation Transient Simulators: Horizon, LEDA
- Need for a Fast and Simple Transient Simulator

Past Studies

- Scoggins (1977), Drift Flux Model, Horizontal Two-Phase Transient
- Dutta-Roy (1982), Two-Fluid Model for Horizontal Two-Phase Stratified Flow
- Sharma (1986,1993), Two-Fluid Model for Stratified and Slug Flow
- Taitel (1978,1989,1990,1997), Flow Patten Dependant Mechanistic Model
- Minami (1991), Pigging Slug Dynamics, Two-Phase Flow

Past Studies …

- Sarica (1991), Terrain Slugging, Two-Phase Flow
- Zhang (2003), Slug Dissipation and Generation in Two-Phase Hilly-Terrain Pipe Flow
- Tengesdal (2003), Severe Slugging, Gas-Liquid Two-Phase Flow
- Beltran (2006), Severe Slugging, Gas-Oil-Water Three Phase Flow

Scope of Current Work

- Consider Transient Phenomena Caused by Boundary Condition Changes
- Gas-Liquid Two-Phase Flow
- All Inclination Angles
- All Flow Patterns

Our Approach

- Attempt 1: Two-Fluid Model for Stratified Flow
- Attempt 2: Drift Flux Model

Attempt 1: Two Fluid Model

- Mass Conservations for Liquid and Gas:

$$\frac{dm_L}{dt} = \dot{m}_{L,i-1} - \dot{m}_{L,i}$$

$$\frac{dm_G}{dt} = \dot{m}_{G,i-1} - \dot{m}_{G,i}$$

Attempt 1: Two Fluid Model …

- **Momentum Conservations for Liquid and Gas:**

$$(P_i - P_{i+1})AH_L = (\tau_L S_L - \tau_I S_I)\Delta x + \rho_L g A H_L \Delta x \, sin\theta$$

$$(P_i - P_{i+1})A(1 - H_L) = (\tau_G S_G + \tau_I S_I)\Delta x + \rho_G g A(1 - H_L)\Delta x \, sin\theta$$

Liquid Mass Flow Rate

- **From Liquid Momentum Conservation**

$$\dot{m}_{L,i}^{K+1} = a_{L,i}^{K+1}(P_i^{K+1} - P_{i+1}^{K+1}) + b_{L,i}^{K+1}$$

$$a_{L,i}^{K+1} = \frac{1}{\frac{(f_L S_L \rho_L - f_I S_I \rho_G)\Delta x \dot{m}_L}{2\rho_L^2 A^3 H_L^3} + \frac{f_I S_I \Delta x \dot{m}_G}{\rho_L A^3 H_L^2 (1-H_L)}}$$

$$b_{L,i}^{K+1} = \frac{\frac{f_I S_I \Delta x \dot{m}_G^2}{2\rho_G A^3 H_L (1-H_L)^2} - \rho_L g sin\theta \Delta x}{\frac{(f_L S_L \rho_L - f_I S_I \rho_G)\Delta x \dot{m}_L}{2\rho_L^2 A^3 H_L^3} + \frac{f_I S_I \Delta x \dot{m}_G}{\rho_L A^3 H_L^2 (1-H_L)}}$$

Gas Mass Flow Rate

- **From Gas Momentum Conservation**

$$\dot{m}_{G,i}^{K+1} = a_{G,i}^{K+1}(P_i^{K+1} - P_{i+1}^{K+1}) + b_{G,i}^{K+1}$$

$$a_{G,i}^{K+1} = \frac{1}{\frac{(f_G S_G + f_I S_I)\Delta x \dot{m}_G}{2\rho_G A^3 (1-H_L)^3} - \frac{f_I S_I \Delta x \dot{m}_L}{\rho_L A^3 H_L (1-H_L)^2}}$$

$$b_{G,i}^{K+1} = \frac{-\frac{f_I S_I \rho_G \Delta x \dot{m}_L^2}{2\rho_L^2 A^3 H_L^2 (1-H_L)} - \rho_G g \sin\theta \Delta x}{\frac{(f_G S_G + f_I S_I)\Delta x \dot{m}_G}{2\rho_G A^3 (1-H_L)^3} - \frac{f_I S_I \Delta x \dot{m}_L}{\rho_L A^3 H_L (1-H_L)^2}}$$

Solution Procedures

- **Unknowns: H_L, P, V_{SL}, V_{SG}**
- **Initial and Boundary Conditions**
- **Time Marching Scheme**

Model Validation

- Experiments by Vigneron *et al.* (1995)
  - Air and Kerosene
  - Horizontal Pipe L=420 m, d=77.9 mm
  - Two Test Sections
  - Transient Caused By:
    - Liquid flow rate change
    - Gas flow rate change
    - Liquid blow out
    - Start up

Test 1-C

- Inlet Liquid Flow Rate 8.4 $m^3/d \rightarrow 32$ m^3/d at t=180 sec
- Inlet Gas Flow Rate 4055 Sm^3/d
- Separator Pressure 1.76 bar

Test 1-C …

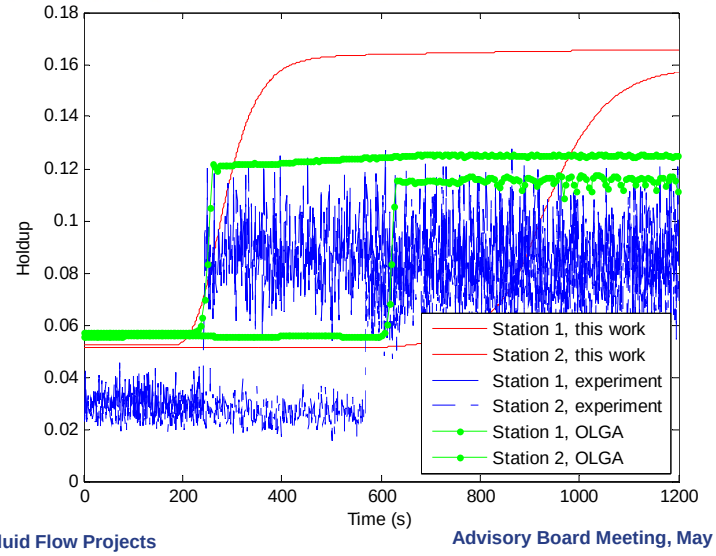

Test 1-C …

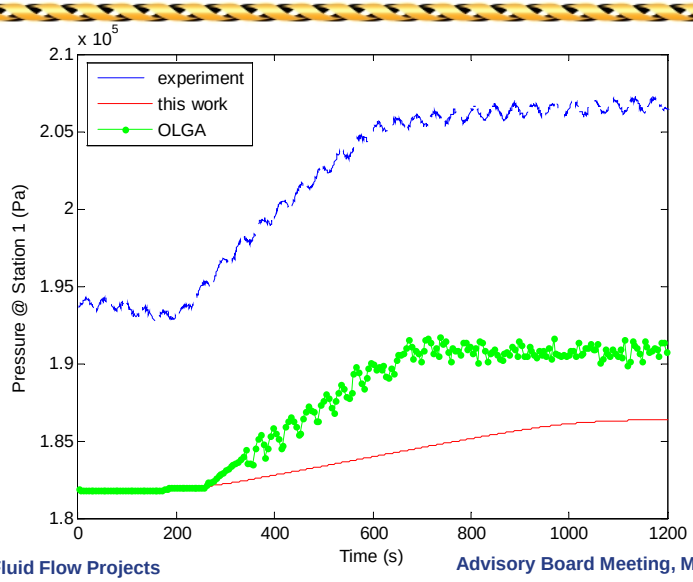

Test 3-A

- Inlet Liquid Flow Rate 48.8 $m^3/d \rightarrow 0$ at t=120 sec
- Inlet Gas Flow Rate 4825 Sm^3/d
- Separator Pressure 1.69 bar

Test 3-A …

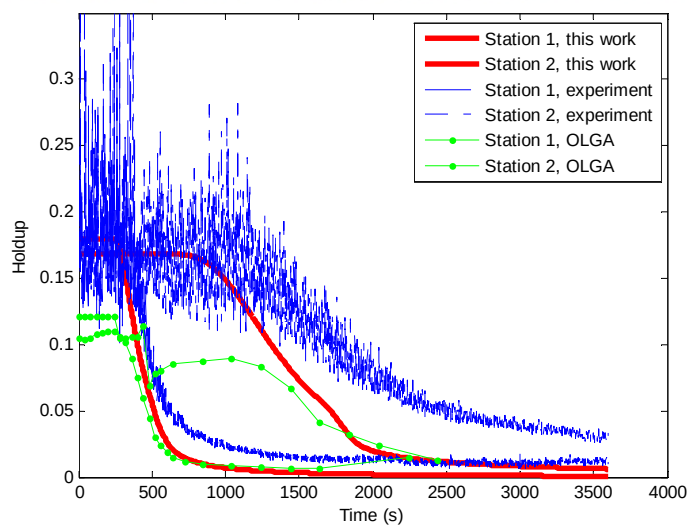

Test 3-A …

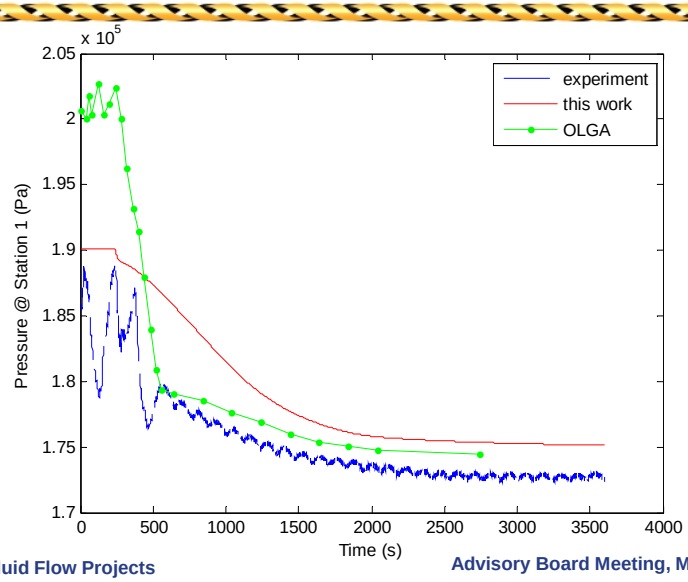

Two Fluid Model Summary

- Two-Fluid Model is Developed for Stratified Flow
- For Liquid Flow Rate Change, Model Simulation Gave Good Prediction
- For Gas Flow Rate Change, Current Model Does Not Converge

Attempt 2: Drift Flux Model

- **Mass Conservations for Liquid and Gas:**

$$\frac{dm_L}{dt} = \dot{m}_{L,i-1} - \dot{m}_{L,i}$$

$$\frac{dm_G}{dt} = \dot{m}_{G,i-1} - \dot{m}_{G,i}$$

Attempt 2: Drift Flux Model …

- **Momentum Conservation for Gas-Liquid Mixture:**

$$(P_i - P_{i+1})A = \frac{1}{2} f_M \rho_M v_M^2 \pi D \Delta x + \rho_M g A \Delta x sin\theta$$

Attempt 2: Drift Flux Model …

- **Drift Flux Model:**

$$v_G = C v_M + v_d$$

$C = 1.0$

$$v_d = 0.54\sqrt{gd}\cos\theta + 0.35\sqrt{gd}\sin\theta$$

Gas Mass Flow Rate

- **From Mixture Momentum Conservation**

$$\dot{m}_{G,i}^{K+1} = a_i^{K+1}(P_i^{K+1} - P_{i+1}^{K+1}) + b_i^{K+1}$$

$$a_i^{K+1} = \frac{2A^2C^2\rho_g(1-H_L)}{f_M\rho_M\pi D\Delta x(V_G - V_d)}$$

$$b_i^{K+1} = \frac{-2A^2C^2\rho_g(1-H_L)g\Delta x\sin\theta}{f_M\pi D\Delta x(V_G - V_d)} + \rho_g A(1-H_L)v_d$$

Solution Procedures

- Unknowns: H_L, P, V_{SL}, V_{SG}
- Initial and Boundary Conditions
- Time Marching Scheme

Model Validation

- Experiments by Vigneron *et al.* (1995)
  - Air and Kerosene
  - Horizontal Pipe L=420 m, d=77.9 mm
  - Two Test Sections
  - Transient Caused By:
    - Liquid flow rate change
    - Gas flow rate change
    - Liquid blow out
    - Start up

Test 1-D

- Slug Flow, Liquid Flow Rate Decrease
- Inlet Liquid Flow Rate 340 m^3/d → 168 m^3/d at t=120 sec
- Inlet Gas Flow Rate 880 Sm^3/d
- Separator Pressure 1.67 bar

Test 1-D …

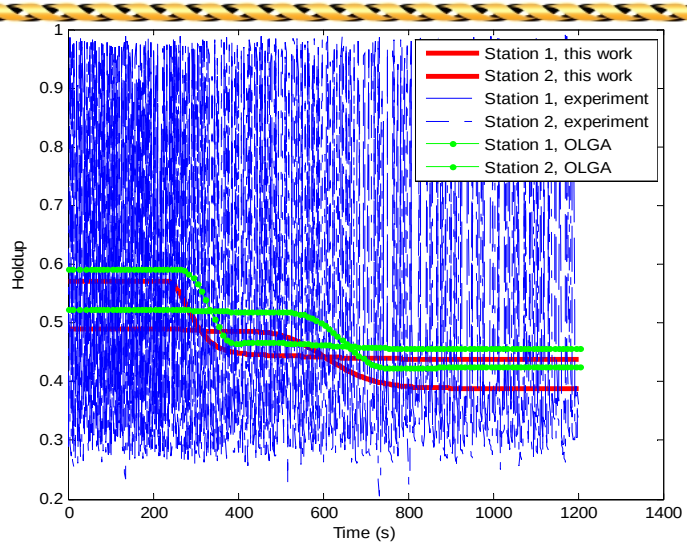

Test 1-D …

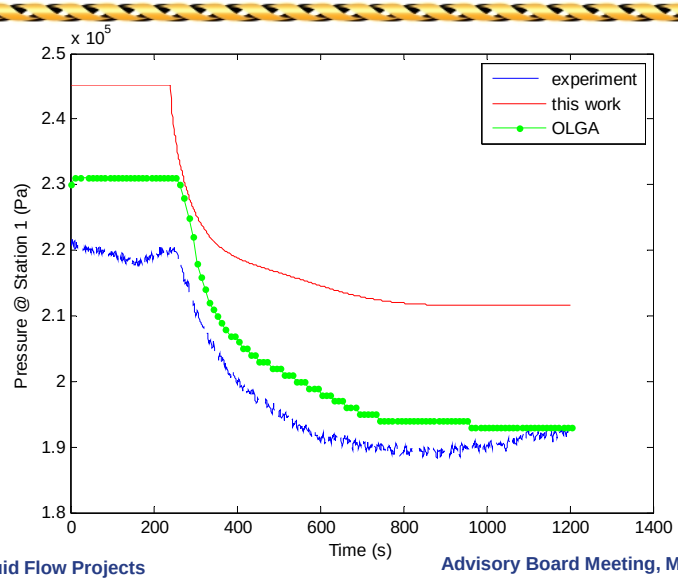

Test 2-D

- Slug Flow, Gas Flow Rate Increase
- Inlet Liquid Flow Rate 195 m^3/d
- Inlet Gas Flow Rate 1875 Sm^3/d → 10840 Sm^3/d at t=125 sec
- Separator Pressure 1.67 bar

Test 2-D …

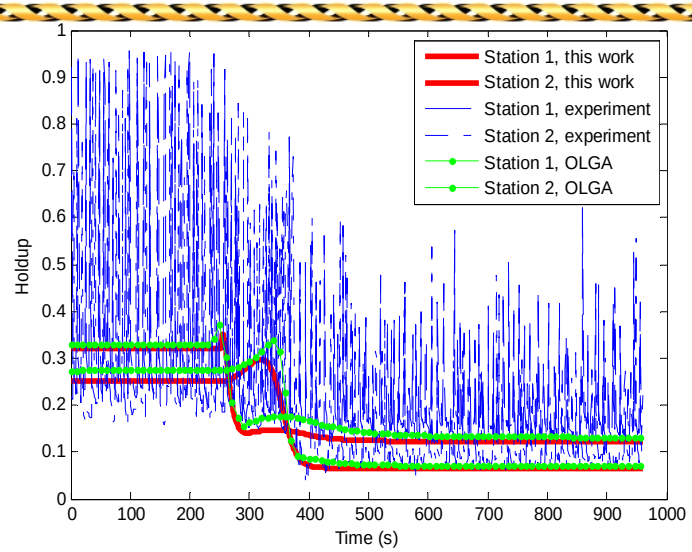

Test 2-D …

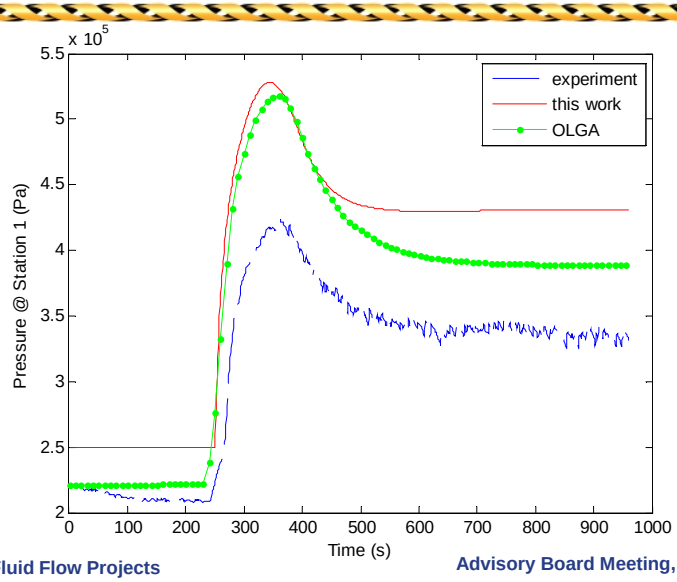

Test 3-B

- Slug Flow, Liquid Blow Out
- Inlet Liquid Flow Rate 204 $m^3/d \rightarrow 0$ at t=95 sec
- Inlet Gas Flow Rate 5880 Sm^3/d
- Separator Pressure 1.69 bar

Test 3-B …

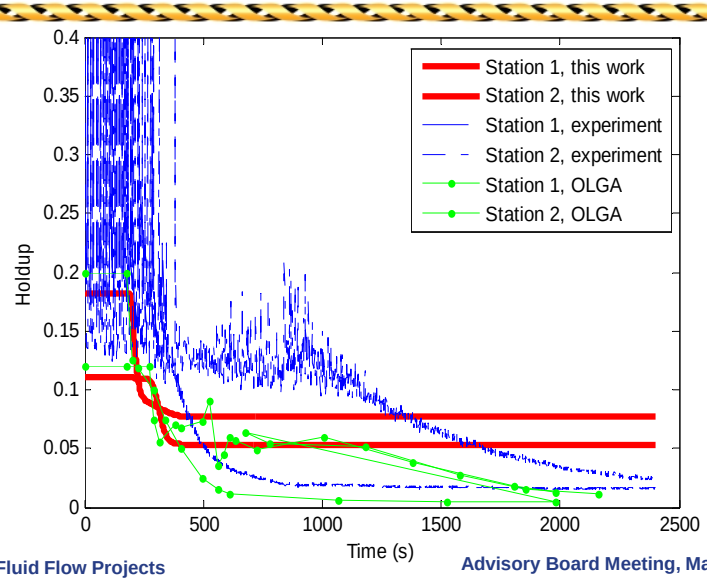

Test 3-B …

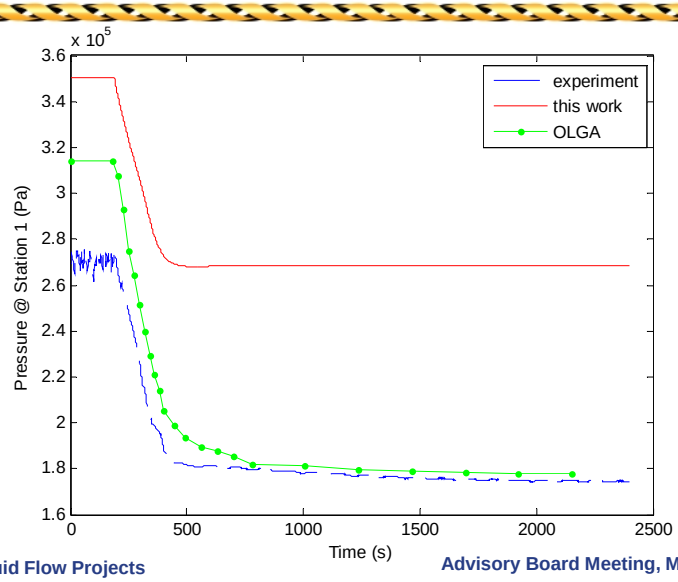

Test 4-B0

- Slug Flow, Startup
- Initial H_L=0.0
- Startup at t=122 sec
- Inlet Liquid Flow Rate 0 → 322.0 m^3/d
- Inlet Gas Flow Rate 0 → 1870 Sm^3/d
- Separator Pressure 1.66 bar

Test 4-B0 …

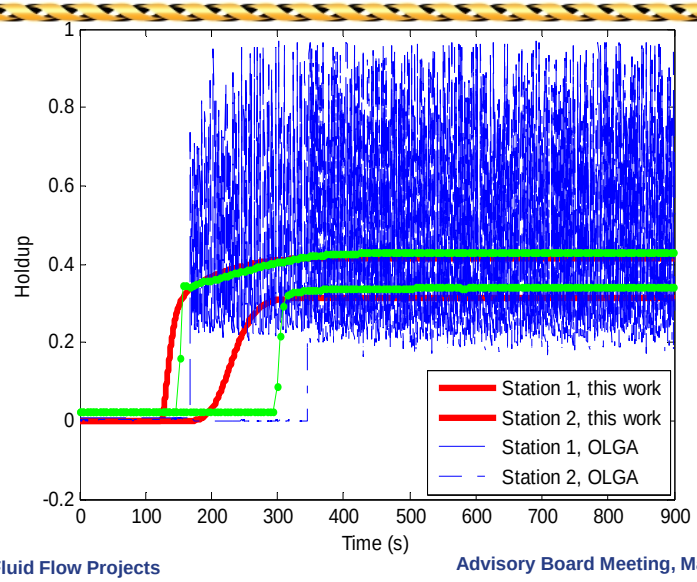

Fluid Flow Projects

Advisory Board Meeting, May 12, 2010

Test 4-B0 …

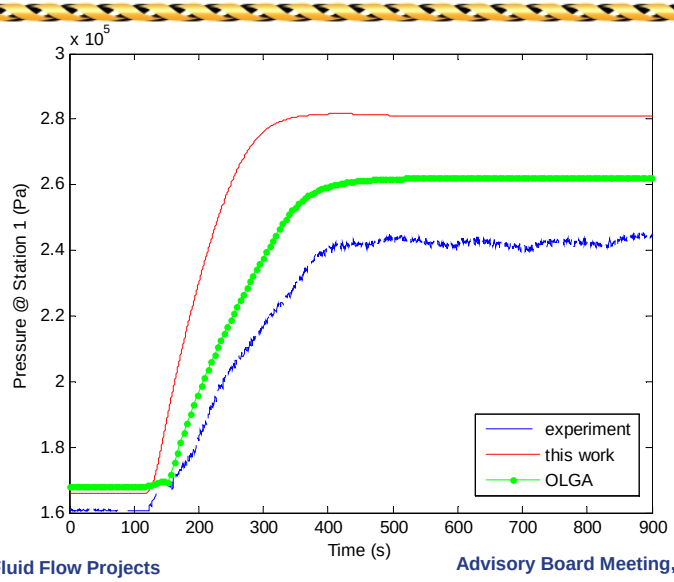

Fluid Flow Projects

Advisory Board Meeting, May 12, 2010

Test 1-C

- Stratified Flow, Liquid Flow Rate Increase
- Inlet Liquid Flow Rate 8.4 m^3/d → 32 m^3/d at t=180 sec
- Inlet Gas Flow Rate 4055 Sm^3/d
- Separator Pressure 1.76 bar

Test 1-C …

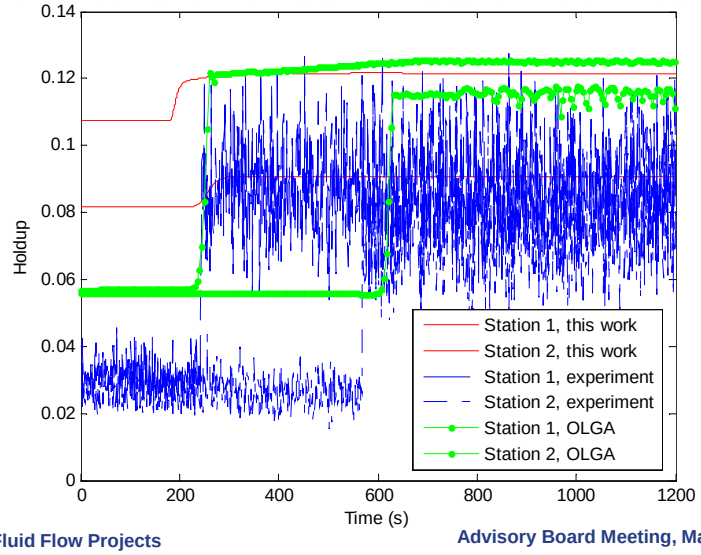

Test 1-C …

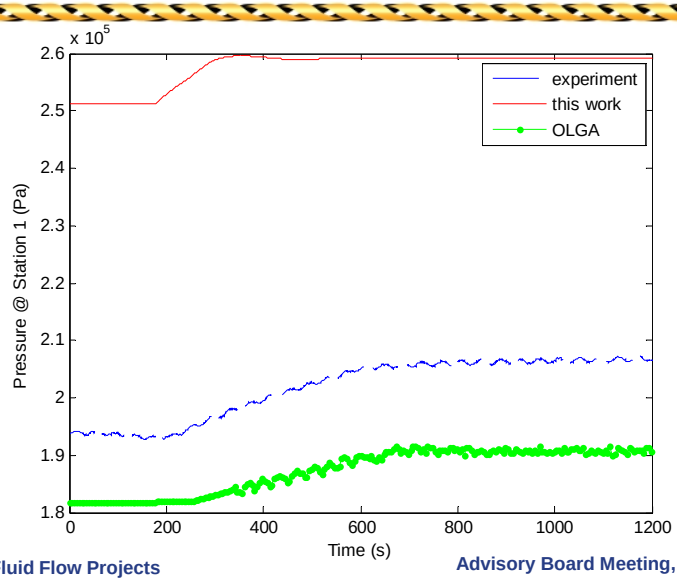

Test 2-B

- Stratified Flow, Gas Flow Rate Increase
- Inlet Liquid Flow Rate 20.2 m^3/d
- Inlet Gas Flow Rate 340 Sm^3/d → 2530 Sm^3/d at t=130 sec
- Separator Pressure 1.67 bar

Test 2-B …

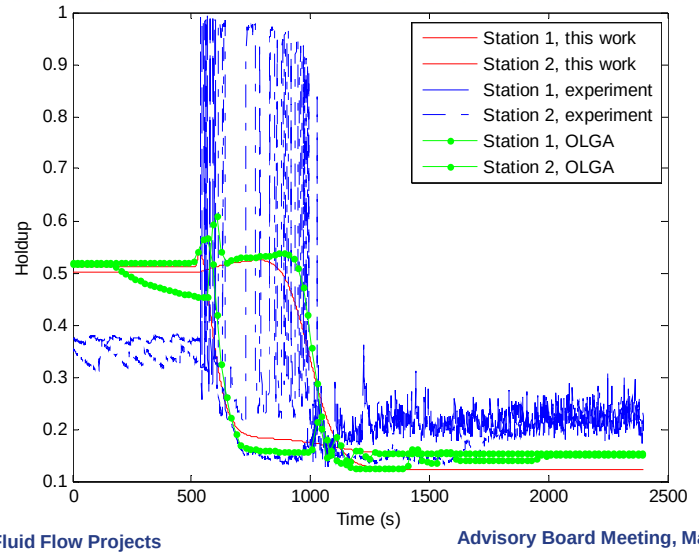

Fluid Flow Projects

Advisory Board Meeting, May 12, 2010

Test 2-B …

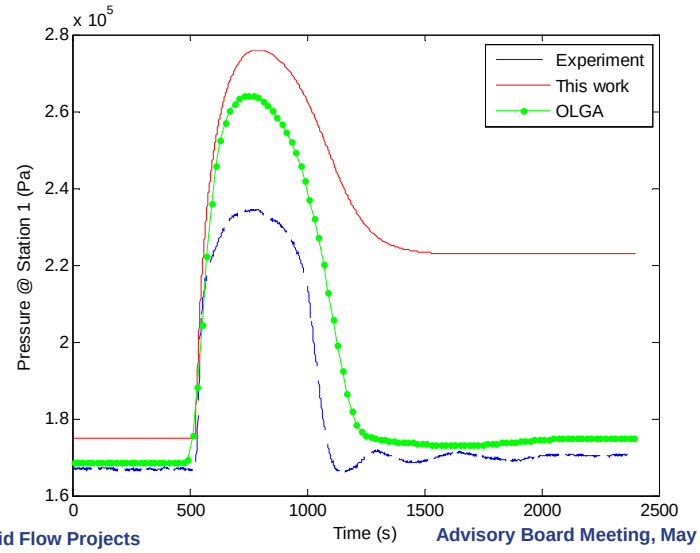

Fluid Flow Projects

Advisory Board Meeting, May 12, 2010

Test 3-A

- Stratified Flow, Liquid Blow Out
- Inlet Liquid Flow Rate 48.8 $m^3/d \rightarrow 0$ at t=120 sec
- Inlet Gas Flow Rate 4825 Sm^3/d
- Separator Pressure 1.69 bar

Test 3-A …

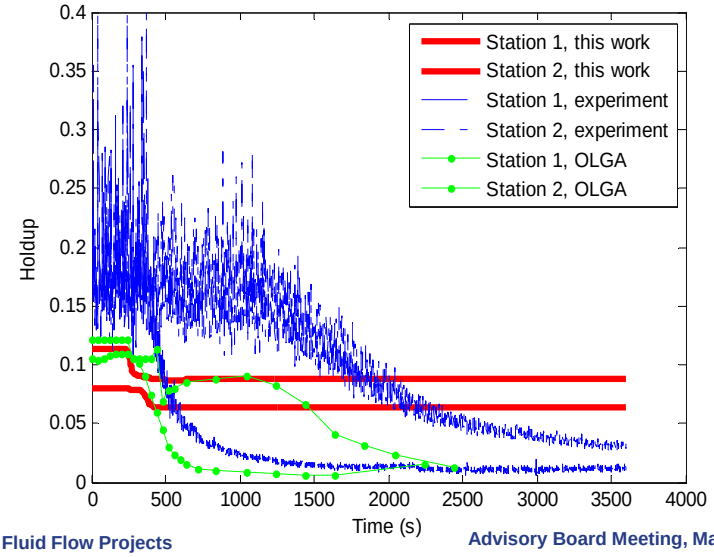

Test 3-A …

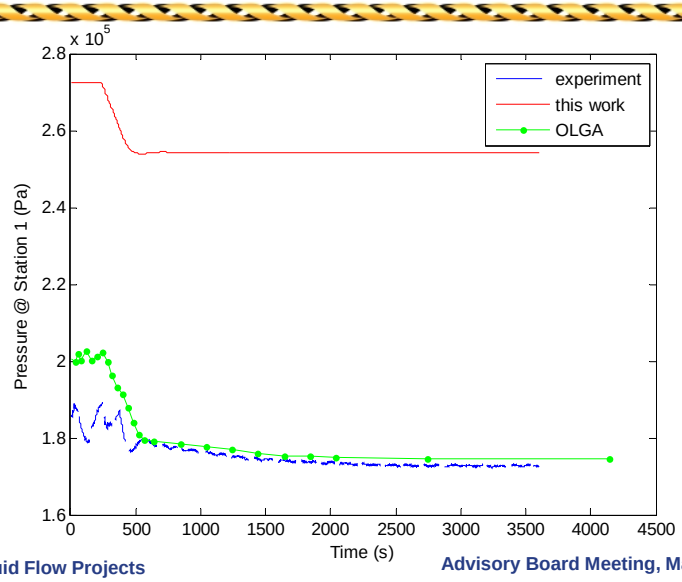

Drift Flux Model Summary

- Good for Slug Flow
- For Stratified Flow
  Good for Gas Flow Rate Change, Why?
  Not Good for Liquid Rate Change, Why?

Efforts in Improving DF Model

- Modify the Drift Flux Correlation for Stratified Flow, How?

Further Work

- Modify the Drift Flux Model for Stratified Flow
- Need to Incorporate the Model with a PVT Package
- Heat Transfer
- Terrain/Severe Slugging
- More Data for Model Validation

Questions and Comments

?

Transient Gas-Liquid Two-Phase Flow Simulation

Michelle Li

Objective

The objective of this study is to develop a simplified simulator for transient gas-liquid two-phase flow in pipelines.

Introduction

Transient phenomena are frequently encountered in pipelines in the oil and gas industry. These phenomena occur when there is a change in inlet and outlet conditions, or when terrain/severe slugging are formed due to the geometry of the pipe. Knowledge of the dynamic behavior is very important to properly design and operate the pipelines, as well as the receiving facilities.

The investigation of transient flow phenomena in petroleum industry started in the late 70's and early 80's. Currently, industry has developed capable all purpose transient simulators such as OLGA, PLAC, TACITE. Further efforts are underway to develop next generation all purpose transient simulators with multidimensional capabilities such as Horizon and LEDA.

These codes normally utilize full set of mass, momentum and energy conservation equations. However, most of the transient phenomena encountered in oil and gas industry are comparatively slow, and the use of full set of equations is probably not necessary. There is a need for a simplified transient flow simulator.

In this study, the transient phenomenon is modeled through unsteady mass conservation equations, while the momentum equation is considered to be in local quasi-steady state. Both two-fluid approach and drift flux approach are tried, and the results are presented.

Attempt 1: Two Fluid Model

Flow pattern is predicted with steady state models. Hydrodynamic behavior of each flow pattern is modeled separately.

1. Method

Unsteady mass conservation equations are used for both gas and liquid. Momentum equations are considered to be in local equilibrium. Gas is compressible, while liquid is considered to be incompressible.

Governing Equations for Stratified Flow:

The mass conservation equations are:

$$\frac{dm_L}{dt} = \dot{m}_{L,i-1} - \dot{m}_{L,i}, \quad (1)$$

$$\frac{dm_G}{dt} = \dot{m}_{G,i-1} - \dot{m}_{G,i}. \quad (2)$$

The momentum conservation equations are:

$$(P_i - P_{i+1})AH_L = (\tau_L S_L - \tau_I S_I)\Delta x + \rho_L g A H_L \Delta x \, sin\theta, \quad (3)$$

$$(P_i - P_{i+1})A(1 - H_L) = (\tau_G S_G + \tau_I S_I)\Delta x + \rho_G g A(1 - H_L)\Delta x \, sin\theta. \quad (4)$$

Where the shear stresses can be correlated as:

$$\tau_L = f_L \frac{\rho_L v_L^2}{2}, \quad (5)$$

$$\tau_G = f_G \frac{\rho_G v_G^2}{2}, \quad (6)$$

$$\tau_I = f_I \frac{\rho_G (v_G - v_L)^2}{2}. \quad (7)$$

Friction factors f_L and f_G can be approximated by the correlation $f = C\ Re^{-n}$, C=0.046, n=0.2 for turbulent

flow, and C=16, n=1 for laminar flow. Interfacial friction factor f_I can be approximated by

$$f_I = f_G\left(1 + 14.3H_L^{0.5}\left(\frac{v_{SG}}{v_{SG,t}} - 1\right)\right). \quad (8)$$

Where $v_{SG,t} = 5\left(\frac{\rho_{GO}}{\rho_G}\right)^{0.5}$, ρ_{GO} is the gas density at atmospheric pressure. The perimeters S_L, S_G, S_I are calculated according to Zhang *et al.* (2003) as follows:

$$S_L = \pi d\Theta, \quad (9)$$

$$S_G = \pi d(1 - \Theta), \quad (10)$$

$$S_I = \frac{S_L(A_{CD} - AH_L) + S_{CD}AH_L}{A_{CD}}, \quad (11)$$

$$S_{CD} = dsin(\pi\Theta), \quad (12)$$

$$A_{CD} = \frac{d^2}{4}\left(\pi\Theta - \frac{\sin(2\pi\Theta)}{2}\right). \quad (13)$$

The wetted wall fraction Θ is calculated with Grolman correlation,

$$\Theta = \Theta_0\left(\frac{\sigma_{water}}{\sigma}\right)^{0.15} + \frac{\rho_G}{\rho_L - \rho_G}\frac{1}{cos\theta}\left(\frac{\rho_L v_{SL}^2 d}{\sigma}\right)^{0.25}\left(\frac{v_{SG}^2}{(1-H_L)^2 gd}\right)^{0.8}. \quad (14)$$

Where Θ_0 is the wetted wall fraction corresponding to a flat gas/liquid interface for a given H_L.

A linear relationship can be obtained from Eq. (3) and Eq. (4) to calculate $\dot{m}_L$ and $\dot{m}_G$ from the pressure difference.

$$\dot{m}_{L,i}^{K+1} = a_{L,i}^{K+1}(P_i^{K+1} - P_{i+1}^{K+1}) + b_{L,i}^{K+1}. \quad (15)$$

$$\dot{m}_{G,i}^{K+1} = a_{G,i}^{K+1}(P_i^{K+1} - P_{i+1}^{K+1}) + b_{G,i}^{K+1}. \quad (16)$$

Where the coefficients $a_{L,i}^{K+1}$, $b_{L,i}^{K+1}$, $a_{G,i}^{K+1}$, $b_{G,i}^{K+1}$ are:

$$a_{L,i}^{K+1} = \frac{1}{\frac{(f_L S_L \rho_L - f_I S_I \rho_G)\Delta x \dot{m}_L}{2\rho_L^2 A^3 H_L^3} + \frac{f_I S_I \Delta x \dot{m}_G}{\rho_L A^3 H_L^2 (1-H_L)}}, \quad (17)$$

$$b_{L,i}^{K+1} = \frac{\frac{f_I S_I \Delta x \dot{m}_G^2}{2\rho_G A^3 H_L (1-H_L)^2} - \rho_L g sin\theta \Delta x}{\frac{(f_L S_L \rho_L - f_I S_I \rho_G)\Delta x \dot{m}_L}{2\rho_L^2 A^3 H_L^3} + \frac{f_I S_I \Delta x \dot{m}_G}{\rho_L A^3 H_L^2 (1-H_L)}}, \quad (18)$$

$$a_{G,i}^{K+1} = \frac{1}{\frac{(f_G S_G + f_I S_I)\Delta x \dot{m}_G}{2\rho_G A^3 (1-H_L)^3} - \frac{f_I S_I \Delta x \dot{m}_L}{\rho_L A^3 H_L (1-H_L)^2}}, \quad (19)$$

$$b_{G,i}^{K+1} = \frac{-\frac{f_I S_I \rho_G \Delta x \dot{m}_L^2}{2\rho_L^2 A^3 H_L^2 (1-H_L)} - \rho_G g sin\theta \Delta x}{\frac{(f_G S_G + f_I S_I)\Delta x \dot{m}_G}{2\rho_G A^3 (1-H_L)^3} - \frac{f_I S_I \Delta x \dot{m}_L}{\rho_L A^3 H_L (1-H_L)^2}}. \quad (20)$$

2. Solution Procedures

Figure 1 shows a flow chart for the two fluid model approach. Detailed descriptions of each step are given below.

1) Initialization: Define pipe geometry, fluid properties, and initial conditions. The pipe is divided into N sections of length Δx. Initial condition at time $t=0$ includes: gas and liquid velocities, liquid holdup, and pressure for each section of the pipe.

2) Specify boundary conditions. Inlet gas and liquid flow rates and outlet pressure at each time step are known.

3) Liquid mass in each section of the pipe at the new time step K+1 is calculated by

$$m_{L,i}^{K+1} = m_{L,i}^{K} + \Delta t\left(\dot{m}_{L,i-1}^{K+1} - \dot{m}_{L,i}^{K+1}\right). \quad (21)$$

4) The new liquid holdup is calculated as

$$H_{L,i}^{K+1} = \frac{m_{L,i}^{K+1}}{\rho_L A_i \Delta x}. \quad (22)$$

5) Gas mass in each section of the pipe at the new time step K+1 is calculated by

$$m_{G,i}^{K+1} = m_{G,i}^{K} + \Delta t(\dot{m}_{G,i-1}^{K+1} - \dot{m}_{G,i}^{K+1}). \quad (23)$$

6) The new gas density is calculated as

$$\rho_{G,i}^{K+1} = \frac{m_{G,i}^{K+1}}{\left(1 - H_{L,i}^{K+1}\right)A_i \Delta x}. \quad (24)$$

7) The new pressure is calculated using the ideal gas equation of state,

$$P_i^{K+1} = \rho_{G,i}^{K+1} RT. \quad (25)$$

8) Calculate wetted wall perimeters S_L, S_G, S_I using Eq. (9) - (14).

9) Calculate the friction factors f_L, f_G, f_I;

10) Calculate the coefficients $a_{L,i}^{K+1}$, $b_{L,i}^{K+1}$, $a_{G,i}^{K+1}$, $b_{G,i}^{K+1}$ using Eq. (17) – (20).

11) Given pressure drop, and the coefficients $a_{L,i}^{K+1}$, $b_{L,i}^{K+1}$, $a_{G,i}^{K+1}$, $b_{G,i}^{K+1}$, the new liquid and gas mass flow

rate at each section of the pipe are calculated using Eq. (15) – (16).

12) The new superficial velocities are calculated as

$$v_{SL,i}^{K+1} = \frac{\dot{m}_{L,i}^{K+1}}{\rho_{L,i}^{K+1} A_i} \ . \quad (26)$$

$$v_{SG,i}^{K+1} = \frac{\dot{m}_{G,i}^{K+1}}{\rho_{G,i}^{K+1} A_i}. \quad (27)$$

13) Compare the newly calculated liquid and gas flow rate with the $\dot{m}_{L,i}^{K+1}$ and $\dot{m}_{G,i}^{K+1}$ calculated from the last iteration, and check the convergence. If converged, change the 'new' variables into 'old' and go to step 3) for the calculation of next time step. If not, go to step 5) for another iteration within the current time step. Convergence criteria are set as

$$\frac{\dot{m}_{L,i}^{K+1,new} - \dot{m}_{L,i}^{K+1}}{\dot{m}_{L,i}^{K+1}} < 1\%. \quad (28)$$

$$\frac{\dot{m}_{G,i}^{K+1,new} - \dot{m}_{G,i}^{K+1}}{\dot{m}_{G,i}^{K+1}} < 1\%. \quad (29)$$

3. Model Validation

The experimental results from Vigneron *et al.* (1995) are used to validate the model simulation. Vigneron *et al.* used air and kerosene as working fluids. The fluid properties are given as

$$\rho_L = 1006.61 - 0.67167 \times T. \quad (30)$$

$$\mu_L = 0.881377 \times 10^{-4} \times \rho_L \times \exp(-0.01277766 \times T) \ . \quad (31)$$

$$\rho_G = \frac{P}{287.0 \times T}. \quad (32)$$

$$\mu_G = 0.867886 \times 10^{-5} \times \exp(0.002513 \times T) + 2.9893 \times 10^{-12} \times P. \quad (33)$$

The test facility is a horizontal steel pipe 420 m in length and 77.9 mm in diameter. Two 2.4 m long test sections, made of transparent PVC pipe, were installed along the loop at distances 61.6 m and 396 m, respectively, from the mixing tee. Experiments were carried out within a wide range of operating conditions, and the flow patterns include stratified flow and slug flow. Transient flows caused by changes in liquid and gas flow rates, liquid blow out and startup were tested. A summary of these tests is given in Table 1. Comparisons of these experimental data with simulation results are presented.

Liquid Flow Rate Change

Test 1C

For this test, the inlet gas flow rate was kept at 4055 Sm^3/d. The inlet liquid flow rate was at 8.4 m^3/d initially, and it was raised to 32 m^3/d at time 180 seconds. Separator pressure was 1.76 bar.

Comparison of experimental measurement and simulation results is presented in Fig. 2. Figure 2(a) shows the variation of liquid holdup with time at the two test sections from experimental measurements, and simulation results from both the current model and OLGA. The liquid holdup predictions for both initial and final states are higher than experimental measurements. From the experiments, the liquid holdup is raised from 0.03 to 0.1, while from the current model simulation, the liquid holdup is raised from 0.06 to 0.16, as a result, the propagation of liquid front is slower in the model prediction.

Figure 2(b) shows the variation of pressure with time at the first test section from experimental measurements, and simulation results from both the current model and OLGA. The predicted pressure drop is much lower than the experimental measurement, which again is related to the holdup prediction. Since the holdup is predicted to be larger than experimental measurements, with the same superficial liquid velocity, the on-site liquid velocity is predicted lower, thus gives lower friction loss, and lower pressure drop.

Test 1G

For test 1-G, the inlet gas flow rate was kept at 2745 Sm^3/d. The inlet liquid flow rate was at 32.9 m^3/d initially, and it was decreased to 8.5 m^3/d at time 120 seconds. Separator pressure was 1.67 bar.

Comparison of experimental measurement and simulation results is presented in Fig. 3. Figure 3(a) shows the variation of liquid holdup with time at the two test sections from experimental measurements, and simulation results from both the current model and OLGA. Figure 3(b) shows the variation of pressure with time at the first test section from experimental measurements, and simulation results from both the current model and OLGA.

Liquid Blow Out

Test 3A

The initial condition is a steady state flow with average inlet flow rates of 4825 Sm^3/d for gas and 48.8 m^3/d for liquid. At 120 seconds, the liquid supply is stopped, while gas supply is unchanged. Separator pressure was 1.69 bar.

Comparison of experimental measurement and simulation results is presented in Fig. 4. Figure 4(a) shows the variation of liquid holdup with time at the two test sections from experimental measurements, and simulation results from both the current model and OLGA. Figure 4(b) shows the variation of pressure with time at the first test section from experimental measurements, and simulation results from both the current model and OLGA.

The current model gives a good prediction for both liquid holdup and pressure.

4. Discussion

Two-fluid model is developed for stratified flow. For cases with liquid flow rate change, the model can predict the trend very well. Further improvement on the gas-liquid interfacial friction factor could be able to improve the quantitative agreements.

For tests with gas flow rate change, the current model has not given a converged result yet.

Attempt 2: Drift Flux Model

Develop a simplified transient simulator with drift flux model, ignoring flow pattern and flow pattern transition.

1. Method

Use unsteady mass conservation equations for both gas and liquid. Gas liquid mixture momentum equation is used and considered to be in local equilibrium. Drift flux model is used. Gas is compressible, while liquid is considered to be incompressible.

Gas liquid mixture momentum conservation equation is written as

$$(P_i - P_{i+1})A = \frac{1}{2} f_M \rho_M v_M^2 \pi D \Delta x + \rho_M g A \Delta x sin\theta. \quad (34)$$

Where, v_M is the mixture velocity ($v_M = v_{SL} + v_{SG}$). ρ_M is the mixture density ($\rho_M = H_L\rho_M + (1-H_L)\rho_G$). H_L is the liquid holdup.

Drift flux model is used to obtain the gas velocity,

$$v_G = Cv_M + v_d. \quad (35)$$

As a starting point, we choose C=1.0, and $v_d = 0.54\sqrt{gd}cos\theta + 0.35\sqrt{gd}sin\theta$ from Bendiksen (1984).

Substituting Eq. (35) into Eq. (34) yields a relationship between gas mass flow rate and pressure difference $P_i - P_{i+1}$. A linear relationship between gas mass flow rate and pressure difference can be obtained as

$$\dot{m}_{G,i}^{K+1} = a_i^{K+1}(P_i^{K+1} - P_{i+1}^{K+1}) + b_i^{K+1}. \quad (36)$$

Where

$$a_i^{K+1} = \frac{2A^2C^2\rho_g(1-H_L)}{f_M\rho_M\pi D\Delta x(V_G - V_d)}, \quad (37)$$

$$b_i^{K+1} = \frac{-2A^2C^2\rho_g(1-H_L)g\Delta x sin\theta}{f_M\pi D\Delta x(V_G - V_d)} + \rho_g A(1-H_L)v_d. \quad (38)$$

2. Solution Procedures

Figure 5 shows a flowchart for the drift flux model approach. Detailed descriptions of each step are given below.

1) Initialization: Define pipe geometry, fluid properties and initial conditions. The pipe is divided into N sections of length Δx. Initial condition at time t=0 includes: gas and liquid velocities, liquid holdup, and pressure for each section of the pipe.

2) Specify boundary conditions: Inlet gas and liquid flow rates and outlet pressure at each time step are given.

3) Liquid mass in each section of the pipe at the new time step K+1 is calculated by

$$m_{L,i}^{K+1} = m_{L,i}^{K} + \Delta t(\dot{m}_{L,i-1}^{K+1} - \dot{m}_{L,i}^{K+1}). \quad (39)$$

4) The new liquid holdup is calculated as

$$H_{L,i}^{K+1} = \frac{m_{L,i}^{K+1}}{\rho_L A_i \Delta x}. \quad (40)$$

5) Gas mass in each section of the pipe at the new time step K+1 is calculated by

$$m_{G,i}^{K+1} = m_{G,i}^{K} + \Delta t(\dot{m}_{G,i-1}^{K+1} - \dot{m}_{G,i}^{K+1}). \quad (41)$$

6) The new gas density is calculated as

$$\rho_{G,i}^{K+1} = \frac{m_{G,i}^{K+1}}{\left(1-H_{L,i}^{K+1}\right)A_i\Delta x}. \quad (42)$$

7) The new pressure is calculated using the ideal gas equation of state,

$$P_i^{K+1} = \rho_{G,i}^{K+1}RT. \quad (43)$$

8) Calculate the mixture properties ρ_M and μ_M, mixture Reynolds number Re_M, mixture friction factor f_M, and the coefficients a_i^{K+1}, b_i^{K+1}.

9) Given pressure drop, and the coefficients a_i^{K+1}, b_i^{K+1}, the new gas mass flowrate at each section of the pipe is calculated using Eq. (36).

10) The new superficial gas velocity is calculated as

$$v_{SG,i}^{K+1} = \frac{\dot{m}_{G,i}^{K+1}}{\rho_{G,i}^{K+1}A_i}. \quad (44)$$

11) The new superficial liquid velocity is calculated from Eq. (35),

$$v_{SL,i}^{K+1} = \frac{v_{SG,i}^{K+1}}{C(1-H_{L,i}^{K+1})} - \frac{v_d}{C} - v_{SG,i}^{K+1}. \quad (45)$$

12) The new liquid mass flow rate is calculated as

$$\dot{m}_{L,i}^{K+1} = v_{SL,i}^{K+1}\rho_L A_i. \quad (46)$$

13) Compare the newly calculated liquid and gas mass flow rates with $\dot{m}_{L,i}^{K+1}$ and $\dot{m}_{G,i}^{K+1}$ calculated from the last iteration, and check the convergence. If converged, change the 'new' variables into 'old' and go to step 3) for the calculation of next time step. If not, go to step 5) for another iteration within the current time step. Convergence criteria are set as

$$\frac{\dot{m}_{L,i}^{K+1,new} - \dot{m}_{L,i}^{K+1}}{\dot{m}_{L,i}^{K+1}} < 1\%, \quad (47)$$

$$\frac{\dot{m}_{G,i}^{K+1,new} - \dot{m}_{G,i}^{K+1}}{\dot{m}_{G,i}^{K+1}} < 1\%. \quad (48)$$

3. Model Validation

The experimental results from Vigneron *et al.* (1995) are used to validate the model simulation. Comparison of experimental data with simulation results is presented in this section.

Liquid Flow Rate Change

Test 1A

The inlet gas flow rate was kept at 815 Sm^3/d. Inlet liquid flow rate increased from 32.5 m^3/d to 168.4 m^3/d at 120 seconds. Separator pressure was kept at 1.67 bar. Both initial and final states are in slug flow pattern. Comparison of experimental measurement and simulation results is presented in Fig. 6. Figure 6(a) shows the variation of liquid holdup with time at the two test sections from experimental measurements, and simulation results from both the current model and OLGA. The liquid holdup predictions for both initial and final states are lower than experimental measurements. From the experiments, the liquid holdup is raised from 0.4 to 0.6, while from the current model simulation, the liquid holdup is raised from 0.34 to 0.46.

Figure 6(b) shows the variation of pressure with time at the first test section from experimental measurements, and simulation results from both the current model and OLGA. The current model prediction of pressure drop is much higher than the experimental measurement.

Test 1B

Inlet gas flow rate was kept at 400 Sm^3/d. Inlet liquid flow rate increased from 8.4 m^3/d to 31.8 m^3/d at 190 seconds. Separator pressure was kept at 1.67 bar. Both initial and final states are in slug flow regime. Comparison of experimental measurement and simulation results is presented in Fig. 7. Figure 7(a) shows the variation of liquid holdup with time at the two test sections from experimental measurements, and simulation results from both the current model and OLGA. Figure 7(b) shows the variation of pressure with time at the first test section from experimental measurements, and simulation results from both the current model and OLGA. The liquid holdup predictions for both initial and final states are higher than experimental measurements. Besides, this model is not able to predict the propagation of liquid wave front correctly. The prediction of pressure drop is much higher than the experimental measurement.

Test 1C

For case 1-C, the inlet gas flow rate was kept at 4055 Sm^3/d. The inlet liquid flow rate was at 8.4 m^3/d initially, and it was increased to 32 m^3/d at time 180 seconds. Separator pressure was at 1.76 bar. Both initial and final steady state flow conditions are in the stratified flow regime. After the increase in inlet liquid flow rate, pressure builds up gradually as the liquid front advances through the pipeline. The liquid holdup vs. time plot (Fig. 8(a)) clearly shows the propagation of liquid front. Comparison of experimental measurement and simulation results is presented in Fig. 8. Figure 8(a) shows the variation of liquid holdup with time at the two test sections from experimental measurements, and simulation results from both the current model and OLGA. The liquid holdup predictions for both initial and final states are higher than experimental measurements. The current model is not able to predict the propagation of liquid wave front correctly.

Figure 8(b) shows the variation of pressure with time at the first test section from experimental measurements, and simulation results from both the current model and OLGA. The prediction of pressure drop is much higher than the experimental measurements.

Test 1D

The inlet gas flow rate was kept at 880 Sm^3/d. Inlet liquid flow rate decreased from 340 m^3/d to 168 m^3/d at 120 seconds. Separator pressure was kept at 1.67 bar. Both initial and final states are in slug flow regime.

Comparison of experimental measurement and simulation results is presented in Fig. 9. Figure 9(a) shows the variation of liquid holdup with time at the two test sections from experimental measurements, and simulation results from both the current model and OLGA. The liquid holdup predictions for both initial and final states are slightly lower than experimental measurements. In the experiment, the liquid holdup at station 1 decreased from 0.6 to 0.45, while in the current model simulation, the liquid holdup at station 1 decreases from 0.57 to 0.45. The current model gives good prediction for the liquid wave front movement.

Figure 9(b) shows the variation of pressure with time at the first test section from experimental measurements, and simulation results from both the current model and OLGA. The prediction of pressure drop is higher than the experimental measurements.

Test 1E

The initial condition is a steady state flow with average inlet flow rates of 2590 Sm^3/d for gas phase and 28.1 m^3/d for liquid phase. Inlet liquid flow rate was increased to 294 m^3/d at 125 seconds. Separator pressure was kept at 1.67 bar during the entire process. Flow pattern was stratified wavy initially and then changed to slug flow.

Comparison of experimental measurement and simulation results is presented in Fig. 10. For holdup prediction, the current model agrees very well with OLGA predictions, however, both initial and final holdups are considerably lower than the measured holdups. The predicted initial and final pressures are higher than the measured values.

Test 1F

The inlet gas flow rate was kept at 7620 Sm^3/d. Inlet liquid flow rate decreased from 295 m^3/d to 172 m^3/d at 120 seconds. Separator pressure was kept at 1.74 bar. Both initial and final states were in slug flow regime.

Comparison of experimental measurement and simulation results is presented in Fig. 11. Figure 11(a) shows the variation of liquid holdup with time at the two test sections from experimental measurements, and simulation results from both the current model and OLGA. The liquid holdup predictions for both initial and final states are lower than experimental measurements. In the experiments, the liquid holdup at station 1 decreased from 0.3 to 0.25, while in the current model simulation, the liquid holdup at station 1 decreased from 0.2 to 0.15.

Figure 11(b) shows the variation of pressure with time at the first test section from experimental measurements, and simulation results from both the current model and OLGA. The prediction of pressure drop is much higher than the experimental measurement.

Test 1G

For case 1-G, the inlet gas flow rate was kept at 2745 Sm^3/d. The inlet liquid flow rate was at 32.9 m^3/d initially, and it was decreased to 8.5 m^3/d at time 120 seconds. Separator pressure was 1.67 bar.

Comparison of experimental measurement and simulation results is presented in Fig. 12. Figure 12(a) shows the variation of liquid holdup with time at the two test sections from experimental measurements, and simulation results from both the current model and OLGA. Figure 12(b) shows the variation of pressure with time at the first test section from experimental measurements, and simulation results from both the current model and OLGA.

Similar as test 1B and test 1C, here the drift flux model is not able to predict the holdup and pressure correctly.

Gas Flow Rate Change

Test 2A

The inlet liquid flow rate was kept at 8.0 m^3/d. Inlet gas flow rate increased from 850 Sm^3/d to 4520 Sm^3/d at 120 seconds. Separator pressure was kept at 1.67 bar. Both initial and final states were in stratified flow regime.

Comparison of experimental measurement and simulation results is presented in Fig. 13. Figure 13(a) shows the variation of liquid holdup with time at the two test sections from experimental measurements, and simulation results from both the current model and OLGA. The liquid holdup predictions for both initial and final states showed good agreements.

The experimental data reveals two different transient phenomena. Immediately after the gas flow rate increase, a compressibility wave moves along the pipe and creates waves throughout the pipe. Some of these waves may form slugs. After the intense slugging, additional time is required to reach the final steady state. The current model is able to predict the first transient phenomenon. However, it failed to predict the second transient phenomenon.

Figure 13(b) shows the variation of pressure with time at the first test section from experimental measurements, and simulation results from both the current model and OLGA. The prediction of pressure drop is higher than the experimental measurement.

Test 2B

The inlet liquid flow rate was kept at 20.2 m^3/d. Inlet gas flow rate increased from 340 Sm^3/d to 2530 Sm^3/d at 130 seconds. Separator pressure was kept at 1.67 bar. Both initial and final states were in stratified flow regime.

Comparison of experimental measurement and simulation results is presented in Fig. 14. Figure 14(a) shows the variation of liquid holdup with time at the two test sections from experimental measurements, and simulation results from both the current model and OLGA. The liquid holdup predictions for both initial and final states showed good agreements.

Similar as in Test 2A, there are two transient phenomena, but the current model is able to predict only the first one.

Figure 14(b) shows the variation of pressure with time at the first test section from experimental measurements, and simulation results from both the current model and OLGA. The prediction of pressure drop is slightly higher than the experimental measurement.

Test 2C

The inlet liquid flow rate was kept at 203 m^3/d. Inlet gas flow rate increased from 870 Sm^3/d to 3690 Sm^3/d at 120 seconds. Separator pressure was kept at 1.76 bar. Both initial and final states were in slug flow regime.

Comparison of experimental measurement and simulation results is presented in Fig. 15. Figure 15(a) shows the variation of liquid holdup with time at the two test sections from experimental measurements, and simulation results from both the current model and OLGA. The current model agrees very well with OLGA predictions.

Figure 15(b) shows the variation of pressure with time at the first test section from experimental measurements, and simulation results from both the current model and OLGA. The prediction of pressure drop is slightly higher than the experimental measurement.

Test 2D

The inlet liquid flow rate was kept at 195 m^3/d. Inlet gas flow rate increased from 1875 Sm^3/d to 10840 Sm^3/d at 125 seconds. Separator pressure was kept at 1.67 bar. Both initial and final states were in slug flow regime.

Comparison of experimental measurement and simulation results is presented in Fig. 16. Figure 16(a) shows the variation of liquid holdup with time

at the two test sections from experimental measurements, and simulation results from both the current model and OLGA. The liquid holdup predictions for both initial and final states are lower than experimental measurements. In the experiments, the liquid holdup at station 1 decreased from 0.4 to 0.2, while in the current model simulation, the liquid holdup at station 1 decreased from 0.32 to 0.13.

Figure 16(b) shows the variation of pressure with time at the first test section from experimental measurements, and simulation results from both the current model and OLGA. The prediction of pressure drop agrees very well with the experimental measurement.

Test 2E

The inlet liquid flow rate was kept at 323 m^3/d. Inlet gas flow rate increased from 815 Sm^3/d to 5000 Sm^3/d at 65 seconds. Separator pressure was kept at 1.67 bar. Both initial and final states were in stratified flow regime.

Comparison of experimental measurement and simulation results is presented in Fig. 17. Figure 17(a) shows the variation of liquid holdup with time at the two test sections from experimental measurements, and simulation results from both the current model and OLGA. Figure 17(b) shows the variation of pressure with time at the first test section from experimental measurements, and simulation results from both the current model and OLGA. Current model gives very good predictions for both holdups and pressure profiles.

Liquid Blow Out

Test 3A

The initial condition was a steady state flow with average inlet flow rates of 4825 Sm^3/d for gas and 48.8 m^3/d for liquid. At 120 seconds, the liquid supply was stopped, while gas supply was unchanged. Separator pressure was kept at 1.69 bar.

Comparison of experimental measurement and simulation results is presented in Fig. 18. Figure 18(a) shows the variation of liquid holdup with time at the two test sections from experimental measurements, and simulation results from both the current model and OLGA. Figure 18(b) shows the variation of pressure with time at the first test section from experimental measurements, and simulation results from both the current model and OLGA. The current model is not able to predict both holdup and pressure profile well for this case.

Test 3B

The initial condition was a steady state flow with average inlet flow rates of 5880 Sm^3/d for gas and 204 m^3/d for liquid. At 95 seconds, the liquid supply was stopped, while gas supply was unchanged. Separator pressure was kept at 1.69 bar.

Comparison of experimental measurement and simulation results is presented in Fig. 19. Figure 19 (a) shows the variation of liquid holdup with time at the two test sections from experimental measurements, and simulation results from both the current model and OLGA. Figure 19(b) shows the variation of pressure with time at the first test section from experimental measurements, and simulation results from both the current model and OLGA.

Startup

Test 4B0

The pipeline was initially empty. Gas and liquid mixture was fed into the pipe at time 122 seconds. The final condition was a steady state flow with average inlet flow rates of 1870 Sm^3/d for gas and 322 m^3/d for liquid. Separator pressure was kept at 1.66 bar.

Comparison of experimental measurement and simulation results is presented in Fig. 20. Figure 20(a) shows the variation of liquid holdup with time at the two test sections from experimental measurements, and simulation results from both the current model and OLGA. Figure 20(b) shows the variation of pressure with time at the first test section from experimental measurements, and simulation results from both the current model and OLGA.

4. Discussion

A drift flux model is developed to simulate the transient two-phase flow behavior in pipelines. The model is based on drift velocity correlation and is flow pattern independent. The result for slug flow shows good agreement with experimental data as well as OLGA simulations.

When this model is applied to stratified flow, it gives good results only for cases with gas flow rate changes. For transient behavior caused by liquid flow rate change, the current model is not able to

simulate it correctly. It seems necessary to modify the drift flux model for stratified flow.

Attempt 3: Power Law Correlation

Develop a simplified transient simulator using power law correlation, ignoring flow pattern and flow pattern transition.

1. Method

Al-Sarkhi and Sarica (2009) developed a closure relationship between pressure gradient and flow rate for stratified gas-liquid two-phase flow in horizontal pipes. Their model performance was tested against more than 1200 published experimental data points and the result showed a good agreement even for flow regimes other than separated flow, and for slightly inclined pipes.

From Al-Sarkhi and Sarica work, the optimized curve which fits the experimental data is expressed as,

$$P^* = 0.075X^{*-1.808} \quad . \tag{49}$$

where

$$P^* = \frac{D(-dP/dx)}{{}^1/_2\rho_L v_{SL}^2} \quad . \tag{50}$$

$$X^* = \frac{\dot{m}_L}{\dot{m}_G}\sqrt{\frac{\rho_G}{\rho_L}} \quad . \tag{51}$$

Substituting Eq. (50) and (51) into Eq. (49), and discretize it in space and time gives a relationship between $\dot{m}_G$ and pressure difference as,

$$\dot{m}_{G,i}^{K+1} = \left(\frac{0.075}{2}\frac{\Delta x}{DA^2(P_i^{K+1}-P_{i+1}^{K+1})}\frac{(\dot{m}_{L,i}^{K+1})^{0.192}(\rho_{G,i}^{K+1})^{-0.904}}{\rho_L^{0.096}}\right)^{-\frac{1}{1.808}} . \tag{52}$$

Eq. (35) could be used as a closure relationship to make the problem solvable. However, the coefficients C and v_d may need to be adjusted so that it is compatible with the power law correlation.

2. Solution Procedure

The solution procedure is the same as in Attempt 2, except in Step 9, Eq. (52) is used to calculate the new gas mass flow rate.

3. Discussion

Converged result for this approach has not been reached yet. Probably, it is because the current drift flux model is not compatible with the power law correlation.

Further Work

- Modify the drift flux model for stratified flow;
- Need to incorporate the model with a PVT package;
- Heat Transfer;
- Consider terrain/severe slugging;
- Compare with more experimental data for validation purpose.

Nomenclature

A	=	cross sectional area [m^2]
d	=	diameter [m]
f	=	friction factor
H	=	holdup
m	=	mass [kg]
$\dot{m}$	=	mass flowrate [kg/s]
P	=	pressure [Pa]
S	=	perimeter over which shear stress acts
v	=	velocity [m/s]
T	=	temperature [Kelvin]

Subscripts

L	=	liquid phase

G	=	gas phase
I	=	interface
M	=	mixture
i	=	the ith section of the pipe

Greek Letters

τ	=	shear stress [Pa]
ρ	=	density [kg/m]
θ	=	inclination angle
Θ	=	wetted wall fraction
σ	=	surface tension [N/m]
μ	=	dynamic viscosity [kg/m·s)

References

1. Bendiksen, K.: "An experimental investigation of the motion of long bubbles in inclined tubes," *Int. J. Multiphase Flow* 10, 467-483 (1984).
2. Zhang, H.Q., Wang, Q., Sarica, C., and Brill, J.P.: "Unified model for gas-liquid pipe flow via slug dynamics – part 1: Model development," ASME *J. Energy Res. Tech.* 125, 266-273 (2003).
3. Vigneron, F., Sarica, C., and Brill, J.P.: "Experimental analysis of imposed two-phase flow transients in horizontal pipelines," Proceedings of the BHR Group 7th international conference, 199-217 (1995).

Table 1: Summary of Vigneron *et al.* (1995) Experiments

TEST #	INITIAL(I) FINAL(F)	FLOW RATE LIQUID(m^3/d)	FLOW RATE GAS(Sm^3/d)	FLOW PATTERN	P_{sep} (Bar)
LIQUID FLOW RATE CHANGE					
1-A	I	32.5	815	Slug	1.67
	F	168.4	815	Slug	
1-B	I	8.4	400	Stratified Smooth	1.67
	F	31.8	400	Stratified Wavy	
1-C	I	8.4	4055	Stratified Wavy	1.76
	F	32.0	4055	Stratified Wavy	
1-D	I	340	880	Slug	1.67
	F	168	880	Slug	
1-E	I	28.1	2590	Stratified Wavy	1.67
	F	294	2590	Slug	
1-F	I	295	7620	Slug	1.74
	F	172	7620	Slug	
1-G	I	32.9	2745	Stratified Wavy	1.67
	F	8.5	2745	Stratified Smooth	
GAS FLOW RATE CHANGE					
2-A	I	8.0	850	Stratified Smooth	1.67
	F	8.0	4520	Stratified Wavy	
2-B	I	20.2	340	Stratified Smooth	1.67
	F	20.2	2530	Stratified Wavy	
2-C	I	203	870	Slug	1.76
	F	203	3690	Slug	
2-D	I	195	1875	Slug	1.67
	F	195	10840	Slug	
2-E	I	323	815	Slug	1.67
	F	323	5000	Slug	
LIQUID BLOW OUT					
3-A	I	48.8	4825	Stratified Wavy	1.69
	F	0.0	4825	Single Phase Gas	
3-B	I	204.0	5880	Slug	1.69
	F	0.0	5880	Single Phase Gas	
STARTUP					
4-A0	I	H_L=0.0			1.68
	F	22.0	2650	Stratified Wavy	
4-A1	I	H_L=1.0			1.68
	F	21.8	2615	Stratified Wavy	
4-B0	I	H_L=0.0			1.66
	F	322.0	1870	Slug	
4-B1	I	H_L=1.0			1.66
	F	322.5	1910	Slug	

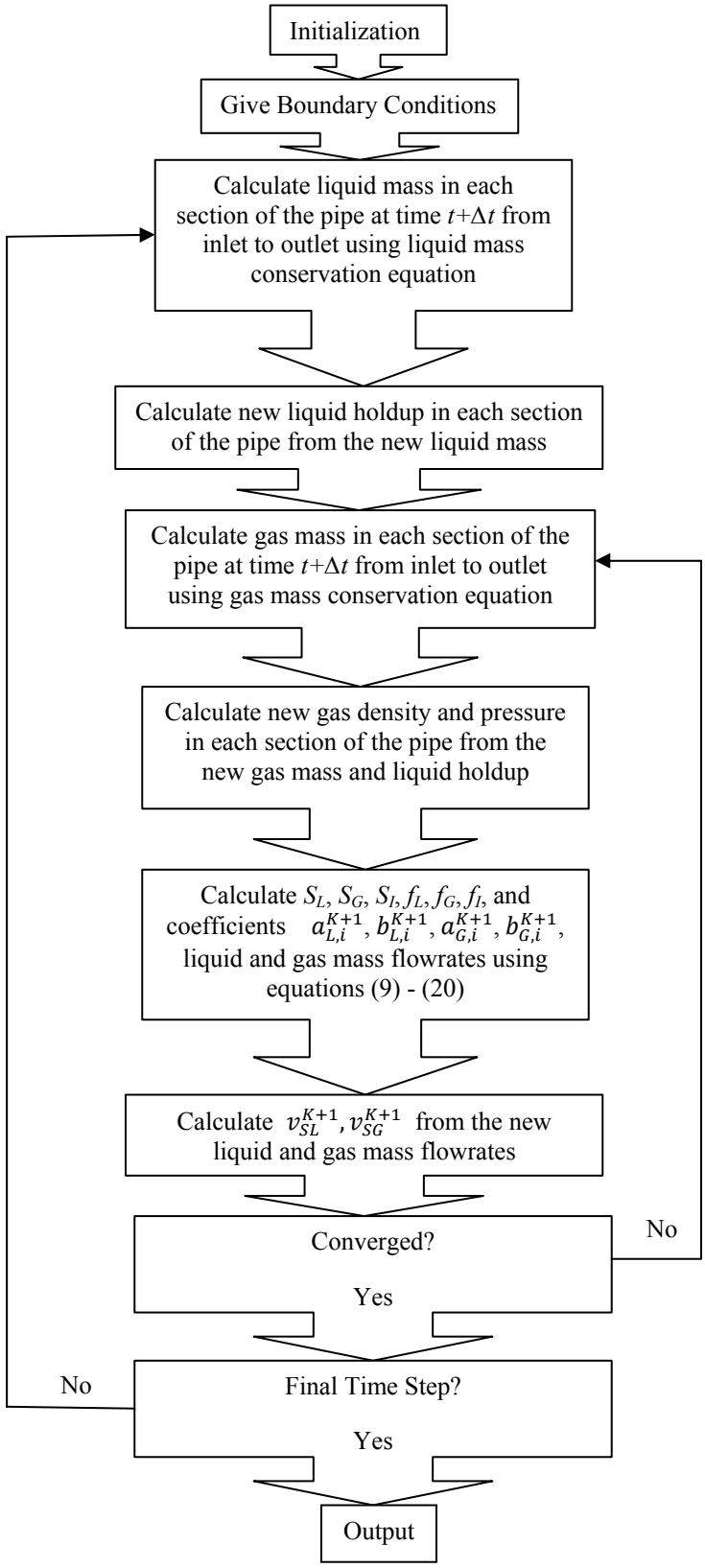

Fig. 1: Flow Chart for Two Fluid Model

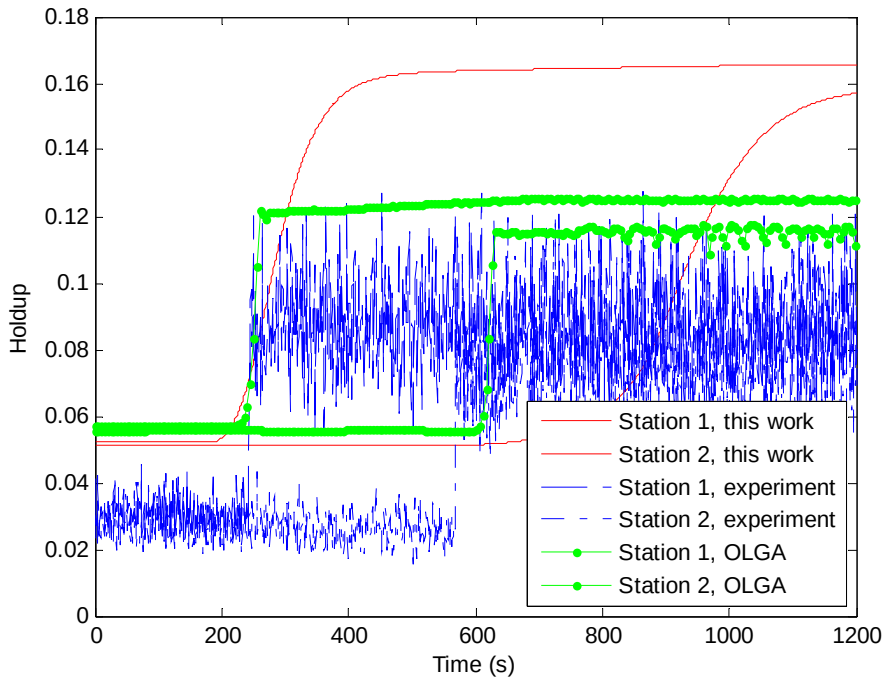

(a) Variation of liquid holdup with time at the two test sections

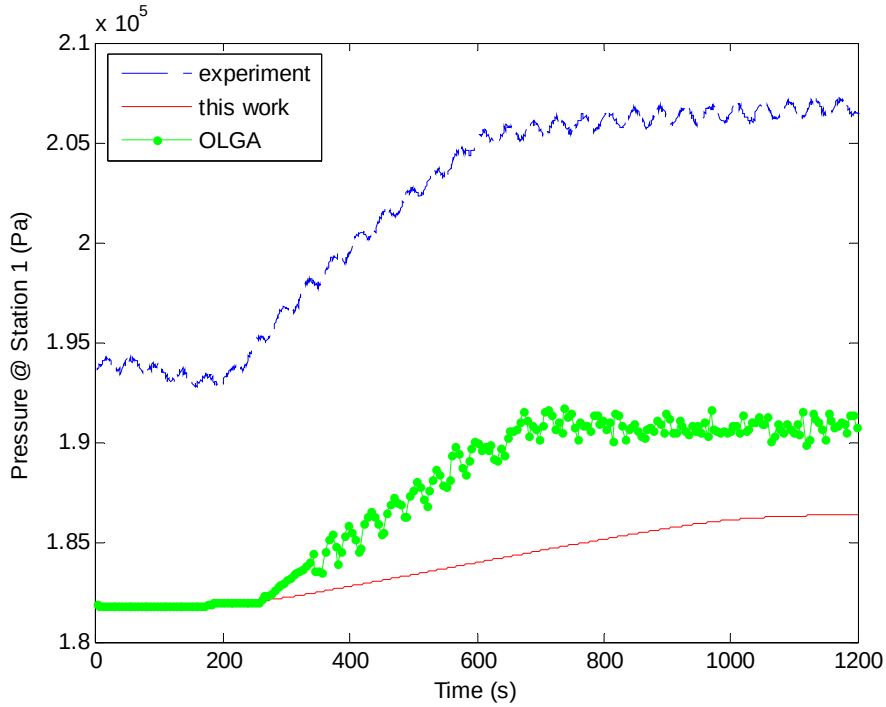

(b) Variation of pressure with time at the first test section

Fig. 2: Results for Test 1-C with two-fluid model

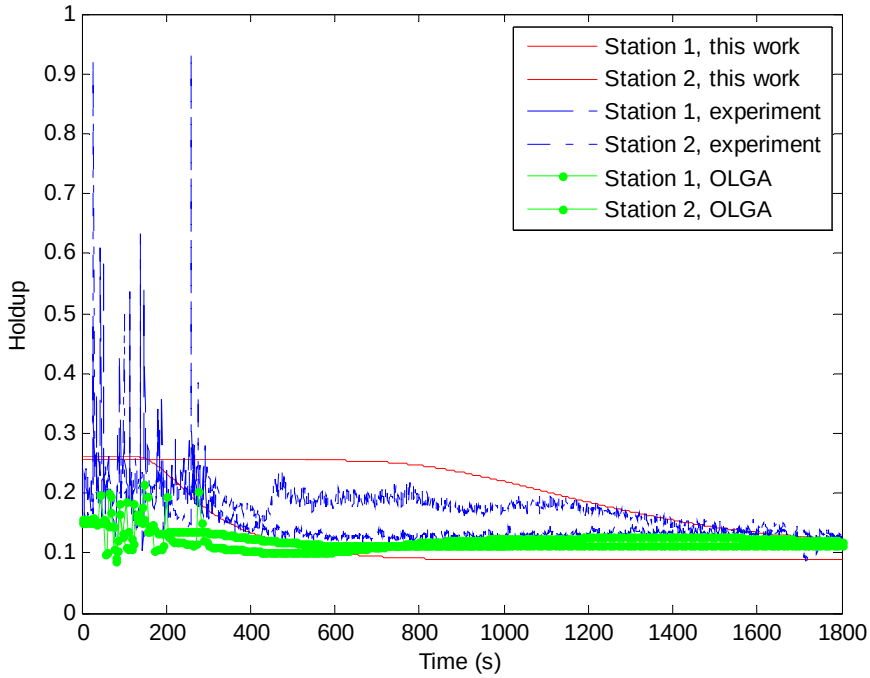

(a) Variation of liquid holdup with time at the two test sections

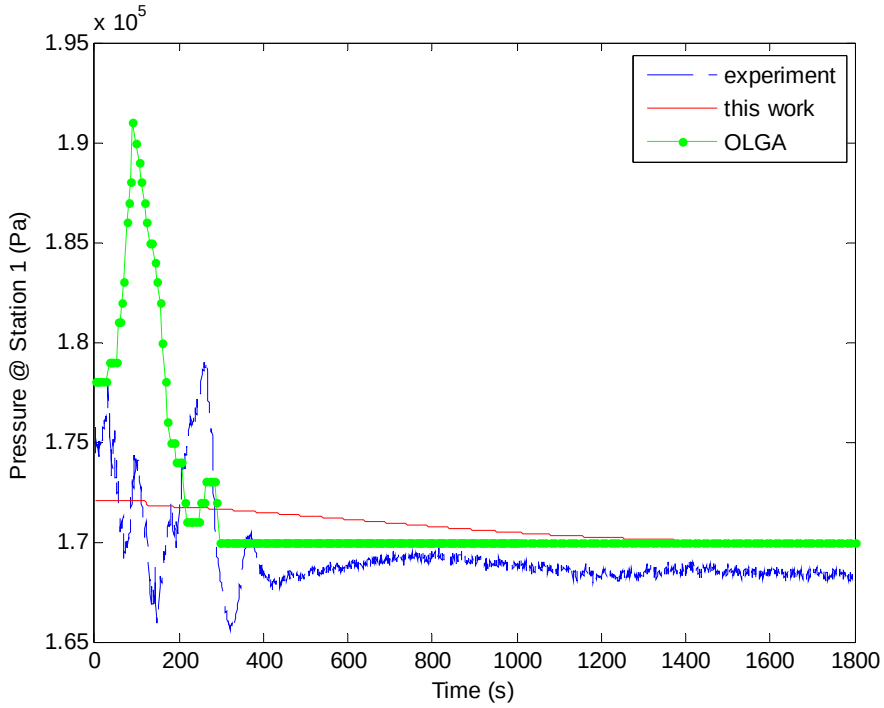

(b) Variation of pressure with time at the first test section

Fig. 3: Results for Test 1-G with two-fluid model

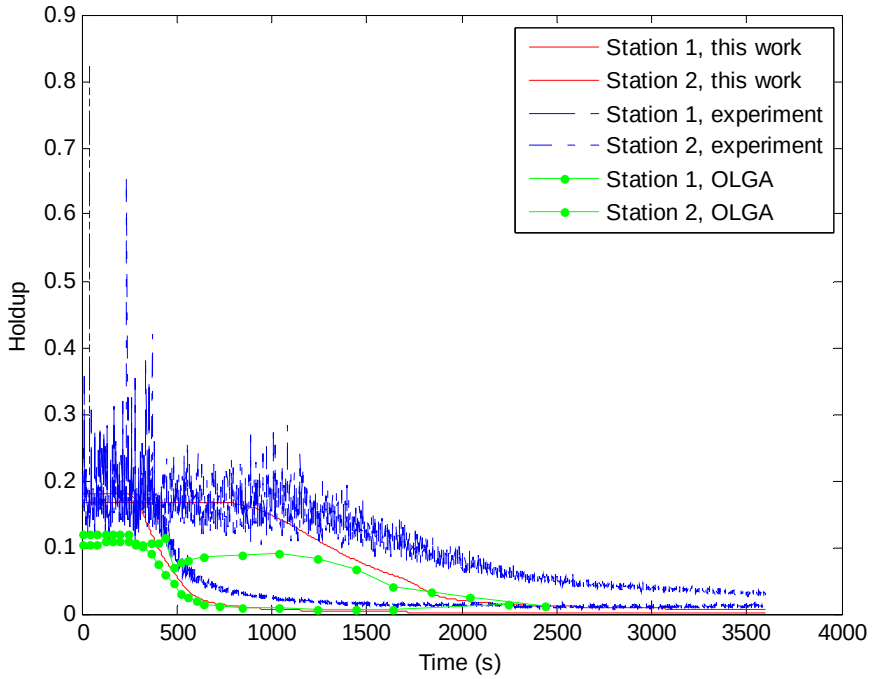

(a) Variation of liquid holdup with time at the two test sections

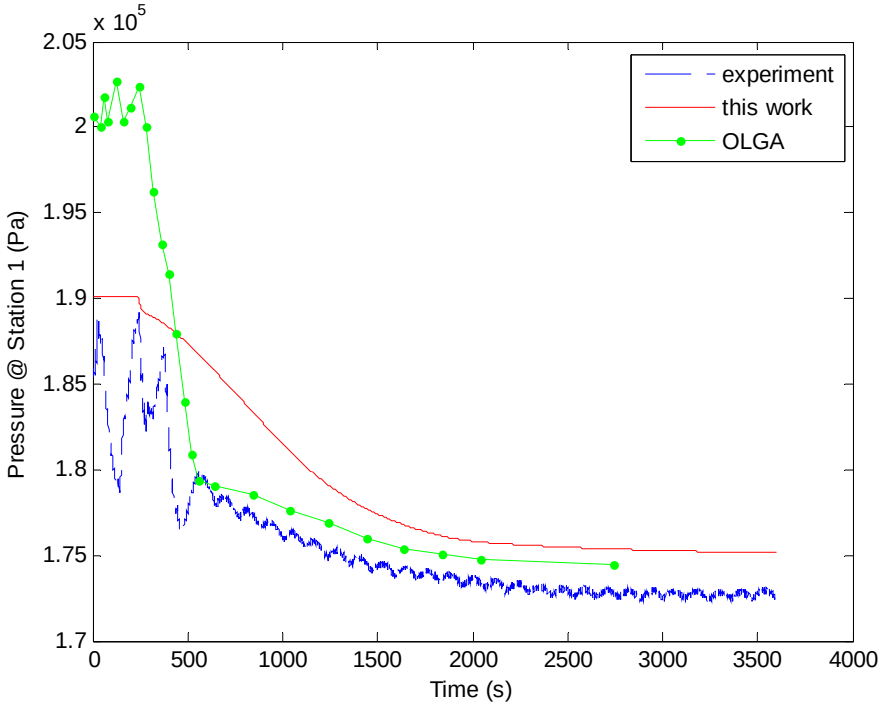

(b) Variation of pressure with time at the first test section

Fig. 4: Results for Test 3-A with two-fluid model

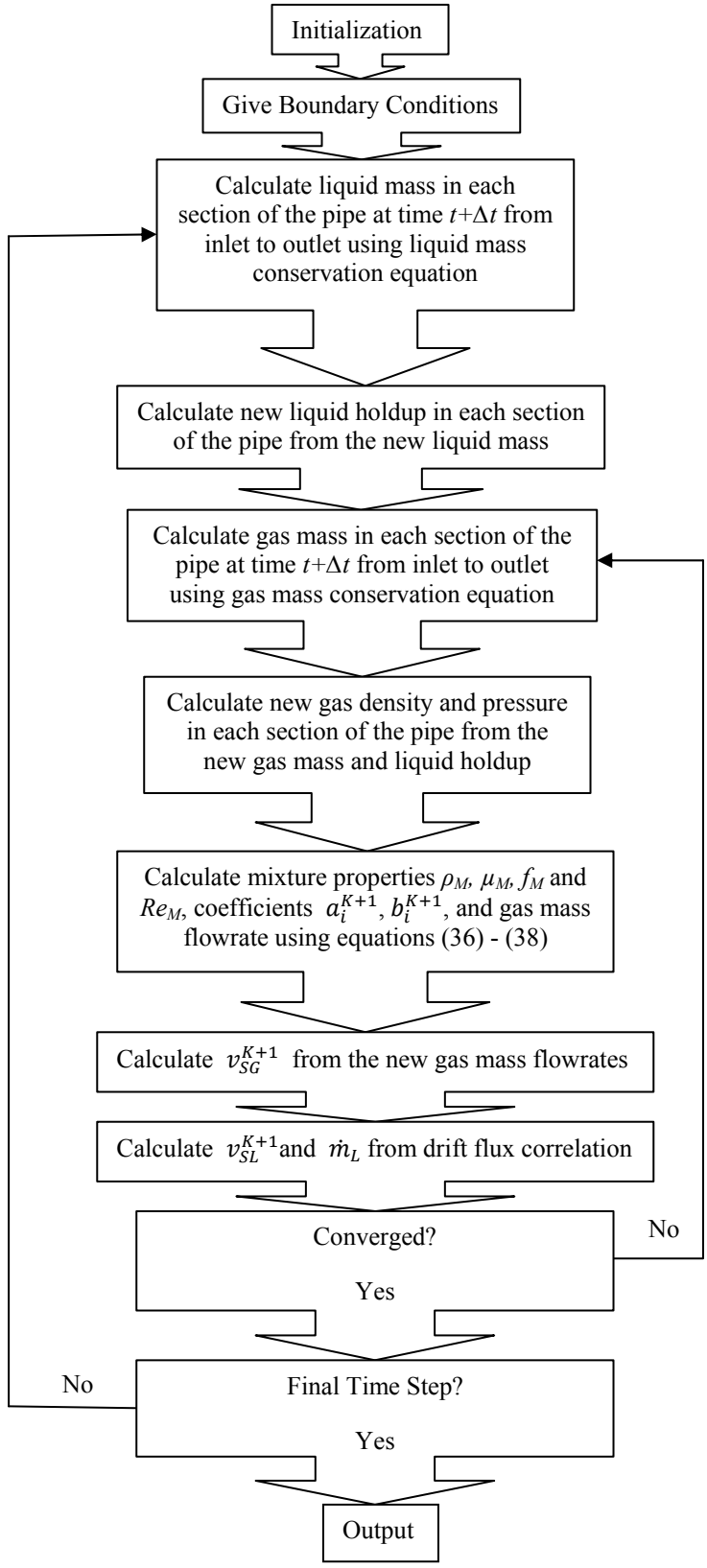

Fig. 5: Flow Chart for Drift Flux Model

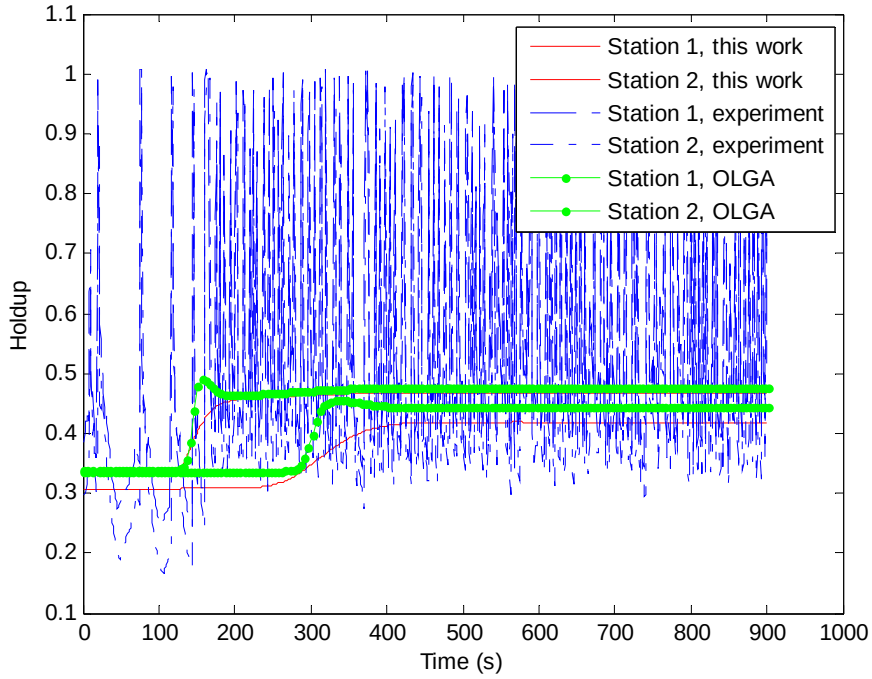

(a) Variation of liquid holdup with time at the two test sections

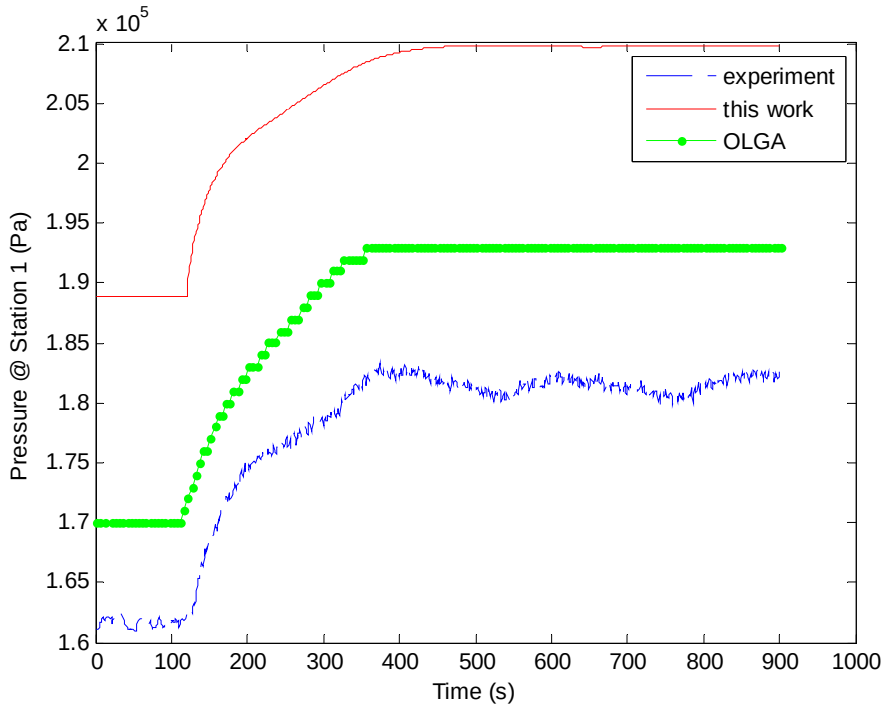

(b) Variation of pressure with time at the first test section

Fig. 6: Results for Test 1-A with drift flux model

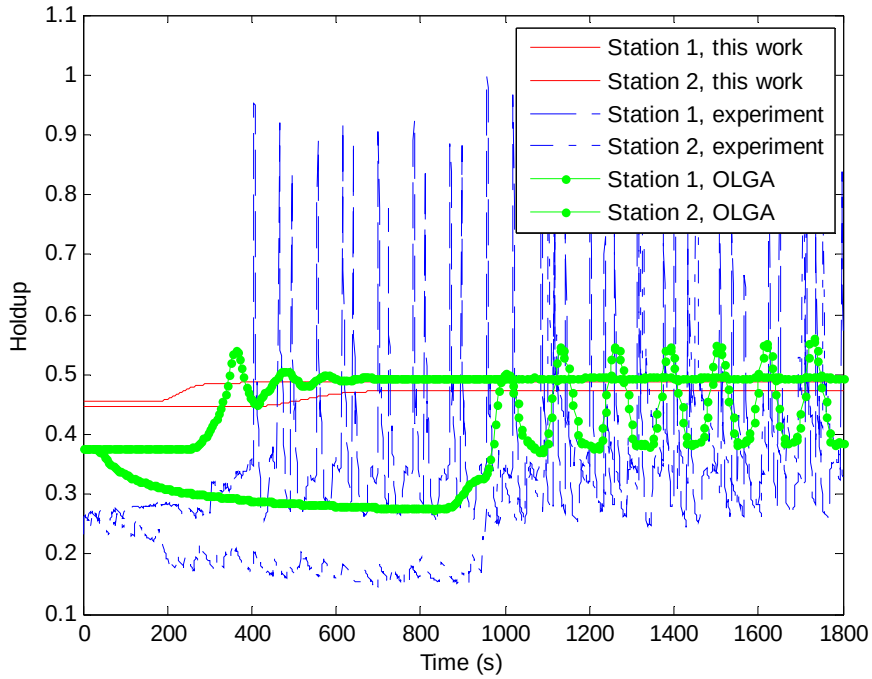

(a) Variation of liquid holdup with time at the two test sections

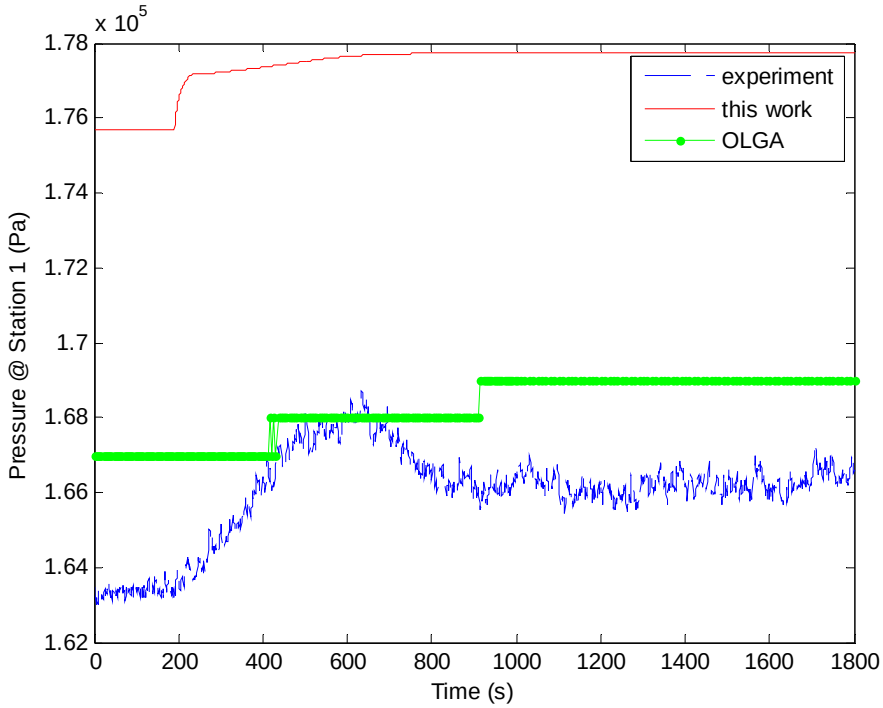

(b) Variation of pressure with time at the first test section

Fig. 7: Results for Test 1-B with drift flux model

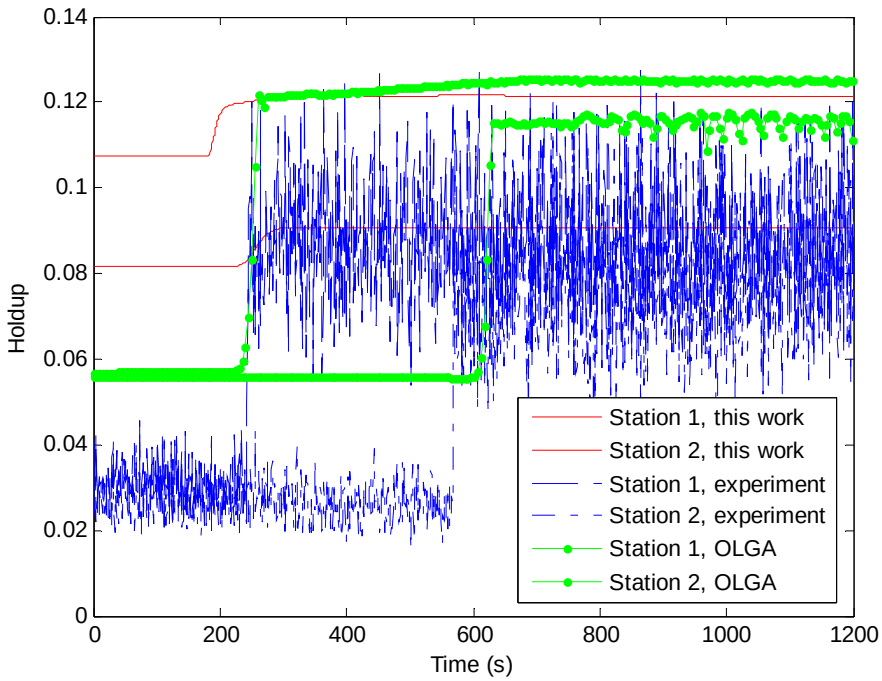

(a) Variation of liquid holdup with time at the two test sections

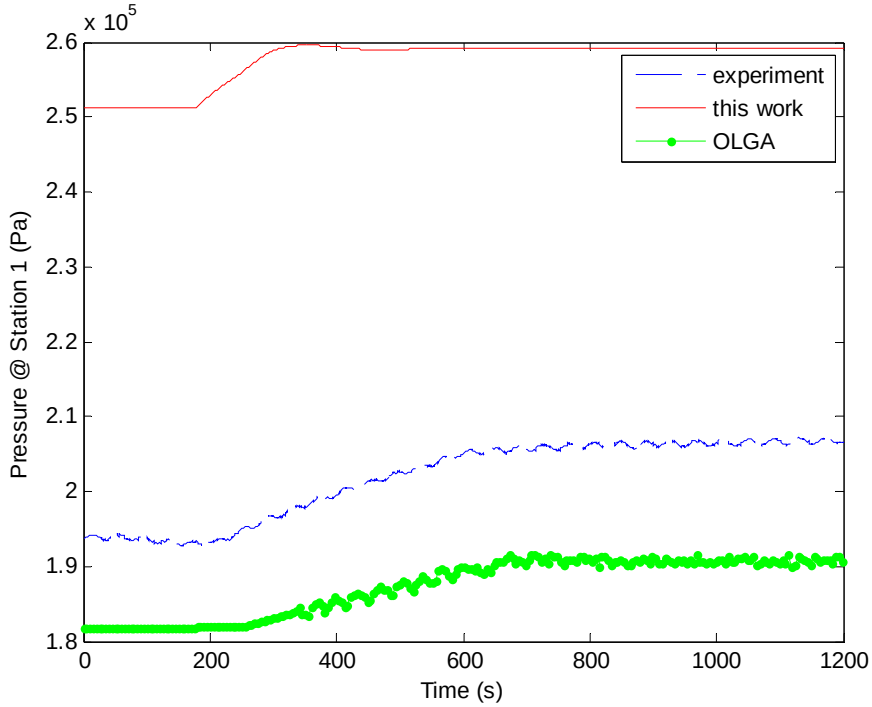

(b) Variation of pressure with time at the first test section

Fig. 8: Results for Test 1-C with drift flux model

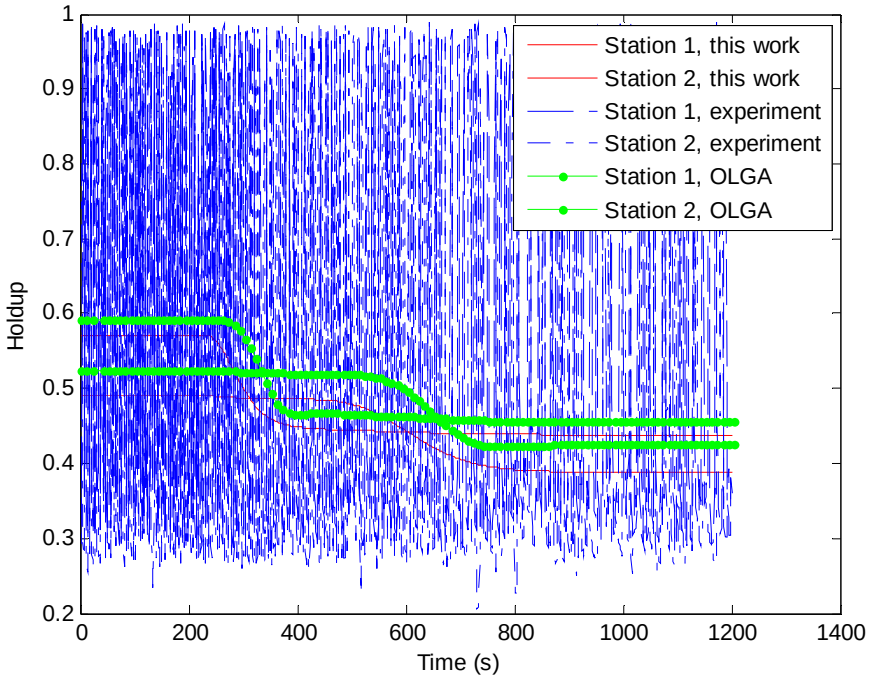

(a) Variation of liquid holdup with time at the two test sections

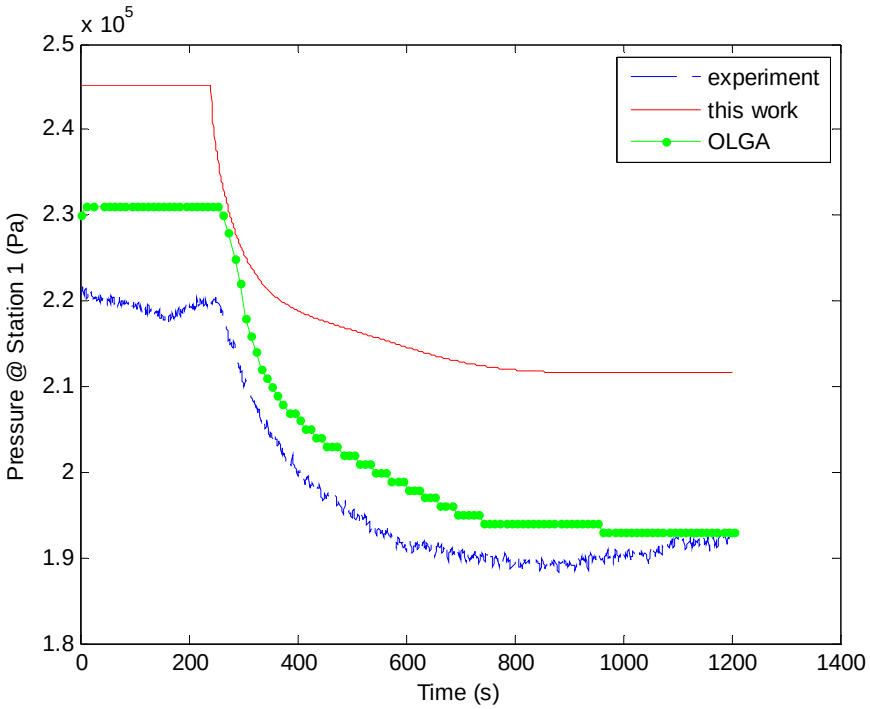

(b) Variation of pressure with time at the first test section

Fig. 9: Results for Test 1-D with drift flux model

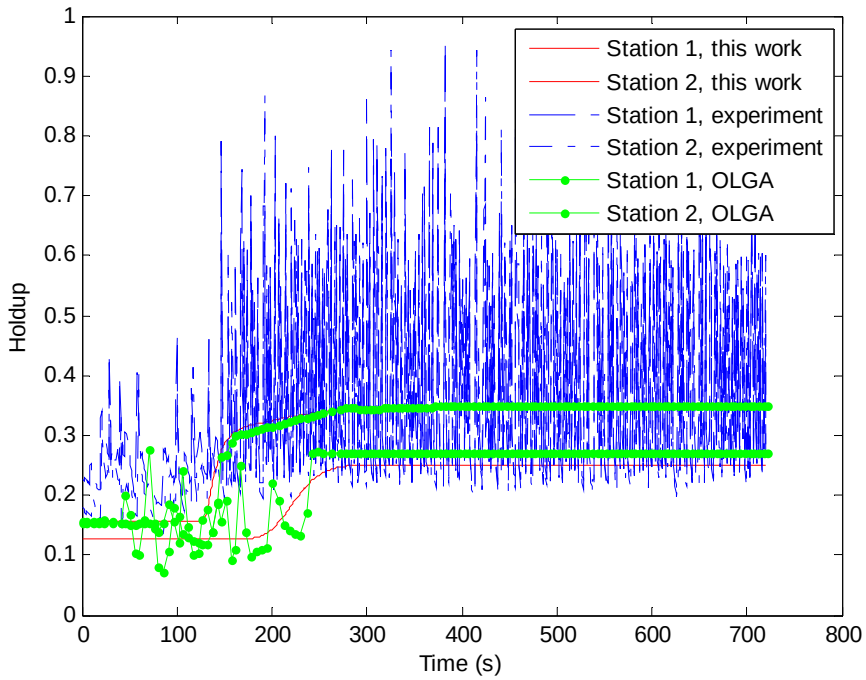

(a) Variation of liquid holdup with time at the two test sections

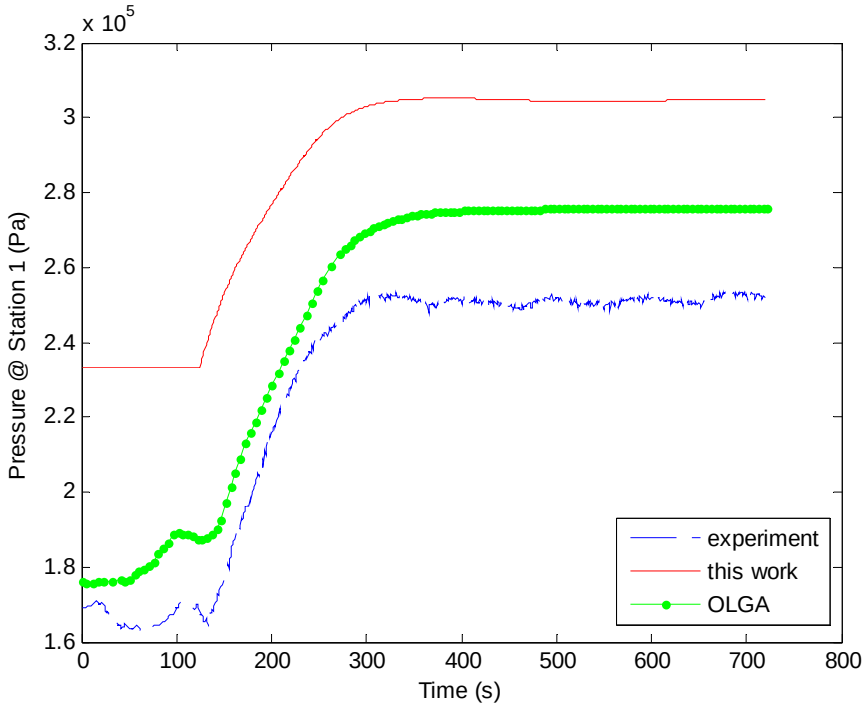

(b) Variation of pressure with time at the first test section

Fig. 10: Results for Test 1-E with drift flux model

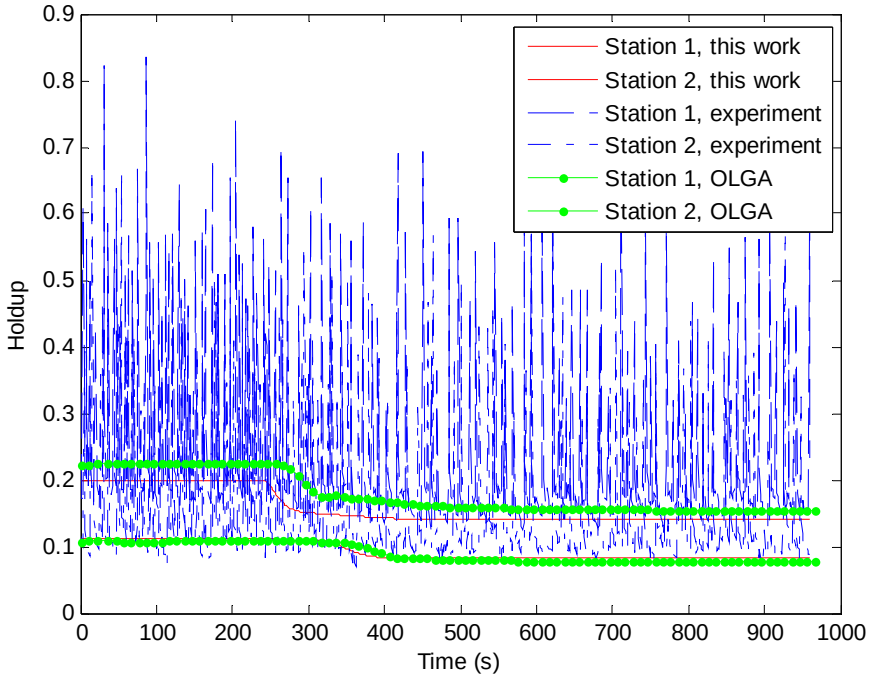

(a) Variation of liquid holdup with time at the two test sections

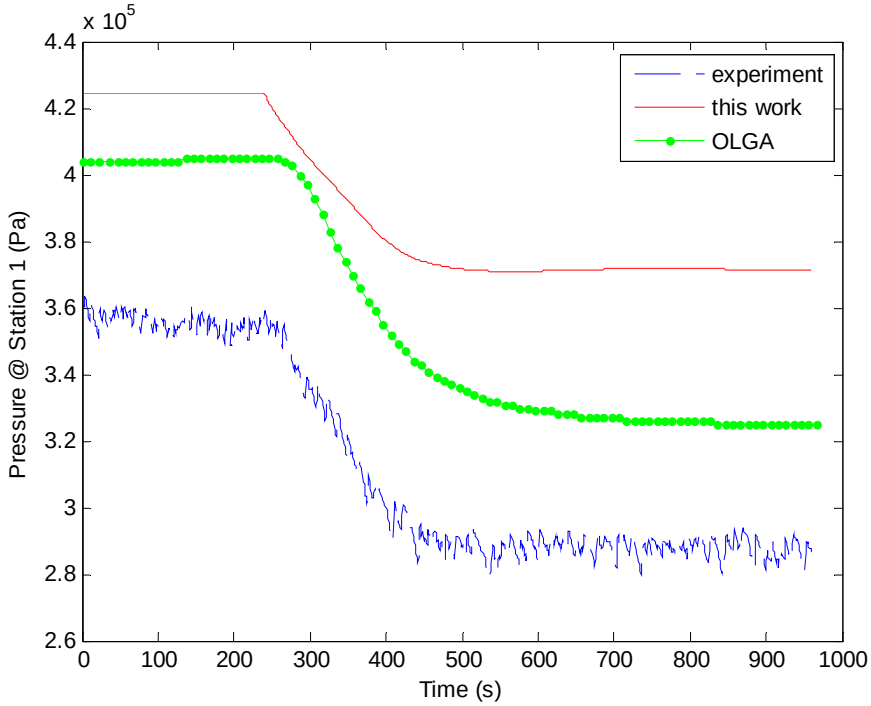

(b) Variation of pressure with time at the first test section

Fig. 11: Results for Test 1-F with drift flux model

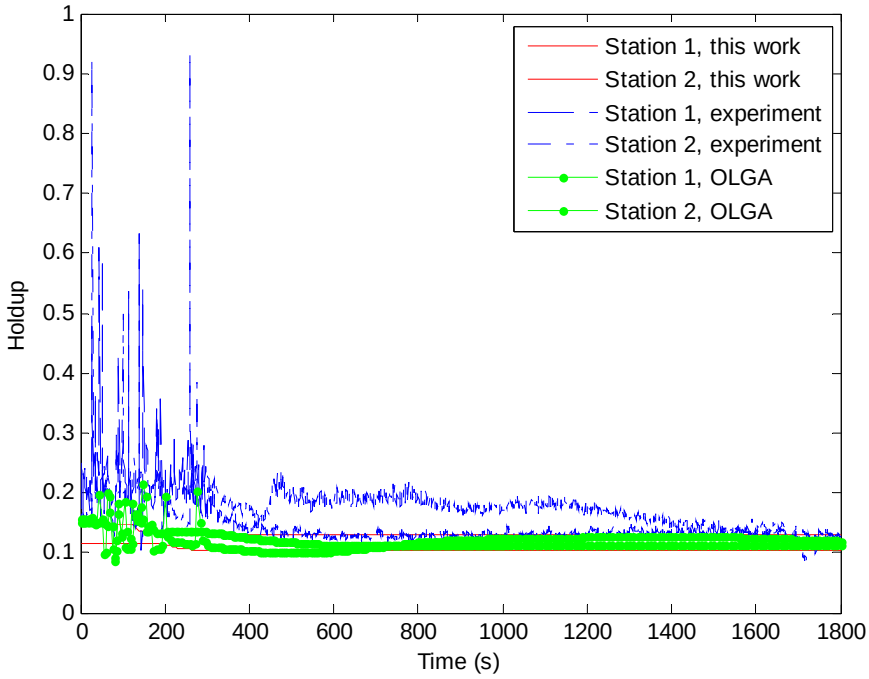

(a) Variation of liquid holdup with time at the two test sections

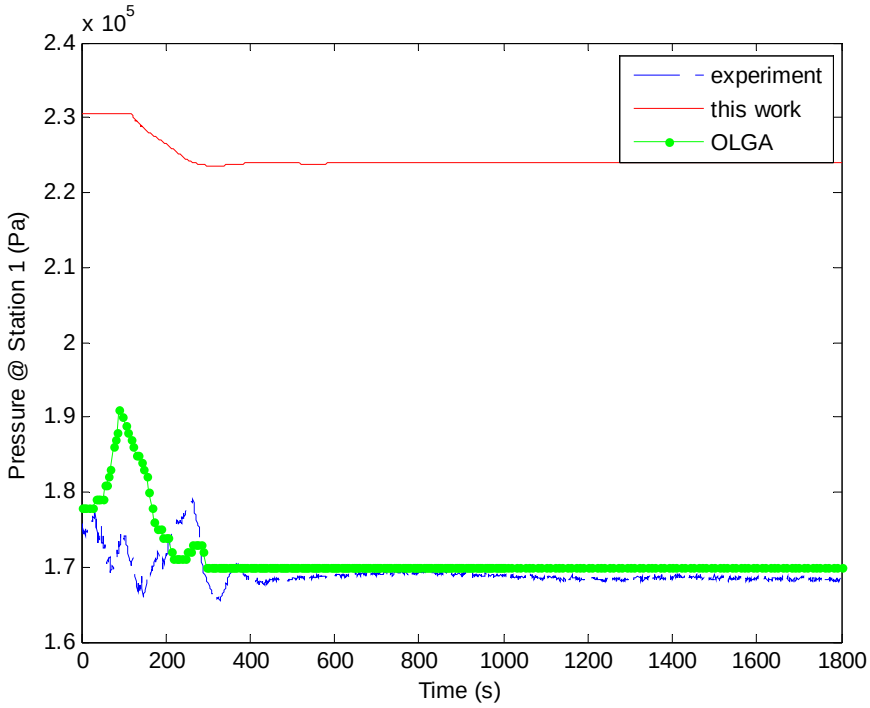

(b) Variation of pressure with time at the first test section

Fig. 12: Results for Test 1-G with drift flux model

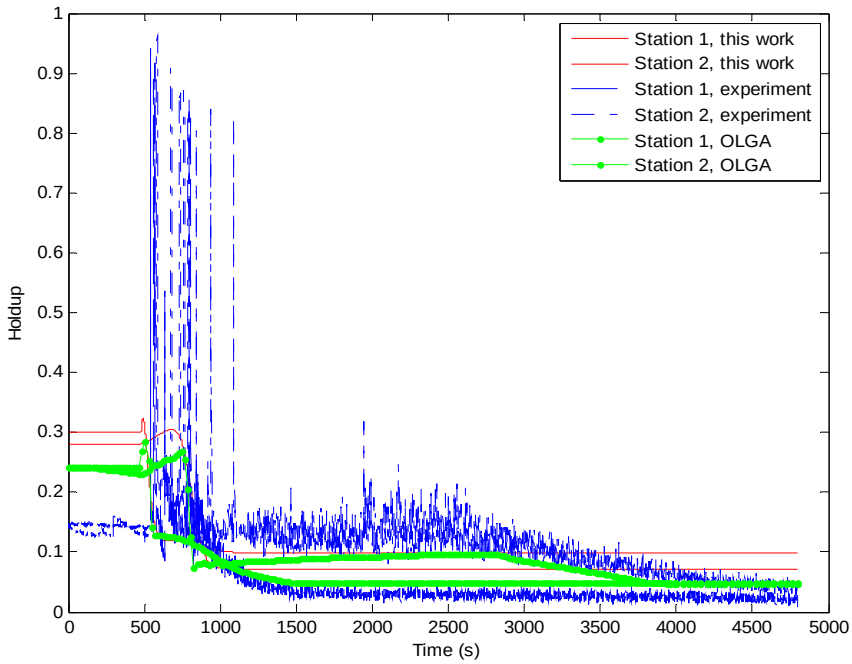

(a) Variation of liquid holdup with time at the two test sections

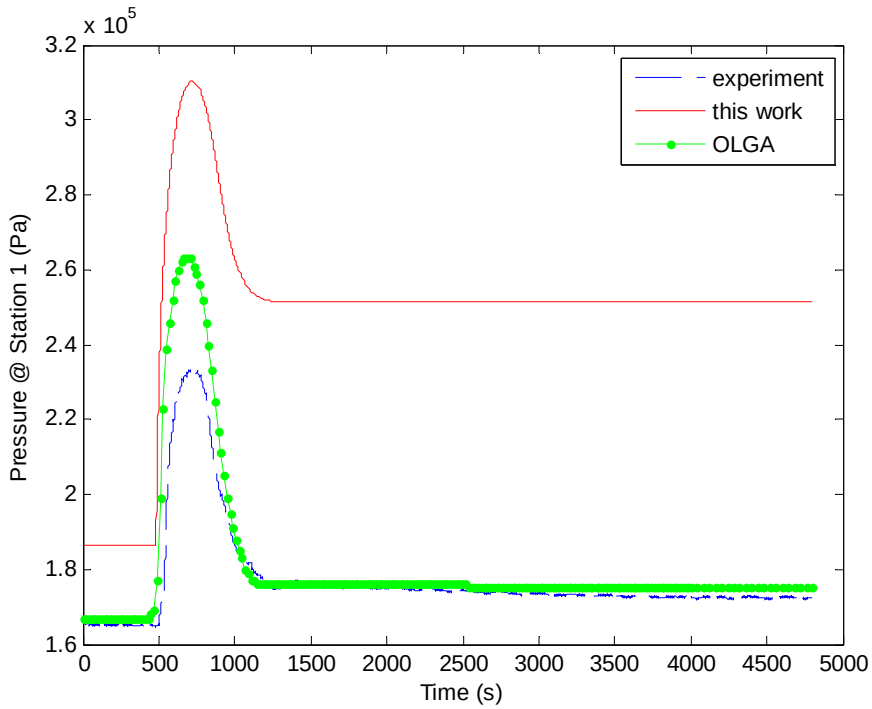

(b) Variation of pressure with time at the first test section

Fig. 13: Results for Test 2-A with drift flux model

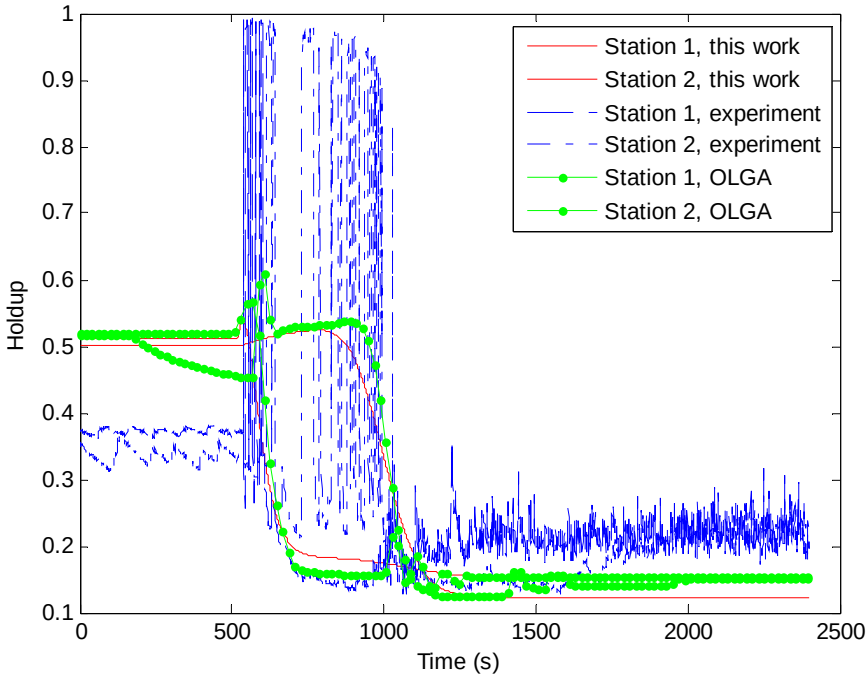

(a) Variation of liquid holdup with time at the two test sections

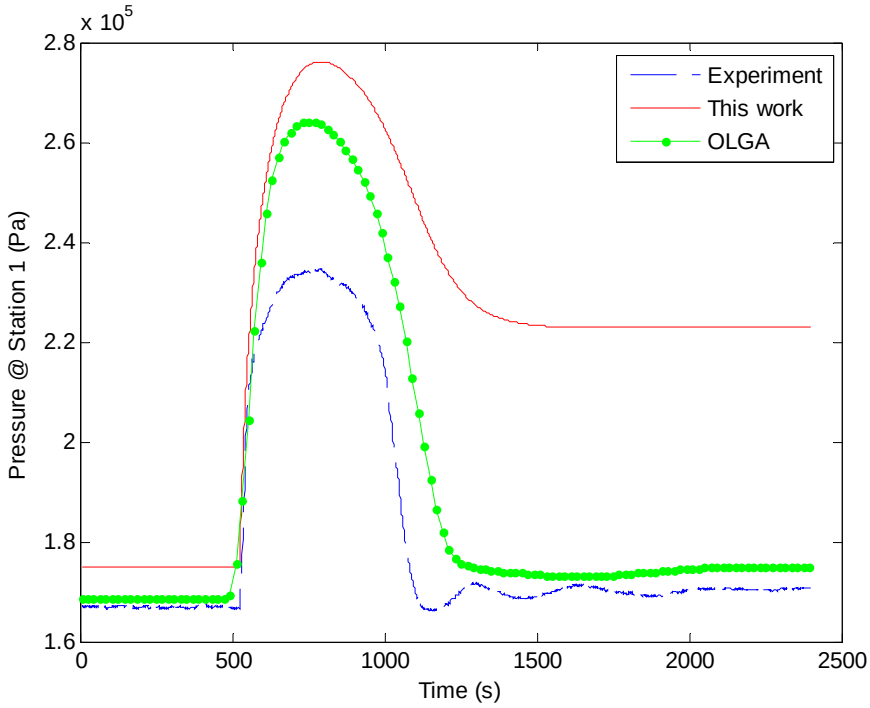

(b) Variation of pressure with time at the first test section

Fig. 14: Results for Test 2-B with drift flux model

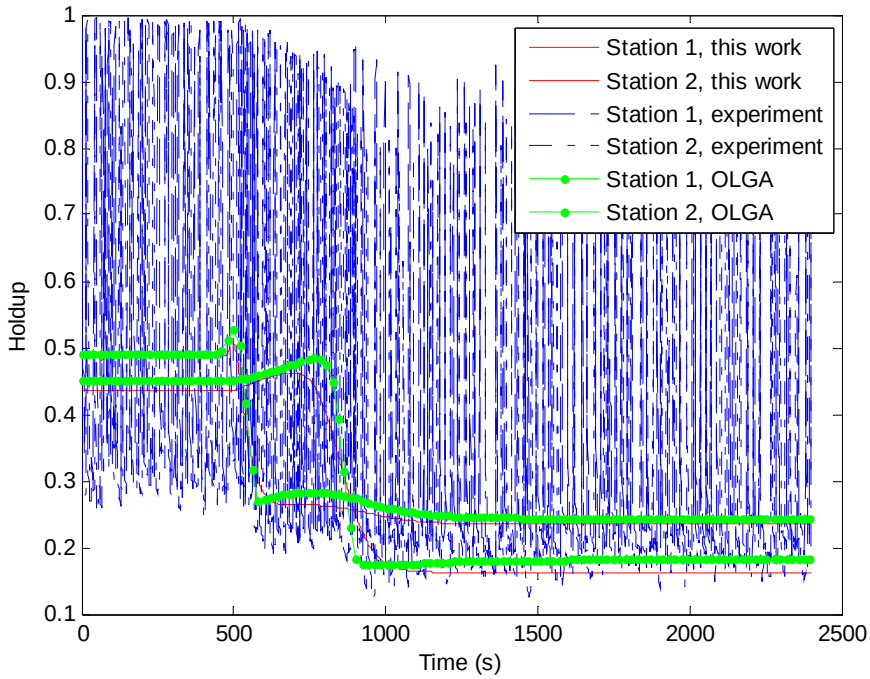

(a) Variation of liquid holdup with time at the two test sections

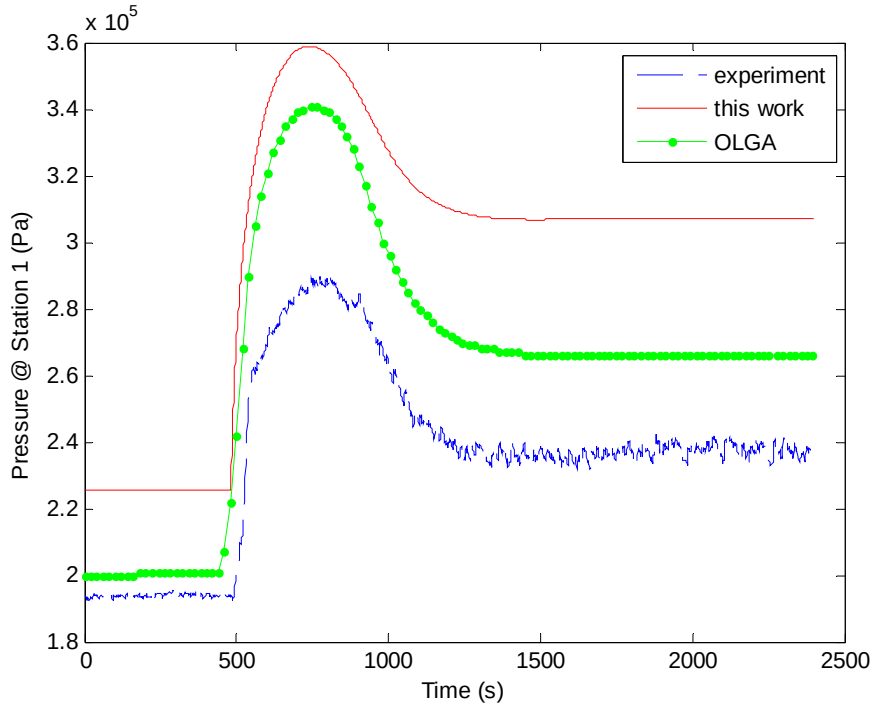

(b) Variation of pressure with time at the first test section

Fig. 15: Results for Test 2-C with drift flux model

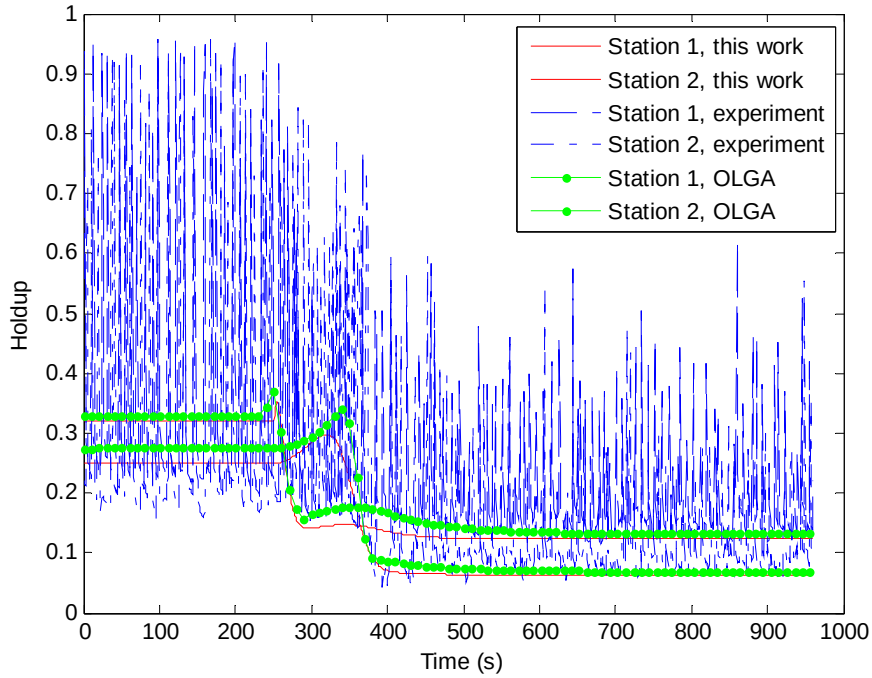

(a) Variation of liquid holdup with time at the two test sections

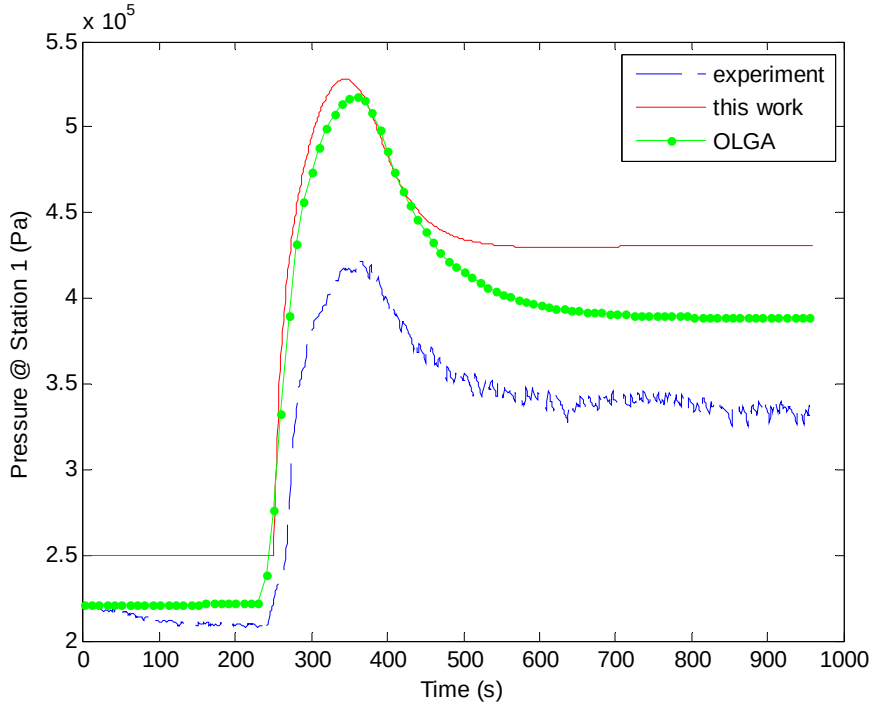

(b) Variation of pressure with time at the first test section

Fig. 16: Results for Test 2-D with drift flux model

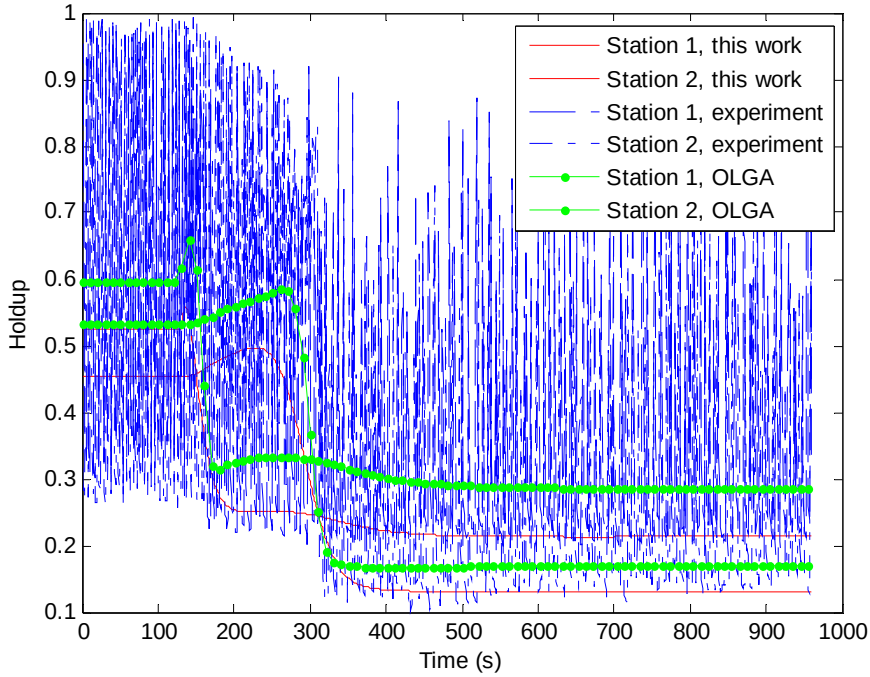

(a) Variation of liquid holdup with time at the two test sections

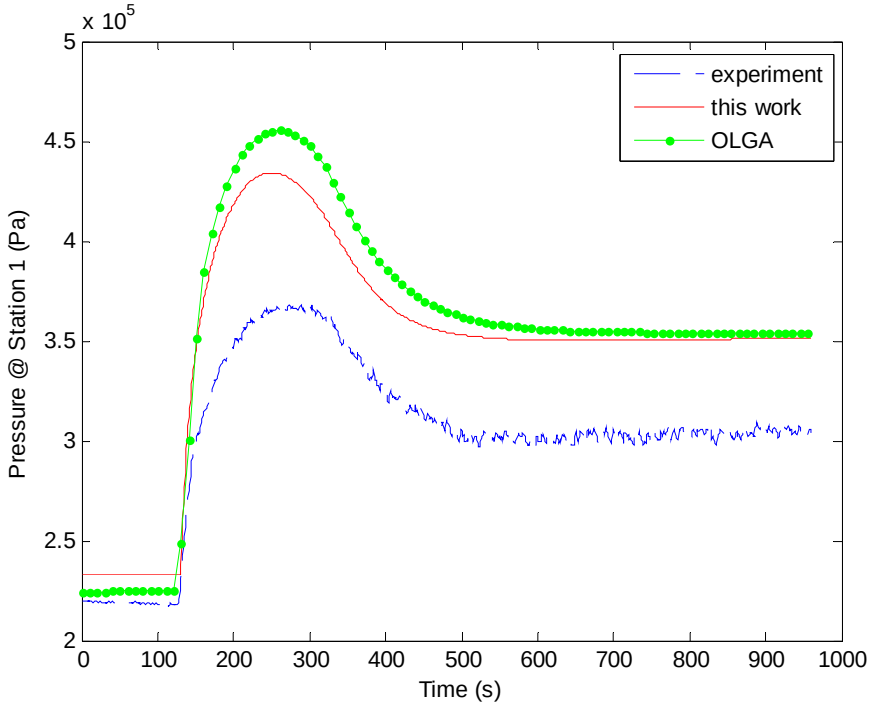

(b) Variation of pressure with time at the first test section

Fig. 17: Results for Test 2-E with drift flux model

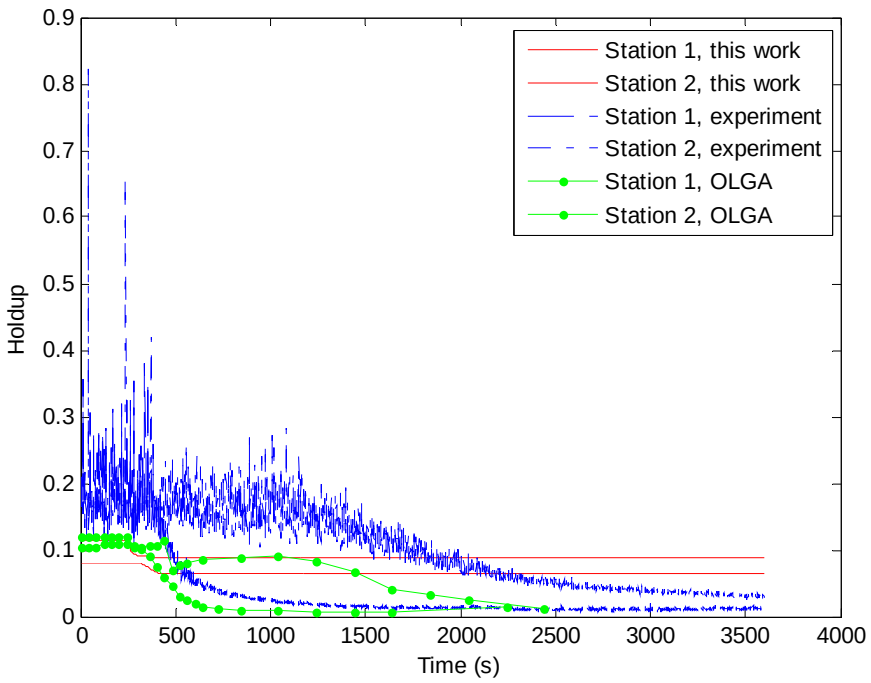

(a) Variation of liquid holdup with time at the two test sections

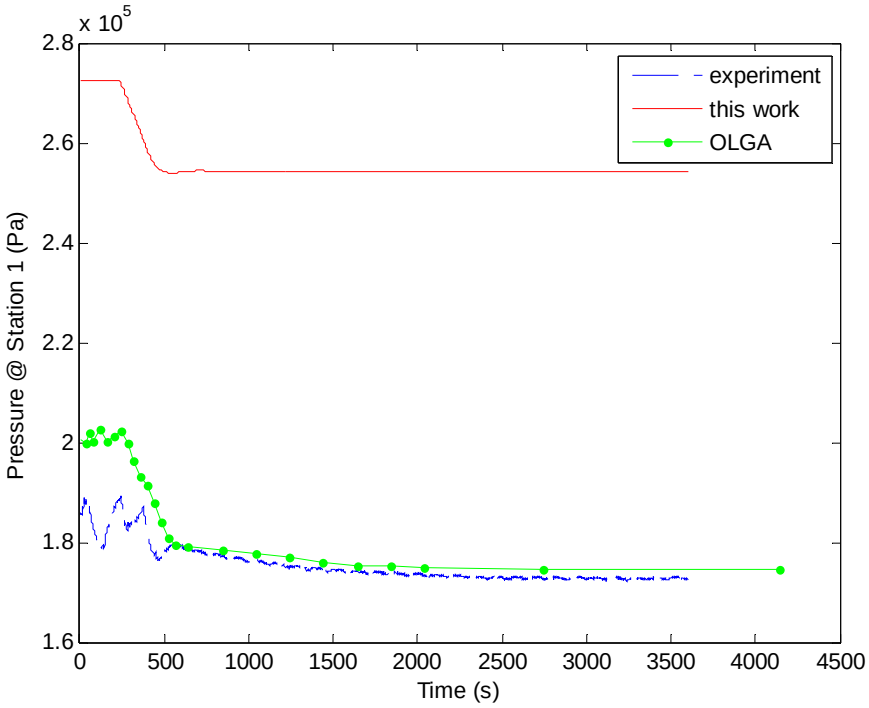

(b) Variation of pressure with time at the first test section

Fig. 18: Results for Test 3-A with drift flux model

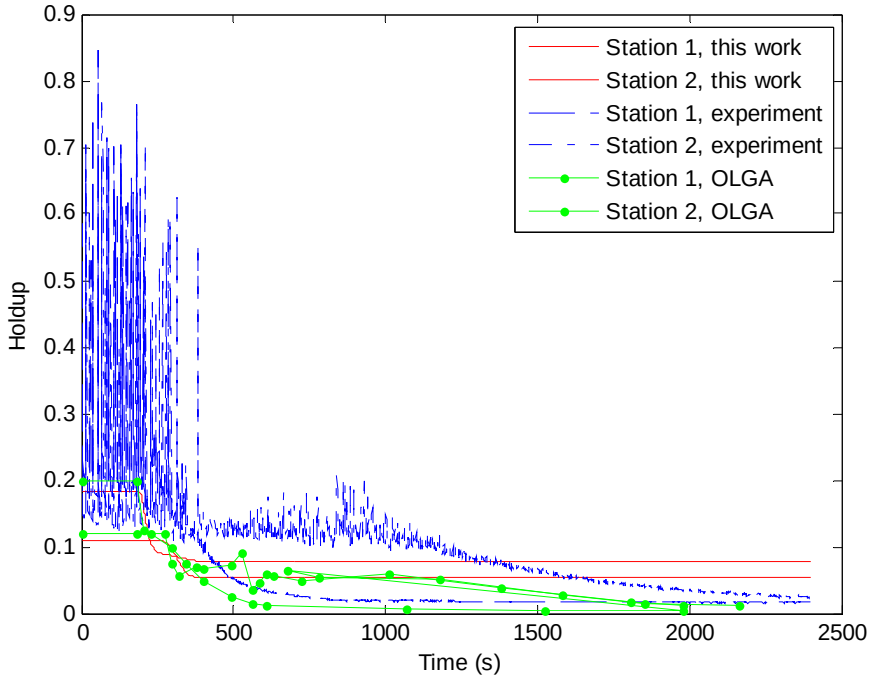

(a) Variation of liquid holdup with time at the two test sections

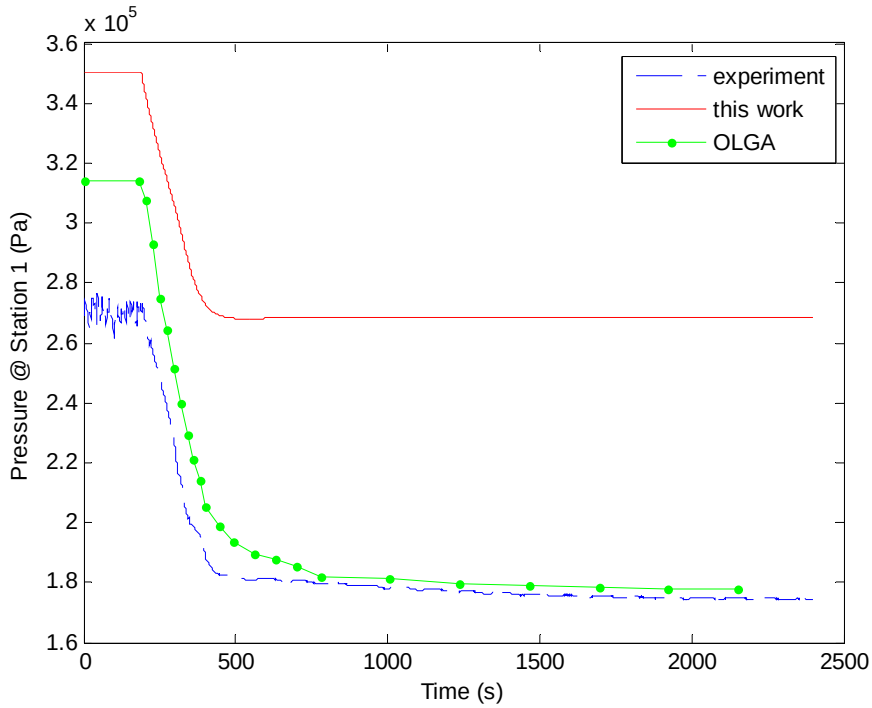

(b) Variation of pressure with time at the first test section

Fig. 19: Results for Test 3-B with drift flux model

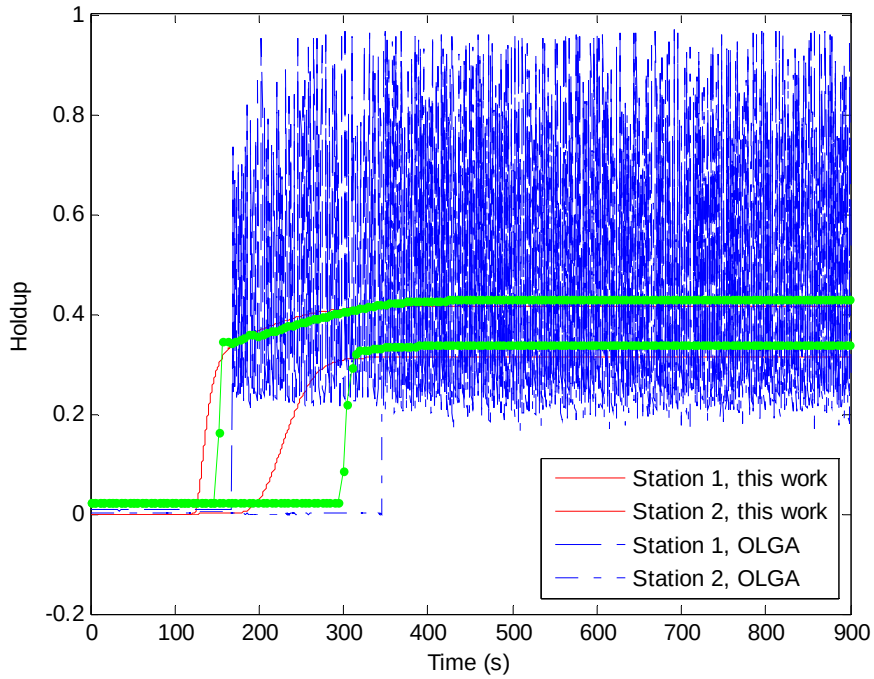

(a) Variation of liquid holdup with time at the two test sections

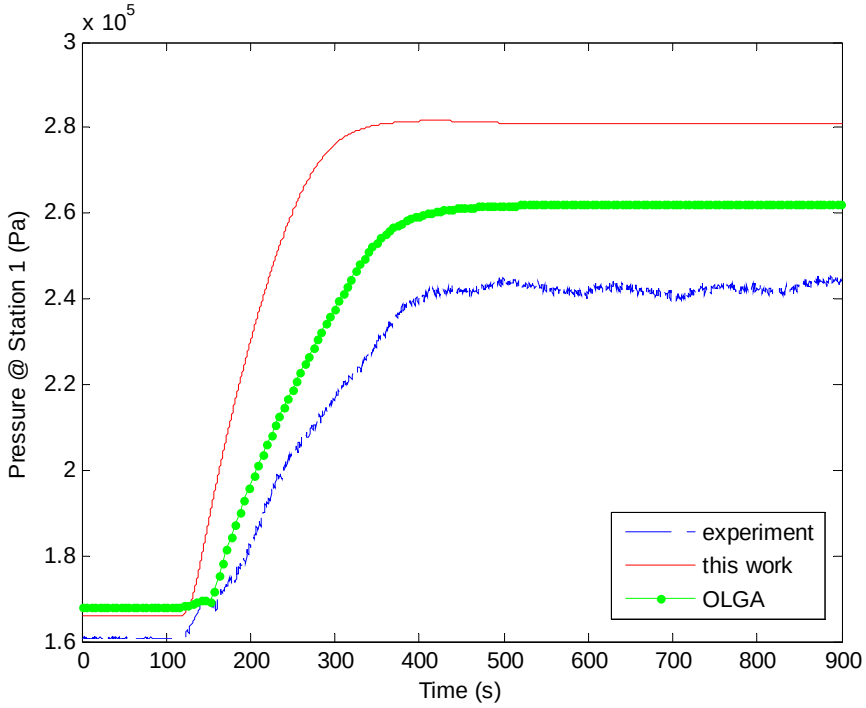

(b) Variation of pressure with time at the first test section

Fig. 20: Results for Test 4-B0 with drift flux model

Fluid Flow Projects

Executive Summary of Research Activities

Cem Sarica

Advisory Board Meeting, May 12, 2010

Liquid Unloading from Gas Wells

- Objectives
  - Explore Mechanism Controlling Onset of Liquid Loading
  - Investigate Effects of Well Deviation on Liquid Loading

Liquid Unloading from Gas Wells …

- Past Studies
  - Primarily on Droplet Transfer {Turner (1969), Coleman(1991), etc.}
  - Film Reversal {Barnea (1987), Veeken (2009)}
  - No Comprehensive Study on Inclination Angle Effect

Liquid Unloading from Gas Wells …

- Status
  - Literature Review is Complete
  - Experimental Study is Being Planned
    - 3 in. ID Severe Slugging Facility Will be Used
    - Facility Modifications to Be Completed by Summer

Fluid Flow Projects

Liquid Unloading from Gas Wells

Ge (Max) Yuan

Advisory Board Meeting, May 12, 2010

Outline

- Objectives
- Introduction
- Literature Review
- Research Proposal
- Experimental Study
- Near Future Tasks
- Project Schedule

Objectives

- Explore Mechanisms Controlling Onset of Liquid Loading
- Investigate Effect of Well Deviation on Liquid Loading

Introduction

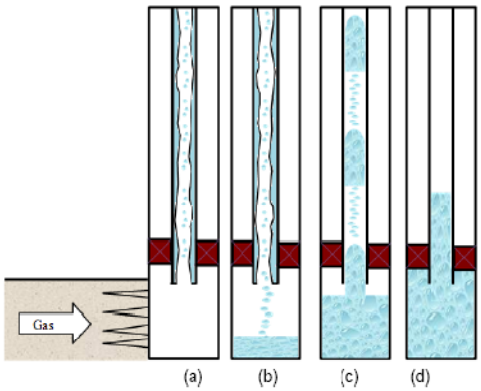

Gas Production Flow Regime Changes from Mist (a) to Annular (b) to Slug/Churn Flow (c) and Eventually Loads up (d).

Introduction …

Important Concepts

- Critical Gas Flow Velocity
  - Minimum gas velocity required to move liquid droplets upward
  - Gas rate at flow pattern transition
  - Gas rate required to move liquid film upward

Introduction …

- Industry Method to Recognize Liquid Loading

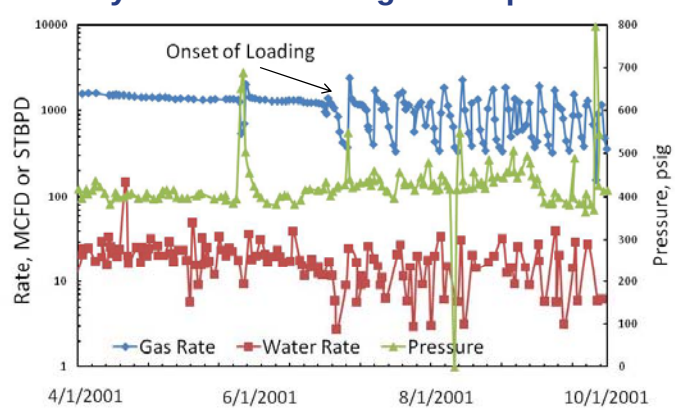

Well Performance Data Indicating Liquid Loading (Sutton *et al.*, 2003)

Introduction …

Important Concepts

- Transitional Annular Flow
  - Two zones
    - Lower part
      - Thick film
      - Direction of film flow is changing
    - Upper part
      - Thinner film
      - Film flow downward

Literature Review

- Influence of Well Deviation on Critical Gas Velocity
  - Belfroid *et al.* (2008) 2 in. ID, air-water flow, only 4 points

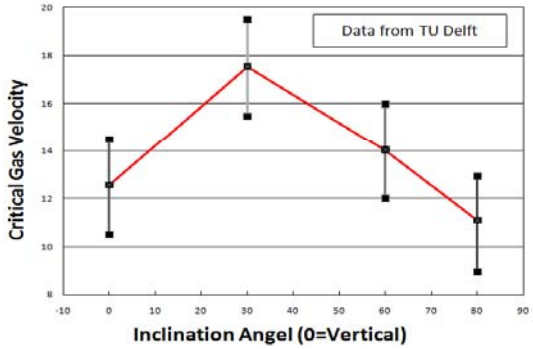

Literature Review …

- Mechanism of Liquid Loading
  - Main mechanisms (Toma 2007)
    - Film drainage
    - System instability
    - Flow pattern change
  - Liquid loading occurs due to liquid film flow reversal rather than droplet flow reversal
    - Christiansen (2009) - Not published
    - Veeken (2009) - Simulation results

Literature Review …

- Modeling of Liquid Loading
  - Turner *et al.* (1969), based on steady-state analysis
    - Continuous film model and entrained droplet model proposed
    - Entrained droplet model adapted because of better performance in matching field data

Literature Review …

- **Entrained Droplet Model**

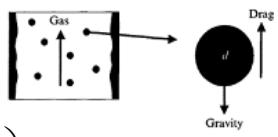

$$F_D = \frac{1}{2} C_d \left(\frac{d_d^2}{4} \right) \rho_g v_g^2 \qquad F_G = \left(\frac{\pi d_d^3}{6} \right) g \left(\rho_L - \rho_g \right)$$

Drag Force **Droplet Weight**

If $F_D > F_G$ → gas velocity > critical velocity
If $F_D < F_G$ → onset of liquid loading

Literature Review …

- **Entrained Droplet Model …**
  - **Solving for gas velocity**

$$v_g = \frac{2}{\sqrt{3}} \left[\frac{g\left(\rho_L - \rho_g\right) d_d}{\rho_g C_D} \right]^{0.5}$$

$$N_{WE} = \frac{d_d \rho_g v_g^2}{\sigma}$$

$$d_d = \frac{N_{WE} \sigma}{\rho_g v_g^2}$$

Literature Review …

- Entrained Droplet Model …

Superficial gas velocity — Liquid surface tension — Liquid & gas density

$$v_g = \left(\frac{4N_{WE}}{3C_D}\right)^{0.25} \frac{\left[\sigma g\left(\rho_l - \rho_g\right)\right]^{0.25}}{\rho_g^{0.5}}$$

Drag coefficient — Weber Number

Literature Review …

- Coleman *et al.* (1991)
  - Used Turner's droplet model
  - Field data with P_{wh} < 500 psia
  - 20% adjustment not needed
  - Wells showing slug flow not obey droplet model

Literature Review …

- Nossier *et al.* (2000)
  - Calculating Reynolds numbers corresponding to field data
  - Data exceeded the assumed range of Re assumed by Turner
  - C_D = 0.2 not 0.44

Literature Review …

- Nossier *et al.* (2000)…
  - C_D = 0.2 not 0.44

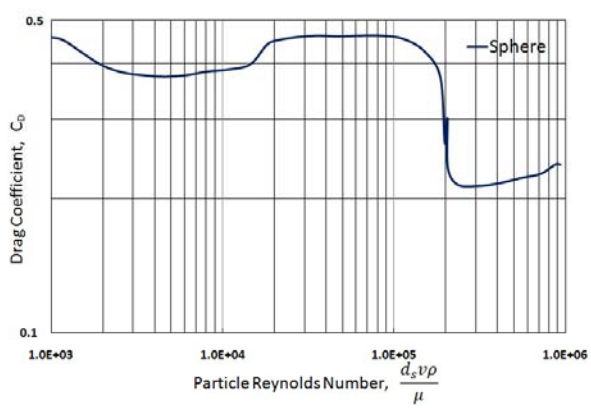

Literature Review …

- Experimental Study
  - Flores-Avila *et al.* (2002)
    - Experiments (air-water flow, deviation angles)
    - Holdup measured at different v_{SG}
    - New expression incorporating inclination angle and drag coefficient

Literature Review …

- Experimental Study
  - Girija (2006)
  - Girija *et al.* (2007)
    - Experiments (air-water flow, vertical annulus)
    - Critical velocities obtained at different conditions
    - Transitional annular flow observed and defined

Literature Summary

- Few Data About Inclination Effect
- No Comprehensive Study on Inclination Effect
- Mechanism In Debate

Research Proposal

Experimental Investigation

- Effect of Well Deviation on Critical Gas Velocity
- Flow Pattern along Wellbore
- Relationship between Liquid Film Flow Direction and Liquid Loading
- Inspection of Phase Distribution of Water

Research Proposal …

Modeling

- Prediction of Critical Gas Velocity Using Existent Models and Comparison with Data
- Improve Current Models or Develop a New Model if Necessary

Experimental Study

- Facility
- Test Fluids
- Testing Range
- Instrumentation

Facility

- Previously Used for Severe Slugging
- 3-in ID Low Pressure Flow Loop
- Needs Modifications

Test Fluids

- Test Fluid
  - Gas – Air
  - Water – Tap Water

Testing Range

➢ **Test Matrix**

v_{SG} (m/s)	v_{SL} (m/s) Inclination Angle: 30, 45, 60, 75, 90				
10	0.005	0.01	0.02	0.05	0.1
15	0.005	0.01	0.02	0.05	0.1
20	0.005	0.01	0.02	0.05	0.1
25	0.005	0.01	0.02	0.05	0.1
30	0.005	0.01	0.02	0.05	0.1

Testing Range …

- **Test Matrix (Vertical)**

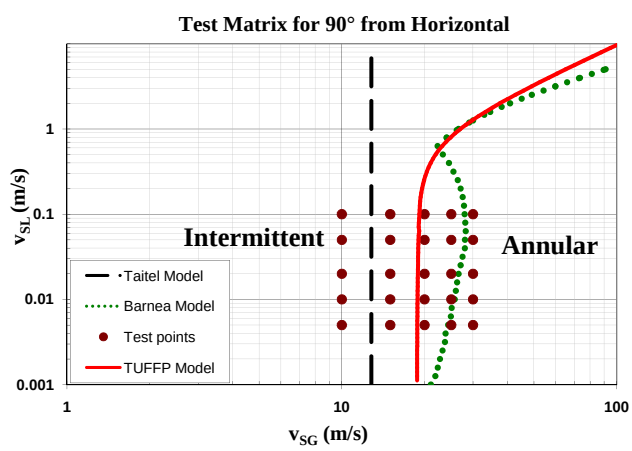

Testing Range …

- Test Matrix (75°)

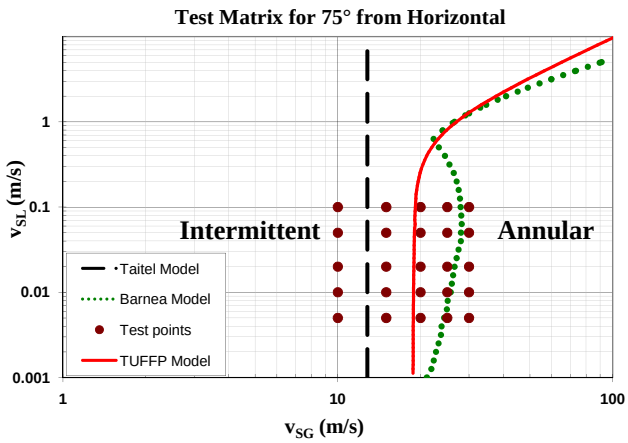

Testing Range …

- Test Matrix (60°)

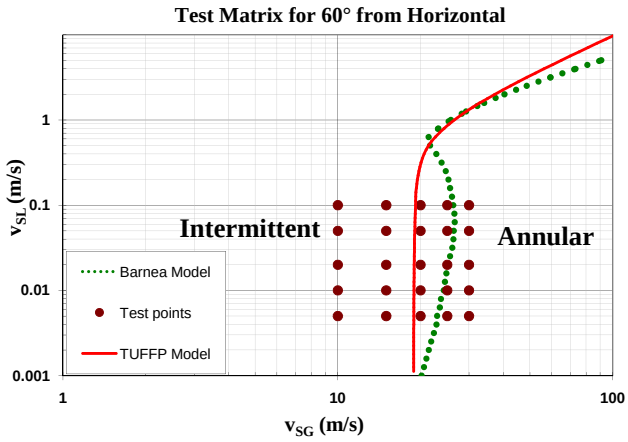

Testing Range …

- Test Matrix (45°)

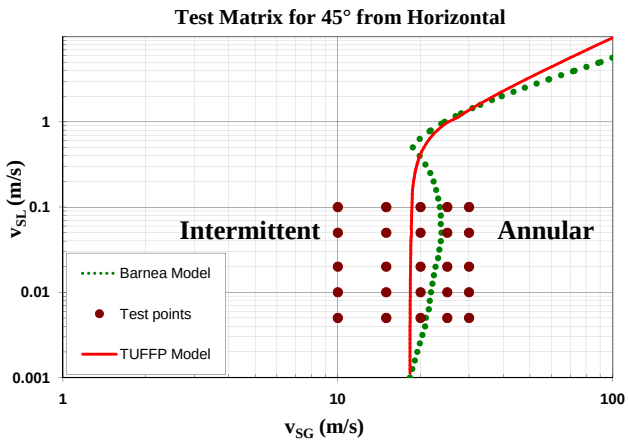

Testing Range …

- Test Matrix (30°)

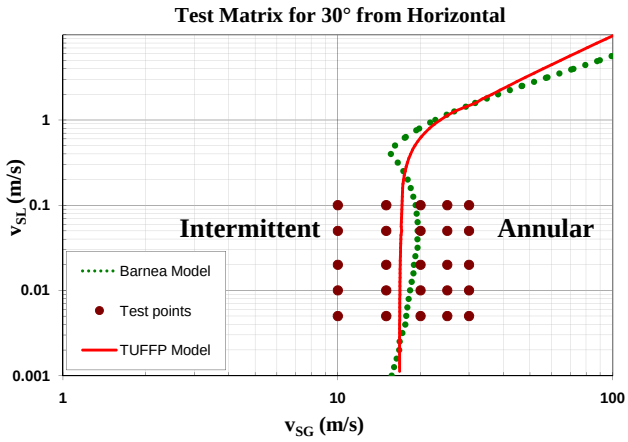

Instrumentation

- Pressure and Temperature: PTs and DPs and TTs
- Holdup: Quick Closing Valves
- Liquid Entrainment Fraction
- Liquid Film Flow Direction
- Liquid Film Thickness
- Liquid Film Velocity

Film Flow Direction

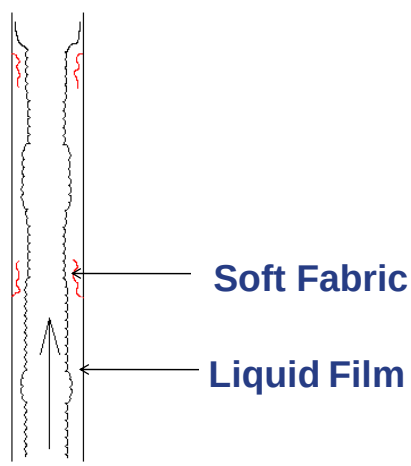

Film Thickness: Conductivity Probe

Conductivity Probe …

- Assembly Configuration

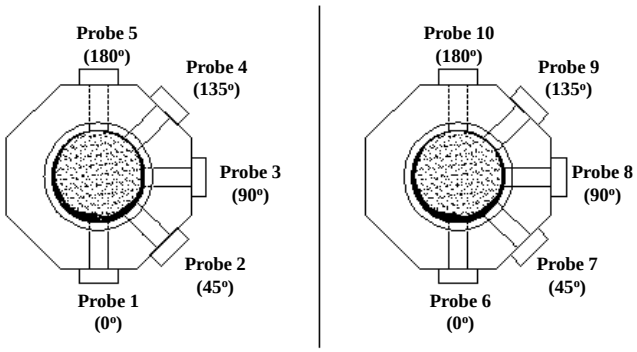

Conductivity Probe …

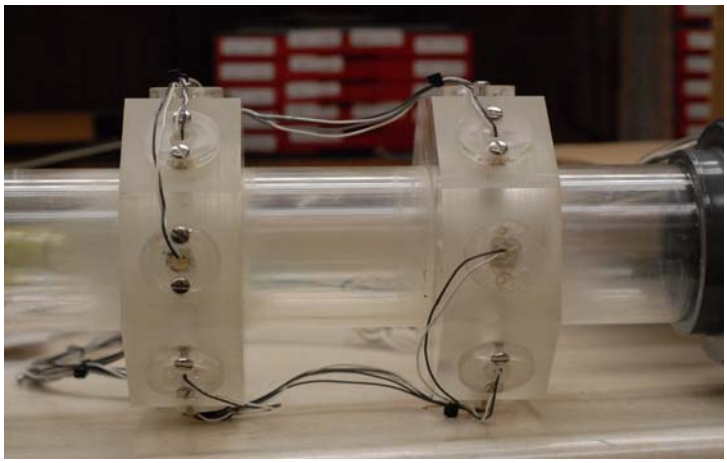

Liquid Entrainment: Iso-kinetic Probe

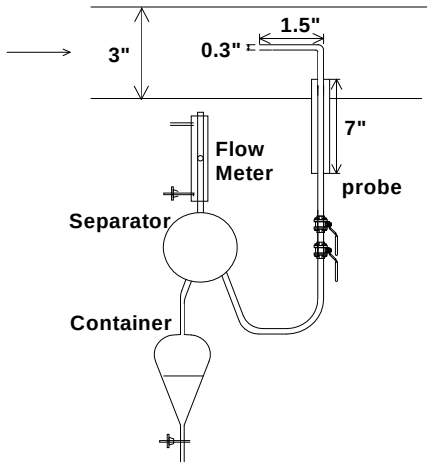

Film Velocity: Cold Liquid Injection

- Detect Temperature Variation
- $\text{Velocity} = \dfrac{\text{Distance}}{\text{Time}}$

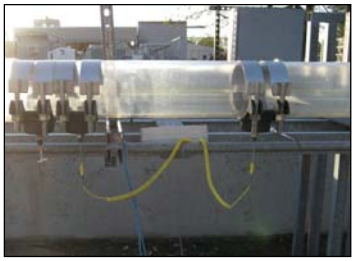

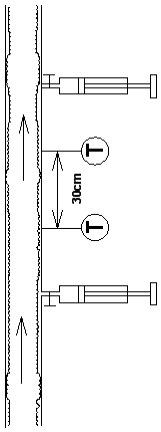

Near Future Tasks

- Test Section Design
- Facility Modification
  - Conversion from Severe Slugging Setup
  - Instrumentation
- Preliminary Testing

Project Schedule

Literature Review	Ongoing
Facility Modification	Summer 2010
Preliminary Testing	September 2010
Experimental Testing	February 2011
Data Analysis	May 2011
Model Comparison	July 2011
Final Report	August 2011

Questions/Comments

Liquid Unloading from Gas Wells

Ge (Max) Yuan

PROJECTED COMPLETION DATES:

Literature Review	Ongoing
Facility Modifications	July 2010
Preliminary Testing	August 2010
Testing	March 2011
Data Analysis	May 2011
Final Report	August 2011

Objectives

The main objectives of this study are:

- Explore the mechanisms controlling the onset of liquid loading and
- Investigate the effect of well deviation on liquid loading process.

Introduction

As natural gas is produced from a reservoir, the simultaneous flow of gas with liquid hydrocarbons and/or water is a common occurrence in both onshore and offshore production systems. Liquid loading in the wellbore has been recognized as one of the most important problems in gas production. In the early time of the production, natural gas carries liquid in the form of mist. The reservoir pressure is sufficient for the gas wells to transport the liquid phase to the surface along with the gas phase. As the gas well matures, the reservoir pressure decreases and gas flow velocity drops. When the gas velocity becomes lower than a critical value, the liquid falls back and the flow pattern changes from annular flow to slug flow. As liquid loading progresses, the accumulation of liquid increases the bottom-hole pressure and further reduces gas production rate. Then, the flow pattern may change to bubbly flow. Eventually, the well can no longer produce. The process of liquid loading is shown in Fig. 1.

In the oil and gas industry, several methods have been developed to solve the liquid loading problem; such as using a down-hole pump to produce water, using velocity string, lowering wellhead pressure, and foam assisted lift. Although a lot of efforts have been made to model the liquid loading process of gas wells, experimental data are very limited. Field data from Turner (1969), Coleman (1991) and Veeken (2009) are the only available data to validate the existent models.

Turner *et al.* (1969) derived a method of predicting the critical gas rate by equating the upward drag and downward gravity forces on the largest possible liquid droplet. The maximum Weber number determines the largest possible droplet size. The so-called Turner expression for liquid loading includes a 20% upward adjustment to best-fit field data. The Turner method has been widely used in the industry for decades because it only requires readily measurable wellhead parameters.

Literature Review

Mechanism of liquid loading is still in debate. The flow pattern transition from annular to churn/slug flow pattern transition from annular to churn/slug flow plays an important role in the process. In practice some other mechanisms may initiate the liquid loading. The main mechanisms for liquid loading may include:

- Film drainage,
- System instability,
- Flow regime change (Toma 2007).

Recent literature has reported that liquid loading occurs due to liquid film flow reversal rather than droplet flow reversal, which is a challenge to the widely used Turner's criterion. Several authors have observed such phenomena in their flow loop experiments. Van't Westende *et al.* (2007) studied liquid transport in a 0.05 m diameter 12 m long air-

water pipe. The maximum observed droplet size was about 1 order of magnitude smaller than the maximum droplet size postulated by the Turner expressions, i.e. the droplets should not cause liquid loading.

It was observed that the onset of liquid loading coincides with liquid film flow reversal rather than liquid droplet flow reversal. Christiansen (2009) carried out similar flow loop testing and observed the same film flow reversal. The results of transient flow modeling provided by Veeken *et al.* (2009) also support the flow loop observation.

The Turner's criterion does not consider the influence of well deviation on critical gas velocity. In deviated wells, there may be different mechanisms. Flow loop testing has also been used to investigate the influence of well deviation on liquid loading rate which cannot be predicted by Turner's model. The results for a 2-inch diameter air-water flow loop are presented in Belfroid *et al.* (2008) as four testing points.

Turner *et al.* (1969) proposed the continuous film model and entrained droplet model and concluded that the droplet falling is the controlling mechanism. They adopted the "droplet model" from fluid particle dynamics to calculate the critical gas velocity necessary to lift the liquid droplets in near vertical wells. In this model, the minimum velocity required to keep liquid droplets in suspension is the result of a force balance between the drag exerted by the surrounding gas and the gravity of the droplets.

Turner *et al.* (1969) pointed out that the interfacial tension can be obtained with sufficient accuracy from handbooks and that the drag coefficient is dependent on the droplet shape and Reynolds number. They suggested that, for typical oil field conditions, the Reynolds number ranges from 10^4 to $2\text{x}10^5$. The drag coefficient of spherical droplets in this range of Reynolds number is approximately 0.44. Considering the range of the Weber number (20 to 30) as suggested by Hinze *et al.* (1955) and selecting its maximum value, Turner *et al.* (1969) introduced the following expression in oilfield units for the critical gas velocity required to keep liquid droplets in suspension:

$$v_{sg} \approx v_g = 17.6 \frac{[\sigma(\rho_l - \rho_g)]^{0.25}}{\rho_g^{0.5}} \qquad (1)$$

Field data of 101 wells were provided for model validation. A 20% upward adjustment was suggested to better match the field data.

Coleman *et al.* (1991) adopted the Turner model to analyze the Exxon field data and found out the 20% adjustment was not needed. The major difference between the two sets of field data is the wellhead pressure. The wellhead pressures of most wells in the Turner's field data were higher than 800 psia while those of Coleman's data were less than 500 psia.

Coleman *et al.* (1991) also noted that gas density, interfacial tension and temperature have little impact on the critical gas velocity calculations, with wellbore diameter and wellhead pressure playing a more significant role. It was observed that wells with slug flow behavior did not obey the entrained droplet model.

Nossier *et al.* (2000) examined the assumption of turbulent flow made by Turner *et al.* (1969) by calculating the Reynolds numbers corresponding to the field data gathered by Turner *et al.* (1969) and Coleman *et al.* (1991). They found that almost all the field data from the first reference exceeded the assumed range (10^4 to $2\text{x}10^5$) of Reynolds number. In particular, it was found that the range was $2\text{x}10^5$ to 10^6, corresponding to a drag coefficient of 0.2 and therefore requiring the 20% adjustment to match field data. The calculated Reynolds numbers from the field data provided by Coleman *et al.* (1991) was in the originally assumed Reynolds number range and therefore requiring little or no adjustment to match field data. Nossier *et al.* (2000) then developed two entrained droplet models: one for low flow rate systems, and one for high flow rate systems. For low flow rate systems, the flow transition criterion proposed by Allen (1900) was used, where the critical gas velocity is calculated as:

$$v_g = 0.2\left[\frac{g(\rho_l - \rho_g)}{\rho_g}\right]^{0.72} \times \frac{d_d^{1.18}}{\left(\frac{\mu_g}{\rho_g}\right)^{0.45}} \qquad (2)$$

For the transition flow regime, the following equation is derived to calculate the critical velocity:

$$v_g = 14.6\sigma^{0.35} \frac{(\rho_l - \rho_g)^{0.2}}{\mu_g^{0.134}\rho_g^{0.134}} \qquad (3)$$

For highly turbulent flow,

$$v_g = \frac{21.3(\rho_l - \rho_g)\sigma^{0.25}}{\rho_g^{0.5}} \qquad (4)$$

The entrained droplet approach is the most widely used in the oil and gas industry to predict the minimum gas flow rate required to prevent the onset of liquid loading. Models based on this approach

have been tested against field data, with varying degrees of success reported by each author.

Veeken *et al.* (2009) presented liquid loading field data from offshore fields that exceed the Turner predicted values by about 40%. The main reason is that the Turner's expression is not applicable for directional wells with inclination angles. It subsequently presents the results of transient multiphase flow modeling which show us that the liquid film velocity may drop to zero in the pipe.

Flores-Avila *et al.* (2002) carried out experiments performed with air and water in a 48 ft long flow loop at 0°, 20°, 40°, 60° and 75° deviation angles from the vertical. Liquid holdup at different superficial gas velocities is measured. A new expression is proposed to predict critical gas velocity based on Turner's droplet model by also considering the flow regime of the continuous phase when evaluating the drag coefficient, as well as the angle of deviation from the vertical. Similarly, the amount of liquid that flows countercurrent into and accumulates in the well is predicted based on the concept of zero net liquid flow (ZNLF) holdup.

$$v_{critical} = 14.27\left[\frac{\sigma(\rho_l - \rho_g)}{C_d \cos\theta \rho_g^2}\right]^{0.25} \quad (5)$$

Girija (2006) investigated critical flow rates in the tubing-casing annulus. Two different methods were used in this study. In the first method (Constant Water-Rate Method), water-rate is kept as constant and gas-rate drops step by step. In the second method (Constant-Level Method), a fixed amount of water was charged to the bottom of the tube. Gas flow rate was incrementally increased, starting at a rate well below the expected critical flow rate. Any produced water was recycled to the base of the test section. The water level in the separator was maintained at a reference level for the duration of the test. Transitional annular flow was observed and defined in this study. Results show that the critical rates were independent of height of the tubing-casing, volume of water charged and eccentricity of the tubing. The observed critical flow rates are 20% to 50% less than estimated from the Turner's expression (without the 20% adjustment) with actual cross-sectional area of the annulus.

Liquid unloading of gas wells becomes an important issue because there is no satisfactory model to predict critical velocity for inclined wells. In Grija's study, a Transitional Annular Flow was observed. In this flow regime, gas flows upward in the central core of the conduit, and a liquid film is on the walls of the conduit. When this regime is observed in the flow loop, it occurs in two zones in the test section. In the lower zone, the liquid film is thick and its direction of flow is changing. In the upper part of the loop, the film is thinner and the direction of flow is downward. The lower zone generates lots of liquid droplets which are lifted to the upper zone in the test section, where they coalesce on the walls and flow downward until they meet the thicker film of the lower zone. Thus, the flow regimes in the loop consist of a lower zone with a gas core and annular film from which droplets are transported upward, and an upper coalescing zone in which droplets strike the wall of the loop and flow downward. There is a distinct interface between the lower zone and the upper zone.

Experimental Study

The 76.2-mm (3-in.) diameter severe slugging facility of the Tulsa University Fluid Flow Projects (TUFFP) will be modified for this project (Fig. 2). The facility is capable of being inclined from horizontal to vertical. Pressure and temperature transducers are placed near the test section to obtain fluid properties and other flowing characteristics.

Test Fluids

Compressed air and Tulsa city tap water will be used in this study. The surface tension of the tap water will be measured frequently to ensure accurate results.

Testing Range

In this study, experiments will be conducted at different flow conditions in terms of flow rates and inclination angle. Superficial water velocities range from 0.005 to 0.1 m/s. Superficial gas velocities range from 10 to 30 m/s. The test range should experience the onset of liquid loading in order to get the critical gas velocity. Figures 5 through 9 display the test matrices for experiments to be conducted at inclination angles of 30°, 45°, 60°, 70°, and 90° from horizontal.

Instrumentation

Quick-closing valves (QCV) will be installed on the test section to measure liquid holdup. A soft fabric will be attached to the interior surface of the pipe to help identity the film flow direction shown in Fig. 10.

Liquid film thickness can be measured using conductivity probe shown in Fig. 11. The probe consists of a single wire which traverses across the pipe cross section. The air-water interface is indicated by change in conductance and hence a change in voltage across the probe. This method relies on visual observation and manually traversing the probe which can introduce considerable error in the measurement. Hence, there is a need to devise a method which can provide real time data on liquid film thickness. A single wire capacitance probe is being examined for measurement of water layer thickness.

Cold liquid injection technique maybe used to determine liquid velocity. A cold liquid injector is placed at a point in the test section to inject cold water into the test section. Two thermal probes are installed 0.5 ft after the injector with a 1 ft interval between them. The time required for the cold liquid to travel between the two probes is measured which gives the velocity of the liquid. The configuration is shown in Fig 12.

An iso-kinetic sampling probe (shown in Fig. 13) has also been installed in the facility to measure entrainment fraction. The iso-kinetic sampling probe will be inserted into the pipe at various radial distances. The liquid sampled from the gas core will be separated in a small gas-liquid separator and collected in a graduated cylinder. From these measurements, the droplet entrainment flux profile will be determined. The entrainment fraction can be calculated by integrating this flux profile. The iso-kinetic sampling probe works best under low liquid flow rates where a more distinct division between the gas core and liquid film exists.

Near Future Tasks

The main tasks for the future are:

- Test section design
- Facility modification
- Evaluate of instrumentation
- Preliminary test

Nomenclature

v	= Velocity [m/s]
C_d	= Drag Coefficient
d_d	= Droplet diameter [mm]
ρ	= Density [kg/m^3]
σ	= Interfacial tension [N/m]
g	= Gravitational constant [m/s^2]
μ	= Viscosity [Pa·s]
θ	= Inclination angle [degree]

Subscripts

g	= Gas
l	= Liquid
critical	= Critical velocity for liquid unloading
SG	= Superficial gas
SL	= Superficial liquid

References

Allen, H.S.: Philos. Mag. (1900) 50, 323.

Coleman, S.B., Clay, H.B., McCurdy, D.G., and Lee Norris, H. III (1991): "A New Look at Predicting Gas-Well Load Up," J. Pet. Tech., March 1991, 329-333.

Belfroid, S.P.C., Schiferli, W., Alberts, G.J.N., Veeken, C.A.M. and Biezen, E.: "Prediction Onset and Dynamic Behavior of Liquid Loading Gas Wells," SPE paper 115567 presented at 2008 SPE ATCE, Denver, CO, 21-24 September 2008.

Flores-Avila, F., Smith, J.R., Bourgoyne Jr., A.T., and Bourgoyne, D.A., "Experimental Evaluation of Control Fluid Fallback during Off-Bottom Well Control: Effect of Deviation Angle," IADC/SPE 74568, IADC/SPE Drilling Conference held in Dallas, Texas, 26–28 February 2002.

Girija, E.G., Christiansen R.L. and Miller M.G. (2007): "Experimental Study of Critical Flow Rates in the Tubing-Casing Annulus of Natural Gas Wells," SPE paper 109609 presented at 2007 SPE ATCE held in Anaheim, California, U.S.A., 11–14 November 2007.

Girija, E.G: "Experimental Study of Gas-Liquid Flow Through a Tubing-Casing Annulus With Application to Natural Gas Wells," M.S. Thesis, Colorado School of Mines (2006)

Hinze, J.O.: "Fundamentals of the Hydrodynamic Mechanism of Splitting in Dispersion Processes," AICHE Jour., Sep. 1955, 1, No. 3, 289.

Nosseir, M.A., Darwich, T.A., Sayyouh, M.H. and El Sallaly, M.: "A New Approach for Accurate Prediction of Loading in Gas Wells Under Different Flowing Conditions," SPE Production & Facilities (November 2000) 241-46.

Solomon F.A., Falcone G. and Teodoriu C. (2008): "Critical Review of Existing Solutions to Predict and Model Liquid Loading in Gas Wells", SPE paper 115933 presented at SPE ATCE held in Denver, Colorado, USA, 21–24 September 2008.

Toma, P., Vegas E., Kuru E., "Prediction of Slug-to Annular Flow Pattern Transition (STA) for Reducing the Risk of Gas-Lift Instabilities and Effective Gas/Liquid Transport for Low-Pressure Reservoirs", SPE Production & Operations November 2007.

Turner, R.G., Hubbard, M.G., and Dukler, A.E. (1969): "Analysis and Prediction of Minimum Flow Rate for The Continuous Removal of Liquids from Gas Wells," J. Pet. Tech., Nov. 1969, 1475-1482.

Van't Westende, J.M.C, Kemp, H.K., Belt, R.J. and Portela, L.M.: "On the Role of Droplets in Cocurrent Annular and Churn-Annular Pipe Flow," International Journal of Multiphase Flow 33 (2007) 595–615.

Veeken K., Hu B. and Schiferli W., (2009): "Transient Multiphase Flow Modeling of Gas Well Liquid Loading," SPE paper 123657 presented at SPE Offshore Europe Oil & Gas Conference & Exhibition held in Aberdeen, UK, 8–11 September 2009.

Table 1 Test Matrix

v_{SG} (m/s)	v_{SL} (m/s) Inclination Angle: 30, 45, 60, 75, 90				
10	0.005	0.01	0.02	0.05	0.1
15	0.005	0.01	0.02	0.05	0.1
20	0.005	0.01	0.02	0.05	0.1
25	0.005	0.01	0.02	0.05	0.1
30	0.005	0.01	0.02	0.05	0.1

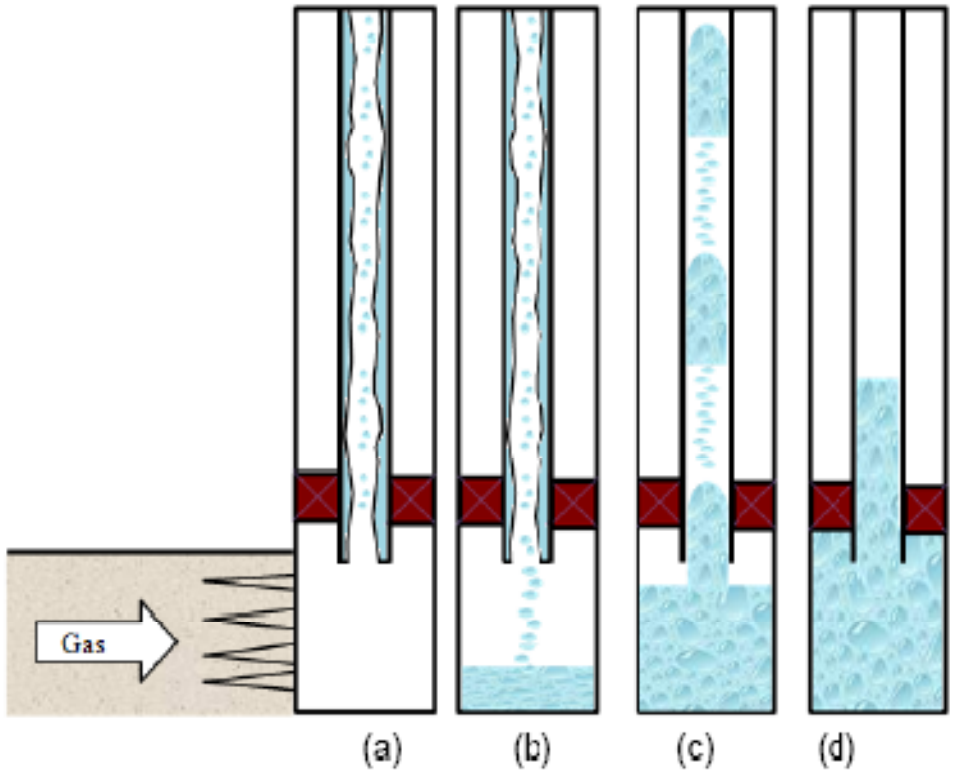

Figure 1: Gas Production Flow Regime Changes from Mist (a) to Annular (b), Slug/Churn Flow (c), and Eventually Loads up (d).

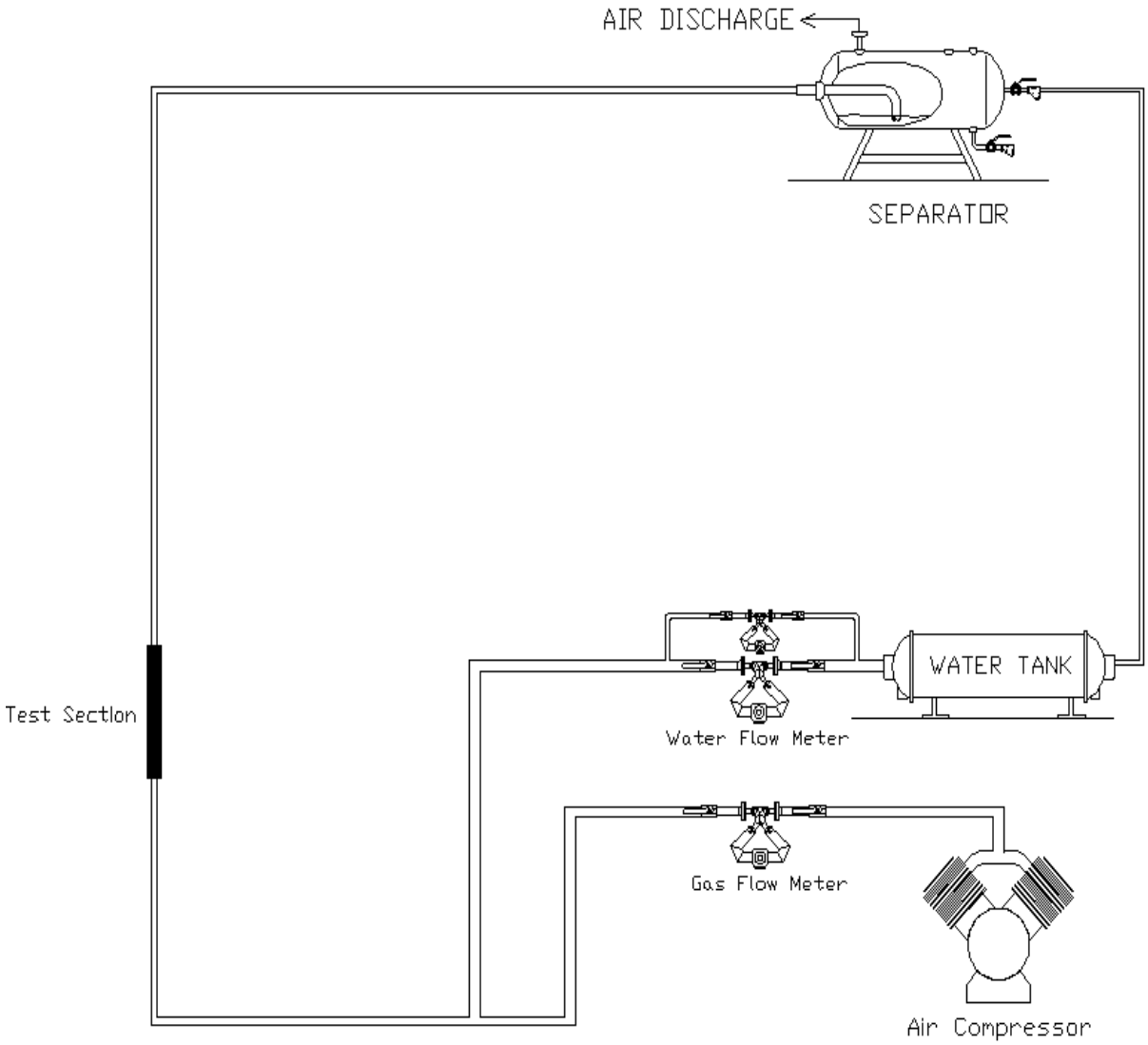

Figure 2: Schematic of Liquid Loading Test Facility of TUFFP

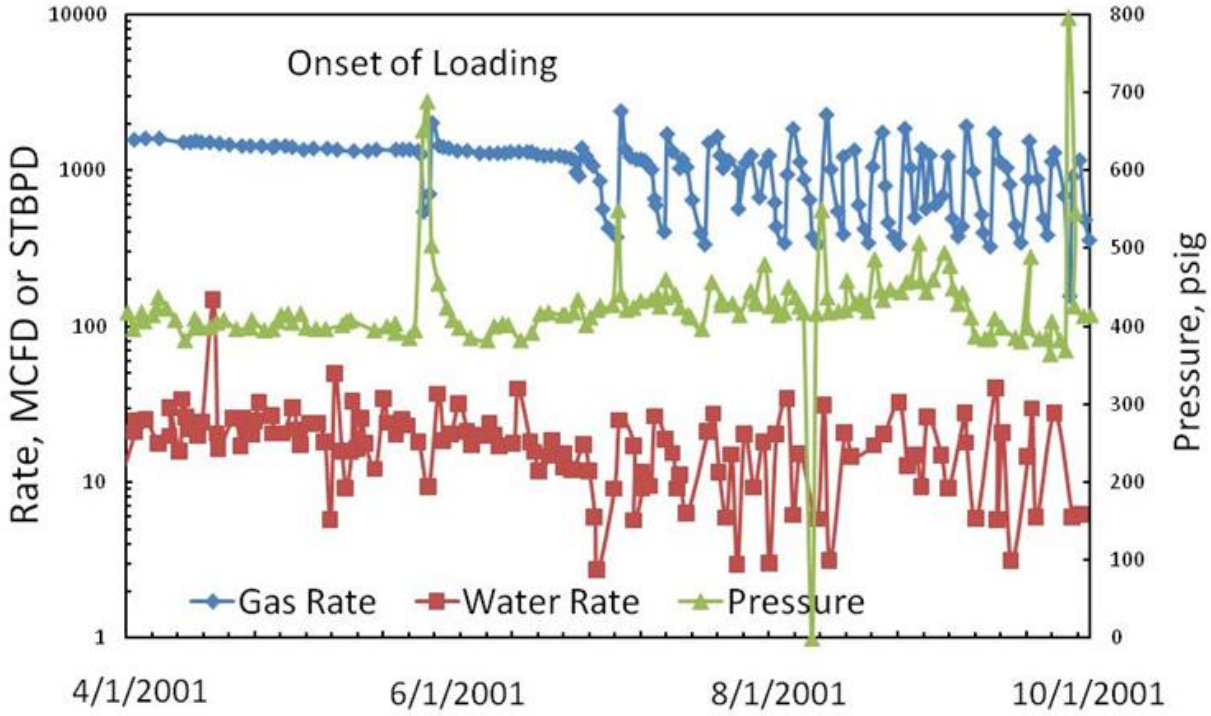

Figure 3: Well Performance Data Indicating Liquid Loading (Sutton *et al*, 2003)

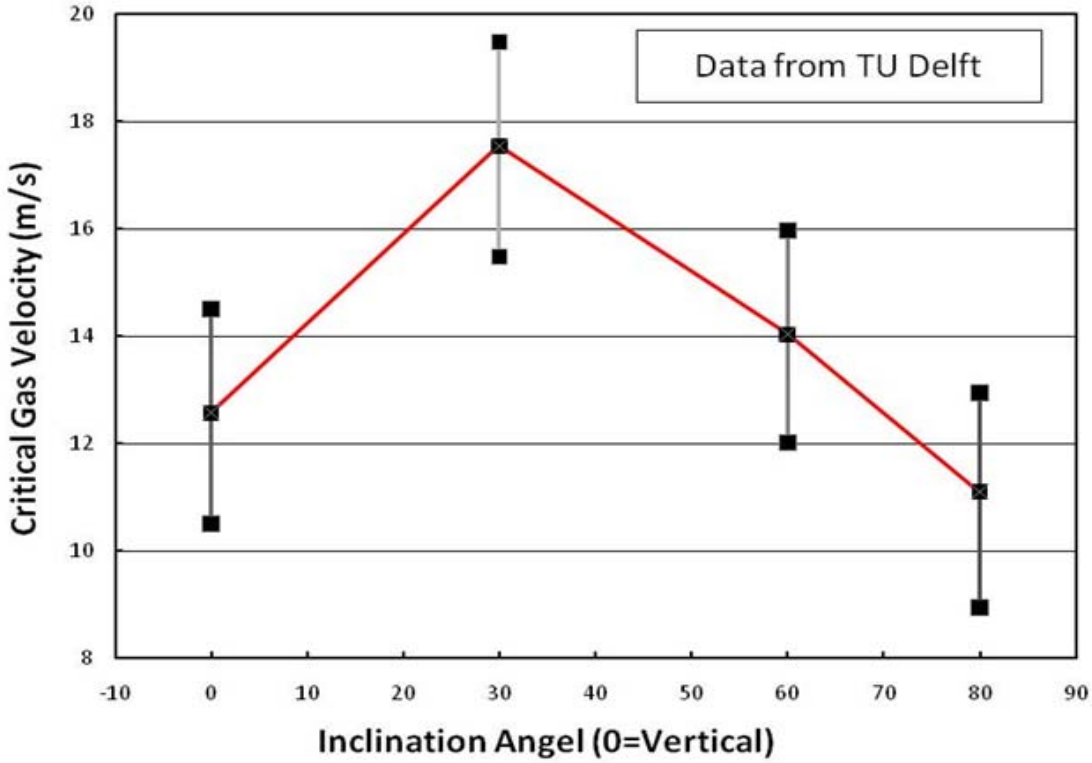

Figure 4: Critical Gas Velocity as Function of Inclination Angle (Belfroid *et al.*, 2008)

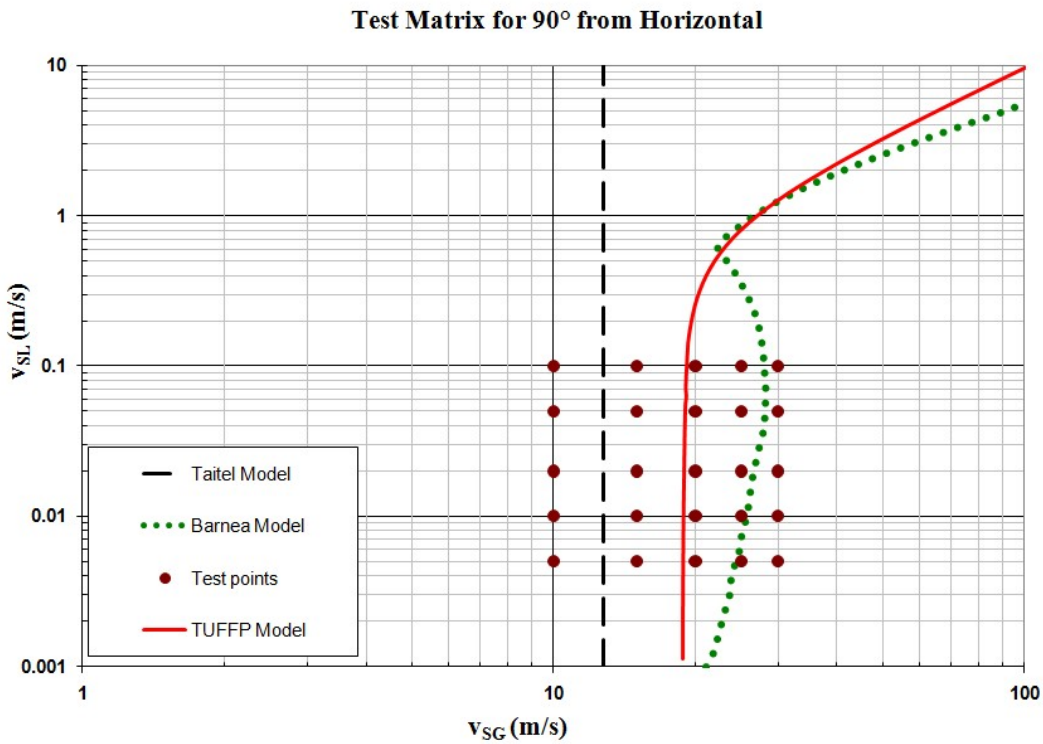

Figure 5: Test Matrix on Annular-Intermittent Transition Map by Different Models (Vertical)

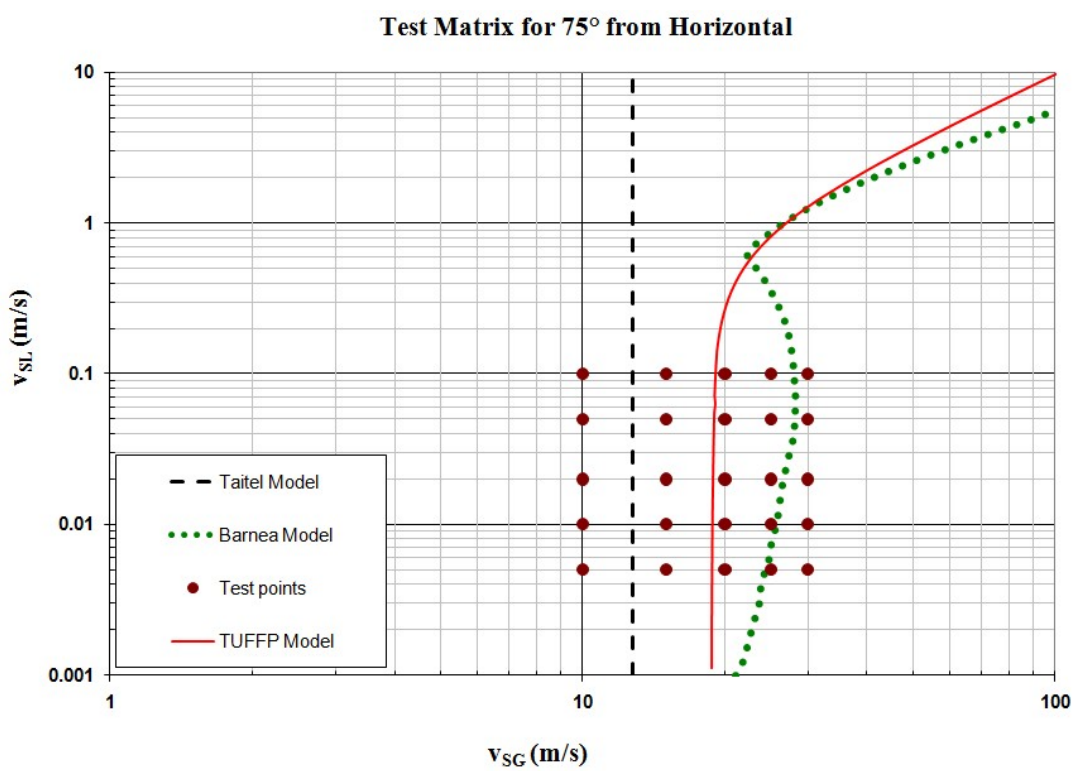

Figure 6: Test Matrix on Annular-Intermittent Transition Map by Different Models (75°)

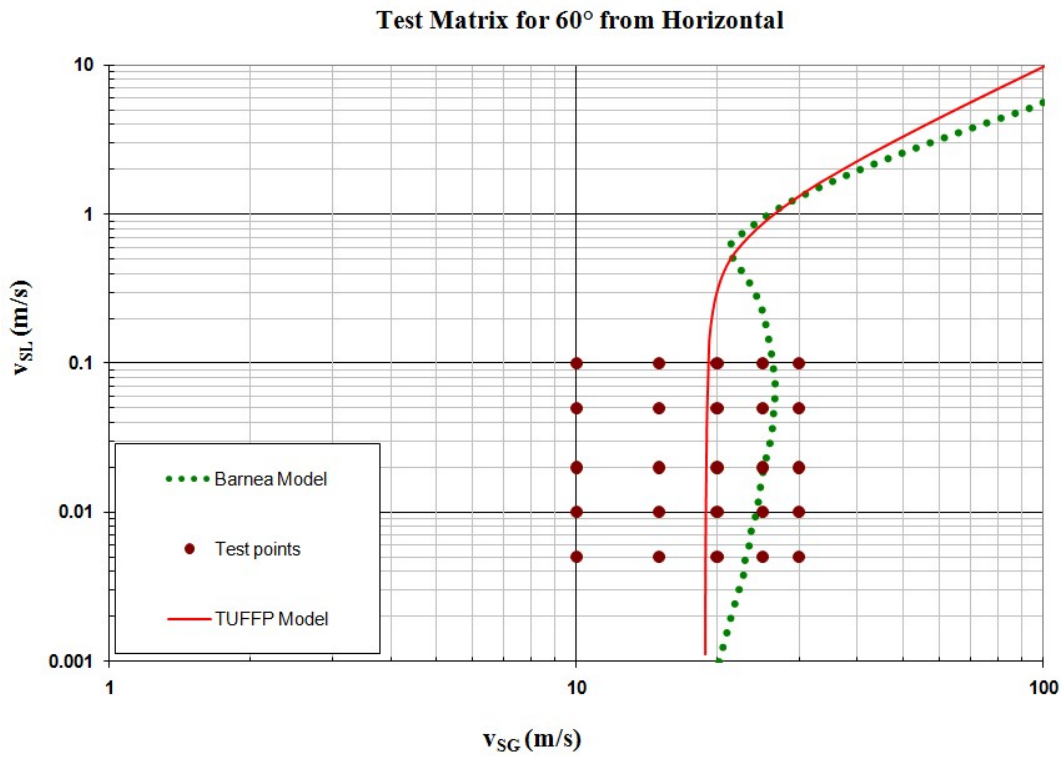

Figure 7: Test Matrix on Annular-Intermittent Transition Map by Different Models (60°)

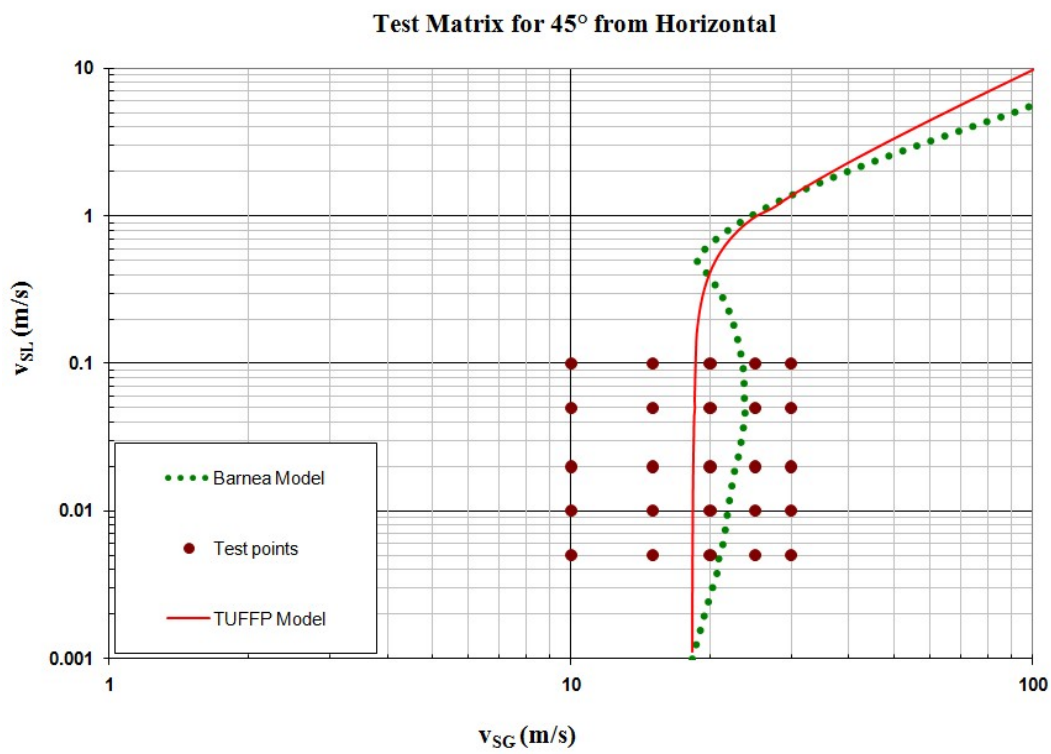

Figure 8: Test Matrix on Annular-Intermittent Transition Map by Different Models (45°)

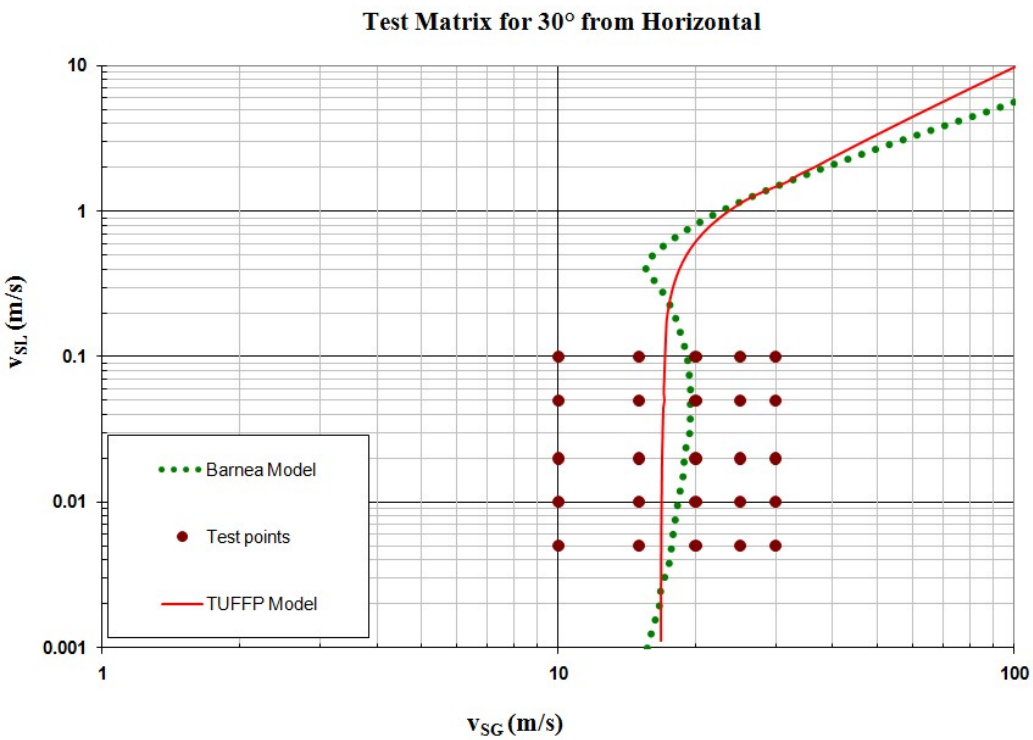

Figure 9: Test Matrix on Annular-Intermittent Transition Map by Different Models (30°)

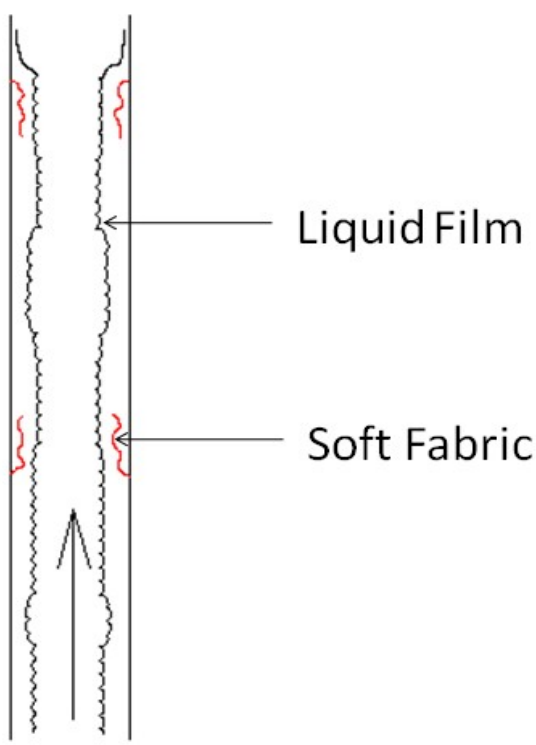

Figure 10: Schematic Map of Film Flow Direction Measurement

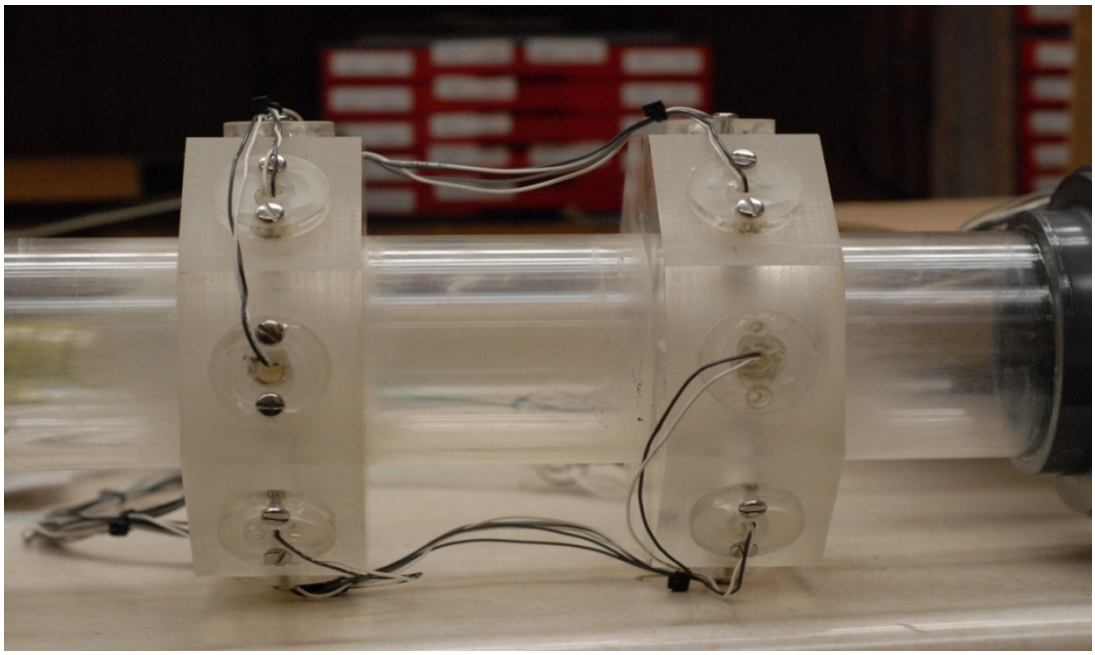

Figure 11: Conductivity Assembly for Film Thickness Measurement

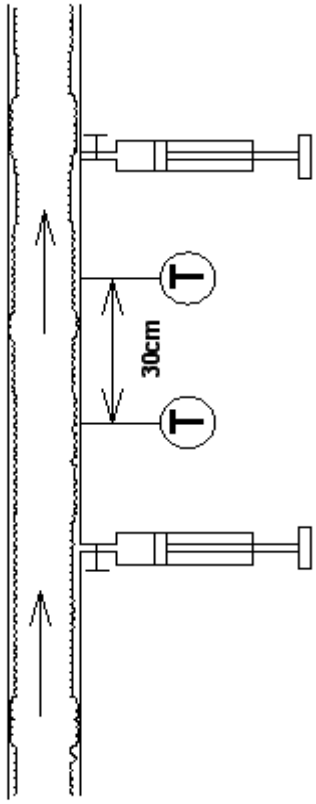

Figure 12: Cold Liquid Injection for Film Velocity Measurement

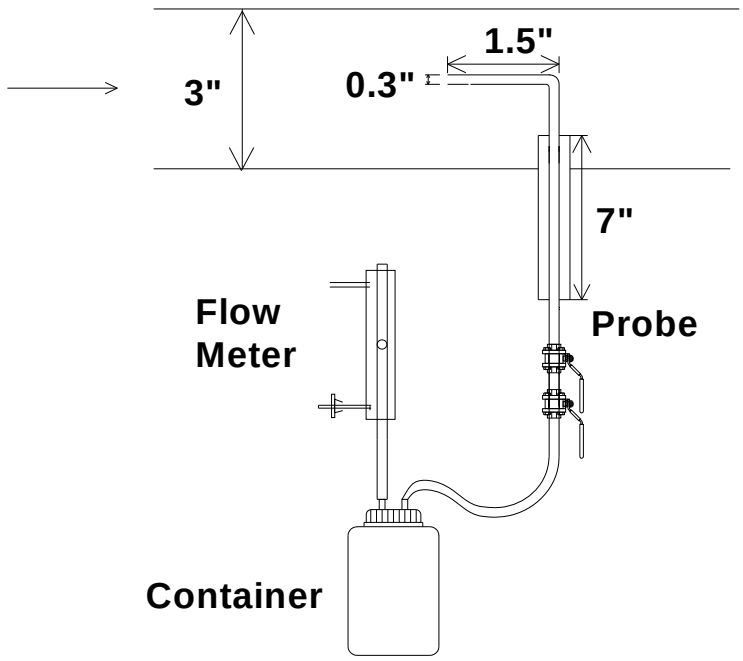

Figure 13: Iso-kinetic Probe for Liquid Entrainment Measurement

Fluid Flow Projects

Business Report

Cem Sarica

Advisory Board Meeting, May 12, 2010

Membership Status

- Current Status
  - Membership Stands at 15
    - 14 Industrial and MMS
  - Efforts Continue to Increase Membership
    - Potential to Reach Out Natural Gas Producers

Personnel Changes

- Dr. Polat Abduvayt Accepts a Position with an Engineering Consulting Company
- Dr. Abdel Al-Sarkhi Rejoins TUFFP Team as Visiting Associate Professor

Papers and Publications

- Gokcal, B., Al-Sarkhi, A. S., Sarica, C., and Al-Safran, M. E.: "Prediction of Slug Frequency for High Viscosity Oils in Horizontal Pipes," To Be Published in *SPE Journal Project Facilities & Construction 2010.*
- Yu, T., Li, M., Zhang, H. Q., and Sarica, C: "A Mechanistic Model for Gas/Liquid Flow in Upward Vertical Annuli," SPE 124181, to Be Published *SPE Production & Operations Journal* in 2010.

Next Advisory Board Meetings

- Tentative Schedule
  - Nov. 2, 2010
    - TUHOP Meeting
    - TUHFP Meeting
    - TUFFP Workshop
    - Facility Tour
    - TUHOP/TUHFP/TUFFP Reception
  - Nov. 3, 2010
    - TUFFP Meeting
    - TUFFP/TUPDP Dinner
  - Nov. 4, 2010
    - TUPDP Meeting
- Venue is The University of Tulsa

Financial Report

- Year 2009 Closing
  - TUFFP Industrial Account
  - TUFFP MMS Account
- Year 2010 Update
  - TUFFP Industrial Account
  - TUFFP MMS Account

2009 Industrial Account Summary

(Prepared April 28, 2010)

Anticipated Reserve Fund Balance on January 1, 2009					**452,358.43**
Income for 2009					
	2009 Membership Fees (14 @ $48,000 - excludes MMS)				**$672,000**
	Two Uncollected 2009 Membership Fees				**(96,000)**
Total Budget					**1,028,358.43**
Projected Budget/Expenditures for 2009					
		Budget	**Revised Budget 2/11/09**	**Expenses 1/8/10**	
90101	Principal Investigator - Sarica	29,251.82	29,074.14	19,562.62	
90103	Co-Principal Investigator - Zhang			-	
90600	Professional Salary - Jones	11,596.24	11,728.00	9,773.32	
90601	Professional Salary - Li	13,157.00	12,875.00	5,031.59	
90602	Professional Salary - Graham	19,923.00	20,149.00	16,790.92	
90603	Professional Salary - Polat	62,000.00	65,000.00	55,434.90	
90701	Technician - Miller	9,943.45	10,016.00	8,036.20	
90702	Technician - Waldron	16,826.00	16,517.00	16,522.92	
90703	Technician - Kelsey	19,097.00	18,746.00	18,746.00	
91000	Graduate Students - Monthly	58,100.00	54,650.00	62,825.00	
91100	Students - Hourly	15,000.00	15,000.00	12,312.97	
91800	Fringe Benefits (33%)	59,992.19	58,805.74	50,132.65	
93100	General Supplies	3,000.00	3,000.00	170,977.31	
93101	Research Supplies	100,000.00	100,000.00	63,248.52	
93102	Copier/Printer Supplies	500.00	500.00	81.99	
93103	Component Parts			1,585.90	
93104	Computer Software	4,000.00	4,000.00	1,023.75	
93106	Office Supplies	2,000.00	2,000.00	1,466.14	
93200	Postage/Shipping	500.00	500.00	3,313.00	
93300	Printing/Duplicating	2,000.00	2,000.00	3,788.79	
93400	Telecommunications	3,000.00	3,000.00	1,649.99	
93500	Membership/Subscriptions	1,000.00	1,000.00	515.00	
93601	Travel - Domestic	10,000.00	10,000.00	9,431.74	
93602	Travel - Foreign	10,000.00	10,000.00	2,203.96	
93700	Entertainment (Advisory Board Meetings)	10,000.00	10,000.00	16,400.50	
94803	Consultants	16,000.00	18,500.00	24,280.33	
94813	Outside Services	20,000.00	20,000.00	25,975.57	
95103	Equipment Rental			2,752.24	
95200	F&A (55.6%)	141,721.35	141,867.93	125,120.26	
98901	Employee Recruiting	3,000.00	3,000.00	3,923.05	
99001	Equipment	600,000.00	400,000.00	319,161.04	
99002	Computers	8,000.00	8,000.00	1,604.61	
99300	Bank Charges	40.00	40.00	30.00	
81801	Tuition/Fees	30,665.00	30,067.00	29,089.00	
81806	Graduate Fellowship			2,608.03	
	Total Expenditures	**1,280,313.05**	**1,080,035.81**	**1,085,399.81**	
Anticipated Reserve Fund Balance as of 12/31/09					**(57,041.38)**

2009 MMS Account Summary

(Prepared January 11, 2010)

Reserve Balance as of 12/31/08			**5,769.94**
2009 Budget			**48,000.00**
Total Budget			**53,769.94**
Projected Budget/Expenditures for 2009			
		Budget	**2009 Anticipated Expenditures**
91000	Students - Monthly	27,900.00	23,925.00
95200	F&A	15,512.40	13,039.13
81801	Tuition/Fees		
Total Anticipated Expenditures as of 12/31/09		**43,412.40**	**36,964.13**
Total Anticipated Reserve Fund Balance as of 12/31/09			**16,805.82**

2010 Industrial Account Projections

(Prepared April 26, 2010)

Anticipated Reserve Fund Balance on January 1, 2010					**($57,041)**
Income for 2010					
	2010 Anticipated Membership Fees (13 @ $48,000 - exludes MMS)				**624,000**
	1 Membership Overpayment				**3,000**
Total Budget					**$ 569,959**
Projected Budget/Expenditures for 2008/2009					
		Projected Budget	**Revised Budget April 2010**	**2010 Expenditures (April 2010)**	
90101 - 90103	Faculty Salaries	29,074.14	918.10	981.10	
90600 - 90609	Professional Salaries	47,628.54	53,310.06	53,310.06	
90700 - 90703	Staff Salaries	35,262.50	35,291.52	35,291.52	
91000	Student Salaries - Monthly	41,550.00	43,725.00	43,725.00	
91100	Student Salaries - Hourly	15,000.00	10,000.00	10,000.00	
91800	Fringe Benefits	38,068.16	30,986.49	30,986.49	
81801	Tuition & Student Fees	17,898.00	26,637.00	26,637.00	
92102	Student Fringe		1,762.00	1,762.00	
93100	General Supplies	3,000.00	3,000.00	156.25	
93101	Research Supplies	50,000.00	60,000.00	34,068.38	
93102	Copier/Printer Supplies	500.00	500.00	-	
93104	Computer Software	4,000.00	3,000.00	538.18	
93106	Office Supplies	2,000.00	2,000.00	654.40	
93200	Postage and Shipping	500.00	500.00	269.83	
93300	Printing and Duplicating	2,000.00	2,000.00	83.31	
93400	Telecommunications	3,000.00	1,700.00	456.99	
93500	Membership	1,000.00	1,000.00	90.00	
93601	Travel - Domestic	10,000.00	10,000.00	1,405.32	
93602	Travel - Foreign	10,000.00	10,000.00	-	
93700	Entertainment	10,000.00	10,000.00	276.87	
94813	Outside Services	20,000.00	20,000.00	9,650.00	
95103	Equipment Rental			500.73	
95200	F&A (55.6%)	93,694.44	79,679.07	79,679.07	
98901	Employee Recruiting	3,000.00			
99001	Equipment	200,000.00	257,868.00	-	
99002	Computers	8,000.00	-	-	
99300	Bank Charges	40.00	40.00		
Total Anticipated Expenditures		**645,215.78**	**663,917.24**	**330,522.50**	
Anticipated Reserve as of 12/31/10					**(93,958.62)**

Salaries are calculated through December 31, 2010

Total TUFFP Income reduced by $136,000 due to uncollected Membership Fees

2010 MMS Account Projections

(Prepared April 9, 2010)

Reserve Balance as of 12/31/09			**16,805.82**
2010 Budget			**48,000.00**
Total Budget			**64,805.82**
Projected Budget/Expenditures for 2010			
		Budget	**2010 Anticipated Expenditures**
91000	Students - Monthly	27,900.00	34,800.00
95200	F&A	15,512.40	18,966.00
Total Anticipated Expenditures as of 12/31/10		**43,412.40**	**53,766.00**
Total Anticipated Reserve Fund Balance as of 12/31/10			**11,039.82**

History – Membership

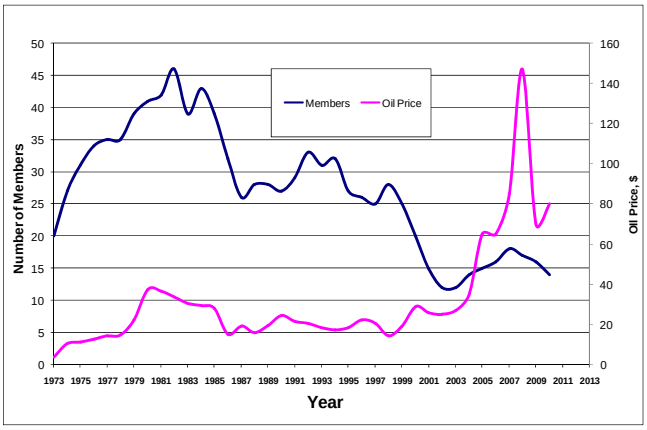

Fluid Flow Projects

Advisory Board Meeting, May 12, 2010

History – Membership Fees

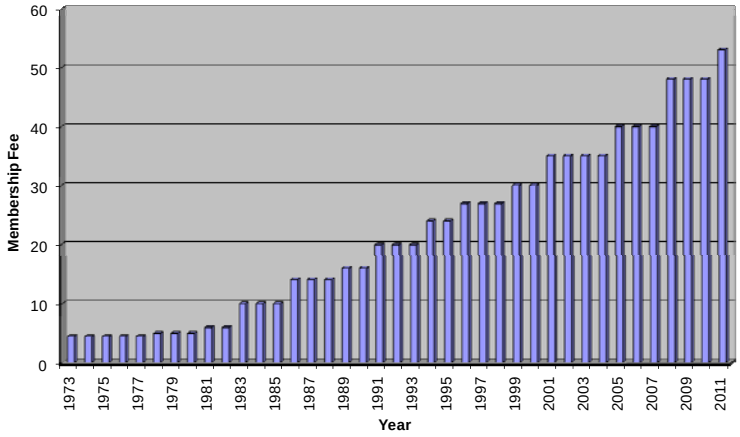

Fluid Flow Projects

Advisory Board Meeting, May 12, 2010

History - Expenditures

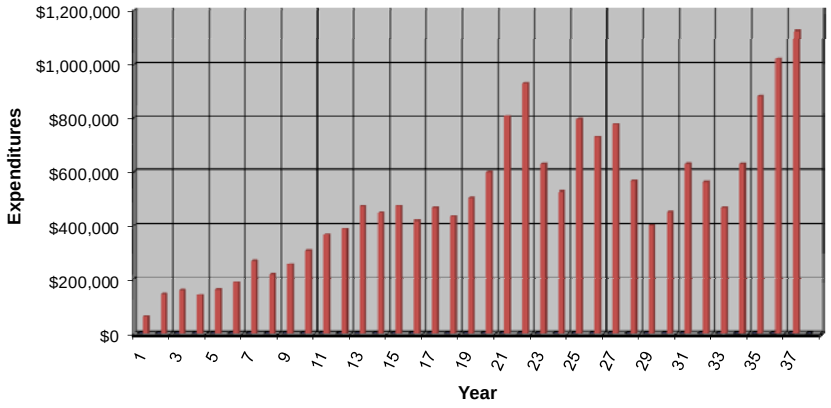

Fluid Flow Projects

Advisory Board Meeting, May 12, 2010

Membership Fees

- 2010 Membership Dues
  - 2 Unpaid
  - Need Prompt Payments

Fluid Flow Projects

Advisory Board Meeting, May 12, 2010

Introduction

This semi-annual report is submitted to Tulsa University Fluid Flow Projects (TUFFP) members to summarize activities since the September 30, 2009 Advisory Board meeting and to assist in planning for the next six months. It also serves as a basis for reporting progress and generating discussion at the 74rd semi-annual Advisory Board meeting to be held in OneOK Club of H. A. Chapman Stadium of the University of Tulsa Main Campus, 3112 East 8th Street, Tulsa, Oklahoma on Wednesday, May 12, 2010.

The activities will start with Tulsa University High Viscosity Projects (TUHOP) Advisory Board meeting on May 11, 2010 between 8:15 a.m. and noon in OneOK Club. Between 1:00 and 3:00 p.m. on May 11, 2010, there will be TUFFP workshop in the same room. There will be presentations made by TUFFP member companies. A facility tour will be held on May 11, 2010 between 3:30 and 5:30 p.m. Following the tour, there will be a TUHOP/TUFFP reception between 6:00 and 9:30 p.m. in OneOK Club.

TUFFP Advisory Board meeting will convene at 8:00 a.m. on May 12th and will adjourn at approximately 5:00 p.m. Following the meeting, there will be a joint TUFFP/TUPDP dinner between 6:00 and 9:00 p.m. in OneOK Club.

The Tulsa University Paraffin Deposition Projects (TUPDP) Advisory Board meeting will be held on May 13th in OneOK Club, between 8:00 a.m. and 1:15 p.m.

The reception and the dinner will provide an opportunity for informal discussions among members, guests, and TU staff and students.

Several TUFFP/TUPDP/TUHOP facilities will be operating during the tour. An opportunity will also be available to view the hydrate flow loop.

The following dates have tentatively been established for Fall 2010 Advisory Board meetings. The venue for Fall 2010 Advisory Board meetings is tentatively set to be the University of Tulsa Main Campus.

2010 Fall Meetings

November 2, 2010	Tulsa University High Viscosity Oil Projects (TUHOP) JIP Meeting
	Tulsa University Fluid Flow Projects (TUFFP) Workshop
	Tulsa University Hydrate Flow Performance (TUHFP) JIP Meeting
	Facility Tour
	TUHOP/TUHFP/TUFFP Reception
November 3, 2010	Tulsa University Fluid Flow Projects (TUFFP) Advisory Board Meeting
	TUFFP/TUPDP Reception
November 4, 2010	Tulsa University Paraffin Deposition Projects (TUPDP) Advisory Board Meeting

Personnel

Dr. Cem Sarica, Professor of Petroleum Engineering, continues as Director of TUFFP and TUPDP, and as Co-Principal Investigator of TUHFP and TUHOP.

Dr. Holden Zhang, Assistant Professor of Petroleum Engineering, serves as Principal Investigator of TUHOP and Associate Director of TUFFP.

Dr. Brill continues to be involved as the director emeritus on a voluntary basis.

Dr. Abdel Al-Sarkhi of King Fahd University of Petroleum and Minerals, former TUFFP Research Associate, is employed as Research Associate Professor for the Summer of 2010.

Dr. Polat Abduvayt continued as TUFFP Post Doctoral Research Associate since the last Advisory Board meeting. Dr. Abduvayt has accepted a job offer from an engineering consulting company in San Francisco, CA. He will be leaving TU effective May 15, 2010. We wish him the best in his future endeavors.

Dr. Mingxiu (Michelle) Li continues to serve as a Research Associate for TUHOP and TUFFP.

Mr. Scott Graham continues to serve as Project Engineer. Scott oversees all of the facility operations and continues to be the senior electronics technician for TUFFP, TUPDP, and TUHOP.

Mr. Craig Waldron continues as Research Technician, addressing our needs in mechanical areas. He also serves as a flow loop operator for TUPDP and Health, Safety, and Environment (HSE) officer for TUFFP, TUPDP and TUHOP.

Mr. Brandon Kelsey serves as an electro-mechanical technician serving TUFFP, TUPDP, and TUHOP projects.

Ms. Linda Jones continues as Project Coordinator of TUFFP, TUPDP and TUHOP projects. She keeps the project accounts in addition to other responsibilities such as external communications, providing computer support for graduate students, publishing and distributing all research reports and deliverables, managing the computer network and web sites, and supervision of part-time office help.

Ms Lori Watts of Petroleum Engineering is the web master for TUFFP/TUPDP/TUHOP websites.

Table 1 updates the current status of all graduate students conducting research on TUFFP projects for the last six months.

Mrs. Gizem Ersoy Gokcal continued her study on slug flow evolution in three-phase gas-oil-water flow in hilly terrain pipelines. She has also been working for Technip in Houston, TX, USA, since September 2009. She successfully defended her Ph.D. dissertation on April 24, 2010.

Ms. Ceyda Kora, from Turkey, is pursuing her MS degree in Petroleum Engineering. Ceyda has received a BS degree in Petroleum and Natural Gas Engineering from Middle East Technical University in 2008. She is studying the effects of high oil viscosity on liquid slug holdup.

Mr. Kiran Gawas, from India, is pursuing his Ph.D. degree in Petroleum Engineering. Kiran has a BS degree in Chemical Engineering from University of Mumbai, Institute of Chemical Technology and a Master of Technology degree from Indian Institute of Technology (IITB). He is studying Low Liquid Loading Three-phase Flow.

Mr. Benin (Ben) Chelinsky Jeyachandra, from India, is pursuing his MS degree in Petroleum Engineering. Ben has received a BS degree in Chemical Engineering from Birla Institute of Technology and Science University in 2008. Ben is studying the high oil viscosity multiphase flow.

Mr. Ge (Max) Yuan, from Peoples Republic of China, is pursuing his MS degree in Petroleum Engineering. Max has received a BS degree in Chemical Engineering and Technology from Dalian University of Technology in 2009. Max is studying Liquid Loading in Gas Wells.

A list of all telephone numbers and e-mail addresses for TUFFP personnel are given in Appendix D.

Table 1

2010 Spring Research Assistant Status

Name	*Origin*	*Stipend*	*Tuition*	*Degree Pursued*	*TUFFP Project*	*Completion Date*
Gizem Ersoy Gokcal	Turkey	No	No	Ph.D. – PE	Slug Flow Evolution in Three-Phase Gas-Oil-Water Flow in Hilly Terrain Pipelines	Spring 2010
Kiran Gawas	India	Yes – TUFFP	Waived (TU)	Ph.D. – PE	Three-phase Gas-Oil-Water Low Liquid Loading	Fall 2012
Ceyda Kora	Turkey	Yes – TUFFP	Waived (MMS)	MS. – PE	Effects of High Viscosity Oil on Liquid Slug Holdup	Fall 2010
Benin (Ben) Chelinsky Jeyachandra	India	Yes – TUFFP	Waived (MMS)	MS – PE	High Viscosity Oil and Gas Flow in Inclined Pipes	Fall 2011
Ge Yuan	PRC	Yes – TUFFP	Yes – TUFFP	MS – PE	Liquid Unloading from Gas Wells	Fall 2011

Membership

The current membership of TUFFP stands at 13 industrial members and Mineral Management Services of Department of Interior (MMS).

Rosneft has terminated their membership. PEMEX has terminated their membership for 2010 due to significant reduction in their technology development budgets.

Our efforts to increase the TUFFP membership level continues.

Table 2 lists all the current 2010 TUFFP members. A list of all Advisory Board representatives for these members with pertinent contact information appears in Appendix B. A detailed history of TUFFP membership is given in Appendix C.

Table 2

2010 Fluid Flow Projects Membership

Baker Atlas	Marathon Oil Company
BP Exploration	Minerals Management Service
Chevron	Petrobras
ConocoPhillips	Schlumberger
Exxon Mobil	Shell Global Solutions
JOGMEG	SPT
KOC	Total

Equipment and Facilities Status

Test Facilities

The 6 in. ID High Pressure Facility construction is underway. Our aim is to complete the construction by the end of 2010. The concrete foundation and steel supporting structures have been completed. All major equipments have been purchased. They are either on-site or scheduled for delivery. The test section will be completed by the end of May. Piping in the circulation area and the instrumentation/control system will be completed by the end of October. Commissioning of the gas compressor will take place in November with shakedown tests of the entire facility beginning in January. The flow loop is expected to be fully operational in March of 2011. A HAZOP analysis will be arranged with the support from Chevron. This will identify the need for additional safety and measurement devices and finalize the operation procedures.

Detailed descriptions of these modification efforts appear in a progress presentation given in this brochure. A site plan showing the location of the various TUFFP and TUPDP test facilities on the North Campus is given in Fig. 1.

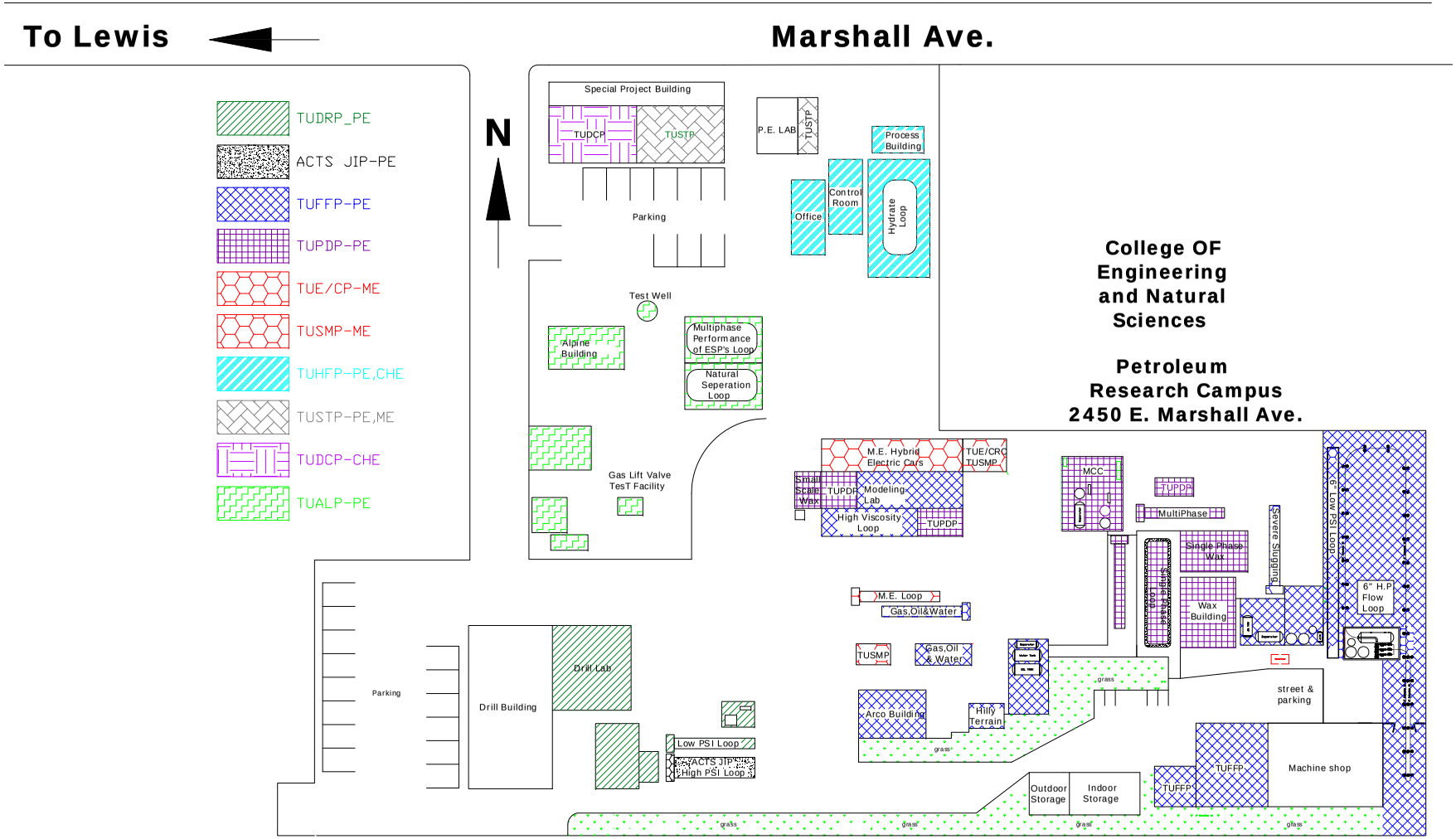

Figure 1 – Site Plan for the North Campus Research Facilities

Financial Status

TUFFP maintains separate accounts for industrial and U.S. government members. Thus, separate accounts are maintained for the MMS funds.

As of April 10, 2009, 14 of the 16 TUFFP members had paid their 2009 membership fees. We have contacted the two delinquent members and pursuing payments. Their memberships are currently suspended.

Table 3 presents a financial analysis of income and expenditures for the 2009 Industrial member account as of April 10, 2010. This serves as unofficial closing budget for 2009. Also shown are previous 2009 budgets that have been reported to the members. The total industry expenditures for 2009 were $1,085,399.81. This resulted in $57,041.38 in deficit for the industry reserve account due to two uncollected membership fee.

Table 4 presents a financial analysis of expenditures and income for the MMS Account for 2009. This account is used primarily for graduate student stipends. A balance of $16,805.82 is carried over to 2010.

The University of Tulsa waives up to 19 hours of tuition for each graduate student that is paid a stipend from the United States government, MMS funds. Moreover, The University of Tulsa has granted tuition waiver for one Ph.D. student. A total of 45 hours of tuition (equivalent of $32,850) were waived for 2009.

Tables 5-6 present the projected budgets and income for the Industrial, and MMS accounts for 2010. The 2010 TUFFP industrial membership is assumed to stay at 13 in this analysis. This will provide $627,000.00 of industrial membership income for 2010. The sum of the 2010 income and the reserve account is projected to be $569,959.00. The expenses for the industrial member account are estimated to be $663,917.24 leaving a negative balance of $93,958.62. The MMS account is expected to have a carryover of $11,039.82.

Despite of the cost cutting measures implemented this year, 2010 budget has a shortfall as presented primarily due to the high pressure facility construction. Since we cannot operate with a negative budget, we have asked the University of Tulsa to help. The University has agreed to loan TUFFP the necessary funds to complete the high pressure facility provided that TUFFP pays back the loaned funds in 2011. Moreover, the operating costs have steadily been increasing every year. Therefore, it is proposed to increase the membership fee from $48,000 to $55,000 effective 2011.

Table 3: TUFFP 2009 Industrial Budget Summary

(Prepared April 28, 2010)

Anticipated Reserve Fund Balance on January 1, 2009					**452,358.43**
Income for 2009					
	2009 Membership Fees (14 @ $48,000 - excludes MMS)				**$672,000**
	Two Uncollected 2009 Membership Fees				**(96,000)**
Total Budget					**1,028,358.43**
Projected Budget/Expenditures for 2009					
		Budget	**Revised Budget 2/11/09**	**Expenses 1/8/10**	
90101	Principal Investigator - Sarica	29,251.82	29,074.14	19,562.62	
90103	Co-Principal Investigator - Zhang			-	
90600	Professional Salary - Jones	11,596.24	11,728.00	9,773.32	
90601	Professional Salary - Li	13,157.00	12,875.00	5,031.59	
90602	Professional Salary - Graham	19,923.00	20,149.00	16,790.92	
90603	Professional Salary - Polat	62,000.00	65,000.00	55,434.90	
90701	Technician - Miller	9,943.45	10,016.00	8,036.20	
90702	Technician - Waldron	16,826.00	16,517.00	16,522.92	
90703	Technician - Kelsey	19,097.00	18,746.00	18,746.00	
91000	Graduate Students - Monthly	58,100.00	54,650.00	62,825.00	
91100	Students - Hourly	15,000.00	15,000.00	12,312.97	
91800	Fringe Benefits (33%)	59,992.19	58,805.74	50,132.65	
93100	General Supplies	3,000.00	3,000.00	170,977.31	
93101	Research Supplies	100,000.00	100,000.00	63,248.52	
93102	Copier/Printer Supplies	500.00	500.00	81.99	
93103	Component Parts			1,585.90	
93104	Computer Software	4,000.00	4,000.00	1,023.75	
93106	Office Supplies	2,000.00	2,000.00	1,466.14	
93200	Postage/Shipping	500.00	500.00	3,313.00	
93300	Printing/Duplicating	2,000.00	2,000.00	3,788.79	
93400	Telecommunications	3,000.00	3,000.00	1,649.99	
93500	Membership/Subscriptions	1,000.00	1,000.00	515.00	
93601	Travel - Domestic	10,000.00	10,000.00	9,431.74	
93602	Travel - Foreign	10,000.00	10,000.00	2,203.96	
93700	Entertainment (Advisory Board Meetings)	10,000.00	10,000.00	16,400.50	
94803	Consultants	16,000.00	18,500.00	24,280.33	
94813	Outside Services	20,000.00	20,000.00	25,975.57	
95103	Equipment Rental			2,752.24	
95200	F&A (55.6%)	141,721.35	141,867.93	125,120.26	
98901	Employee Recruiting	3,000.00	3,000.00	3,923.05	
99001	Equipment	600,000.00	400,000.00	319,161.04	
99002	Computers	8,000.00	8,000.00	1,604.61	
99300	Bank Charges	40.00	40.00	30.00	
81801	Tuition/Fees	30,665.00	30,067.00	29,089.00	
81806	Graduate Fellowship			2,608.03	
	Total Expenditures	**1,280,313.05**	**1,080,035.81**	**1,085,399.81**	
Anticipated Reserve Fund Balance as of 12/31/09					**(57,041.38)**

Table 4: TUFFP 2009 MMS Budget Summary

2009 TUFFP MMS Budget Summary
(Prepared January 11, 2010)

Reserve Balance as of 12/31/08			**5,769.94**
2009 Budget			**48,000.00**
Total Budget			**53,769.94**

Projected Budget/Expenditures for 2009

		Budget	**2009 Anticipated Expenditures**
91000	Students - Monthly	27,900.00	23,925.00
95200	F&A	15,512.40	13,039.13
81801	Tuition/Fees		
Total Anticipated Expenditures as of 12/31/09		**43,412.40**	**36,964.13**

Total Anticipated Reserve Fund Balance as of 12/31/09	**16,805.82**

Table 5: 2010 TUFFP Industrial Budget

(Prepared April 26, 2010)

Anticipated Reserve Fund Balance on January 1, 2010					**($57,041)**
Income for 2010					
	2010 Anticipated Membership Fees (13 @ $48,000 - exludes MMS)				**624,000**
	1 Membership Overpayment				**3,000**
Total Budget					**$ 569,959**
Projected Budget/Expenditures for 2008/2009					
		Projected Budget	**Revised Budget April 2010**	**2010 Expenditures (April 2010)**	
90101 - 90103	Faculty Salaries	29,074.14	918.10	981.10	
90600 - 90609	Professional Salaries	47,628.54	53,310.06	53,310.06	
90700 - 90703	Staff Salaries	35,262.50	35,291.52	35,291.52	
91000	Student Salaries - Monthly	41,550.00	43,725.00	43,725.00	
91100	Student Salaries - Hourly	15,000.00	10,000.00	10,000.00	
91800	Fringe Benefits	38,068.16	30,986.49	30,986.49	
81801	Tuition & Student Fees	17,898.00	26,637.00	26,637.00	
92102	Student Fringe		1,762.00	1,762.00	
93100	General Supplies	3,000.00	3,000.00	156.25	
93101	Research Supplies	50,000.00	60,000.00	34,068.38	
93102	Copier/Printer Supplies	500.00	500.00	-	
93104	Computer Software	4,000.00	3,000.00	538.18	
93106	Office Supplies	2,000.00	2,000.00	654.40	
93200	Postage and Shipping	500.00	500.00	269.83	
93300	Printing and Duplicating	2,000.00	2,000.00	83.31	
93400	Telecommunications	3,000.00	1,700.00	456.99	
93500	Membership	1,000.00	1,000.00	90.00	
93601	Travel - Domestic	10,000.00	10,000.00	1,405.32	
93602	Travel - Foreign	10,000.00	10,000.00	-	
93700	Entertainment	10,000.00	10,000.00	276.87	
94813	Outside Services	20,000.00	20,000.00	9,650.00	
95103	Equipment Rental			500.73	
95200	F&A (55.6%)	93,694.44	79,679.07	79,679.07	
98901	Employee Recruiting	3,000.00			
99001	Equipment	200,000.00	257,868.00	-	
99002	Computers	8,000.00	-	-	
99300	Bank Charges	40.00	40.00		
Total Anticipated Expenditures		**645,215.78**	**663,917.24**	**330,522.50**	
Anticipated Reserve as of 12/31/10					**(93,958.62)**

Salaries are calculated through December 31, 2010

Total TUFFP Income reduced by $136,000 due to uncollected Membership Fees

Table 6: TUFFP 2010 MMS Budget

2010 TUFFP MMS Budget Summary
(Prepared April 9, 2010)

Reserve Balance as of 12/31/09			**16,805.82**
2010 Budget			**48,000.00**
Total Budget			**64,805.82**

Projected Budget/Expenditures for 2010

		Budget	**2010 Anticipated Expenditures**
91000	Students - Monthly	27,900.00	34,800.00
95200	F&A	15,512.40	18,966.00
Total Anticipated Expenditures as of 12/31/10		**43,412.40**	**53,766.00**

Total Anticipated Reserve Fund Balance as of 12/31/10 **11,039.82**

Miscellaneous Information

Fluid Flow Projects Short Course

The 34th TUFFP "Two-Phase Flow in Pipes" short course offering is scheduled for May 17-21, 2010. Current enrollment stands at 7.

Dr. Abdel Al-Sarkhi Returns to TUFFP

We are happy to announce that Dr. Abdel Al-Sarkhi has accepted our offer to take a Research Associate Professor position in the department to be part of TUFFP team again. He will spend his summers in Tulsa working with TUFFP Research Assistants and Associates.

BHR Group Conference on Multiphase Technology

Since 1991, TUFFP has participated as a co-supporter of BHR Group Conferences on Multiphase Production. TUFFP personnel participate in reviewing papers, serving as session chairs, and advertising the conference to our members. This conference is one of the premier international event providing delegates with opportunities to discuss new research and developments, to consider innovative solutions in multiphase production area.

7th North American Conference on Multiphase Technology, sponsored and supported by Neotechnology Consultants of Calgary, Canada, sponsored by Bornemann Pumps Kongsberg and SPT Group and supported by TUFFP, is scheduled to be held 2-4 of June 2010 in Banff, Canada. The conference will benefit anyone engaged in the application, development and research of multiphase technology for the oil and gas industry. Applications in the oil and gas industry will also be of interest to engineers from other industries for which multiphase technology offers a novel solution to their problems. The conference will also be of particular value to designers, facility and operations engineers, consultants and researchers from operating, contracting, consultancy and technology companies. The conference brings together experts from across the American Continents and Worldwide.

The scope of the conference includes variety of subjects pertinent to Multiphase Production in both technology development and applications of the existing technologies. The detailed information about the conference can be found in BHRg's (www.brhgroup.com).

There are three papers either fully or partially resulted from the research conducted at TUFFP.

Publications & Presentations

Since the last Advisory Board meeting, the following publications and presentations are made.

1) Gokcal, B., Al-Sarkhi, A. S., Sarica, C., and Al-Safran, M. E.: "Prediction of Slug Frequency for High Viscosity Oils in Horizontal Pipes," To Be Published in *SPE Journal Project Facilities & Construction 2010.*
2) Yu, T., Li, M., Zhang, H. Q., and Sarica, C: "A Mechanistic Model for Gas/Liquid Flow in Upward Vertical Annuli," SPE 124181, to Be Published *SPE Production & Operations Journal* in 2010.

Tulsa University Paraffin Deposition Projects (TUPDP) Activities

The forth three year phase of TUPDP has recently started. The studies concentrate on the paraffin deposition characterization of single-phase turbulent flow with new oils, gas-oil-water paraffin deposition, restart of gelled flow lines and field verification. The yearly budget of the project is projected to be $660,000.

Tulsa University Heavy Oil Projects (TUHOP) Activities

TUHOP is an outgrowth of one of the projects initiated through Tulsa University Center of Research Excellence (TUCoRE) initiated by Chevron. Up to this date, Chevron has provided TU to $680,000 for improvement of an existing high pressure multiphase flow facility. Current members of the JIP are BP, Chevron, ConocoPhillips, and Petrobras. The primary objective of the JIP is to investigate the effects of high oil viscosity on multiphase flow behavior.

Two-Phase Flow Calendar

Several technical meetings, seminars, and short courses involving two-phase flow in pipes are scheduled for 2010 and 2011. Table 9 lists meetings that would be of interest to TUFFP members.

Table 9

Meeting and Conference Calendar

2010

May 11	TUHOP Advisory Board Meeting, Tulsa, Oklahoma
	TUFFP Spring Workshop, Tulsa, Oklahoma
May 12	TUFFP Spring Advisory Board Meeting, Tulsa, Oklahoma
May 13	TUPDP Spring Advisory Board Meeting, Tulsa, Oklahoma
May 17 - 21	TUFFP Short Course, Tulsa, Oklahoma
May 30 – June 4	International Conference on Multiphase Flow, Tampa, Florida
June 2 - 4	BHRg's 7th North American Conference on Multiphase Technology, Banff, Canada
September 20 - 22	SPE Annual Technical Conference and Exhibition, Florence, Italy
November 2	TUHOP Advisory Board Meeting, Tulsa, Oklahoma
	TUFFP Fall Workshop, Tulsa, Oklahoma
	TUHFP Advisory Board Meeting, Tulsa, Oklahoma
November 3	TUFFP Advisory Board Meeting, Tulsa, Oklahoma
November 4	TUPDP Advisory Board Meeting, Tulsa, Oklahoma

Appendix A

Fluid Flow Projects Deliverables[1]

1. "An Experimental Study of Oil-Water Flowing Mixtures in Horizontal Pipes," by M. S. Malinowsky (1975).

2. "Evaluation of Inclined Pipe Two-Phase Liquid Holdup Correlations Using Experimental Data," by C. M. Palmer (1975).

3. "Experimental Evaluation of Two-Phase Pressure Loss Correlations for Inclined Pipe," by G. A. Payne (1975).

4. "Experimental Study of Gas-Liquid Flow in a Pipeline-Riser Pipe System," by Z. Schmidt (1976).

5. "Two-Phase Flow in an Inclined Pipeline-Riser Pipe System," by S. Juprasert (1976).

6. "Orifice Coefficients for Two-Phase Flow Through Velocity Controlled Subsurface Safety Valves," by J. P. Brill, H. D. Beggs, and N. D. Sylvester (Final Report to American Petroleum Institute Offshore Safety and Anti-Pollution Research Committee, OASPR Project No. 1; September, 1976).

7. "Correlations for Fluid Physical Property Prediction," by M. E. Vasquez A. (1976).

8. "An Empirical Method of Predicting Temperatures in Flowing Wells," by K. J. Shiu (1976).

9. "An Experimental Study on the Effects of Flow Rate, Water Fraction and Gas-Liquid Ratio on Air-Oil-Water Flow in Horizontal Pipes," by G. C. Laflin and K. D. Oglesby (1976).

10. "Study of Pressure Drop and Closure Forces in Velocity- Type Subsurface Safety Valves," by H. D. Beggs and J. P. Brill (Final Report to American Petroleum Institute Offshore Safety and Anti-Pollution Research Committee, OSAPR Project No. 5; July, 1977).

11. "An Experimental Study of Two-Phase Oil-Water Flow in Inclined Pipes," by H. Mukhopadhyay (September 1, 1977).

12. "A Numerical Simulation Model for Transient Two-Phase Flow in a Pipeline," by M. W. Scoggins, Jr. (October 3, 1977).

13. "Experimental Study of Two-Phase Slug Flow in a Pipeline-Riser Pipe System," by Z. Schmidt (1977).

14. "Drag Reduction in Two-Phase Gas-Liquid Flow," (Final Report to American Gas Association Pipeline Research Committee; 1977).

15. "Comparison and Evaluation of Instrumentation for Measuring Multiphase Flow Variables in Pipelines," Final Report to Atlantic Richfield Co. by J. P. Brill and Z. Schmidt (January, 1978).

16. "An Experimental Study of Inclined Two-Phase Flow," by H. Mukherjee (December 30, 1979).

---

[1] Completed TUFFP Projects – each project consists of three deliverables – report, data and software. Please see the TUFFP website

17. "An Experimental Study on the Effects of Oil Viscosity, Mixture Velocity and Water Fraction on Horizontal Oil-Water Flow," by K. D. Oglesby (1979).

18. "Experimental Study of Gas-Liquid Flow in a Pipe Tee," by S. E. Johansen (1979).

19. "Two Phase Flow in Piping Components," by P. Sookprasong (1980).

20. "Evaluation of Orifice Meter Recorder Measurement Errors in Lower and Upper Capacity Ranges," by J. Fujita (1980).

21. "Two-Phase Metering," by I. B. Akpan (1980).

22. "Development of Methods to Predict Pressure Drop and Closure Conditions for Velocity-Type Subsurface Safety Valves," by H. D. Beggs and J. P. Brill (Final Report to American Petroleum Institute Offshore Safety and Anti-Pollution Research Committee, OSAPR Project No. 10; February, 1980).

23. "Experimental Study of Subcritical Two-Phase Flow Through Wellhead Chokes," by A. A. Pilehvari (April 20, 1981).

24. "Investigation of the Performance of Pressure Loss Correlations for High Capacity Wells," by L. Rossland (1981).

25. "Design Manual: Mukherjee and Brill Inclined Two-Phase Flow Correlations," (April, 1981).

26. "Experimental Study of Critical Two-Phase Flow through Wellhead Chokes," by A. A. Pilehvari (June, 1981).

27. "Experimental Study of Pressure Wave Propagation in Two-Phase Mixtures," by S. Vongvuthipornchai (March 16, 1982).

28. "Determination of Optimum Combination of Pressure Loss and PVT Property Correlations for Predicting Pressure Gradients in Upward Two-Phase Flow," by L. G. Thompson (April 16, 1982).

29. "Hydrodynamic Model for Intermittent Gas Lifting of Viscous Oils," by O. E. Fernandez (April 16, 1982).

30. "A Study of Compositional Two-Phase Flow in Pipelines," by H. Furukawa (May 26, 1982).

31. "Supplementary Data, Calculated Results, and Calculation Programs for TUFFP Well Data Bank," by L. G. Thompson (May 25, 1982).

32. "Measurement of Local Void Fraction and Velocity Profiles for Horizontal Slug Flow," by P. B. Lukong (May 26, 1982).

33. "An Experimental Verification and Modification of the McDonald-Baker Pigging Model for Horizontal Flow," by S. Barua (June 2, 1982).

34. "An Investigation of Transient Phenomena in Two-Phase Flow," by K. Dutta-Roy (October 29, 1982).

35. "A Study of the Heading Phenomenon in Flowing Oil Wells," by A. J. Torre (March 18, 1983).

36. "Liquid Holdup in Wet-Gas Pipelines," by K. Minami (March 15, 1983).

37. "An Experimental Study of Two-Phase Oil-Water Flow in Horizontal Pipes," by S. Arirachakaran (March 31, 1983).

38. "Simulation of Gas-Oil Separator Behavior Under Slug Flow Conditions," by W. F. Giozza (March 31, 1983).

39. "Modeling Transient Two-Phase Flow in Stratified Flow Pattern," by Y. Sharma (July, 1983).

40. "Performance and Calibration of a Constant Temperature Anemometer," by F. Sadeghzadeh (August 25, 1983).

41. "A Study of Plunger Lift Dynamics," by L. Rosina (October 7, 1983).

42. "Evaluation of Two-Phase Flow Pressure Gradient Correlations Using the A.G.A. Gas-Liquid Pipeline Data Bank," by E. Caetano F. (February 1, 1984).

43. "Two-Phase Flow Splitting in a Horizontal Pipe Tee," by O. Shoham (May 2, 1984).

44. "Transient Phenomena in Two-Phase Horizontal Flowlines for the Homogeneous, Stratified and Annular Flow Patterns," by K. Dutta-Roy (May 31, 1984).

45. "Two-Phase Flow in a Vertical Annulus," by E. Caetano F. (July 31, 1984).

46. "Two-Phase Flow in Chokes," by R. Sachdeva (March 15, 1985).

47. "Analysis of Computational Procedures for Multi-Component Flow in Pipelines," by J. Goyon (June 18, 1985).

48. "An Investigation of Two-Phase Flow Through Willis MOV Wellhead Chokes," by D. W. Surbey (August 6, 1985).

49. "Dynamic Simulation of Slug Catcher Behavior," by H. Genceli (November 6, 1985).

50. "Modeling Transient Two-Phase Slug Flow," by Y. Sharma (December 10, 1985).

51. "The Flow of Oil-Water Mixtures in Horizontal Pipes," by A. E. Martinez (April 11, 1986).

52. "Upward Vertical Two-Phase Flow Through An Annulus," by E. Caetano F. (April 28, 1986).

53. "Two-Phase Flow Splitting in a Horizontal Reduced Pipe Tee," by O. Shoham (July 17, 1986).

54. "Horizontal Slug Flow Modeling and Metering," by G. E. Kouba (September 11, 1986).

55. "Modeling Slug Growth in Pipelines," by S. L. Scott (October 30, 1987).

56. "RECENT PUBLICATIONS" - A collection of articles based on previous TUFFP research reports that have been published or are under review for various technical journals (October 31, 1986).

57. "TUFFP CORE Software Users Manual, Version 2.0," by Lorri Jefferson, Florence Kung and Arthur L. Corcoran III (March 1989)

58. "Simplified Modeling and Simulation of Transient Two Phase Flow in Pipelines," by Y. Taitel (April 29, 1988).

59. "RECENT PUBLICATIONS" - A collection of articles based on previous TUFFP research reports that have been published or are under review for various technical journals (April 19, 1988).

60. "Severe Slugging in a Pipeline-Riser System, Experiments and Modeling," by S. J. Vierkandt (November 1988).

61. "A Comprehensive Mechanistic Model for Upward Two-Phase Flow," by A. Ansari (December 1988).

62. "Modeling Slug Growth in Pipelines" Software Users Manual, by S. L. Scott (June 1989).

63. "Prudhoe Bay Large Diameter Slug Flow Experiments and Data Base System" Users Manual, by S. L. Scott (July 1989).

64. "Two-Phase Slug Flow in Upward Inclined Pipes", by G. Zheng (Dec. 1989).

65. "Elimination of Severe Slugging in a Pipeline-Riser System," by F. E. Jansen (May 1990).

66. "A Mechanistic Model for Predicting Annulus Bottomhole Pressures for Zero Net Liquid Flow in Pumping Wells," by D. Papadimitriou (May 1990).

67. "Evaluation of Slug Flow Models in Horizontal Pipes," by C. A. Daza (May 1990).

68. "A Comprehensive Mechanistic Model for Two-Phase Flow in Pipelines," by J. J. Xiao (Aug. 1990).

69. "Two-Phase Flow in Low Velocity Hilly Terrain Pipelines," by C. Sarica (Aug. 1990).

70. “Two-Phase Slug Flow Splitting Phenomenon at a Regular Horizontal Side-Arm Tee,” by S. Arirachakaran (Dec. 1990)

71. "RECENT PUBLICATIONS" - A collection of articles based on previous TUFFP research reports that have been published or are under review for various technical journals (May 1991).

72. "Two-Phase Flow in Horizontal Wells," by M. Ihara (October 1991).

73. "Two-Phase Slug Flow in Hilly Terrain Pipelines," by G. Zheng (October 1991).

74. "Slug Flow Phenomena in Inclined Pipes," by I. Alves (October 1991).

75. "Transient Flow and Pigging Dynamics in Two-Phase Pipelines," by K. Minami (October 1991).

76. "Transient Drift Flux Model for Wellbores," by O. Metin Gokdemir (November 1992).

77. "Slug Flow in Extended Reach Directional Wells," by Héctor Felizola (November 1992).

78. "Two-Phase Flow Splitting at a Tee Junction with an Upward Inclined Side Arm," by Peter Ashton (November 1992).

79. "Two-Phase Flow Splitting at a Tee Junction with a Downward Inclined Branch Arm," by Viswanatha Raju Penmatcha (November 1992).

80. "Annular Flow in Extended Reach Directional Wells," by Rafael Jose Paz Gonzalez (May 1994).

81. "An Experimental Study of Downward Slug Flow in Inclined Pipes," by Philippe Roumazeilles (November 1994).

82. "An Analysis of Imposed Two-Phase Flow Transients in Horizontal Pipelines Part-1 Experimental Results," by Fabrice Vigneron (March 1995).

83. "Investigation of Single Phase Liquid Flow Behavior in a Single Perforation Horizontal Well," by Hong Yuan (March 1995).

84. “1995 Data Documentation User’s Manual”, (October 1995).

85. “Recent Publications” A collection of articles based on previous TUFFP research reports that have been published or are under review for various technical journals (February 1996).

86. “1995 Final Report - Transportation of Liquids in Multiphase Pipelines Under Low Liquid Loading Conditions”, Final report submitted to Penn State University for subcontract on GRI Project.

87. “A Unified Model for Stratified-Wavy Two-Phase Flow Splitting at a Reduced Tee Junction with an Inclined Branch Arm”, by Srinagesh K. Marti (February 1996).

88. “Oil-Water Flow Patterns in Horizontal Pipes”, by José Luis Trallero (February 1996).

89. “A Study of Intermittent Flow in Downward Inclined Pipes” by Jiede Yang (June 1996).

90. “Slug Characteristics for Two-Phase Horizontal Flow”, by Robert Marcano (November 1996).

91. “Oil-Water Flow in Vertical and Deviated Wells”, by José Gonzalo Flores (October 1997).

92. “1997 Data Documentation and Software User’s Manual”, by Avni S. Kaya, Gerad Gibson and Cem Sarica (November 1997).

93. “Investigation of Single Phase Liquid Flow Behavior in Horizontal Wells”, by Hong Yuan (March 1998).

94. “Comprehensive Mechanistic Modeling of Two-Phase Flow in Deviated Wells” by Avni Serdar Kaya (December 1998).

95. “Low Liquid Loading Gas-Liquid Two-Phase Flow in Near-Horizontal Pipes” by Weihong Meng (August 1999).

96. “An Experimental Study of Two-Phase Flow in a Hilly-Terrain Pipeline” by Eissa Mohammed Al-Safran (August 1999).

97. “Oil-Water Flow Patterns and Pressure Gradients in Slightly Inclined Pipes” by Banu Alkaya (May 2000).

98. “Slug Dissipation in Downward Flow – Final Report” by Hong-Quan Zhang, Jasmine Yuan and James P. Brill (October 2000).

99. “Unified Model for Gas-Liquid Pipe Flow – Model Development and Validation” by Hong-Quan Zhang (January 2002).

100. “A Comprehensive Mechanistic Heat Transfer Model for Two-Phase Flow with High-Pressure Flow Pattern Validation” Ph.D. Dissertation by Ryo Manabe (December 2001).

101. “Revised Heat Transfer Model for Two-Phase Flow” Final Report by Qian Wang (March 2003).

102. “An Experimental and Theoretical Investigation of Slug Flow Characteristics in the Valley of a Hilly-Terrain Pipeline” Ph.D. Dissertation by Eissa Mohammed Al-safran (May 2003).

103. “An Investigation of Low Liquid Loading Gas-Liquid Stratified Flow in Near-Horizontal Pipes” Ph.D. Dissertation by Yongqian Fan.

104. “Severe Slugging Prediction for Gas-Oil-Water Flow in Pipeline-Riser Systems,” M.S. Thesis by Carlos Andrés Beltrán Romero (2005)

105. “Droplet-Homophase Interaction Study (Development of an Entrainment Fraction Model) – Final Report,” Xianghui Chen (2005)

106. “Effects of High Oil Viscosity on Two-Phase Oil-Gas Flow Behavior in Horizontal Pipes” M.S. Thesis by Bahadir Gokcal (2005)

107. “Characterization of Oil-Water Flows in Horizontal Pipes” M.S. Thesis by Maria Andreina Vielma Paredes (2006)

108. “Characterization of Oil-Water Flows in Inclined Pipes” M.S. Thesis by Serdar Atmaca (2007).

109. “An Experimental Study of Low Liquid Loading Gas-Oil-Water Flow in Horizontal Pipes” M.S. Thesis by Hongkun Dong (2007).

110. “An Experimental and Theoretical Investigation of Slug Flow for High Oil Viscosity in Horizontal Pipes” Ph.D. Dissertation by Bahadir Gokcal (2008).

111. “Modeling of Gas-Liquid Flow in Upward Vertical Annuli” M.S. Thesis by Tingting Yu (2009).

112. “Modeling of Hydrodynamics of Oil-Water Pipe Flow using Energy Minimization Concept” M.S. Thesis by Anoop Kumar Sharma (2009).

113. “Liquid Entrainment in Annular Gas-Liquid Flow in Inclined Pipes” M.S. Thesis by Kyle L. Magrini (2009).

Appendix B

2010 Fluid Flow Projects Advisory Board Representatives

Baker Atlas

Michael R. Wells
Director of Research
Baker Hughes
Phone: (281) 363-6769
Fax: (281) 363-6099
Email Mike.Wells@bakerhughes.com

Dan Georgi
Baker Atlas
2001 Rankin Road
Houston, Texas 77073
Phone: (713) 625-5841
Fax: (713) 625-6795
Email: dan.georgi@bakeratlas.com

Datong Sun
Baker Atlas
2001 Rankin Road
Houston, Texas 77073
Phone: (713) 625-5791
Fax: (713) 625-6795
Email: datong.sun@bakeratlas.com

BP

Official Representative & UK Contact
Paul Fairhurst
BP
Flow Assurance Engineering – UTG
Building H
Chertsey Road
Sunbury on Thames, Middlesex TW16 7LN
England
Phone: (44 1 932) 774818
Fax: (44 7 787) 105183
Email: fairhucp@bp.com

Alternate UK Contact
Andrew Hall
BP
Pipeline Transportation Team, EPT
1H-54 Dyce
Aberdeen, AB21 7PB
United Kingdom
Phone: (44 1224) 8335807
Fax:
Email: halla9@bp.com

Alternate UK Contact
Trevor Hill
BP
E&P Engineering Technical Authority – Flow Assurance
Chertsey Road
Sunbury on Thames, Middlesex TW16 7BP
United Kingdom
Phone: (44) 7879 486974
Fax:
Email: trevor.hill@uk.bp.com

US Contact
Taras Makogon
BP
501 Westlake Park Blvd.
Houston, Texas 77079
Phone: (281) 366-8638
Fax:
Email: taras.makogon@bp.com

US Contact
George Shoup
BP
501 Westlake Park Blvd.
Houston, Texas 77079
Phone: (281) 366-7238
Fax:
Email: shoupgj@bp.com

US Contact
Oris Hernandez
Flow Assurance Engineer
BP
501 Westlake Park Blvd.
Houston, Texas 77079
Phone: (281) 366-5649
Fax:
Email: oris.hernandez@bp.com

Chevron

Lee Rhyne
Chevron
Flow Assurance Team
1400 Smith Street, Room 23188
Houston, Texas 77002
Phone: (713) 372-2674
Fax: (713) 372-5991
Email: lee.rhyne@chevron.com

Sam Kashou
Chevron
1500 Louisiana Street
Houston, Texas 77002
Phone: (832) 854-3917
Fax: (832) 854-6425
Email: samkashou@chevron.com

Jeff Creek
Chevron
Flow Assurance Team
1600 Smith Street
Houston, Texas 77002
Phone: (713) 754-7347
Fax: (713) 754-7300
Email: lcre@chevron.com

Hariprasad Subramani
Chevron
Flow Assurance
1400 Smith Street, Room 23192
Phone: (713) 372-2657
Fax: (713) 372-5991
Email: hjsubramani@chevron.com

ConocoPhillips, Inc.

Tom Danielson
ConocoPhillips, Inc.
600 N. Dairy Ashford
1036 Offshore Building
Houston, Texas 77079
Phone: (281) 293-6120
Fax: (281) 293-6504
Email: tom.j.danielson@conocophillips.com

Kris Bansal
ConocoPhillips, Inc.
1034 Offshore Building
600 N. Dairy Ashford
Houston, Texas 77079
Phone: (281) 293-1223
Fax: (281) 293-3424
Email: kris.m.bansal@conocophillips.com

Yongqian Fan
ConocoPhillips, Inc.
600 N. Dairy Ashford
1052 Offshore Building
Houston, Texas 77079
Phone: (281) 293-4730
Fax: (281) 293-6504
Email: yongqian.fan@conocophillips.com

ExxonMobil

Don Shatto
ExxonMobil
P. O. Box 2189
Houston, Texas 77252-2189
Phone: (713) 431-6911
Fax: (713) 431-6387
Email: don.p.shatto@exxonmobil.com

Jiyong Cai
ExxonMobil
P. O. Box 2189
Houston, Texas 77252-2189
Phone: (713) 431-7608
Fax: (713) 431-6387
Email: jiyong.cai@exxonmobil.com

Nader Berchane
ExxonMobil Upstream Research Company
Gas & Facilities Division
P. O. Box 2189
Houston, Texas 77252-2189
Phone: (713) 431-6059
Fax: (713) 431-6322
Email: nader.berchane@exxonmobil.com

JOGMEC

Tomoko Watanabe
JOGMEC
1-2-2, Hamada, Mihama-ku
Chiba, 261-0025 Japan
Phone: (81 43) 2769281
Fax: (81 43) 2764063
Email: watanabe-tomoko@jogmec.go.jp

Masaru Nakamizu
JOGMEC
One Riverway, Suite 450
Houston, Texas 77056
Phone: (713) 622-0204
Fax: (713) 622-1330
Email: nakamizu-masaru@jogmec.go.jp

Kuwait Oil Company

Eissa Alsafran
Kuwait University
College of Engineering and Petroleum
Petroleum Engineering Department
P. O. Box 5969
Safat – 13060 – Kuwait
Phone: (965) 4987699
Fax: (965) 4849558
Email: eisa@kuniv.edu.kw
dr_ealsafran@yahoo.com

Adel Al-Abbasi
Manager, Research and Technology
Kuwait Oil Company (K.S.C.)
P. O. Box 9758
Ahmadi – Kuwait 61008
Phone: (965) 398-8158
Fax: (965) 398-2557
Email: aabbasi@kockw.com

Ahmad K. Al-Jasmi
Team Leader R & T (Surface)
Research and Technology Group
Industrial Area
Kuwait Oil Company
P. O. Box 9758
Ahmadi – Kuwait 61008
Phone: (965) 3984126
(965) 3866771
Fax: (965) 3989414
Email: ajasmi@kockw.com

Bader S. Al-Matar
Snr. Reservoir Engineer
R & T Subsurface Team
Kuwait Oil Company
P. O. Box 9758
Ahmadi – Kuwait 61008
Phone: (965) 398-9111 ext. 67708
Email: bmatar@kockw.com

Marathon Oil Company

Rob Sutton
Marathon Oil Company
P. O. Box 3128
Room 3343
Houston, Texas 77253
Phone: (713) 296-3360
Fax: (713) 296-4259
Email: rpsutton@marathonoil.com

Minerals Management Services

Sharon Buffington
Minerals Management Services
Technology Research Assessment Branch
381 Elden Street
Mail Stop 2500
Herndon, VA 20170-4817
Phone: (703) 787-1147
Fax: (703) 787-1555
Email: sharon.buffington@mms.gov

Kurt Stein
Program Analyst
Minerals Management Services
Engineering and Research Branch
Mail Stop 4021
381 Eldon Street
Herndon, VA 20170-4817
Phone: (703) 787-1687
Fax: (703) 767-1549
Email: Kurt.Stein@mms.gov

Petrobras

Rafael Mendes
Petrobras
Cidade Universitaria – Quadra 7 – Ilha do Fundao
CENPES/PDEP/TEEA
Rio de Janeiro 21949-900
Brazil
Phone: (5521) 38652008
Fax:
Email: rafael.mendes@petrobras.com.br

Kazuoishi Minami
Petrobras
Av. Republica do Chile
65 – 17° Andar – Sala 1703
Rio de Janerio 20035-900
Brazil
Phone: (55 21) 5346020
Fax: (55 21) 5341128
Email: minami@petrobras.com.br

Marcelo Goncalves
Petrobras
Cidade Universitaria – Quadra 7 – Ilha do Fundao
CENPES/PDEP/TEEA
Rio de Janeiro 21949-900
Brazil
Phone: (5521) 38656712
Fax: (5521) 38656796
Email: marcelog@petrobras.com.br

Ibere Alves
Petrobras
Phone: (55 21) 5343720
Email: ibere@petrobras.com.br

Schlumberger

Mack Shippen
Schlumberger
5599 San Felipe
Suite 1700
Houston, Texas 77056
Phone: (713) 513-2532
Fax: (713) 513-2042
Email: mshippen@slb.com

William Bailey
Principal
Schlumberger – Doll Research
1 Hampshire Street, MD-B213
Cambridge, MA 02139
Phone: (617) 768-2075
Fax:
Email: wbailey@slb.com

Sammy Haddad
GFM Reservoir Domain Champion & Res. Eng. Advisor
Schlumberger Middle East S.A.
Mussafah
P. O. Box 21
Abu Dhabi, UAE
Phone: (971 2) 5025212
Fax:
Email: shaddad@abu-dhabi.oilfield.slb.com

Shell Global Solutions

Rusty Lacy
Fluid Flow (OGUF)
Shell Global Solutions (US) Inc.
Westhollow Technology Center
3333 Hwy 6 South
Houston, Texas 77082-3101
Phone: (281) 544-7309
Fax: (281) 544-8427
Email: rusty.lacy@shell.com

Ulf Andresen
Fluid Flow Engineer
Shell Global Solutions (US) Inc.
Westhollow Technology Center
3333 Hwy 6 South
Houston, Texas 77082
Phone: (281) 544-6424
Fax:
Email: ulf.andresen@shell.com

SPT

Richard Shea
SPT
11490 Westheimer, Suite 720
Houston, Texas 77077
Phone: (281) 496-9898 ext. 11
Fax: (281) 496-9950
Email: richard.shea@sptgroup.com

Yordanka Gomez-Markovich
SPT
Flow Assurance
DEV-GP6-1438
Phone: (281) 654-7549
Fax: (281) 654-6202
Email: yordanka.e.gomez@exxonmobil.com

Lee Norris
SPT
11490 Westheimer, Suite 720
Houston, Texas 77077
Phone: (281) 496-9898 ext. 14
Fax: (281) 496-9950
Email: hln@sptgroup.com

Gunnar Staff
SPT Group A/S
P. O. Boks 113, Instituttveien 10
N-2027 Kjeller, Norway
Phone: 47 63 89 04 94
Fax: 47 64 84 45 00
Email: gunnar.staff@sptgroup.com

TOTAL

Benjamin Brocart
Research Engineer
Rheology and Disperse Systems
TOTAL Petrochemicals France
Research & Development Centre Mont/Lacq
B. P. 47 – F – 64170
Lacq, France
Phone: (33 559) 926611
Fax: (33 559) 926765
Email: Benjamin.brocart@total.com

Emmanuel Duret
TOTAL Exploration & Production
DGEP/SCR/ED/ECP
2, place Jean Millier – La Defense 6
92078 Paris la Defense Cedex - France
Phone: (33) 1 47 44 35 03
Fax:
Email: emmanuel-denis.duret@total.com

Appendix C

History of Fluid Flow Projects Membership

1973			
1.	TRW Reda Pump	12 Jun. '72	T: 21 Oct. '77
2.	Pemex	15 Jun. '72	T: 30 Sept. ’96 R: Dec ’97 T: 2010
3.	Getty Oil Co.	19 Jun. '72	T: 11 Oct. '84 with sale to Texaco
4.	Union Oil Co. of California	7 Jul. '72	T: for 2001
5.	Intevep	3 Aug. '72	TR: from CVP in '77; T: 21 Jan ’05 for 2006
6.	Marathon Oil Co.	3 Aug. '72	T: 17 May ‘85 R: 25 June '90 T: 14 Sept. ‘94 R: 3 June ‘97 **Current**
7.	Arco Oil and Gas Co.	7 Aug. '72	T: 08 Dec. ‘97
8.	AGIP	6 Sep. '72	T: 18 Dec. '74
9.	Otis Engineering Corp.	4 Oct. '72	T: 15 Oct. '82
10.	ConocoPhillips, Inc.	5 Oct. '72	T: Aug. '85 R: 5 Dec. '86 **Current**
11.	Mobil Research and Development Corp.	13 Oct. '72	T: 27 Sep. 2000
12.	Camco, Inc.	23 Oct. '72	T: 15 Jan. '76 R: 14 Mar. '79 T: 5 Jan. '84
13.	Crest Engineering, Inc.	27 Oct. '72	T: 14 Nov. '78 R: 19 Nov. '79 T: 1 Jun. '84
14.	Chevron	3 Nov. '72	**Current**
15.	Aminoil	9 Nov. '72	T: 1 Feb. '77

16.	Compagnie Francaise des Petroles (TOTAL)	6 Dec. '72	T: 22 Mar. '85 R: 23 Oct. '90 T: 18 Sep. '01 for 2002 R: 18 Nov. '02 **Current**
17.	Oil Service Co. of Iran	19 Dec. '72	T: 20 Dec. '79
18.	Sun Exploration and Production Co.	4 Jan. '73	T: 25 Oct. '79 R: 13 Apr. '82 T: 6 Sep. '85
19.	Amoco Production Co. (now as BP Amoco)	18 May '73	
20.	Williams Brothers Engrg. Co.	25 May '73	T: 24 Jan. '83
	1974		
21.	Gulf Research and Development Co.	20 Nov. '73	T: Nov. '84 with sale to Chevron
22.	El Paso Natural Gas Co.	17 Dec. '73	T: 28 Oct. '77
23.	Arabian Gulf Exploration Co.	27 Mar. '74	T: 24 Oct. '82
24.	ExxonMobil Upstream Research	27 Mar. '74	T: 16 Sep. '86 R: 1 Jan. '88 T: 27 Sep. 2000 R: 2007 **Current**
25.	Bechtel, Inc.	29 May '74	T: 14 Dec. '76 R: 7 Dec. '78 T: 17 Dec. '84
26.	Saudi Arabian Oil Co.	11 Jun. '74	T: for 1999
27.	Petrobras	6 Aug. '74	T: for 2000 R: for 2005 **Current**
	1975		
28.	ELF Exploration Production (now as TotalFina Elf)	24 Jul. '74	T: 24 Feb. '76 Tr. from Aquitaine Co. of Canada 19 Mar. '81 T: 29 Jan. '87 R: 17 Dec. '91
29.	Cities Service Oil and Gas Corp.	21 Oct. '74	T: 25 Oct. '82 R: 27 Jun. '84 T: 22 Sep. '86

30.	Texas Eastern Transmission Corp.	19 Nov. '74	T: 23 Aug. '82
31.	Aquitaine Co. of Canada, Ltd.	12 Dec. '74	T: 6 Nov. '80
32.	Texas Gas Transmission Corp.	4 Mar. '75	T: 7 Dec. '89
	1976		
33.	Panhandle Eastern Pipe Line Co.	15 Oct. '75	T: 7 Aug. '85
34.	Phillips Petroleum Co.	10 May '76	T: Aug. 94 R: Mar 98 T: 2002
	1977		
35.	N. V. Nederlandse Gasunie	11 Aug. '76	T: 26 Aug. '85
36.	Columbia Gas System Service Corp.	6 Oct. '76	T: 15 Oct. '85
37.	Consumers Power Co.	11 Apr. '77	T: 14 Dec. '83
38.	ANR Pipeline Co.	13 Apr. '77	TR: from Michigan- Wisconsin Pipeline Co. in 1984 T: 26 Sep. '84
39.	Scientific Software-Intercomp	28 Apr. '77	TR: to Kaneb from Intercomp 16 Nov. '77 TR: to SSI in June '83 T: 23 Sep. '86
40.	Flopetrol/Johnston-Schlumberger	5 May '77	T: 8 Aug. '86
	1978		
41.	Norsk Hydro a.s	13 Dec. '77	T: 5 Nov. '82 R: 1 Aug. '84 T: 8 May ‘96
42.	Dresser Industries Inc.	7 Jun. '78	T: 5 Nov. '82
	1979		
43.	Sohio Petroleum Co.	17 Nov. '78	T: 1 Oct. '86
44.	Esso Standard Libya	27 Nov. '78	T: 2 Jun. '82
45.	Shell Internationale Petroleum MIJ B.V. (SIPM)	30 Jan. '79	T: Sept. 98 for 1999
	1980		
46.	Fluor Ocean Services, Inc.	23 Oct. '79	T: 16 Sep. '82
47.	Texaco	30 Apr. '80	T: 20 Sep. ’01 for 2002
48.	BG Technology (Advantica)	15 Sep. '80	T: 2003

	1981		
49.	Det Norske Veritas	15 Aug. '80	T: 16 Nov. '82
	1982		
50.	Arabian Oil Co. Ltd.	11 May '82	T: Oct.'01 for 2002
51.	Petro Canada	25 May '82	T:28 Oct. '86
52.	Chiyoda	3 Jun. '82	T: 4 Apr '94
53.	BP	7 Oct. '81	**Current**
	1983		
54.	Pertamina	10 Jan. '83	T: for 2000 R: March 2006
	1984		
55.	Nippon Kokan K. K.	28 Jun. '83	T: 5 Sept. '94
56.	Britoil	20 Sep. '83	T: 1 Oct. '88
57.	TransCanada Pipelines	17 Nov. '83	T:30 Sep. '85
58.	Natural Gas Pipeline Co. of America (Midcon Corp.)	13 Feb. '84	T:16 Sep. '87
59.	JGC Corp.	12 Mar. '84	T: 22 Aug. '94
	1985		
60.	STATOIL	23 Oct. '85	T:16 Mar. '89
	1986		
61.	JOGMEC (formerly Japan National Oil Corp.)	3 Oct. '86	T: 2003 R: 2007 **Current**
	1988		
62.	China National Oil and Gas Exploration and Development Corporation	29 Aug. '87	T:17 Jul. '89
63.	Kerr McGee Corp.	8 Jul. '88	T:17 Sept. '92
	1989		
64.	Simulation Sciences, Inc.	19 Dec. '88	T: for 2001
	1991		
65.	Advanced Multiphase Technology	7 Nov. '90	T:28 Dec. '92

66.	Petronas	1 Apr. ‘91	T: 02 Mar. 98 R: 1 Jan 2001 T: Nov. 2008 for 2009
		1992	
67.	Instituto Colombiano Del Petroleo	19 July ‘91	T: 3 Sep. ’01 for 2002
68.	Institut Francais Du Petrole	16 July. '91	T: 8 June 2000
69.	Oil & Natural Gas Commission of India	27 Feb. '92	T: Sept. 97 for 1998
		1994	
70.	Baker Jardine & Associates	Dec. ‘93	T: 22 Sept. ‘95 for 1996
		1998	
71.	Baker Atlas	Dec. 97	**Current**
72.	Minerals Management Service (Department of Interior’s)	May. 98	**Current**
		2002	
73.	Schlumberger Overseas S.A.	Aug. 02	**Current**
74.	Saudi Aramco	Mar. 03	T: for 2007
		2004	
75.	YUKOS	Dec. ‘03	T: 2005
76.	Landmark Graphics	Oct. ‘04	T: 2008
		2005	
77.	Rosneft	July ‘05	T: 2010
		2006	
78.	Tenaris		T: Sept 2008 – for 2009
79.	Shell Global		**Current**
80.	Kuwait Oil Company		**Current**
		2009	
81.	SPT		**Current**

Note: T = Terminated; R = Rejoined; and TR = Transferred

Appendix D

Contact Information

Director	
Cem Sarica	(918) 631-5154 cem-sarica@utulsa.edu
Associate Director	
Holden Zhang	(918) 631-5142 hong-quan-zhang@utulsa.edu
Director Emeritus	
James P. Brill	(918) 631-5114 brill@utulsa.edu
Project Coordinator	
Linda M. Jones	(918) 631-5110 jones@utulsa.edu
Project Engineer	
Scott Graham	(918) 631-5147 sdgraham@utulsa.edu
Research Associates	
Polat Abduvayt	(918) 631-5138 polat-abduvayt@utulsa.edu
Mingxiu (Michelle) Li	(918) 631-5107 michelle-li@utulsa.edu
Research Technicians	
Brandon Kelsey	(918) 631-5133 brandon-kelsey@utulsa.edu
Craig Waldron	(918) 631-5131 craig-waldron@utulsa.edu
Research Assistants	
Gizem Ersoy	(918) 631-5119 gizem-ersoy@utulsa.edu
Kiran Gawas	(918) 631-5117 kiran-gawas@utulsa.edu
Benin Jeyachandra	(918) 631-5119 bjeyachandra@utulsa.edu
Ceyda Kora	(918) 631-5117 ceyda-kora@utulsa.edu
Ge Yuan	(918) 631-5124 ge-yuan@utulsa.edu
Web Administrator	
Lori Watts	(918) 631-2979 lori-watts@utulsa.edu
Fax Number:	**(918) 631-5112**
Web Sites:	**www.tuffp.utulsa.edu**